SPECTROSCOPY AND PHOTOCHEMISTRY OF NOVEL ORGANOMETALLIC COMPLEXES

by

TODD DOUGLAS JAEGER

(Under the Direction of Michael A. Duncan)

ABSTRACT

Metal-benzene complexes of the form $M^+(benzene)_n$ (M=Ti, V, Fe, Co, Ni) are produced in the gas phase using laser vaporization in a pulsed nozzle cluster source. Several different laser photodissociation techniques are used to elucidate structures, examine fragmentation patterns, and obtain vibrational spectra for investigation of trends in shifts of the ligand based vibrational modes. First, fixed frequency photodissociation at 532 nm and 355 nm is used to probe the photochemistry of several transition metal ion-benzene and cyclooctatetraene systems. Complexes with different metals follow different fragmentation pathways including simple ligand elimination, ligand decomposition, and photo-induced charge-transfer. Next, the vibrational spectra of several transition metal-ion benzene complexes are obtained in the 600 to 1700 cm^{-1} region via Infrared Resonance Enhanced Multiple-photon Photodissociation (IR-REMPD) spectroscopy with a free electron laser. Photodissociation of all complexes occurs by the elimination of intact neutral benzene molecules, and this process is enhanced on resonances in the vibrational spectrum, making it possible to measure vibrational spectra for size-selected complexes by monitoring fragment yield versus IR excitation wavelength. Finally, vibrational spectra for metal ion-benzene and metal ion-benzene-argon complexes are obtained by

employing infrared photodissociation spectroscopy in the C-H stretch region (2700-3300 cm^{-1}) using an Optical Parametric Oscillator/Amplifier (OPO/OPA). Density functional theory calculations are employed to investigate the structures, energetics and vibrational frequencies of these complexes. The comparison between experiment and theory provides fascinating new insight into the bonding in these prototypical organometallic complexes.

INDEX WORDS: Spectroscopy, Clusters, Organometallics, Sandwich Complexes, Ion Chemistry, Photochemistry, Infrared, Photodissociation, Density Functional Theory

SPECTROSCOPY AND PHOTOCHEMISTRY OF NOVEL ORGANOMETALLIC COMPLEXES

by

TODD DOUGLAS JAEGER

B.S., Southwest Missouri State University, 2000

A Dissertation Submitted to the Graduate Faculty of The University of Georgia in Partial Fulfillment of the Requirements for the Degree

DOCTOR OF PHILOSOPHY

ATHENS, GEORGIA

2004

SPECTROSCOPY AND PHOTOCHEMISTRY OF NOVEL ORGANOMETALLIC COMPLEXES

by

TODD DOUGLAS JAEGER

Major Professor:	Michael A. Duncan
Committee:	Lionel A. Carreira
	Henning H. Meyer

Electronic Version Approved:

Maureen Grasso
Dean of the Graduate School
The University of Georgia
December 2004

DEDICATION

I don't know any children who say they want to be a chemist when they grow up. I can't say that I was any different, yet here I am embarking down that pathway. I have no regrets about this decision, be it a conscious or unconscious one, and I must take this time to trace backwards in time so that I might thank those responsible for nudging me toward this point in my life.

First, I would like to thank the Father, the Son, and the Holy Spirit. Without them there would be no yesterday, no today, and no hope of a tomorrow. Although my religious practices may have wavered and changed over the years, my faith in a higher power has never ceased. In fact, I believe my work in the hard sciences has strengthened my relationship with that higher power. I definitely know that I never prayed harder in my life until I had to take quantum mechanics.

Next, I want to thank my parents, Wayne and Nancy, for years of dedicated support, physically, mentally, and, of course, financially. Each has been a rock foundation for me to build my life upon, a soft shoulder for me to cry on, and a pair of strong arms to pick me up after I have fallen, time and time again. For this I could not possible say thanks enough, so instead I hope that my success in life, from here forward, will be a constant reminder of how grateful I am to have two wonderful parents in my life. Mom and Dad, this work is dedicated to you. Thanks for being you and having me. It was you two, remember, that inspired my interest in science: car-pooling to WINGS every Wednesday, countless trips to museums, numerous books on dinosaurs, nature, etc. God bless you both, I would not be the man I am today without you both.

Along with my parents, I have been blessed with a wonderful group of siblings. Chad, my oldest brother, has taught me many lessons in life. The lesson that shines above all others, though, is this: never stop chasing your dreams, no matter how rough the road gets. Chad, as many may know, could make magic with a soccer ball. But for all of the glorious goals he scored and victories he enjoyed, he endured mountains of pain from broken bones, physical exhaustion or knocked-out teeth. Don't think for a minute, though, while he groped in the mud with a mouth full of blood looking for his incisors, that he ever had a doubt in his mind that he would lace his boots back up and be back on the pitch for his next match. Chad continues chasing on his dreams now, though they've changed from his own dreams and aspirations to those of his son, Cole. He is blessed with a loving wife and partner, Holly, to help make those dreams a reality. I wish them many more happy years together

My sister Mel has played a vital role in my life as female role model. She has taught me to respect the female gender, in all aspects of life. She also taught me that I should not fear a little hard work, a lesson that rings true daily. I should also thank Mel for the "head-start" program she instituted in our home when I was young. While most older sisters force their little brothers to play house, Mel used to have us play school with her. To this date, I have not had a tougher teacher, but I could probably thank tougher corporal punishment laws for that... Mel and her husband Jason are the proud parents of twins, Camden and Cayden. I know they will raise these children properly and enjoy many years of health and happiness together.

My older brother Jared is the final sibling in my family. Jared holds a special place in my life as a coworker, a brother, and, above all, my best friend. I know I would not have made it through graduate school if he and his wife, Erin, had not moved down here after my first year. Jared, you are a source of strength and inspiration, and I love you. I wish you luck in the future,

and I want you to know that I am always here for you. You are fortunate to have a wonderful wife, and I will miss you both immensely. I hope we will all remain as close as we have as the days go by. Erin, you have become a sister to me and I will never forget all that you have done for me.

Outside of my family, I have had the fortune of working with many great scientists and friends. I first would like to thank Dr. Michael A. Duncan for giving me the opportunity to work in his lab for the past four and a half years. You are a brilliant scientist, a wonderful teacher, and a so-so golfer. Did I mention that you have a great sense of humor? When I came to this lab four years ago, Mike was given a blank slate in me to work with. I think he has done a damn good job filling it. I know he will have much success in the future. Mike, we are all still waiting for that Nobel Prize.

In my lab I have had the fortune of working with some young aspiring scientists that I am sure will influence the world in positive ways. This work is also dedicated to them for their help in the lab and, basically, for putting up with my rantings during my tenure at Georgia. In no particular order, I would like to thank Gilles, Deniz, Rich, Jared, Nick, Brian, Prosser, Greg, Karen, Tim, and Dinesh. Good luck to you all in the future, I know you will do well. We have made many memories together and experienced some wild times, and I thank certain ones of you (you know who you are) for not bringing those up in professional circles...only joking.

Last but not least, I dedicate this work to my dog Sam. Thanks for listening.

TABLE OF CONTENTS

CHAPTER 1

INTRODUCTION

Metal ion-ligand systems are prevalent throughout chemistry, biology, atmospheric science and astrophysics. Metal ions in various oxidation states are responsible for much of condensed phase inorganic chemistry. Many enzymes present in biological systems possess metal ions at their active sites that influence their structure and function.[1] Electrostatic forces are thought to govern selective metal ion transport through cell membranes.[2] The binding on metal oxide catalytic surfaces is attributed to interactions with ionic metal lattice sites.[3-5] Meteor ablation in the earth's atmosphere deposits surprisingly large quantities of metal ions on a daily basis.[6-10] These same results are observed in the atmospheres of other planets in our solar system,[11] specifically after the impact of comet Shoemaker-Levy 9 on Jupiter.[12] Complexes of metal ions with polyaromatic hydrocarbons (PAH's) are thought to be components of interstellar dust clouds and imbedded in dust and ice grains in these environments.[13-20] It is evident from these examples that metal ion-ligand interactions are responsible for a variety of important chemical processes. It is unfortunate that theory has trouble dealing with many of these complex systems, especially those in which multiple ligands are involved. When theory fails, it is important to produce such complexes and directly measure their properties. Gas-phase metal ion-ligand complexes provide models for metal-ligand bonding, metal ion solvation, and metal-surface adsorbate interactions. This study focuses, in conjunction with theory, on the production,

fixed-frequency photodissociation, and infrared spectroscopy of metal ion-ligand systems in an attempt to better understand their bonding, structure, coordination and solvation.

Metal ion-ligand and molecular ions can be produced in a variety of ways. Electron impact (EI) ionization of volatile hydrocarbons has been used extensively in the past.[21-22] Although ion production is efficient and simple in such sources, production of larger ion densities requires incident electron energy to be well above the ionization potential (IP) of the hydrocarbons being studied. This excess energy can cause internal heating of these molecules as well as extensive fragmentation. Chemical ionization has also been used as a "soft" ionization alternative,[23] however even in this scheme a broad distribution of internal states may be produced, leading to broad, ambiguous vibrational and/or electronic spectra.[24] Another limitation of these two techniques is the variety of species that can be produced or studied. Molecules must have high vapor pressures or low boiling points to put them in the gas-phase for study. This eliminates the possibility of studying metals or other high refractory materials using these methods.

Metal-containing species have also been previously produced utilizing various forms of electrical discharge sources, i.e. hollow-cathode or glow-discharge sources.[25,26] Metal atom as well as larger metal clusters can be produced by these sources as a continuous beam of thermalized ions. Unfortunately, instantaneous sample densities are somewhat low. The substance to be studied must also be a conductor, which limits the materials that can be studied. A similar source to these is the corona discharge source. This source, used by Saykally and co-workers[27] as well as others, produces ions via a discharge then cools them in a mild supersonic expansion.

For better cooling, many groups have coupled supersonic expansions with electron impact ionization sources.[26,28-55] In these sources clusters produced in a supersonic expansion are ionized downstream by an electron impact source. Although the clusters are cooled efficiently the expansion, the ionization event can impart excess energy into the molecular cluster. Some cooling occurs by evaporation of rare gas or molecular units. Unfortunately gas density is much lower downstream from the ionization region so collisional cooling is limited. Although these sources have the advantage of low cost and easy assembly, spectroscopy of ions produced this way has shown that they are somewhat hot internally.

More recently electrospray ionization sources have been utilized.[56-78] These sources are effective for producing multiply charged ions. In the ionization sources described previously singly charged cations and anions are primarily produced. Small ions in low-pressure gas-phase environments usually cannot support multiple charges without spontaneously decomposing into two or more singly charged species. In solution, however, solvation stabilizes multiply charged species. Electrospray sources effectively extract these ions directly from solution, preserving their charge. For samples that have high melting points and cannot readily be accessed in solution, laser vaporization has become the method of choice. To avoid fragmentation of large biomolecules Matrix Assisted Laser Desorption Ionization has become a popular technique.[79-87] Samples of interest are prepared in a matrix and put under vacuum. A low power laser is then fired at this target. The matrix absorbs the brunt of the incident laser energy and the resulting shockwave. Molecules trapped in the matrix are subsequently desorbed and ionized without extensive fragmentation. Similarly, highly refractory samples can be vaporized using a high power pulsed laser system.

Laser ablation sources were originally used to make neutral metal clusters.[88] Because virtually any solid can be used in such a setup, a vast variety of chemically interesting substances have been produced in this way including not only metal clusters,[89-92] but carbon[93] and semiconductor clusters[94,95] as well. To study the neutral complexes created from this plasma, EI as well as photoionization has been employed. These techniques have the possibility of imparting excess internal energy on the cluster, leading to broad spectra. It has been found recently that this type of source coupled with a supersonic expansion is also excellent at producing cold cations and anions directly. By seeding a ligand of interest into the expansion gas, cold metal ion-ligand complexes can be produced efficiently and at higher sample densities than previous techniques.

Metal ion-ligand systems have been the focus of gas-phase chemical studies for many years. Much early work focused on the reactivities and thermodynamics of such systems.[96-98] Equilibrium mass spectrometry,[99-101] collision-induced dissociation,[102-104] radiative association,[105] as well as various theoretical studies[106-126] have been performed to elucidate bond energies and infer coordination numbers. UV-vis laser photodissociation has also been applied to various metal-ligand systems such as $M^+(PAH)_n$,[127-130,132] $M^+(C_{60})_n$,[131-133] $M^+(benzene)_n$[134,135] complexes and, in this study, $M^+(cyclooctatetraene)_n$[136] to investigate fragmentation patterns for evidence of stable metal-ligand cores and the appearance of novel photochemistry. Although these techniques give some insight into the bonding in these systems, they provide no spectroscopic data to give definitive structures.

Because metal ion-ligand complexes can only be produced in low densities, typical absorption spectroscopy is not possible. Instead, various forms of "action spectroscopy" have been employed on metal ion-ligand complexes including Laser Induced Fluorescence (LIF),[137]

laser Photoelectron Spectroscopy (PES) of size-selected anions,[138-144] Resonance Enhanced Photodissociation (REPD) spectroscopy,[52,145-230] Mass Analyzed Threshold Ionization (MATI) spectroscopy,[139] and Zero Electron Kinetic Energy (ZEKE) spectroscopy.[139-144,231-242] Most of the early studies focused on electronic spectroscopy in the ultraviolet/visible region of the spectrum due to the strength of these transitions and the availability of tunable laser light sources in this area. Dye lasers and, more recently, Optical Parametric Oscillator (OPO) systems have provided the necessary high energy to make these experiments successful. Electronic spectroscopy has been applied to both main group[145-182] and transition metal[183-196] ion complexes with small molecules and rare gas atoms. Metals with known electronic transitions in the UV/VIS are usually selected. If a weakly bound electrostatic complex can be formed, then the electronic transition of the complex can usually be found close by. Early success was achieved using group II metal ions which possess strong $^2P \leftarrow ^2S$ atomic transitions.[145-181] Duncan and coworkers,[150-161] Fuke and coworkers,[162-166] and Kleiber and coworkers[167-172] employed photodissociation spectroscopy on Mg^+ and Ca^+ complexes with such small molecules as H_2O, CO_2, N_2, C_2H_2, C_2H_4, and CH_3OH. Farrar and coworkers[145-149] as well as Velegrakis and coworkers[173-177] made similar measurements on strontium complexes. For complexes where no low lying electronic transitions exist, i.e. Al^+-Ar[182] and Al^+-(C_2H_2),[172] vacuum UV techniques have been employed to obtain the electronic spectra. Transition metal cation complexes with some of the above mentioned small molecules were investigated by Brucat and coworkers[183-192] and, more recently, Metz and coworkers.[193-196] Several other groups have used similar techniques to investigate multiply charged transition metal cation complexes.[197,198] Theoretical predictions complement these studies by calculating ground and electronic state geometries.[106-126]

Many of the above studies have been performed on cold molecules using high-resolution laser systems giving vibrationally resolved spectra for mono-ligand systems and, in some cases, beautiful rotationally resolved spectra, allowing for determination of structures for these single-ligand complexes.[135b,152b,153b,154,157a,158] These studies give information on excited and ground state electronic structures as well as the ability, for certain systems, to extrapolate ground state bond energies from progressions in the metal-ligand stretching coordinate. Although, much information can be gained from these investigations, electronic spectroscopy has several limitations.[161] First, it is often difficult to gain the same information for multiple ligand systems as can be gleaned for mono-ligand systems. Predissociation is often prevalent in these systems, leading to extremely broad spectra with no vibrational resolution.[161] Also, although weakly bound metal ion-ligand complexes may form in an ion's ground state, the energy of the light absorbed is often enough to overcome reaction barriers causing photo-induced metal-ligand reactions. This often leads to severe lifetime broadening and the inability to vibrationally resolve spectra. Finally, ground state reactions can occur due to solvation effects of multiple ligands. This phenomenon has been previously observed in the mass spectrometry patterns of several systems, including metal ion-water clusters. Fragmentation patterns in these systems show spontaneous formation of M^{2+} and OH^- in larger clusters.[243-247] These reactions again lead to broad, featureless spectra.

Because of the limitations of electronic spectroscopy, investigations that probe the ground state of these clusters systems is absolutely necessary. One method used previously is ZEKE/MATI.[139-144,231-242] Studies have been performed by Duncan and coworkers on Al^+-Ar[139] and Al^+-H_2O[143] and by Blake and coworkers on Na^+-H_2O.[144] Miller and coworkers have also investigated $MgCH_3$[140] and $ZnCH_3$[141] using this technique. Recently Yang and coworkers have

successfully applied ZEKE to a variety of metal-ligand systems.[231-242] Because of large changes in the bonding going from a neutral to a cation, Franck-Condon activity is usually limited to the metal-ligand stretching coordinate. These studies are limited in their ability to size-select the cluster being studied.

IR spectroscopy is the method of choice for ground state structural studies in condensed phase systems. Since ion density is too low in a pulsed molecular beam, direct absorption measurements are not possible. IR photodissociation work has been previously applied using line-tunable CO_2 laser systems.[248-251] These early studies were limited in their scope because the laser systems used were severely limited in their scanning range. Many non-metal cation, anion, and neutral systems have been investigated using IR photodissociation spectroscopy.[40,48,51,53,54,252-259] Knickelbein and coworkers have also obtained IR photodissociation spectra for several neutral metal-ligand complexes.[249-251] However, Lisy and coworkers were the first to apply such techniques to metal complexes with their studies of alkali metal ion-ligand systems.[199-204]

Since these initial attempts, advances in laser systems and the coupling of these systems to a laser ablation pulsed nozzle cluster source have allowed the field of IR photodissociation spectroscopy to expand to more and more metal ion-ligand systems. Our lab has applied Infrared Resonance Enhanced Photodissociation (IR-REPD) spectroscopy to several metal ion-ligand systems using an IR OPO system.[206-208, 211-216, 218] This work is coupled to a laser vaporization cluster source allowing for many more high melting materials to be studied. IR spectra in the mid to near IR region have been obtained for complexes with both main group and transition metals with a variety of ligands (e.g. CO_2, H_2O, C_2H_2, etc.).[206-208, 211-216, 218] Much work has also been done recently using Free Electron Lasers (FEL's) in the far IR for a variety of metal-ligand

systems[209,210,217,219-230] including Cr^+(aniline)[230] and various Fe^+(ether) systems.[222] The results of these experiments have shown that IR-REPD is a proven technique for elucidating data on ground state geometries of multi-ligand systems, determining coordination numbers, investigating solvation effects, and discovering the occurrence of intracluster reactions.

IR-REPD is not without its faults. One major issue is incident photon energy versus the energy required to fragment a molecule. In UV/VIS photodissociation experiments incident photon energy is high, between 10,000 to 50,000 cm^{-1}. Vibrational resonances, on the other hand, occur below about 4,000 cm^{-1}.[260] Incident photon energy in an IR-REPD must also be below 4,000 cm^{-1} if the fundamental vibration is to be excited. As shown in Table 1.1, the binding energy of a metal ion to a ligand is rather high, usually between 5,000-20,000 cm^{-1}.[102,104,106,107,109,110,112,117-119,122-126,150,151,154,157,244] The vibrational resonances for several ligands are also listed in Table 1.1. It is clear from these values that a single photon absorbed on resonance would not be enough to induce fragmentation in these systems. However, as cluster size grows with the addition of more ligands the binding energy per ligand is expected to decrease. This is especially true once coordination around the metal ion has been filled. Additional ligands cannot attach directly to the ion and instead attach to other ligands. The binding energies in these systems are expected to decrease dramatically. The bond strength for this interaction is more akin to the binding in a dimer or trimer of the isolated molecule. It is expected then that dissociation yields would be quite small or even non-existent when only one to three ligands are attached, but would increase as more ligands attach. This hypothesis is consistent with experimental observations. The dissociation yield is rate dependent, however, and decreases as clusters become too large to fragment on a time scale consistent with detection.

Table 1.1 Binding Energies versus Vibrational Resonance of Various Metal-Ion Ligand Complexes

Complex	Bond Energy	Vibrational Resonance Excited
M^+-H_2O	8,700-12,000 cm^{-1}	3650 cm^{-1} 3750 cm^{-1}
H_2O-H_2O	1750 cm^{-1}	
M^+-CO_2	5250 cm^{-1}	2349 cm^{-1}
CO_2-CO_2	500 cm^{-1}	
M^+-N_2	3500 cm^{-1}	2358 cm^{-1}
M^+-benzene	10,500-17,500 cm^{-1}	700-3100 cm^{-1}
M^+-He	70-1550 cm^{-1}	
M^+-Ne	175-1200 cm^{-1}	
M^+-Ar	500-4500 cm^{-1}	
M^+-Kr	1900-5400 cm^{-1}	

It is possible to obtain IR spectra of the smaller, more strongly bound systems. Two general approaches exist. First, multiphoton photodissociation (MPD) might occur. The intricacies of MPD for both neutral and ionic species have been investigated and described previously.[248,261-265] MPD processes are dependent on laser energy and pulse structure, metal-ligand bond energy, the efficiency and completeness of Intramolecular Vibrational Redistribution (IVR), and the density of states of the system. High power OPO and FEL systems often satisfy the power requirements for MPD by supplying a high flux of photons at a given IR energy. If the density of states is high above the single-photon resonance, then this resonance can be preserved regardless of anharmonicity allowing for multiple photons to be absorbed. If IVR is fast and efficient this energy can be redistributed from the IR chromophore into the dissociation coordinate. Finally, if enough energy is absorbed to exceed the bond energy of the dissociation coordinate, the molecule will undergo fragmentation. As cluster size grows, the density of states increases while bond energy decreases making MPD, in general, more efficient. The temporal structure of a nanosecond OPO allows for MPD, but it is inefficient. However, the temporal structure of a FEL consists of a train of picosecond micropulses in each macropulse from the laser.[266] This allows for several absorption and redistribution events to occur in one macropulse, increasing the overall efficiency of the process.

Unfortunately, multiphoton processes cause broadening of peaks by saturation and are known to red-shift observed resonances from their true value.[267,268] Because of this fact it is important to utilize another technique for acquiring spectra of strongly bound complexes. One method used by this group and others is to attach a weakly bound spectator atom or molecule (e.g. Ne, Ar, H_2, etc.) to the cluster.[48,51,206,207,211-216,218,252,254,269,270] As Table 1.1 shows, the binding energy for these complexes is small and the interaction of the tag is weak, therefore the

perturbation on the cluster structure and its vibrational spectrum is small. The chromophore in the cluster is still the ligand vibration, however the weakest bond is now that of the metal ion with the tag, thereby making this the dissociation coordinate. The dissociation yield increases due to several factors. First, the addition of a weakly bound entity adds low frequency vibrational modes to the cluster increasing the overall density of states. Secondly, the binding of the tag is generally weak enough such that single-photon excitation can now lead to fragmentation. Due to the weak nature of the metal ion-tag bond, tagged clusters must have low internal energy. The combination of cold clusters and single-photon dissociation generally lead to narrow linewidths and increased signal to noise when compared to non-tagged or "neat" clusters.

The work presented here concentrates on applying fixed-frequency photodissociation as well as IR single and multiphoton dissociation to organometallic metal ion-ligand systems, and, in particular, those containing benzene. Metal ion-benzene complexes are attractive because of their relevance for catalysis and biological processes,[1,271] as well as the fundamental importance that aromatic π-bonding has for organometallic chemistry.[272,273] These complexes are also interesting because they are known to form sandwich structures and, hence, can be compared to similar complexes isolated in conventional synthetic chemistry.[272,273] Shortly after the discovery of ferrocene,[274] a charge-transfer stabilized organometallic complex consisting of two cyclopentadienyl rings sandwiching an iron atom, bis-benzene chromium was first synthesized.[275] Its structure is analogous to that of ferrocene: a sandwich of two benzene ligands with a chromium center. The relative stability of the complex was attributed to the 18-electron rule, with 6 electrons donated from each benzene and the remaining six from chromium's valence shell.[275] Other neutral metal-benzene systems have been synthesized via conventional

techniques.[272,273] Some charge species have also been synthesized via these techniques and stabilized by counterions.[272,273] These complexes have been studied with traditional infrared spectroscopy to investigate their bonding via spectral shifts in the benzene ligand based vibrations. Condensed phase measurements are somewhat troublesome, though, due to effects from solid or solvent environments or the presence of counterions. Gas-phase measurements would circumvent these problems, but, until now, no spectroscopic studies exist.

Gas-phase studies have been performed on many metal-ion benzene systems using mass spectrometry.[102c,105a,134,135,276-279] Bond energies have also been determined by using collision-induced dissociation,[102c,276] equilibrium mass spectrometry,[105a,277] as well as UV-vis photodissociation measurements.[134,135] Many extensive theoretical studies have also been performed to investigate the energetics of these fascinating systems.[96,97,122-126,281,282] Kaya and coworkers found that certain early transition metal-benzene systems form multiple-decker sandwiched based on mass spectrometric measurements with prominent $M_x(C_6H_6)_y$ stoichiometries where $y = x+1$.[278] Ion mobility measurements have also been performed on vanadium-benzene complexes by Bowers and coworkers,[279] confirming multiple-decker sandwich structures. Magnetic deflection experiments also verified these structures.[278] Photoelectron spectroscopy has been applied to metal-benzene anions.[278b,283] Recently, an IR spectrum was obtained for $V(C_6H_6)$ size-selected as a cation and then deposited in a rare gas matrix.[284] Lisy and coworkers have obtained IR spectra for mixed-ligand alkali cation-$(water)_x(benzene)_y$ complexes in the O-H stretch region.[204] To date, the IR spectra of size-selected transition metal cation-benzene complexes have not been obtained. The goal of this work is to combine fixed-frequency photodissociation and IR-REPD using an OPO system for mid-IR and a FEL for the fingerprint region to elucidate the structure and bonding in transition

metal cation-benzene complexes and compare these results with those predicted by theory. Furthermore, this work will show that the coordination number for the systems studied here is two and that the onset of solvation occurs after this point.

References

(1) a) Ma, J.C.; Dougherty, D.A. *Chem. Rev.* **1997**, *97*, 1303. b) Dougherty, D.A. *Science* **1996**, *271*, 163.

(2) Krumpf, R.A.; Dougherty, D.A. *Science*. **1993**, *261*, 1708.

(3) Henrich, V.E.; Cox, P.A. *The Surface Science of Metal Oxides,* Royal Society of Chemistry, Cambridge, 1994.

(4) *The Surface Science of Metal Oxides,* Faraday Discussions of the Royal Society of Chemistry, Cambridge, 1999.

(5) Kim, Y.D.; Stultz, J.; Goodman, D.W. *J. Phys. Chem.* **2002**, *106*, 1515.

(6) Plane, J.M.C.; *Int. Rev. Phys. Chem.* **1991**, *10*, 55.

(7) Gardner, J.A.; Viereck, R.A.; Murad, E.; Knecht, D.J., Pike, C.P.; Broadfoot, A.L.; Anderson, E.R. *Geophys. Res. Lett.* **1995**, *22*, 2119.

(8) McNeil, W.J.; Lai, S.T., Murad, E. *J. Geophys. Res.* **1996**, *101*, 5251.

(9) Viereck, R.A.; Murad, E.; Lai, S.T.; Knecht, D.J.; Pike, C.P.; Gardner, J.A.; Broadfoot, A.L.; Anderson, E.R.; McNeil, W.J. *Adv. Space Res.* **1996**, *18*, 61.

(10) McNeil, W.J.; Lai, S.T.; Murad, E. *J. Geophys. Res.* **1998**, *103*, 10899.

(11) Lyons, J.R. *Science*. **1995**, *267*, 648.

(12) Noll, K.S.; McGrath, M.A.; Trafton, L.M.; Atreya, S.K.; Caldwell, J.J, et al. *Science.* **1995**, *267*, 1307.

(13) Millar, T.J.; Williams, D.A., eds. *Dust and Chemistry in Atronomy*, Institute of Physics, London, 1993.

(14) Henning, T.; *Chem. Soc. Rev.* **1998**, *27*, 315.

(15) Serra, G.; Chaudret, B.; Saillard, J.Y.; Le Beuze, A.; Rabaa, H.; Ristorcelli, I.; Klotz A. *Astron. Astrophys.*, **1992**, *260*, 489.

(16) Chaudret, B.; Le Beuze, A.; Rabaa, H.; Saillard, J.Y.; Serra, G. *New J. Chem.* **1991**, *15*, 791.

(17) Marty, P.; Serra, G.; Chaudret, B.; Ristorcelli, I. *Astron. Astrophys.* **1994**, *282*, 916.

(18) Klotz, A; Marty, P.; Boissel, P.; Serra, G.; Chaudret, B.; Daudey, J.P. *Astron. Astrophys.* **1995**, *304*, 520.

(19) Klotz, A; Marty, P.; Boissel, P.; De Caro, D.; Serra, G.; Mascetti, J.; De Parseval, P.; Derouault, J.; Duadey, J.P.; Chaudret, B. *Planet. Space Sci.* **1996**, *44*, 957

(20) Patrie, S.; Becker, H.; Baranov, V.; Bohme, D.K. *Astrophys. J.* **1997**, *476*, 191.

(21) Massey, H.S.W. *Electron Collisions with Molecules and Photoionization*, Oxford University Press, Oxford, 1969.

(22) Blausen, B.D., ed. "Chemical Reactions in Electrical Discharges" *Advances in Chemistry Series No. 80*, American Chemical Society, Washington D.C., 1969

(23) Setser, D.W., ed. *Reactive Intermediates in the Gas Phase,* Academic, New York, 1979.

(24) Berkowitz, J. *Photoabsorption, Photoionization and Photoelectron Spectroscopy,* Academic, New York, 1979.

(25) a) Leopold, D.; Ho, J.; Lineberger, W.C. *J. Chem. Phys.* **1987**, *86*, 1715. b) Ho, J.; Ervin, K.M.; Lineberger, W.C. *ibid.* **1990**, *93*, 6987. c) Ervin, K.M.; Ho, J.; Lineberger, W.C. *ibid.* **1989**, *91*, 5974.

(26) Taylor, W.S.; Everett, W.R.; Babcock, L.M.; McNeal, T.L.; *Int. J. Mass Spectrom. Ion Processes*. **1993**, *125*, 45.

(27) a) Coe, J.V.; Owrutsky, J.; Keim, E.; Agman, N.; Saykally, R.J. *J. Chem. Phys.* 1989, 90, 3893. b) Coe, J.V.; Saykally, R.J. in *Ion and Cluster Ion Spectroscopy and Structure*, Maier, J.P., ed., Elsevier, Amsterdam, 1989, p.131.

(28) Corderman, R.R.; Lineberger, W.C. *Annu. Rev. Phys. Chem.* **1979**, *30*, 347.

(29) Neumark, D.M.; Lykke, K.R.; Anderson, T.; Lineberger, W.C. *J. Chem. Phys.* **1985**, *83*, 4364.

(30) a) Johnson, M.A.; Lineberger, W.C. *Tech. Chem. (Tech. Study Ion-Mol. React.)* **1988**, *20*, 591. b) Johnson, M.A.; Alexander, M.L.; Lineberger, W.C. *Chem. Phys. Lett.* **1984**, *112*, 285.

(31) Dessent, C.E.H.; Johnson, M.A. *NATO ASI Ser., Ser. C.* **1999**, *521*, 287.

(32) Lee, G.H; Arnold, S.T.; Eaton, J.G.; Bowen, K.H. *Chem. Phys. Lett.* **2000**, *321*, 333.

(33) Hendricks, J.H.; de Clercq, H.L.; Lyapustina, S.A.; Bowen, K.H. *J. Chem. Phys.* **1997**, *107*, 2962.

(34) Zanni, M.T.; Frischkorn, C.; Davis, A.V.; Neumark, D.M. *J. Phys. Chem. A* **2000**, *104*, 2527.

(35) Greenblatt, B.J.; Zanni, M.T.; Neumark, D.M. *J. Chem. Phys.* **2000**, *112*, 601.

(36) Greenblatt, B.J.; Zanni, M.T.; Neumark, D.M. *J. Chem. Phys.* **1999**, *111*, 10566

(37) Lenzer, T.; Furlanetto, M.R.; Pivonka, N.L.; Neumark, D.M. *J. Chem. Phys.* **1999**, *110*, 6714.

(38) Asmis, K.R.; Taylor, T.R.; Xu, C.; Neumark, D.M. *J. Chem. Phys.* **1998**, *109*, 4389.

(39) Xu, C.; Burton, G.R.; Taylor, T.R.; Neumark, D.M. *J. Chem. Phys.* **1997**, *107*, 3428.

(40) Lehr, L.; Zanni, M.T.; Frischkorn, C.; Weinkauf, R.; Neumark, D.M. *Science*. **1999**, *284*, 635.

(41) Sanov, A.; Sanford, T.; Nandi, S.; Lineberger, W.C. *J. Chem. Phys.* **1999**, *111*, 664.

(42) Vorsa, V.; Nandi, S.; Campagnola, P.J.; Larsson, M.; Lineberger, W.C. *J. Chem. Phys.* **1997**, *106*, 1402.

(43) Vorsa, V.; Campagnola, P.J.; Nandi, S.; Larsson, M.; Lineberger, W.C. *J. Chem. Phys.* **1995**, *105*, 2298.

(44) Nielson, S.B.; Ayotte, P.; Kelley, J.A.; Weddle, G.H.; Johnson, M.A. *J. Chem. Phys.* **1999**, *111*, 10464.

(45) Ayotte, P.; Nielson, S.B.; Weddle, G.H.; Johnson, M.A.; Xantheas, S.S. *J. Phys. Chem. A.* **1999**, *103*, 10665.

(46) Ayotte, P.; Kim, J.; Kelley, J.A.; Nielson, S.B.; Johnson, M.A. *J. Am. Chem. Soc.* **1999**, *121*, 6950.

(47) Ayotte, P.; Weddle, G.H.; Johnson, M.A. *J. Chem. Phys.* **1999**, *110*, 7129.

(48) Ayotte, P.; Weddle, G.H.; Bailey, C.G.; Johnson, M.A.; Vila, F.; Jordan, K.D. *J. Chem. Phys.* **1999**, *110*, 6268.

(49) Ayotte, P.; Weddle, G.H.; Kim, J.; Johnson, M.A. *Chem. Phys.* **1998**, *239*, 485.

(50) Ayotte, P.; Weddle, G.H.; Kim, J.; Johnson, M.A. *J. Am. Chem. Soc.* **1998**, *120*, 12361.

(51) Ayotte, P.; Bailey, C.G.; Kim, J.; Johnson, M.A. *J. Chem. Phys.* **1998**, *108*, 444.

(52) Cabarcos, O.M.; Weinheimer, C.J.; Lisy, J.M.; Xantheas, S.S. *J. Chem. Phys.* **1999**, *110*, 5.

(53) Cabarcos, O.M.; Weinheimer, C.J.; Lisy, J.M.; Xantheas, S.S. *J. Chem. Phys.* **1999**, *110*, 9516.

(54) a) Choi, J.H.; Kuwata, K.T.; Cao, Y.B.; Okumura, M. *J. Phys. Chem. A.* **1998**, *102*, 503. b) Johnson, M.S.; Kuwata, K.T.; Wong, C.K.; Okumura, M. *Chem. Phys. Lett.* **1996**, *260*, 551.

(55) Ruchti, T.; Rohrbacher, A.; Speck, T.; Connelly, J.P.; Bieske, E.J.; Maier J.P. *Chem. Phys.* **1996**, *209*, 169.

(56) Yamashita, M.; Fenn, J.B. *J. Phys. Chem.* **1984**, *88*, 4451.

(57) Whitehouse, C.M.; Dreyer, R.N.; Yamashita, M. Fenn, J.B. *Anal. Chem.* **1985**, *57*, 675.

(58) Fenn, J.B.; Mann, M.; Meng, C.K.; Wong, S.F.; Whitehouse, C.M. *Science.* **1989**, *246*, 64.

(59) Fenn, J.B.; Mann, M.; Meng, C.K.; Wong, S.F.; Whitehouse, C.M. *Mass. Spectrom. Rev.* **1990**, *9*, 37.

(60) Zhan, D.; Rosell, J.; Fenn, J.B. *J. Am. Soc. Mass Spectrom.* **1998**, *9*, 1241.

(61) Klassen, J.S.; Ho, Y.; Blades, A.T.; Kebarle, P. *Adv. Gas Phase Ion Chem.* **1998**, *3*, 225.

(62) Burns, T.D.; Spence, T.G.; Mooney, M.A.; Posey, L.A. *Chem. Phys. Lett.* **1996**, *258*, 669.

(63) Spence, T.G.; Burns, T.D.; Posey, L.A. *J. Phys. Chem. A.* **1997**, *101*, 139.

(64) Spence, T.G.; Burns, T.D.; Guckenberger, G.B.; Posey, L.A. *J. Phys. Chem. A.* **1997**, *101*, 1081.

(65) Spence, T.G.; Trotter, B.T.; Burns, T.D.; Posey, *J. Phys. Chem. A.* **1998**, *102*, 6101.

(66) Spence, T.G.; Trotter, B.T.; Posey, *J. Phys. Chem. A.* **1998**, *102*, 7779.

(67) Spence, T.G.; Trotter, B.T.; Posey, *Int. J. Mass Spectrom.* **1998**, *177*, 187.

(68) Wang, X.B.; Wang, L.S. *J. Am. Chem. Soc.* **2000**, *122*, 2339.

(69) Wang, L.S.; Wang, X.B. *J.Phys. Chem. A.* **2000**, *104*, 1978.

(70) Wang, X.B.; Ferris, K.; Wang, L.S. *J.Phys. Chem. A.* **2000**, *104*, 25.

(71) Wang, X.B.; Wang, L.S. *Phys. Rev. Lett.* **1999**, *83*, 3402.

(72) Li, X.; Wang, L.S. *J. Chem. Phys.* **1999**, *111*, 8389.

(73) Wang, X.B.; Wang, L.S. *Nature*. **1999**, *400*, 245.

(74) Wang, L.S.; Ding, C.F.; Wang, X.B.; Barlow, S.E. *Rev. Sci. Instrum.* **1999**, *70*, 1957.

(75) Wang, X.B.; Ding, C.F.; Wang, L.S. *Phys. Rev. Lett.* **1998**, *81*, 3351.

(76) Ding, C.F.; Wang, X.B.; Wang, L.S. *J. Phys. Chem. A.* **1998**, *102*, 8633.

(77) Wang, L.S.; Ding, C.F.; Wang, X.B.; Nicholas, J.B. *Phys. Rev. Lett.* **1998**, *81*, 2667.

(78) Li, X.; Wu, H.; Wang, X.B.; Wang, L.S. *Phys. Rev. Lett.* **1998**, *81*, 1909.

(79) Karas, M.; Hillenkamp, F. *Int. J. Mass Spectrom. Ion Processes*. **1987**, *78*, 53.

(80) Beavis, R.C.; Chait, B.T. *Rapid Commun. Mass Sp.* **1989**, *3*, 432.

(81) Beavis, R.C.; Chait, B.T. *Org. Mass. Spectrom.* **1992**, *27*, 156.

(82) Karas, M.; Hillenkamp, F. *Org. Mass. Spectrom.* **1993**, *28*, 1476.

(83) Tanaka, K., et al. *Rapid Commun. Mass Sp.* **1988**, *2*, 151.

(84) Tanka, K. *Angew. Chem. Int. Edit.* **2003**, *42*, 3861.

(85) Karas, M., et al. *Mass Spectrom. Rev.* **1991**, *10*, 335.

(86) Beavis, R.C. *Org. Mass. Spectrom.* **1992**, *27*, 653.

(87) Bahr, U.; Karas, M.; Hillenkamp, F. *Fres. J. Anal. Chem.* **1994**, *348*, 783.

(88) Dietz, T.G.; Duncan, M.A.; Powers, D.E.; Smalley, R.E. *J. Chem. Phys.* **1981**, *74*, 6511.

(89) Brucat, P.J.; Zheng, L.S.; Pattiette, C.L.; Yang, S.; Smalley, R.E. *J. Chem. Phys.* **1986**, *84*, 3078.

(90) Zheng, L.S.; Brucat, P.J.; Pettiette, C.L.; Yang, S.; Smalley, R.E. *J. Chem. Phys.* **1985**, *83*, 4273.

(91) Zheng, L.S.; Carner, C.M.; Brucat, P.J.; Yang, S.H.; Pettiette, C.L.; Craycraft, M.J.; Smalley, R.E. *J. Chem. Phys.* **1986**, *85*, 1681.

(92) Chesnovsky, O.; Taylor, K.J.; Conceicao, J.; Smalley, R.E. *Phys. Rev. Lett.* **1990**, *64*, 1785.

(93) Yang, S.; Taylor, K.J.; Craycraft, M.J.; Conceicao, J.; Pettiette, C.L.; Chesnovsky, O.; Smalley, R.E. *Chem. Phys. Lett.* **1988**, *144*, 431.

(94) Jin, C.; Taylor, K.J.; Conceicao, J.; Smalley, R.E. *Chem. Phys. Lett,* **1990**, *175*, 17.

(95) Chesnovsky, O.; Yang, S.H.; Pettiette, C.L.; Craycraft, M.J.; Liu, Y.; Smalley, R.E. *Chem. Phys. Lett.* **1987**, *138*, 119.

(96) Eller, K.; Schwarz, H. *Chem. Rev.* **1991**, *91*, 1121.

(97) Freiser, B.S. *Organometallic Ion Chemistry*. Kluwer, Dordrecht, 1996.

(98) Weisshaar, J.C. *Acc. Chem. Res.* **1993**, *26*, 213.

(99) Kabarle, P. *Ann. Rev. Phys. Chem.* **1977**, *28*, 445.

(100) a) Klassen, J.S.; Ho, Y.; Blades, A.T.; Kebarle, P. *Adv. Gas Phase. Ion Chem.* **1998**, *3*, 255. b) Peschke, M.; Blades, A.T.; Kebarle, P. *Adv. Met. Semicond. Clusters.* **2001**, *5*, 77.

(101) Kemper, P.R.; Bushnell, J.; Bowers, M.T.; Gellene, G.I. *J. Phys. Chem. A.* **1998**, *102*, 8590.

(102) a) Dalleska, N.F.; Tjelta, B.L.; Armentrout, P.B. *J. Phys. Chem.* **1994**, *98*, 4191. b) Armentrout, P.B.; Baer, T. *J. Phys. Chem.* **1996**, *100*, 12866. c) Rodgers, M.T.; Armentrout, P.B. *Mass Spectrom. Rev.* **2000**, *19*, 215. d) Anderson, A.; Muntean, F.; Derek, W.; Rue, C.; Armentrout, P.B. *J. Phys. Chem.* **2000**, *104*, 692.

(103) Shoeib, T.; Milburn, R.K.; Koyanagi, G.K.; Lavrov, V.V.; Bohme, D.K.; Siu, K.W.M.; Hopkinson, A.C. *Int. J. Mass Spectrom.* **2000**, *201*, 87.

(104) Rodriguez-Cruz, S.; Jockusch, R.A.; Williams, E.R. *J. Am. Chem. Soc.* **1986**, *121*, 1986.

(105) a) Dunbar, R.C.; Klippenstein, S.J.; Hrusak, J.; Stöckigt, D.; Schwarz, H. *J. Am. Chem. Soc.* **1996**, *118*, 5277. b) Petrie, S.; Dunbar, R.C. *J. Phys. Chem. A.* **2000**, *104*, 4480.

(106) Bauschlicher, C.W., Jr.; Sodupe, M.; Partridge, H. *J. Chem. Phys.* **1992**, *96*, 4453.

(107) Sodupe, M.; Bauschlicher, C.W., Jr.; Partridge, H. *Chem. Phys. Lett.* **1992**, *192*, 185.

(108) a) Partridge, H.; Bauschlicher, C.W., Jr.; Langhoff, S.R. *J. Phys. Chem.* **1992**, *96*, 5350. b) Bauschlicher, C.W., Jr.; Partridge, H. *Chem. Phys. Lett.* **1995**, *239*, 241. c) Heineman, C.; Koch, W.; Partridge, H. *Chem. Phys. Lett.* **1998**, *286*, 131.

(109) Partridge, H.; Bauschlicher, C.W., Jr. *Chem. Phys. Lett.* **1992**, *195*, 494.

(110) a) Sodupe, M.; Bauschlicher, C.W., Jr.; Langhoff, S.R. *J. Phys. Chem.* **1992**, *96*, 5350. b) Sodupe, M.; Bauschlicher, C.W., Jr. *J. Phys. Chem.* **1991**, *95*, 8640.

(111) a) Maitre, P.; Bauschlicher, C.W., Jr. *Chem. Phys.* **1994**, *225*, 467. b) Rodriguez,-Santiago, L.; Bauschlicher, C.W., Jr. *Spectrochim. Acta A.* **1999**, *55*, 457.

(112) Sodupe, M.; Branchadell, V.; Rosi, M.; Bauschlicher, C.W., Jr. *J. Phys. Chem. A.* **1997**, *101*, 7854.

(113) Kirschner, K.N.; Ma, B.; Bowen, J.P.; Duncan, M.A. *Chem. Phys. Lett.* **1998**, *295*, 204.

(114) Bauschlicher, C.W., Jr. *Chem. Phys. Lett.* **1993**, *201*, 11.

(115) Matsika, S.; Pitzaer, R.M. *J. Phys. Chem. A.* **1998**, *102*, 1652.

(116) a) Hoffman, B.C.; Schaefer, H.F. *Int. J. Mass Spectrom.* **1999**, *185-187*, 961 b) Weslowski, S.S.; King, R. A.; Schaefer, H.F.; Duncan, M.A. *J. Chem. Phys.* **2000**, *113*, 701.

(117) a) Watanabe, H.; Iwata, S.; Hashimoto, K.; Misaizu, F.; Fuke, K. *J. Am. Chem. Soc.* **1995**, *117*, 755. b) Watanabe, H.; Iwata, S. *J. Phys. Chem.* **1997**, *101*, 487. c) Watanabe,

H.; Iwata, S. *J. Chem. Phys.* **1998**, *108*, 10078. d) Fuke, K.; Hashimoto, K.; Iwata, S. *Adv. Chem. Phys.* **1999**, *110*, 431.

(118) Hrušák, J.; Stöckigt, D.; Schwarz, H. *Chem. Phys. Lett.* **1994**, *221*, 518.

(119) Dudev, T.; Cowan, J.A.; Lim, C. *J. Am. Chem. Soc.* **1999**, *121*, 7665.

(120) Markham, G.D.; Glusker, J.P.; Bock, C.W. *J. Phys. Chem. B.* **2002**, *106*, 5118.

(121) Petrie, S. *J. Phys. Chem.* **2002**, *106*, 7034.

(122) Stöckigt, D. *J. Phys. Chem.* **1997**, *101*, 3800.

(123) Bauschlicher, C.W., Jr.; Partridge, H.; Langhoff, S.R. *J. Phys. Chem.* **1992**, *96*, 3273.

(124) a) Yang, C.N.; Klippenstein, S.J. *J. Phys. Chem.* **1999**, *103*, 1094. b) Klippenstein, S.J.; Yang, C.N. *Int. J. Mass Spectrom.* **2000**, *201*, 253.

(125) Chaquin, P.; Costa, D.; Lepetit, C.; Che, M. *J. Phys. Chem. A.* **2001**, *105*, 4541.

(126) Pandey, R.; Rao, B.K.; Jena, P. Alvarez-Blanco, M. *J. Am. Chem. Soc.* **2001**, *123*, 3799.

(127) Foster, N.R.; Buchanan, J.W.; Flynn, N.D.; Duncan, M.A. *Chem. Phys. Lett.* **2001**, *341*, 476

(128) Foster, N.R.; Grieves, G.A.; Buchanan, J.W.; Flynn, N.D.; Duncan, M.A. *J. Phys. Chem.* **2000**, *104*, 11055.

(129) Buchanan, J.W.; Grieves, G.A.; Flynn, N.D.; Duncan, M.A. *Int. J. Mass Spectrom.* **1999**, *185-187*, 617.

(130) Buchanan, J.W.; Reddic, J.E.; Grieves, G.A.; Duncan, M.A. *J. Phys. Chem.* **1998**, *102*, 6390.

(131) Grieves, G.A.; Buchanan, J.W.; Reddic, J.E.; Duncan, M.A. *Int. J. Mass Spectrom.* **2001**, *204*, 223.

(132) Buchanan, J.W.; Grieves, G.A.; Reddic, J.E; Duncan, M.A. *Int. J. Mass Spectrom.* **1999**, *182*, 323.

(133) Reddic, J.E.; Robinson, J.C.; Duncan, M.A. *Chem. Phys. Lett.* **1997**, *279*, 203.

(134) a) Jacobson, D.B.; Freiser, B.S. *J. Am. Chem. Soc.* **1984**, *106*, 3900. b) Jacobson, D.B.; Freiser, B.S. *J. Am. Chem. Soc.* **1984**, *106*, 4623 c) Rufus, D.; Ranatunga, A.; Freiser, B.S. *Chem. Phys. Lett.* **1995**, *233*, 319.

(135) a) Willey, K.F.; Cheng, P.Y.; Bishop, M.B.; Duncan, M.A. *J. Am. Chem. Soc.* **1991**, *113*, 4721. b) Willey, K.F.; Yeh, C.S.; Robbins, D.L.; Duncan, M.A. *J. Phys. Chem.* **1992**, *96*, 9106.

(136) Jaeger, T.D.; Duncan, M.A. *J. Phys. Chem. A,* Submitted.

(137) Panov, S.I.; Williamson, J.M.; Miller, T.A. *J. Chem. Phys.* **1995**, *102*, 7359.

(138) Duncan, M.A.; Knight, A.M.; Negeshi, Y.; Nagoa, S.; Nakamura, Y.; Kato, A.; Nakajima, A.; Kaya, K. *J. Phys. Chem. A* **2001**, *105*, 10093.

(139) Willey, K.F.; Yeh, C.S.; Duncan, M.A. *Chem. Phys. Lett.* **1993**, *211,* 156.

(140) Panov, S.I.; Powers, D.E.; Miller, T.A. *J. Chem. Phys.* **1998**, *108,* 1335.

(141) Barckholtz, T.A.; Powers, D.E.; Miller, T.A.; Bursten, B.E. *J. Am. Chem. Soc.* **1999**, *121*, 2576.

(142) Yang, D.S.; Miyawaki, J. *Chem. Phys. Lett.* **1999**, *313*, 514.

(143) Agreiter, J.K.; Knight, A.M.; Duncan, M.A. *Chem. Phys. Lett,* **1999**, *313*, 162.

(144) a) Wang, K.; Rodham, D.A.; McKoy, V.; Blake, G.A. *J. Chem. Phys.* **1998**, *108*, 4817. b) Rodham, D.A.; Blake, G.A. *Chem. Phys. Lett.* **1997**, *264*, 522.

(145) Shen, M.H.; Winniczek, J.W.; Farrar, J.M. *J. Phys. Chem.* **1987,** *91*, 6447.

(146) Shen, M.H.; Farrar, J.M. *J Phys. Chem.* **1989**, *93*, 4386.

(147) Shen, M.H.; Farrar, J.M. *J. Chem. Phys.* **1991,** *94*, 3322.

(148) Donnelly, S.G.; Farrar, J.M. *J. Chem. Phys.* **1993**, *98*, 5450.

(149) Qian, J.; Midey, A.J.; Donnelly, S.G.; Lee, J.I.; Farrar, J.M. *Chem. Phys. Lett.* **1995**, *244*, 414.

(150) Willey, K.F.; Yeh, C.S; Robbins, D.L.; Pilgrim, J.S.; Duncan, M.A. *J. Chem. Phys.* **1992**, *97*, 8886.

(151) a) Yeh, C.S.; Willey, K.F.; Robbins, D.L.; Duncan, M.A. *J. Chem. Phys.* **1993**, *98*, 1867. b) Scurlock, C.T.; Pullins, S.H.; Duncan, M.A. *ibid.* **1996**, *105*, 3579.

(152) a) Pilgrim, J.S.; Yeh, C.S.; Berry, K.R.; Duncan, M.A. *J. Chem. Phys.* **1994**, *100*, 7945; erratum: **1996**, *105*, 7876. b) Sucrlock, C.T.; Pilgrim, J.S.; Duncan, M.A. *J. Chem. Phys.* **1995**, *103*, 3293.

(153) a) Robbins, D.L.; Brock, L.R.; Pilgrim, J.S.; Duncan, M.A. *J. Chem. Phys.* **1995**, *102*, 1481. b) Pullins, S.H.; Reddic, J.E.; France, M.R.; Duncan, M.A. *J. Chem. Phys.* **1998**, *108*, 2725.

(154) Scurlock, C.T.; Pullins, S.H.; Reddic, J.E.; Duncan, M.A. *J. Chem. Phys.* **1996**, *104*, 4591.

(155) Pullins, S.H.; Scurlock, C.T.; Reddic, J.E.; Duncan, M.A. *J. Chem. Phys.* **1996**, *104*, 7518.

(156) Duncan, M.A. *Annu. Rev. Phys. Chem.* **1997**, *48*, 63.

(157) a) France, M.R.; Pullins, S.H.; Duncan, M.A. *J. Chem. Phys.* **1998**, *109*, 8842. b) Reddic, J.E.; Duncan, M.A. *Chem. Phys. Lett.* **1999**, *312*, 96.

(158) a) Reddic, J.E.; Duncan, M.A. *J. Chem. Phys.* **1999**, *110*, 9948. b) Reddic, J.E.; Duncan, M.A. *J. Chem. Phys.* **2000**, *112*, 4974.

(159) France, M.R.; Pullins, S.H.; Duncan, M.A. *Chem. Phys.* **1998**, *239*, 447.

(160) Duncan, M.A. *Int. J. Mass. Spectrom.* **2000**, *200*, 545.

(161) Velasquez, J.; Kirschner, K.N.; Reddic, J.E.; Duncan, M.A. *Chem. Phys. Lett.* **2001**, *343*, 613.

(162) Misaizu, F.; Sanekata, M.; Tsukamoto, K.; Fuke, K.; Iwata, S. *J. Phys. Chem.* **1992**, *96*, 8259.

(163) Sanekata, M.; Misaizu, F.; Fuke, K.; Iwata, S.; Hashimoto, K.; *J. Am. Chem. Soc.* **1995**, *117*, 747.

(164) Sanekata, M.; Misaizu, F.; Fuke, K. *J. Chem. Phys.* **1996**, *104*, 9768.

(165) Fuke, K.; Hashimoto, K.; Takasu, R. *Adv. Met. Semicond. Clusters* **2001**, *5*, 1.

(166) Yoshida, S.; Okai, N.; Fuke, K. *Chem. Phys. Lett.* **2001**, *347*, 93.

(167) Cheng, Y.C.; Chen, J.; Ding, L.N.; Wong, T.H.; Kleiber, P.D.; Liu, D.-K. *J. Chem. Phys.* **1996**, *104*, 6452.

(168) Chen, J.; Cheng, Y.C.; Kleiber, P.D. *J. Chem. Phys.* **1997**, *106*, 3884.

(169) Chen, J.; Wong, T.H.; Kleiber, P.D. *Chem. Phys. Lett.* **1997**, *279*, 185.

(170) Kleiber, P.D.; Chen, J. *Int. Rev. Phys. Chem.* **1998**, *17*, 1.

(171) Chen, J.; Wong, T.H.; Cheng, Y.C.; Montgomery, K.; Kleiber, P.D. *J. Chem. Phys.* **1998**, *108*, 2285.

(172) Chen, J.; Wong, T.H.; Kleiber, P.D.; Wang, K.H. *J. Chem. Phys.* **1999**, *110*, 11798.

(173) Luder, C.; Velegrakis, M. *J. Chem. Phys.* **1996**, *105*, 2167.

(174) Luder, C.; Prekas, D.; Vourliotaki, A.; Velegrakis, M. *Chem. Phys. Lett.* **1997**, *267*, 149.

(175) Fanourgakis, G.S.; Farantos, S.C.; Luder, C.; Velegrakis, M.; Xantheas, S.S. *J. Chem. Phys.* **1998**, *109*, 108.

(176) Prekas, D.; Feng, B.H.; Velegrakis, M.; *J. Chem. Phys.* **1998**, *108*, 2712.

(177) Xantheas, S.; Fanourgakis, G.S.; Farantos, S.C.; Velagrakis, M. **1998**, *108*, 46.

(178) Yang, X.; Hu, Y.; Yang, S. *J. Phys. Chem. A* **2000**, *104*, 8496.

(179) Liu, H.;Guo, W.; Yang, S. *J. Chem. Phys.* **2001**, *115*, 4612.

(180) Guo, W.; Liu, H.; Yang, S. *J. Chem. Phys.* **2002**, *116*, 9690.

(181) Guo, W.; Liu, H.; Yang, S. *J. Chem. Phys.* **2002**, *116*, 2896.

(182) Lie, J.; Dagdigian, P.J. *Chem. Phys. Lett.* **1999**, *304*, 317.

(183) Asher, R.L.; Bellert, D.; Buthelezi, T.; Lessen, D.; Brucat, P.J. *Chem. Phys. Lett.* **1995**, *234*, 119.

(184) Buthelezi, T.; Bellert, D.; Lewis, V.; Brucat, P.J. *Chem. Phys. Lett.* **1995**, *246*, 145.

(185) Buthelezi, T.; Bellert, D.; Lewis, V.; Brucat, P.J. *Chem. Phys. Lett.* **1995**, *242*, 627.

(186) Bellert, D.; Buthelezi, T.; Lewis, V.; Dezfulian, K.; Brucat, P.J. *Chem. Phys. Lett.* **1995**, *240*, 495.

(187) Asher, R.L.; Bellert, D.; Buthelezi, T.; Brucat, P.J. *J. Phys. Chem.* **1995**, *99*, 1068.

(188) Bellert, D.; Buthelezi, Dezfulian, K.; T.; Hayes, T.; Brucat, P.J. *Chem. Phys. Lett.* **1996**, *260*, 458.

(189) Bellert, D.; Buthelezi, T.; Hayes, T.; Brucat, P.J. *Chem. Phys. Lett.* **1997**, *277*, 27.

(190) Hayes, T.; Bellert, D.; Buthelezi, T.; Brucat, P.J. *Chem. Phys. Lett.* **1997**, *264*,220.

(191) Hayes, T.; Bellert, D.; Buthelezi, T.; Brucat, P.J. *Chem. Phys. Lett.* **1998**, *287*, 22.

(192) Bellert, D.; Buthelezi, T.; Brucat, P.J. *Chem. Phys. Lett.* **1998**, *290*, 316.

(193) Husband, J.; Aguirre, F.; Thompson, C.J.; Laperle, C.M.; Metz, R.B. *J. Phys. Chem. A* **2000**, *104*, 2020.

(194) Thompson, C.J.; Husband, J.; Aguirre, F.; Metz, R.B. *J. Phys. Chem. A* **2000**, *104*, 8155.

(195) Thompson, C.J.; Aguirre, F.; Husband, J.; Metz, R.B. *J. Phys. Chem. A* **2000**, *104*, 9901.

(196) Faherty, K.P.; Thompson, C.J.; Aguirre, F.; Michen, J.; Metz, R.B. *J. Phys. Chem. A* **2001**, *105*, 10054.

(197) Stace, A.J. *Adv. Met. Semicond. Clusters* **2001**, *5*, 121.

(198) Posey, L.A. *Adv. Met. Semicond. Clusters* **2001**, *5*, 145

(199) Lisy, J.M. *Cluster Ions,* Ng. C; Baer, T.; Powis, I. (Eds.) Wiley, Chichester, 1993.

(200) Weinheimer, C.J.; Lisy, J.M. *Int. J. Mass Spectrom Ion Process* **1996**, *159*, 197.

(201) Weinheimer, C.J.; Lisy, J.M. *J. Phys. Chem.* **1996**, *100*, 15303.

(202) Weinheimer, C.J.; Lisy, J.M. *J. Chem. Phys.* **1996**, *105*, 2938.

(203) Lisy, J.M. *Int. Rev. Phys. Chem.* **1997**, *16*, 267.

(204) a) Cabarcos, O.M.; Weinheimer, C.J.; Lisy, J.M. *J. Chem. Phys.* **1998**, *108*, 5151. b) Cabarcos; O.M.; Weinheimer, C.J.; Lisy, J.M., *J. Chem. Phys.* **1999**, *110*, 8429.

(205) Vaden, T.D.; Forinash, B.; Lisy, J.M. *J. Chem. Phys.* **2002** *117*, 4628.

(206) Gregoire, G.; Velasquez, J.; Duncan, M.A. *Chem. Phys. Lett.* **2001**, *349*, 451.

(207) Gregoire, G.; Duncan, M.A. *J. Chem. Phys.* **2002**, *117*, 2120.

(208) Walters, R.S.; Jaeger, T.D.; Duncan, M.A. *J. Phys. Chem. A* **2002**, *106*, 10482.

(209) van Heijnsbergen, D.; von Helden, G.; Meijer, G.; Maitre, P.; Duncan, M.A. *J. Am. Chem. Soc.* **2002**, *124*, 1562.

(210) van Heijnsbergen, D.; Jaeger, T.D.; von Helden, G.; Meijer, G.; Duncan, M.A. *Chem. Phys. Lett.* **2002**, *364*, 345.

(211) Gergoire, G.; Brinkmann, N.R.; van Heijnsbergen, D.; Schaefer, H.F.; Duncan, M.A. *J. Phys. Chem. A* **2003**, *107*, 218.

(212) Walters, R.S.; Brinkman, N.R.; Schaefer, H.F.; Duncan, M.A. *J. Phys. Chem. A* **2003**, *107*, 7396.

(213) Duncan, M.A. *Int. Rev. Phys. Chem.* **2003**, *22*, 407.

(214) Walker, N.R.; Walters, R.S.; Pillai, E.D.; Duncan, M.A. *J. Chem. Phys.* **2003**, *119*, 10471.

(215) Walker, N.R.; Greives, G.A.; Walters, R.S.; Duncan, M.A. *Chem. Phys. Lett.* **2003**, *380*, 230.

(216) Walker, N.R.; Walters, R.S.; Duncan, M.A. *J. Chem. Phys.* **2004**, *120*, 10037.

(217) Jaeger, T.D.; Fielicke, A.; von Helden, G.; Meijer, G.; Duncan, M.A. *Chem. Phys. Lett.* **2004**, *392*, 409.

(218) Jaeger, T.D.; Pillai, E.D.; Duncan, M.A. *J. Phys. Chem. A* **2004**, *108*, 6605.

(219) Jaeger, T.D.; van Heijnsbergen, D.; Klippenstein, S.J.; von Helden, G.; Meijer, G.; Duncan, M.A. *J. Am. Chem. Soc.* **2004**, *126*, 10981.

(220) Lemaire, J.; Boissel, P.; Heninger, M.; Mauclaire, G.; Bellec, G.; Mestdagh, H.; Simon, A.; Le Caer, S.; Ortega, J.M.; Glotin, F.; Maitre, P *Phys. Rev. Lett.* **2002**, *89*, 273002/1.

(221) Lemaire, J.; Boissel, P.; Heninger, M.; Mestdagh, H.; Mauclaire, G.; Le Caer, S.; Ortega, J.M.; Maitre, P. *Spectra Anal.* **2003**, *32*, 28.

(222) Le Caer, S.; Heninger, M.; Lemaire, J.; Boissel, P.; Maitre, P.; Mestdagh, H. *Chem. Phys. Lett.* **2004**, *385*, 273.

(223) Simon, A.; Jones, W.; Ortega, J.M.; Boissel, P.; Lemaire, J.; Maitre, P. *J. Am. Chem. Soc.* **2004**, *126*, 11666.

(224) Fielicke, A.; Meijer, G.; von Helden, G. *J. Am. Chem. Soc.* **2003**, *125*, 3659.

(225) Fielicke, A.; Meijer, G.; von Helden, G. *Eur. Phys. J. D.* **2003**, *24*, 69.

(226) Fielicke, A.; Meijer, G.; von Helden, G.; Simard, B.; Denommee, S.; Rayner, D. *J. Am. Chem. Soc.* **2003**, *125*, 11184.

(227) Fielicke, A.; Mitric, R.; Meijer, G.; Bonacic-Koutecky, V.; von Helden, G. *J. Am. Chem. Soc.* **2003**, *125*, 15716.

(228) Fielicke, A.; von Helden, G. ; Meijer, G. *J. Phys. Chem. B* **2004**, *108*, 14591.

(229) Fielicke, A.; Kirilyuk, A.; Ratsch, C.; Behler, J.; Scheffler, M.; von Helden, G. ; Meijer, G. *Phys. Rev. Lett.* **2004**, *93*, 023401/1.

(230) Oomens, J.; Moore, D.T.; von Helden, G. ; Meijer, G.; Dunbar, R.C. *J. Am. Chem. Soc.* **2004**, *126*, 724.

(231) Yang, D.S.; Hackett, P.A. *J. Electron Spetrosc.* **2000**, *106*, 153.

(232) Rothschopf, G.K.; Perkins, J.S.; Li, S.; Yang, D.S. *J. Phys. Chem. A* **2000**, *104*, 8178.

(233) Rothschopf, G.K.; Li, S.; Perkins, J.S.; Yang, D.S. *J. Chem. Phys.* **2001**, *115*, 4565.

(234) Li, S.; Rothschopf, G.K.; Pillai, E.D.; Sohnlein, B.R.; Wilson, B.M.; Yang, D.S. *J. Chem. Phys.* **2001**, *115*, 7968.

(235) Pederson, D.B.; Zgierski, M.Z.; Anderson, S.; Rayner, D.M.; Simard, B.; Li, S.; Yang, D.S. *J. Phys. Chem. A* **2001**, *105*, 11462.

(236) Li, S.; Rothschopf, G.K.; Yang, D.S. *J. Chem. Phys.* **2002**, *116*, 6589.

(237) Rothschopf, G.K.; Li, S.; Yang, D.S. *J. Chem. Phys.* **2002**, *117*, 8800.

(238) Li, S.; Rothschopf, G.K.; Fuller, J.F.; Yang, D.S. *J. Chem. Phys.* **2003**, *118*, 8636.

(239) Miyawaki, J.; Yang, D.S.; Sugawar, K.I. *Chem. Phys. Lett.* **2003**, *372*, 627.

(240) Li, S.; Sohnlein, B.R.; Rothschopf, G.K.; Fuller, J.F.; Yang, D.S. *J. Chem. Phys.* **2003**, *119*, 5406.

(241) Li, S.; Fuller, J.F.; Sohnlein, B.R.; Yang, D.S. *J. Chem. Phys.* **2003**, *119*, 8882.

(242) Wang, X.; Yang, D.S. *J. Phys. Chem. A* **2004**, *108*, 6449.

(243) Harms, A.C.; Khanna, S.N.; Chem, B.; Castleman, A.W., Jr. *J. Chem. Phys.* **1994**, *100*, 3540.

(244) Watanabe, H.; Iwata, S. *J. Phys. Chem.* **1996**, *100*, 3377.

(245) a) Beyer, M.; Berg, C.; Görlitzer, H.W.; Schindler, T.; Achatz, U.; Albert, G.; Niedner-Schatteburg, G.; Bondybey, V.E. *J. Am. Chem. Soc.* **1996**, *118,* 7386. b) Beyer, M.; Achatz, U.; Berg, C.; Joos, S.; Niedner-Schatteburg, G.; Bondybey, V.E. *J. Phys. Chem. A* **1999**, *103*, 671. c) Bondybey, V.E.; Beyer, M.K. *Int. Rev. Phys. Chem.* **2002**, *21*, 277. d) Fox, B.S.; Balteanu, I.; Balaj, O.P.; Liu, H.; Beyer, M.K; Bondybey, V.E. *Phys. Chem. Chem. Phys.* **2002**, *4*, 2224. e) Berg C.; Achatz, U.; Beyer, M.; Joos, S.; Albert, G.; Schindler, T.; Niedner-Schattburg, G.; Bondybey, V.E. *Int. J. Mass Spectrom.* **1997**, *167-168*, 723. f) Berg, C.; Beyer, M.; Achatz, U.; Joos, S.; Niedner-Schattburg, G.; Bondybey, V.E. *Chem. Phys.* **1998**, *239*, 379.

(246) Lu, W.; Yang, S. *J. Phys. Chem.* **1998**, *102*, 825.

(247) a) Reinhard, B.M.; Niedner-Schattburg, G. *J. Phys. Chem. A* **2002**, *106*, 7988. b) Reinhard, B.M.; Niedner-Schattburg, G. *Phys. Chem. Chem. Phys.* **2002**, *4*, 1471.

(248) Thorne, L.R.; Beauchamp, J.L. *Gas Phase Ion Chemistry,* **1984**, *3*, 41.

(249) Knickelbein, M.B. *Chem. Phys. Lett.* **1995**, *239*, 11.

(250) Knickelbein, M.B. *J. Chem. Phys.* **1996**, *104*, 3217.

(251) Koretsky, G.M.; Knickelbein, M.B. *Chem. Phys. Lett.* **1997**, *267*, 485.

(252) a) Okumura, M.; Yeh, L.I.; Lee, Y.T. *J. Chem. Phys.* **1985**, *83*, 3705. b) Okumura, M.; Yeh, L.I.; Lee, Y.T. *J. Chem. Phys.* **1988**, *88*, 79. c) Yeh, L.I.;Okumura, M.; Meyers, J.D.; Price, J.M.; Lee, Y.T. *J. Chem. Phys.* **1989**, *91*, 7319. d) Yeh, L.I.; Lee, Y.T.;

Hougen, J.T. *J. Mol. Spectrosc.* **1994**, *164*, 473 e) Crofteon, M.W.; Price, J.M.; Lee, Y.T. *Springer Ser. Chem. Phys.* **1994**, *56*, 44. f) Boo, D.W.; Liu, Z.F.; Suits, A.G.; Tse, J.S.; Lee, Y.T. *Science* **1995**, *269*, 57. g) Wu, C.C.; Jiang, J.C.; Boo, D.W.; Lin, s.H.; Lee, Y.T. Chang, H.C.; *J. Chem. Phys.* **2000**, *112*, 176. h) Wu, C.C.; Jian, J.C.; Hahndorf, I.; Choudhuri, C.; Lee, Y.T.; Chang, H.C. *J. Phys.Chem. A* **2000**, *104*, 9556.

(253) a) Linnartz, H.; Speck, T.; Maier, J.P. *Chem. Phys. Lett.* **1998**, *288*, 504 b) Dopfer, O; Nizkorodov, S.A.; Meuwly, M.; Bieske, E.J.; Maier, J.P. *Chem. Phys. Lett.* **1996**, *260*, 545. c) Ruchti, T.; Speck, T.; Connelly, J.P.; Bieskes, E.J.; Linnartz, H.; Maier, J.P. *J. Chem. Phys.* **1995**, *105*, 2592. d)Meuwly, M.; Nizkorodov, S.A.; Maier, J.P.; Bieske, E.J. *J. Chem. Phys.* **1996**, *104,* 3876. e) Bieske, E.J.; Dopfer, O. *Chem. Rev.* **2000**, *100*, 3963. f) Roth, D.; Dopfer, O.; Maier, J.P. *Phys. Chem. Chem. Phys,* **2000**, *2*, 5013. g) Dopfer, O.; Roth, D.; Maier, J.P. *J. Phys. Chem. A* **2000**, *104*, 11702. h) Dopfer, O.; Roth, D.; Maier, J.P. *J. Chem. Phys.* **2001**, *114*, 7081. i) Verdes, D.; Linnartz, H.; Maier, J.P. *Physics and Chemistry of Clusters, Proceedings of the 117th NObel Symposium ,* Edited by E.E.B. Campbell and M.Larsson. World Scientific Publishing, Singapore, **2000** j) Dopfer, O.; Roth, D.; Maier, J.P. *J. Am. Chem. Soc.* **2002**, *124*, 494 . k) Dopfer, Roth, D.;O.; Maier, J.P *Int. J. Mass. Spectrom.* **2002**, *218*, 281. l) Linnartz, H.; Verdes, D.; Maier, J.P. *Science*, **2002**, *297*, 1166. m) Olkhov, R.V.; Nizkorodov, S.A>; Dopfer, O. *Chem. Phys.* **1998**, *239*, 393.

(254) a) Ayotte, P.; Bailey, C.G.; Johnson, M.A. *J. Phys. Chem.* **1998**, *102*, 3067. b) Bailey, C.G.; Kim, J.; Dessent, C.E.H.; Johnson, M.A. *Chem. Phys. Lett.* **1997**, *269*, 122. c) Bailey, C.G.; Kim, J.; Johnson, M.A. *J. Phys. Chem.* **1996**, *100*, 16782.

(255) Choi, J.H.; Kuwata, K.T.; Haas, B.M.; Cao, Y.B.; Johnson, M.A.; Okumura, M. *J. Chem. Phys.* **1994**, *100*, 7153.

(256) a) Sawamura, T.; Fujii, A.; Sato, S.; Ebata, T.; Mikami, N. *J. Phys. Chem.* **1996**, *100*, 8131. b) Ebata, T.; Fujii, A.; Mikami, N. *Int. Rev. Phys. Chem.* **1998**, *17*, 331.

(257) Huisken, F.; Kaloudis, M.; Kulckes, A. *J. Chem. Phys.* **1996**, *104*, 17.

(258) a) Buck, U.; Ettischer, I.; Melzer, M.; Buch, V.; Sadlej, J. *Phys. Rev. Lett.* **1998**, *80*, 2578. b) Buck, U.; Huisken, F. *Chem. Rev.* **2000**, *100*, 3863.

(259) a) Carney, J.R.; Hagemeister, F.C.; Zweir, T.S. *J. Chem. Phys.* **1998**, *108*, 3379. b) Gruenloh, C.J.; Carney, J.R.; Arrington, C.A.; Zweir, T.S.; Frederick, S.Y.; Jordan, K.D. *Science* **1997**, *276*,1678. c) Zwier, T.S. *Annu. Rev. Phys. Chem.* **1996**, *47*, 205. d) Frost, R.K.; Hagemeister, F.C.; Arrington, C.A.; Schleppenbach, D.; Zweir, T.S.; Jordan, K.D. *J. Chem. Phys.* **1996**, *105*, 2605. e) Pribble, R.N.; Garrett, A.W.; Haber, K.; Zweir, T.S. *J. Chem. Phys.* **1995**, *103*, 531. f) Pribble, R.N.; Zweir, T.S. *Science,* **1994**, *265*, 75.

(260) Shimanouchi, T. Molecular Vibrational Frequencies. *NIST Chemistry, Webbook*, NIST Standard Reference, Database no. 69, edited by P.J. Linstrom and W.G. Mallard. National Institute of Standards and Technology, Gathersburg, MD, 2001.

(261) Bloembergen, N.; Cantrell, C.D.; Larssen, D.M. *SPringer Ser. Opt. Sci.* **1976**, *3*, 162.

(262) Letokhov, V.S.; *Multiphoton Processes,* Proceedings of International Conference, **1978**, 331.

(263) Marcus, R.A.; Noid, D.W.; Koszykowski, M.L. *Springer Ser. Chem. Phys.* **1978**, *3*, 298.

(264) Kung, A.H.; Dai, H.L.; Berman, M.R.; Moore, C.B. *Springer Ser. Opt. Sci.* **1979**, *21*, 309.

(265) King, D.S. *Adv. Chem. Phys.* **1982**, *50*, 105.

(266) Oepts, D.; van der Meer, A.F.G.; van Amersfoort, P.W. *Infrared. Phys. Technol.* **1995**, *36*, 297.

(267) a)von Helden, G.; Holleman, I; Meijer, G.; Sartakov, B. *Opt. Express* **1999**, *4*, 46. b) von Helden, G.; Holleman, I.; Knippels, G.M.H.; van der Meer, A.F.G.; Meijer, G. *Phys. Rev. Lett.* **1997**, *79*, 5234.

(268) van Heijnsbergen, D.; von Helden, G.; Meijer, G. *J. Phys. Chem. A* **2003**, *107*, 1671.

(269) a) Knickelbein, M.B.; Menezes, W.J.C. *Phys. Rev. Lett.* **1992**, *69*, 1046. b) Menezes, W.J.C.; Knickelbein, M.B. *J. Chem. Phys.* **1993**, *98*, 1856. c) Knickelbein, M.B. *J. Chem. Phys.* **1993**, *99*, 2377.

(270) Pino, T.; Boudin, N.; Brechignac, P. *J. Chem. Phys.* **1999**, *111*, 7337.

(271) Caldwell, J.W.; Kollman, P.A. *J. Am. Chem. Soc.* **1995**, *117*, 4177.

(272) Muetterties, E.L.; Bleeke, J.R.; Wucherer, E.J.; Albright, T.A. *Chem. Rev.* **1982**, *82*, 499.

(273) Long, N.J. *Metallocenes,* Blackwell Sciences, Oxford, U.K., 1998.

(274) Kealy, T.J.; Paulson, P.L. *Nature*, **1951**, *168*, 1039.

(275) Fischer, E.O.; Hafner, W. *Z. Naturforsch.* **1955**, *10B*, 665.

(276) a) Chen, Y.M.; Armentrout, P.B., *Chem. Phys. Lett.* **1993**, *210*, 123. b) Meyer, F.; Khan, F.A.; Armentrout, P.B., *J. Am. Chem. Soc.* **1995**, *117*, 9740. c) Armentrout, P.B.; Hales, D.A.; Lian, L., *Adv. Metal Semicon. Clusters* (M.A. Duncan, editor) **1994**, *2*, 1 (JAI Press, Greenwich, CT).

(277) Ho, Y.P.; Yang, Y.C.; Klippenstein, S.J.; Dunbar, R.C., *J. Phys. Chem. A* **1997**, *101*, 3338.

(278) a) Hoshino, K.; Kurikawa, T.; Takeda, H.; Nakajima, A.; Kaya, K., *J. Phys. Chem.* **1995**, *99*, 3053. b) Judai, K.; Hirano, M.; Kawamata, H.; Yabushita, S.; Nakajima, A.; Kaya,

K., *Chem. Phys. Lett.* **1997**, *270*, 23. c) Yasuike, T.; Nakajima, A.; Yabushito, S.; Kaya, K., *J. Phys. Chem. A* **1997**, *101*, 5360. d) Kurikawa, T.; Takeda, H.; Hirano, M.; Judai, K.; Arita, T.; Nagoa, S.; Nakajima, A.; Kaya, K., *Organometallics* **1999**, *18*, 1430. e) Nakajima, A.; Kaya, K., *J. Phys. Chem. A*, **2000**, *104*, 176. f) Miyajima, K; Nakajima, A; Yabushita, S; Knickelbein, M.B.; Kaya, K. *J. Am Chem. Soc.* **2004**, *126*, 13202.

(279) Weis, P.; Kemper, P.R.; Bowers, M.T., *J. Phys. Chem. A* **1997**, *101*, 8207.

(280) a) Sodupe, M.; Bauschlicher, C.W., *J. Phys. Chem.* **1991**, *95*, 8640. b) Sodupe, M.; Bauschlicher, C.W.; Langhoff, S.R.; Partridge, H., *J. Phys. Chem.* **1992**, *96*, 2118. c) Sodupe, M.; Bauschlicher, *Chem. Phys.* **1994**, *185*, 163.

(281) Li, Y.; Baer, T. *J. Phys. Chem. A* **2002**, *106*, 9820.

(282) Kaczorwska, M.; Harvey, J.M. *Phys. Chem. Chem. Phys.* **2002**, *4*, 5227.

(283) Gerhards, M.; Thomas, O.C.; Nilles, J.M.; Zheng, W.-J.; Bowen, K.H., Jr. *J. Chem. Phys.* **2002**, *116*, 10247.

(284) Judai, K; Sera, K.; Amatsutsumi, S.; Yagi, K.; Yasuike, T.; Nakajima, A.; Kaya, K., *Chem. Phys. Lett.* **2001**, *334*, 277.

CHAPTER 2

EXPERIMENTAL

The experimental data in this work was obtained on two similar but different machines, one located here at the University of Georgia Department of Chemistry (referred to as the "Georgia system") and one at the F.O.M. Plasma Physics Institute in the Netherlands (referred to as the "Dutch system"). Both systems are designed to employ laser ablation of a metal target in a pulsed nozzle cluster source to produce metal ion-ligand systems for photofragmentation studies. The lasers used and mass analysis techniques for each system differ and therefore will be described separately.

The Georgia System

A schematic of the Georgia system is shown in Figure 2.1.[1-31] The system consists of a laser ablation pulsed nozzle cluster source coupled to a reflectron time-of-flight mass spectrometer. In this setup the second (532 nm) or third (355 nm) harmonic of an Nd:YAG laser is focused onto a metal rod which is both rotating and translating to ensure a new ablation surface for subsequent laser shots. This forms a plasma which is then entrained in a gas pulse provide by a General Valve Series 9 nozzle with a 1mm orifice. The nozzle is typically operated with a backing pressure between 40-80 psig and a pulse duration of 180-410 μsec. Typical laser

Figure 2.1 Georgia Molecular Beam Machine with Reflectron Time-of-Flight Mass Spectrometer

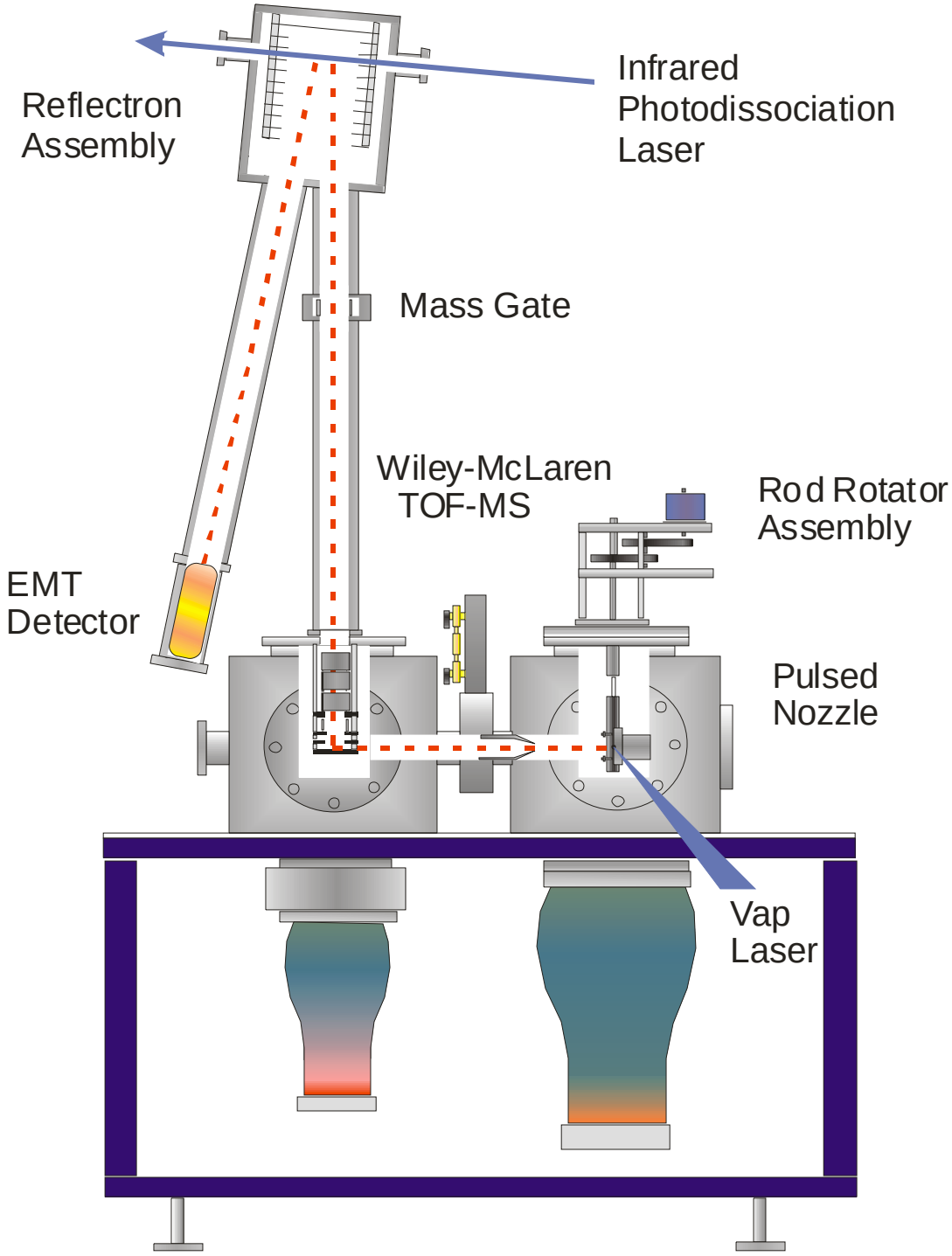
Reflectron
Assembly
Infrared
Photodissociation
Laser
Mass Gate
Wiley-McLaren
TOF-MS
Rod Rotator
Assembly
EMT
Detector
Pulsed
Nozzle
Vap
Laser

pulse energies are attenuated to 1-20 mJ per laser shot. Pressures are kept on the range of 10^{-4} to 10^{-6} torr during operation by a Varian VHS-10 diffusion pump capable of moving ~5300 L of helium per second. Because different metal targets, expansion gases, and ligands can be used, the variety of species that can be produced is virtually limitless. Additionally, although the plasma created is neutral, it contains neutral, cationic and anionic species.

The form of the rod holder influences the cluster distribution produced in such a source. In order to produce clusters of pure metal, for example, many three-body collisions are necessary for cluster growth due to atom recombination. For experiments such as these the laser induced plasma and subsequent expansion would flow through a growth channel where many collisions could occur. Clusters formed in this way tend to be strongly bound complexes with higher internal energy due to bond formation and inefficient cooling from a hindered expansion. This work concentrates on single metal atoms with multiple ligands. These systems are much more weakly bound and hence require a source with greater cooling and an unhindered expansion. Such conditions can be satisfied with a "cutaway" type source as shown in Figure 2.2. The rod holder in these experiments is cut in half down the laser input axis leaving half of the rod exposed to the vacuum. This limits metal atom recombination and clusters primarily of a single metal atom with multiple ligands are created. The ligands are introduced either as the carrier gas (i.e. Ar or CO_2) or seeded into it (i.e. a few drops of C_6H_6 in Ar). Ar has been the preferred carrier gas for these experiments. It is efficient at cooling and quenching the plasma allowing for cluster distributions with multiple ligands to be formed rather easily.

As mentioned earlier, this laser ablation cluster source is coupled to a reflectron time-of-flight (RTOF) mass spectrometer for mass analysis. The RTOF is contained in a separate

Figure 2.2 Pulsed Molecular Beam Valve with Cutaway Style Laser Ablation Source

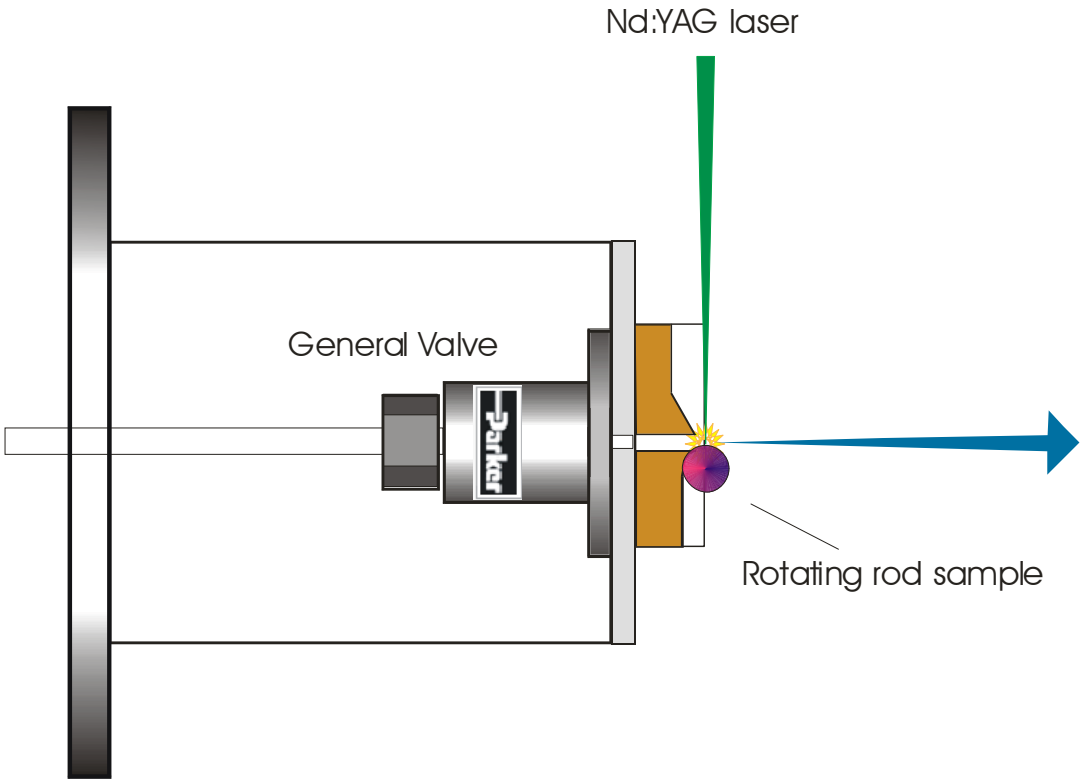
Nd:YAG laser
General Valve
Parker
Rotating rod sample

differentially pumped chamber (Varian VHS-6, 10^{-6}-10^{-8} torr, 2400 L/sec). A schematic of this section of the instrument is shown in Figure 2.3. The molecular beam created in the above mentioned cluster source enters this region via a conical skimmer with a 3 mm aperture (Beam Dynamics, Inc.). This skimmer collimates the molecular beam by significantly deflecting molecules with velocities off the beam axis. This collimated beam now enters the extraction region of the two stage Wiley-McLaren type time-of-flight mass spectrometer.[32] Because these experiments are concerned with cold cation clusters created directly in the source, the ions must be pulse extracted. The repeller plate and draw out grid are kept at ground until the ions contained in the beam pass between them. Once they are in position the plates are rapidly pulsed to 1000 V for the repeller and 900 V for the draw out grid using fast response high voltage pulsers (Behlke Corporation HTS-50, 50 nsec rise time). This accelerates the ions down the first flight tube and towards the reflectron.

As shown in Figure 2.3, a deflection plate and an einzel lens are located just after the repeller, draw out grid, and ground plate. Because the ions are extracted perpendicular to the molecular beam, the deflection plate must be used to help compensate for downstream beam velocity imparted by the carrier gas. An adjustable DC voltage (10 to 100 V) is applied to this plate for this purpose. In order to better focus the ion beam an einzel lens is utilized. This consists of three rings where the two outside rings are held at ground and the central ring has an adjustable DC voltage (0 to 500 V). By optimizing this voltage, the ion packet can be better focused on the detector. Once the ions have passed these focusing elements they enter the field free region of the first flight tube.

A time-of-flight machine mass analyzes ions based on this relationship:

Figure 2.3 Georgia System Reflectron Time-of-Flight Mass Spectrometer

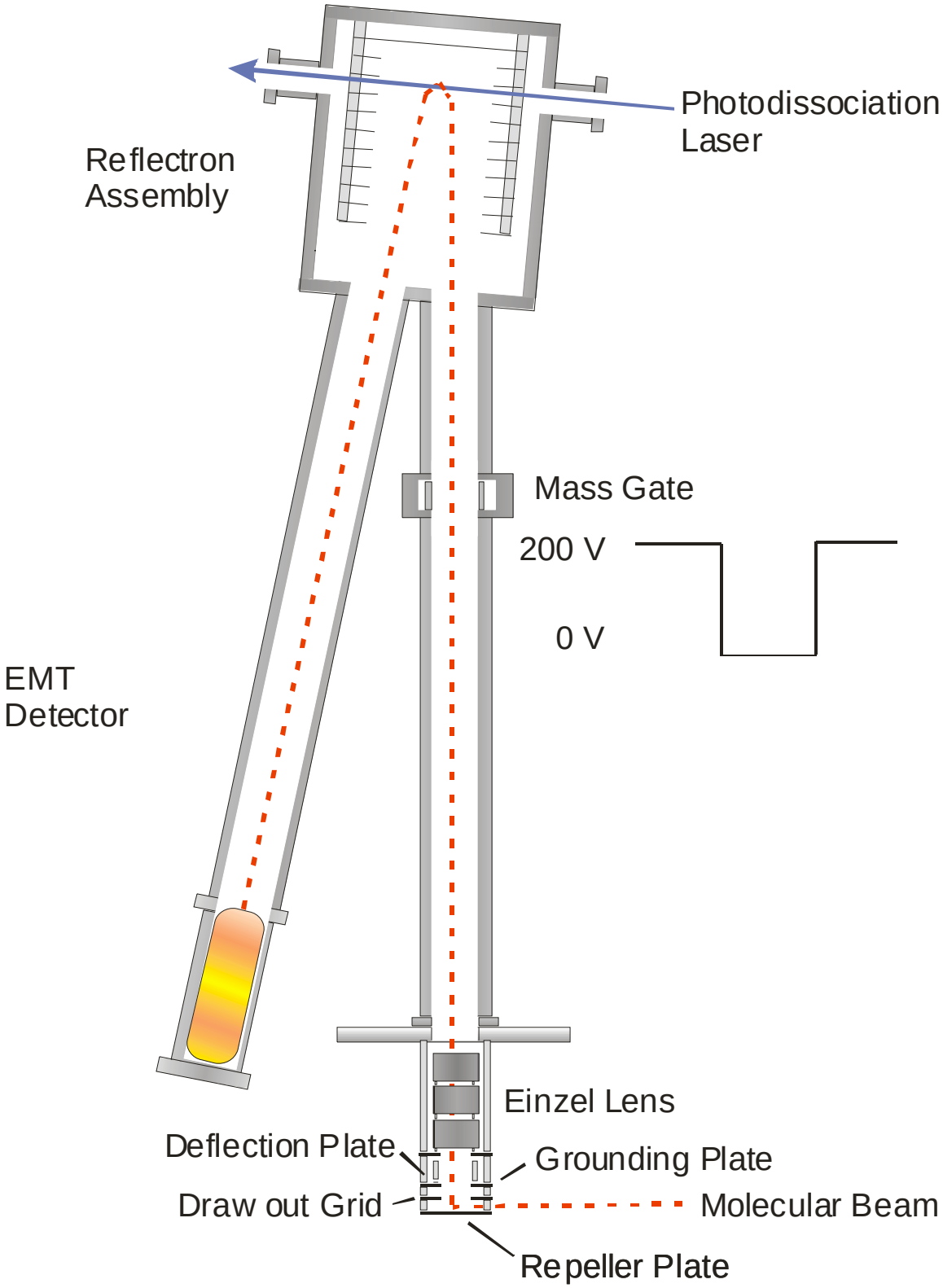
Photodissociation
Laser
Reflectron
Assembly
Mass Gate
200 V
0 V
EMT
Detector
Einzel Lens
Deflection Plate
Grounding Plate
Draw out Grid
Molecular Beam
Repeller Plate

$$\text{Kinetic Energy} = 1/2*\text{Mass}*\text{Velocity}^2$$

where the kinetic energy comes from the acceleration voltages applied to the repeller and draw out grid. Because all ions see the same field here, their kinetic energy is the same, but because their masses are different their velocities must also be different. For instance a heavy ion would move slower down the flight tube than a lighter ion, causing the two ions to become spatially separated. Logically a longer flight tube would lead to better mass separation. This tube is approximately one and a half meters in length, which allows for significant ion separation before entering the reflectron region. This fact is essential for mass selection in this experiment and will be discussed in more detail later.

After traversing the first flight tube, the ions enter the reflectron region of the machine. The reflectron consists of eleven 2" by 4" steel plates with rectangular holes stacked and spaced by approximately 1.5 cm. The two front plates are wired separately and are usually kept at ground for these experiments. 200 kΩ resistors between each plate connect the remaining plates. When a voltage is applied to the back plate a voltage gradient is established along the length of the reflectron stack. Ions enter the reflectron and are slowed down gradually by this field. At the turning point, the initial kinetic energy of the ions has been fully converted to potential energy and the ions are momentarily at a standstill. The ions are then reaccelerated out of the field and continue down the second leg of the flight tube to an electron multiplier tube (EMT) detector where signals are recorded by an oscilliscope (LeCroy Waverunner) and transferred to a PC via an IEEE interface. A mass spectrum of $Ti^+(benzene)_x$ clusters obtained in this way is shown in Figure 2.4. This distribution was created using the above mentioned cutaway source and is therefore dominated by $Ti^+(benzene)_x$ as well as $TiO^+(benzene)_x$ and pure benzene clusters.

Figure 2.4 Time of Flight Mass Spectrum of $Ti^{+}(benzene)_x$ Clusters

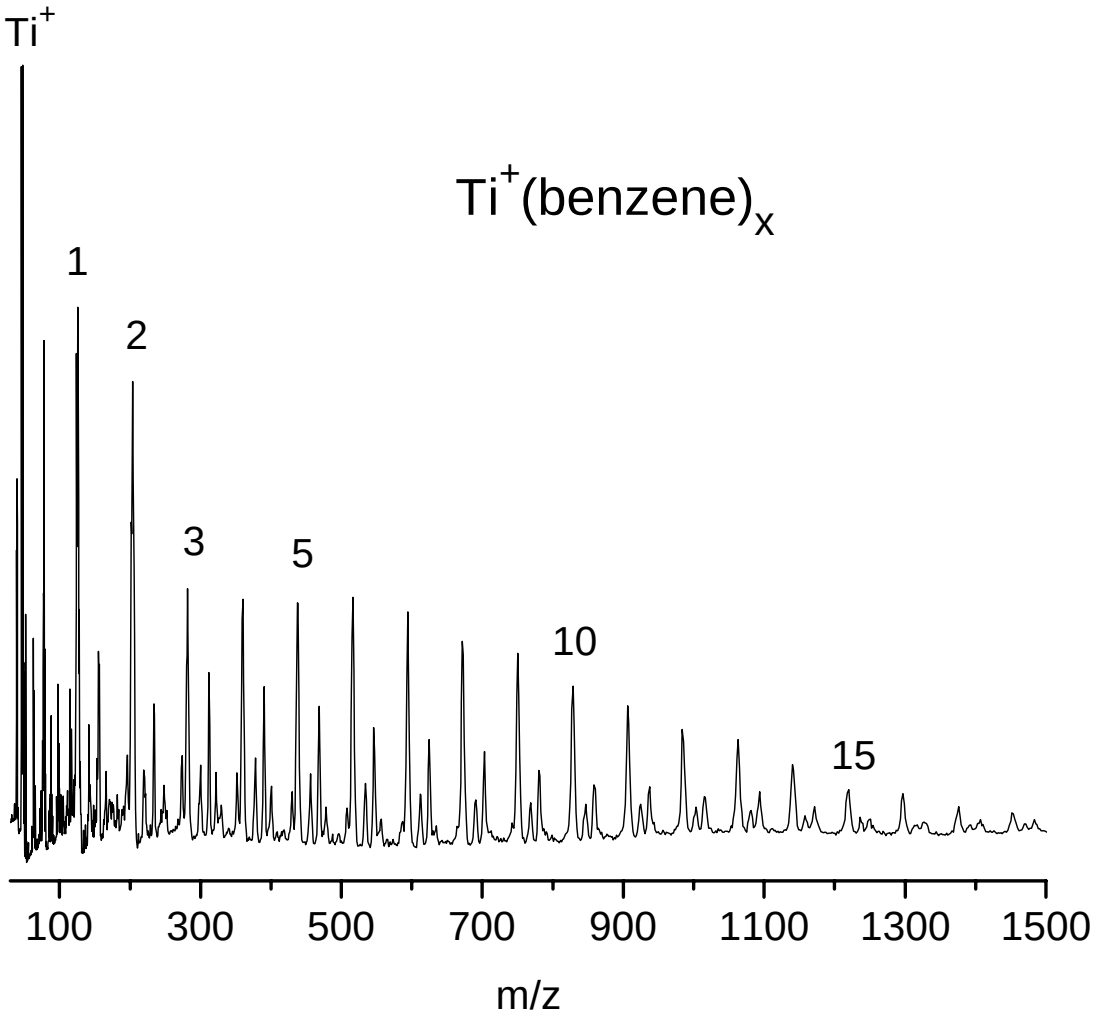
Ti+
Ti+(benzene)x
1
2
3
5
10
15
100
300
500
700
900
1100
1300
1500
m/z

These masses are well resolved and distinguishable from each other over the entire mass range of this data.

Although a reflectron improves mass resolution,[33,34] it is not the primary reason one is used in these experiments. The turning point of the reflectron serves as a convenient spot to overlap the ion packet with a laser beam for photoexcitation. Because the ions are at a virtual standstill a beam can easily be overlapped both spatially and temporally. Additionally, if excitation leads to photofragmentation, the parent and fragment ions follow essentially the same path to the detector, allowing for their simultaneous mass analysis. To create a zero-background for monitoring these fragments, it is necessary to mass select the parent ion of interest. This is accomplished by a set of deflection plates, known as a "mass gate," located in the first flight tube of the machine prior to the reflectron. For mass selection, a voltage of 200 to 400 V is placed on the plates. This pushes the ions off the beam axis and prevents them from entering the reflectron and subsequently being detected. These deflection plates are pulsed to ground at the time the ion packet of interest drifts between them. A mass selected parent ion, in this case Ti^+(benzene) is shown in the top portion of Figure 2.5. The multiplet of peaks corresponds to the naturally occurring isotopes of titanium (46,47,48,49, 50). As can be seen, all ions of higher and lower masses are blocked by the mass gate leaving a zero background for monitoring photofragments in a photodissociation experiment. When a laser is overlapped with this mass selected parent ion, in this case 355 nm light from an Nd:YAG, photoexcitation leads to fragmentation. As shown in the middle panel of Figure 2.5, photofragments are mass analyzed simultaneously with the parent. If the mass selected parent mass spectrum is subtracted from the photofragmentation spectrum then a difference spectrum like that in the lower panel of Figure 2.5 is generated. This

Figure 2.5 Mass Selection, Photofragmentation, and Difference Mass Spectra. The difference mass spectrum is generated by subtracting the mass spectrum with the laser off from the mass spectrum with the laser on.

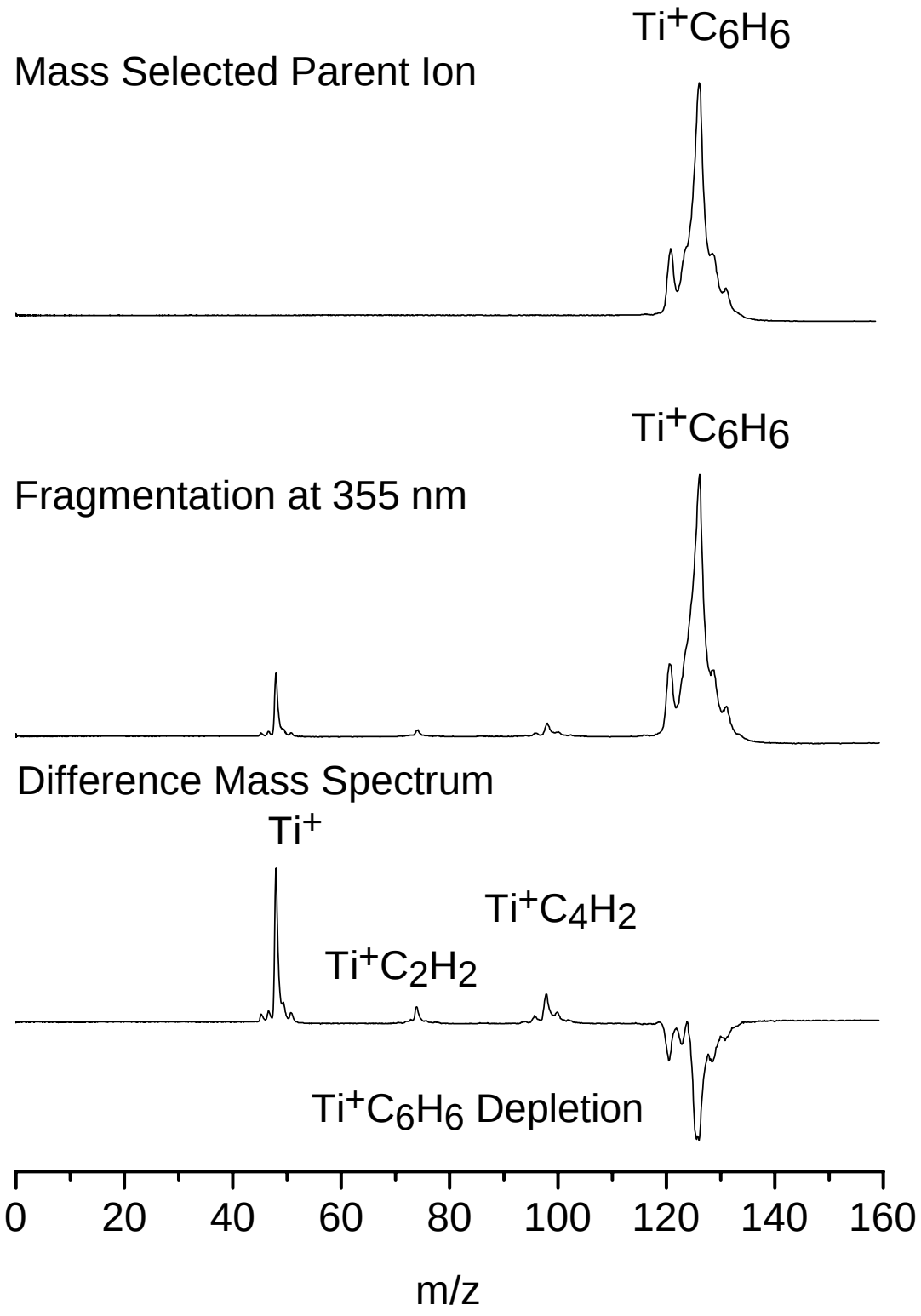
Mass Selected Parent Ion
Ti+C6H6
Fragmentation at 355 nm
Ti+C6H6
Difference Mass Spectrum
Ti+
Ti+C4H2
Ti+C2H2
Ti+C6H6 Depletion
0
20
40
60
80
100
120
140
160
m/z

type of spectrum highlights the depletion of the parent ion by showing it as a negative going peak while presenting fragment ions as positive peaks.

Experiments such as this, where the laser wavelength is held constant, are known as fixed frequency photodissociation experiments. UV and visible photodissociation studies have been performed in this group for many metal-cation ligand systems including $M^+(benzene)_n$,[2] $M^+(C_{60})_n$,[18-20] $M^+(PAH)_n$,[14-17,19] and, as will be discussed in a later chapter, $M^+(cot)_n$.[21] In many cases photodissociation occurs by simple ligand elimination in which an intact neutral ligand cleaves from the cluster leaving the metal cation behind. This is attributed to either the stability of the ligand or a metal-ion ligand binding which is strictly electrostatic in nature. In some cases ligand decomposition can occur where the backbone of the ligand breaks and its components fragment as neutral leaving groups. In systems where this occurs, fragmentation patterns can be attributed to a weak ligand, a photo-chemically activated rearrangement, or evidence of bonding with some charge-transfer character. Yet another pathway is observed with photo-induced charge-transfer reactions as seen with certain M^+(benzene) systems.[2] Fragmentation of these systems yields a charged organic and a neutral metal atom by either direct excitation into a charge-transfer state at an energy above the dissociation limit or via an electronic curve crossing which places the system above the dissociation limit. Fixed frequency experiments are helpful in characterizing the general bonding of a system by revealing relative bond energetics and elucidating novel photochemistry. However, because no actual spectroscopy is performed, exact structural determination is not possible with such an experiment.

Early gas phase metal ion spectroscopic studies focused on the electronic properties of such complexes.[2-13,35-76] This was due to the availability of pulsed laser systems in this spectral range and the strength of electronic transitions. These studies lead to much insight into structure

and energetics of these systems. Unfortunately these studies have been limited to systems of pure metal clusters or to small systems involving a single metal ion and ligand. Larger systems could not be studied because predissociation as well as photo-induced reactions lead to broad ambiguous spectra.[13] In traditional condensed phase inorganic and organometallic chemistry infrared spectroscopy has been an irreplaceable technique for structural determination. Shifts in ligand-based vibrations give direct information as to the charge transfer character in metal-ligand systems.[77-79] Analysis of vibrational spectra based on selection rules established by group theory allows for nearly unambiguous determination of a molecule's structure.[80] Unfortunately the ion density of a molecular beam such as the one used in this experiment is too low for direct absorption experiments. However, the recent advent of high power, pulsed, widely tunable infrared systems has made Infrared Resonance Enhanced Photodissociation (IR-REPD) experiments possible.[81-105] Early work in the field utilized line tunable CO_2 lasers to probe photodissociation yield versus incident photon wavelength.[82-84] These preliminary experiments yielded partial photodissociation spectra for such systems as metal-ethylene[83,84] and others but were severely limited in their spectral range. Fortunately, new technologies have spawned widely tunable IR Optical Parametric Oscillator/Amplifier (OPO/OPA) laser systems that provide high power pulsed IR light from 2000 cm^{-1} to 4500 cm^{-1}.

The OPO/OPA system (LaserVision, Dean Guyer) used at Georgia is shown in Figure 2.6. The pump laser is a Continuum 9010 injection-seeded Nd:YAG laser which provides 550-600 mJ/pulse of horizontally polarized 1064 nm light. This light is split as it enters the OPO/OPA with half sent through a doubling crystal (KTP) and the other half sent through a delay line and on to the amplifier section. The doubled light (532 nm) passes through the grating

Figure 2.6 LaserVision Optical Parametric Oscillator/Optical Parametric Amplifier System

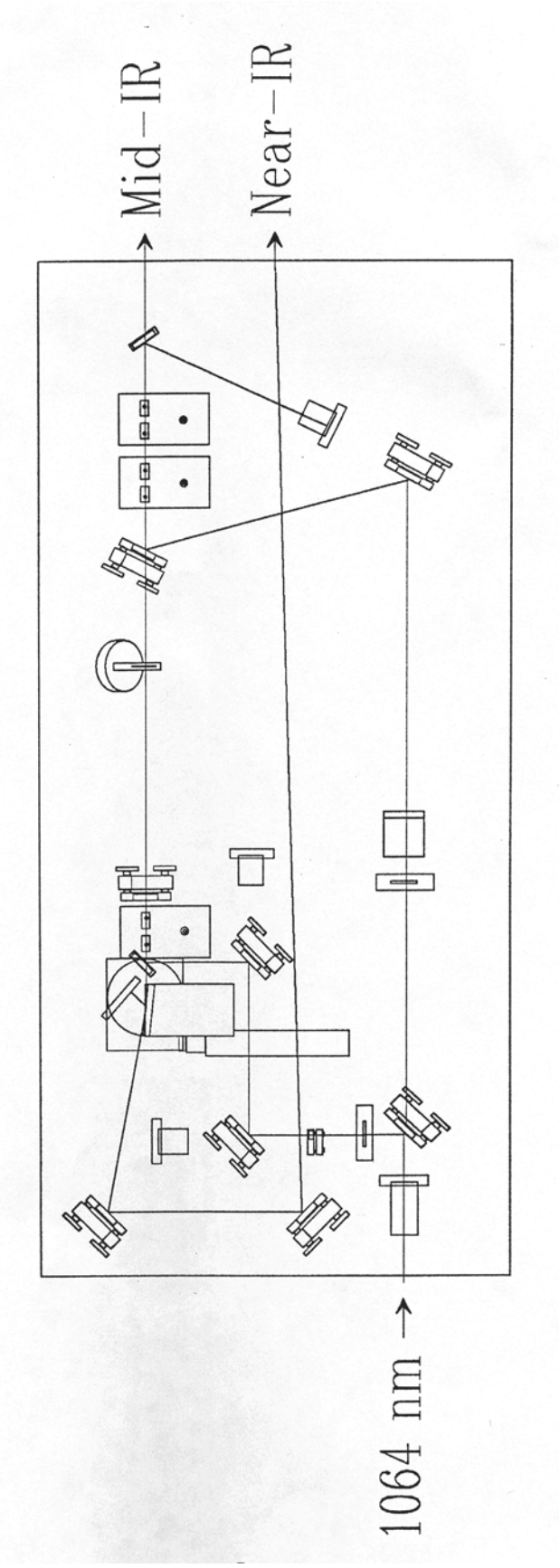
Mid−IR
Near−IR
1064 nm

tuned oscillator section where two angle tuned KTP crystals split the incident photon to produce two photons, the signal and the idler with this relationship:

$$\omega_{pump} = \omega_{signal} + \omega_{idler}$$

$$\text{where } \omega_{signal} \neq \omega_{idler}$$

$$\text{and } \omega_{signal} > \omega_{idler}$$

where ω is the frequency in cm^{-1} of the photon.[106] These crystals provide a signal output from 710-880 nm (~14,000-11,000 cm^{-1}) and an idler output from 1.35-5 μm (~7,000-2,000 cm^{-1}). The idler from the oscillator then passes into the amplifier section where it is recoupled with the 1064 nm light from the delay line. The four KTA crystals in the amplifier utilize difference frequency generation between the idler and the 1064 nm to provide light from 2,000-7,000 cm^{-1} with pulse energies from 1-15 mJ/pulse and a linewidth of ~0.3 cm^{-1}. This light is then sent through the reflectron region of the instrument as described earlier. Fragmentation is enhanced on resonance and an IR-REPD spectrum is obtained by monitoring the fragment intensity versus IR OPO wavelength. Typical spectra are recorded with 1.0 cm^{-1} steps and 30-50 laser shots per point.

The Dutch System

The Dutch system, shown in Figure 2.7,[91,92,94] employs a laser vaporization pulsed nozzle cluster source that utilizes a PSV Pulsed Supersonic Valve (R.M. Jordan, Co.). This valve is operated with a backing pressure from 20-100 psig with a pulse duration of ~55 μsec. Cluster production is similar to that described for the Georgia system. Briefly, the focused second harmonic output of an Nd:YAG laser impinges on a metal target that is both rotating and

Figure 2.7 The Dutch Reflectron Time of Flight Mass Spectrometer with Quadrupole Ion Trap

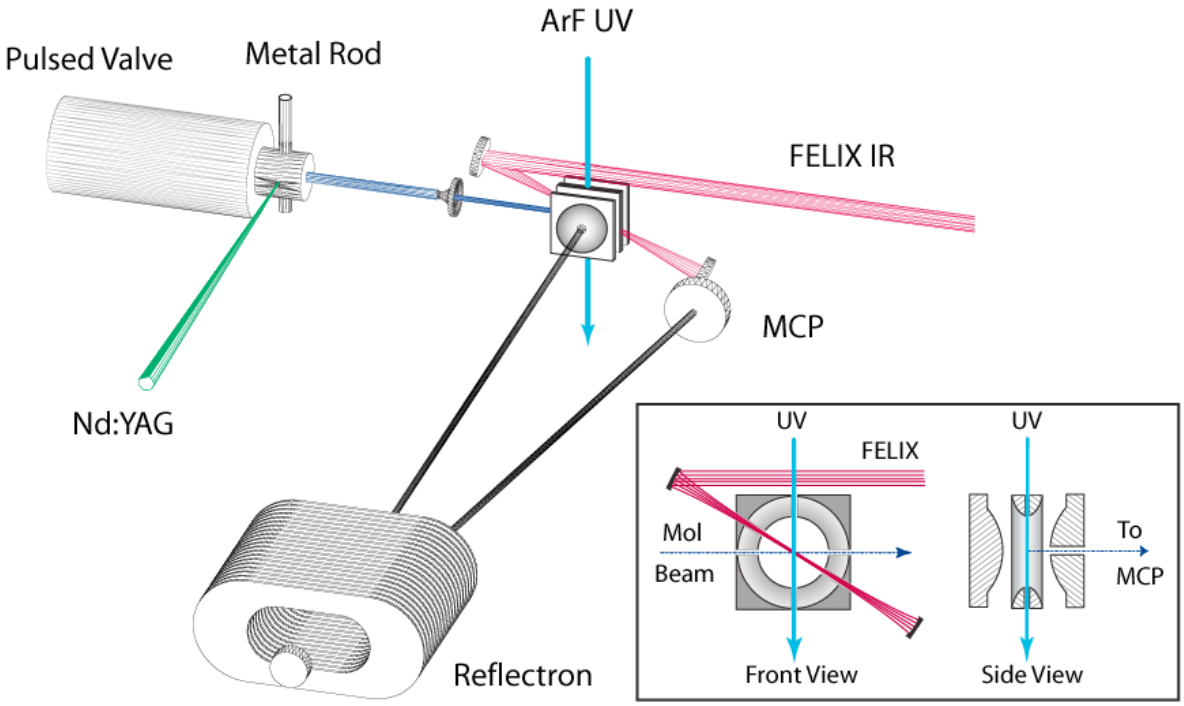
ArF UV
Pulsed Valve
Metal Rod
FELIX IR
MCP
Nd:YAG
Reflectron
UV
FELIX
Mol
Beam
Front View
UV
To
MCP
Side View

translating. A plasma is created and subsequently quenched by a pulse from the valve. For these experiments, a few percent benzene is seeded in with the Ar carrier gas to make complexes of the form $M(benzene)_x$. The expansion is then skimmed before it enters the mass spectrometer portion of the instrument.

Due to experimental constraints, this setup is not designed to examine the nascent cluster ion distribution from the ablation source. Instead, positive deflection plates block ions skimmed from the source. The remaining neutral clusters enter a quadrupole ion trap where they are photoionized using an ArF excimer laser system. At this point the ions can be trapped and held for up to a few seconds if desired. It should be noted that this ion trap does not perform any mass analysis whatsoever. On the contrary, it is used as a means of mass selection. Ions are trapped by use of RF potentials to keep the ions cycling. By adjusting the RF potential ions of lighter mass may be forced into trajectories that cause collisions with the trap walls, essentially eliminating these ions from the system. This leaves a mass threshold where ions below a certain mass may be eliminated. This setup unfortunately does not allow for the elimination of masses above this threshold. Experimentally, all masses below the desired parent ion are eliminated leaving a zero background for the appearance of fragments. Photofragmentation is achieved via light from the Free Electron Laser for Infrared eXperiments (FELIX).[107,108] The characteristics of FELIX will be discussed in detail later. FELIX enters through an aperture in the side of the trap and ion fragmentation is enhanced on vibrational resonance. After laser excitation the potential on the front of the ion trap is pulsed to ground. The trap now functions as the repeller and draw out grid of a Wiley-McLaren TOF, accelerating the ions down the first flight tube, turning in the reflectron, and finally arriving at the Micro Channel Plate (MCP) detector. The IR

Resonance Enhanced Multiple-photon Photodissociation (IR-REMPD) spectrum is obtained by monitoring the fragment yield versus the wavelength of FELIX.

The FELIX laser system warrants some discussion on its own.[107,108] Most lasers are comprised of some lasing medium: a gas, a liquid, or a solid. This medium limits the range through which a laser can function due to self-absorption. In a free electron laser this is not the case. The lasing medium is the electrons themselves, moving at relativistic speeds through a magnetic field. Because of this fact, a free electron laser can function at almost any wavelength. A basic schematic of FELIX is shown in Figure 2.8. A relativistic beam of electrons from a linear accelerator is injected into a collection of permanent magnets with alternating magnetic poles known as an undulator. The undulator is located inside a large optical cavity with highly reflective mirrors at each end. The magnetic field of the undulator is situated perpendicular to the electron beam. Because the polarity alternates periodically along this undulator the subsequent force causes the electrons to move sideways back and forth along the length of the undulator, essentially "wiggling" along their entire flight path. This wiggling is analogous to the behavior of electrons in a stationary dipole antenna and therefore results in emission of radiation with a frequency equal to the oscillation frequency. Although this spontaneous emission is rather weak, successive round trips in the optical cavity result in a large gain in power through stimulated emission from fresh electrons giving laser pulse energies around 50 mJ in a 5-7 μsec pulse and repetition rate of 5 Hz .

The frequency of light emitted can be tuned in either or both of two ways. The first method is to change the velocity of the electron beam. Slower moving electrons will encounter more of a bend while traversing the undulator resulting in longer

Figure 2.8 Schematic of the Free Electron Laser for Infrared eXperiments (FELIX)

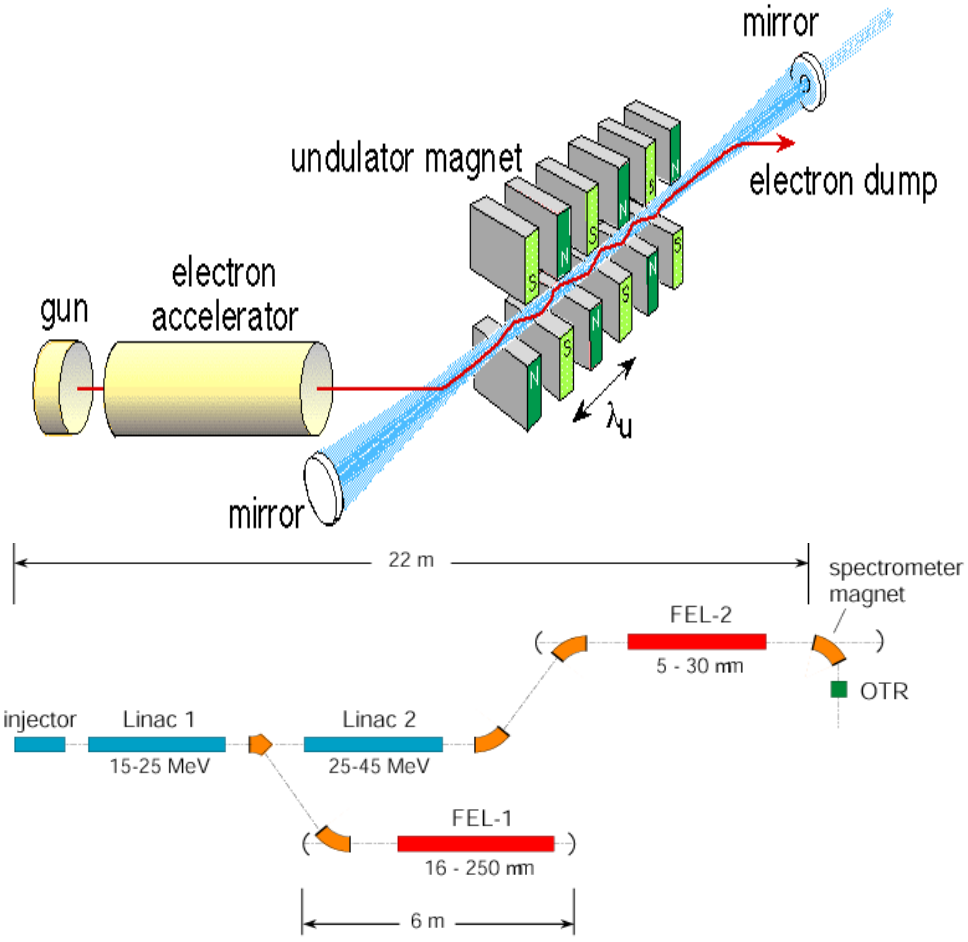

Pulse-structure:

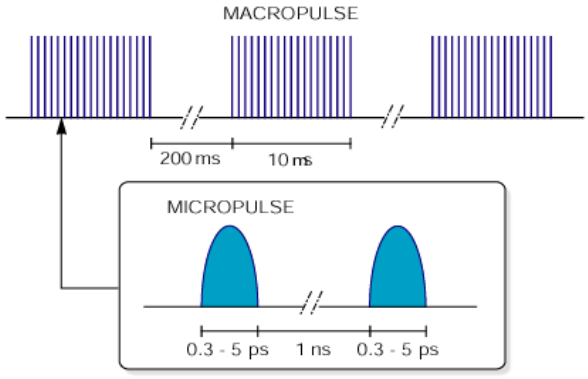

wavelengths and vice versa for faster electrons. This technique is somewhat difficult to do as all electron-focusing elements of the linear accelerator would have to be adjusted specifically for each electron velocity selected. This amounts to time-consuming adjustments for the sake of tunability. The other, more convenient method, employed at FELIX, is to adjust the magnetic field. This is accomplished by attaching a stepping motor to each permanent magnet in the undulator. The magnets can then be moved such that the vertical gap is smaller or larger allowing for adjustment of the amount of bend of the electron path and therefore the frequency of light emitted. This design allows for tuning over a range of 5-30 μm or 15-250 μm (depending on which linear accelerator is used) in a matter of minutes. The peak width of FELIX's output is 5-10 cm^{-1} for the spectral range used in these experiments (600-1700 cm^{-1}).

As is shown if Figure 2.8, FELIX has a somewhat complicated temporal pulse structure. Each cycle consists of a macropulse that is a few microseconds in length. This macropulse consists of a train of smaller micropulses. These micropulses are a few picoseconds in length and spaced apart in time by a nanosecond. The pulse structure allows for molecules to undergo photoexcitation and intramolecular vibrational redistribution several times in one macropulse. Previous studies on C_{60} have shown IR Resonance Enhanced Multiphoton Ionization (IR-REMPI) spectra where up to 300 photons are thought to be absorbed.[109] Although this helps to overcome photon energy versus bond energy inequalities, these multiple-photon events can lead to saturation and broadening of spectral peak widths.[109-112] Typical peak widths are larger than the laser linewidth at about 20-50 cm^{-1}.

References

(1) Willey, K.F.; Yeh, C.S; Robbins, D.L.; Pilgrim, J.S.; Duncan, M.A. *J. Chem. Phys.* **1992**, *97*, 8886.

(2) a) Willey, K.F.; Cheng, P.Y.; Bishop, M.B.; Duncan, M.A. *J. Am. Chem. Soc.* **1991**, *113*, 4721. b) Willey, K.F.; Yeh, C.S.; Robbins, D.L.; Duncan, M.A. *J. Phys. Chem*. **1992**, *96*, 9106.

(3) a) Yeh, C.S.; Willey, K.F.; Robbins, D.L.; Duncan, M.A. *J. Chem. Phys.* **1993**, *98*, 1867. b) Scurlock, C.T.; Pullins, S.H.; Duncan, M.A. *ibid.* **1996**, *105*, 3579.

(4) a) Pilgrim, J.S.; Yeh, C.S.; Berry, K.R.; Duncan, M.A. *J. Chem. Phys.* **1994**, *100*, 7945; erratum: **1996**, *105*, 7876. b) Sucrlock, C.T.; Pilgrim, J.S.; Duncan, M.A. *J. Chem. Phys.* **1995**, *103*, 3293.

(5) a) Robbins, D.L.; Brock, L.R.; Pilgrim, J.S.; Duncan, M.A. *J. Chem. Phys.* **1995**, *102*, 1481. b) Pullins, S.H.; Reddic, J.E.; France, M.R.; Duncan, M.A. *J. Chem. Phys.* **1998**, *108*, 2725.

(6) Scurlock, C.T.; Pullins, S.H.; Reddic, J.E.; Duncan, M.A. *J. Chem. Phys.* **1996**, *104*, 4591.

(7) Pullins, S.H.; Scurlock, C.T.; Reddic, J.E.; Duncan, M.A. *J. Chem. Phys.* **1996**, *104*, 7518.

(8) Duncan, M.A. *Annu. Rev. Phys. Chem.* **1997**, *48*, 63.

(9) a) France, M.R.; Pullins, S.H.; Duncan, M.A. *J. Chem. Phys.* **1998**, *109*, 8842. b) Reddic, J.E.; Duncan, M.A. *Chem. Phys. Lett.* **1999**, *312*, 96.

(10) a) Reddic, J.E.; Duncan, M.A. *J. Chem. Phys.* **1999**, *110*, 9948. b) Reddic, J.E.; Duncan, M.A. *J. Chem. Phys.* **2000**, *112*, 4974.

(11) France, M.R.; Pullins, S.H.; Duncan, M.A. *Chem. Phys.* **1998**, *239*, 447.

(12) Duncan, M.A. *Int. J. Mass. Spectrom.* **2000**, *200*, 545.

(13) Velasquez, J.; Kirschner, K.N.; Reddic, J.E.; Duncan, M.A. *Chem. Phys. Lett.* **2001**, *343*, 613.

(14) Foster, N.R.; Buchanan, J.W.; Flynn, N.D.; Duncan, M.A. *Chem. Phys. Lett.* **2001**, *341*, 476

(15) Foster, N.R.; Grieves, G.A.; Buchanan, J.W.; Flynn, N.D.; Duncan, M.A. *J. Phys. Chem.* **2000**, *104*, 11055.

(16) Buchanan, J.W.; Grieves, G.A.; Flynn, N.D.; Duncan, M.A. *Int. J. Mass Spectrom.* **1999**, *185-187*, 617.

(17) Buchanan, J.W.; Reddic, J.E.; Grieves, G.A.; Duncan, M.A. *J. Phys. Chem.* **1998**, *102*, 6390.

(18) Grieves, G.A.; Buchanan, J.W.; Reddic, J.E.; Duncan, M.A. *Int. J. Mass Spectrom.* **2001**, *204*, 223.

(19) Buchanan, J.W.; Grieves, G.A.; Reddic, J.E; Duncan, M.A. *Int. J. Mass Spectrom.* **1999**, *182*, 323.

(20) Reddic, J.E.; Robinson, J.C.; Duncan, M.A. *Chem. Phys. Lett.* **1997**, *279*, 203.

(21) Jaeger, T.D.; Duncan, M.A. *J. Phys. Chem. A,* Submitted.

(22) Gregoire, G.; Velasquez, J.; Duncan, M.A. *Chem. Phys. Lett.* **2001**, *349*, 451.

(23) Gregoire, G.; Duncan, M.A. *J. Chem. Phys.* **2002**, *117*, 2120.

(24) Walters, R.S.; Jaeger, T.D.; Duncan, M.A. *J. Phys. Chem. A* **2002**, *106*, 10482.

(25) Gergoire, G.; Brinkmann, N.R.; van Heijnsbergen, D.; Schaefer, H.F.; Duncan, M.A. *J. Phys. Chem. A* **2003**, *107*, 218.

(26) Walters, R.S.; Brinkman, N.R.; Schaefer, H.F.; Duncan, M.A. *J. Phys. Chem. A* **2003**, *107*, 7396.

(27) Duncan, M.A. *Int. Rev. Phys. Chem.* **2003**, *22*, 407.

(28) Walker, N.R.; Walters, R.S.; Pillai, E.D.; Duncan, M.A. *J. Chem. Phys.* **2003**, *119*, 10471.

(29) Walker, N.R.; Greives, G.A.; Walters, R.S.; Duncan, M.A. *Chem. Phys. Lett.* **2003**, *380*, 230.

(30) Walker, N.R.; Walters, R.S.; Duncan, M.A. *J. Chem. Phys.* **2004**, *120*, 10037.

(31) Jaeger, T.D.; Pillai, E.D.; Duncan, M.A. *J. Phys. Chem. A* **2004**, *108*, 6605.

(32) Wiley, W.C.; McLaren, I.H. *Rev. Sci. Instrum.* **1955**, *26*, 1150.

(33) Mamyrin, B.A.; Karataeu, V.I.; Shmikk, D.V.; Zagulin, V.A. *Zh. Eksp. Teor. Fiz.* **1973**, *64*, 82.

(34) Boesl, U.; Neusser, H.J.; Weinkauf, R.; Schlag, E.W. *J. Phys. Chem.* **1982**, *86*, 4857.

(35) Shen, M.H.; Winniczek, J.W.; Farrar, J.M. *J. Phys. Chem.* **1987,** *91*, 6447.

(36) Shen, M.H.; Farrar, J.M. *J Phys. Chem.* **1989**, *93*, 4386.

(37) Shen, M.H.; Farrar, J.M. *J. Chem. Phys.* **1991,** *94*, 3322.

(38) Donnelly, S.G.; Farrar, J.M. *J. Chem. Phys.* **1993**, *98*, 5450.

(39) Qian, J.; Midey, A.J.; Donnelly, S.G.; Lee, J.I.; Farrar, J.M. *Chem. Phys. Lett.* **1995**, *244*, 414.

(40) Misaizu, F.; Sanekata, M.; Tsukamoto, K.; Fuke, K.; Iwata, S. *J. Phys. Chem.* **1992**, *96*, 8259.

(41) Sanekata, M.; Misaizu, F.; Fuke, K.; Iwata, S.; Hashimoto, K.; *J. Am. Chem. Soc.* **1995**, *117*, 747.

(42) Sanekata, M.; Misaizu, F.; Fuke, K. *J. Chem. Phys.* **1996**, *104*, 9768.

(43) Fuke, K.; Hashimoto, K.; Takasu, R. *Adv. Met. Semicond. Clusters* **2001**, *5*, 1.

(44) Yoshida, S.; Okai, N.; Fuke, K. *Chem. Phys. Lett.* **2001**, *347*, 93.

(45) Cheng, Y.C.; Chen, J.; Ding, L.N.; Wong, T.H.; Kleiber, P.D.; Liu, D.-K. *J. Chem. Phys.* **1996**, *104*, 6452.

(46) Chen, J.; Cheng, Y.C.; Kleiber, P.D. *J. Chem. Phys.* **1997**, *106*, 3884.

(47) Chen, J.; Wong, T.H.; Kleiber, P.D. *Chem. Phys. Lett.* **1997**, *279*, 185.

(48) Kleiber, P.D.; Chen, J. *Int. Rev. Phys. Chem.* **1998**, *17*, 1.

(49) Chen, J.; Wong, T.H.; Cheng, Y.C.; Montgomery, K.; Kleiber, P.D. *J. Chem. Phys.* **1998**, *108*, 2285.

(50) Chen, J.; Wong, T.H.; Kleiber, P.D.; Wang, K.H. *J. Chem. Phys.* **1999**, *110*, 11798.

(51) Luder, C.; Velegrakis, M. *J. Chem. Phys.* **1996**, *105*, 2167.

(52) Luder, C.; Prekas, D.; Vourliotaki, A.; Velegrakis, M. *Chem. Phys. Lett.* **1997**, *267*, 149.

(53) Fanourgakis, G.S.; Farantos, S.C.; Luder, C.; Velegrakis, M.; Xantheas, S.S. *J. Chem. Phys.* **1998**, *109*, 108.

(54) Prekas, D.; Feng, B.H.; Velegrakis, M.; *J. Chem. Phys.* **1998**, *108*, 2712.

(55) Xantheas, S.; Fanourgakis, G.S.; Farantos, S.C.; Velagrakis, M. **1998**, *108*, 46.

(56) Yang, X.; Hu, Y.; Yang, S. *J. Phys. Chem. A* **2000**, *104*, 8496.

(57) Liu, H.;Guo, W.; Yang, S. *J. Chem. Phys.* **2001**, *115*, 4612.

(58) Guo, W.; Liu, H.; Yang, S. *J. Chem. Phys.* **2002**, *116*, 9690.

(59) Guo, W.; Liu, H.; Yang, S. *J. Chem. Phys.* **2002**, *116*, 2896.

(60) Lie, J.; Dagdigian, P.J. *Chem. Phys. Lett.* **1999**, *304*, 317.

(61) Asher, R.L.; Bellert, D.; Buthelezi, T.; Lessen, D.; Brucat, P.J. *Chem. Phys. Lett.* **1995**, *234*, 119.

(62) Buthelezi, T.; Bellert, D.; Lewis, V.; Brucat, P.J. *Chem. Phys. Lett.* **1995**, *246*, 145.

(63) Buthelezi, T.; Bellert, D.; Lewis, V.; Brucat, P.J. *Chem. Phys. Lett.* **1995**, *242*, 627.

(64) Bellert, D.; Buthelezi, T.; Lewis, V.; Dezfulian, K.; Brucat, P.J. *Chem. Phys. Lett.* **1995**, *240*, 495.

(65) Asher, R.L.; Bellert, D.; Buthelezi, T.; Brucat, P.J. *J. Phys. Chem.* **1995**, *99*, 1068.

(66) Bellert, D.; Buthelezi, Dezfulian, K.; T.; Hayes, T.; Brucat, P.J. *Chem. Phys. Lett.* **1996**, *260*, 458.

(67) Bellert, D.; Buthelezi, T.; Hayes, T.; Brucat, P.J. *Chem. Phys. Lett.* **1997**, *277*, 27.

(68) Hayes, T.; Bellert, D.; Buthelezi, T.; Brucat, P.J. *Chem. Phys. Lett.* **1997**, *264*,220.

(69) Hayes, T.; Bellert, D.; Buthelezi, T.; Brucat, P.J. *Chem. Phys. Lett.* **1998**, *287*, 22.

(70) Bellert, D.; Buthelezi, T.; Brucat, P.J. *Chem. Phys. Lett.* **1998**, *290*, 316.

(71) Husband, J.; Aguirre, F.; Thompson, C.J.; Laperle, C.M.; Metz, R.B. *J. Phys. Chem. A* **2000**, *104*, 2020.

(72) Thompson, C.J.; Husband, J.; Aguirre, F.; Metz, R.B. *J. Phys. Chem. A* **2000**, *104*, 8155.

(73) Thompson, C.J.; Aguirre, F.; Husband, J.; Metz, R.B. *J. Phys. Chem. A* **2000**, *104*, 9901.

(74) Faherty, K.P.; Thompson, C.J.; Aguirre, F.; Michen, J.; Metz, R.B. *J. Phys. Chem. A* **2001**, *105*, 10054.

(75) Stace, A.J. *Adv. Met. Semicond. Clusters* **2001**, *5*, 121.

(76) Posey, L.A. *Adv. Met. Semicond. Clusters* **2001**, *5*, 145

(77) Fritz, H.R.; *Adv. Organomet. Chem.* **1964**, *1*, 239.

(78) Aleksanyan, V.T.; IVib. Spectra Struct. **1982,** *11,* 107.

(79) Nakamoto, K. *Infrared and Raman Spectra of Inorganic and Organometallic Compounds*, 5th ed.; Wiley-Interscience: New York, 1997, Part B.

(80) Cotton, F.A. *Chemical Applications of Group Theory*, 3rd ed.; Wiley-Interscience: New York, 1990.

(81) Thorne, L.R.; Beauchamp, J.L. *Gas Phase Ion Chemistry,* **1984**, *3*, 41.

(82) Knickelbein, M.B. *Chem. Phys. Lett.* **1995**, *239*, 11.

(83) Knickelbein, M.B. *J. Chem. Phys.* **1996**, *104*, 3217.

(84) Lisy, J.M. *Cluster Ions,* Ng. C; Baer, T.; Powis, I. (Eds.) Wiley, Chichester, 1993.

(85) Weinheimer, C.J.; Lisy, J.M. *Int. J. Mass Spectrom Ion Process* **1996**, *159*, 197.

(86) Weinheimer, C.J.; Lisy, J.M. *J. Phys. Chem.* **1996**, *100*, 15303.

(87) Weinheimer, C.J.; Lisy, J.M. *J. Chem. Phys.* **1996**, *105*, 2938.

(88) Lisy, J.M. *Int. Rev. Phys. Chem.* **1997**, *16*, 267.

(89) a) Cabarcos, O.M.; Weinheimer, C.J.; Lisy, J.M. *J. Chem. Phys.* **1998**, *108*, 5151. b) Cabarcos; O.M.; Weinheimer, C.J.; Lisy, J.M., *J. Chem. Phys.* **1999**, *110*, 8429.

(90) Vaden, T.D.; Forinash, B.; Lisy, J.M. *J. Chem. Phys.* **2002** *117*, 4628.

(91) van Heijnsbergen, D.; von Helden, G.; Meijer, G.; Maitre, P.; Duncan, M.A. *J. Am. Chem. Soc.* **2002**, *124*, 1562.

(92) van Heijnsbergen, D.; Jaeger, T.D.; von Helden, G.; Meijer, G.; Duncan, M.A. *Chem. Phys. Lett.* **2002**, *364*, 345.

(93) Jaeger, T.D.; Fielicke, A.; von Helden, G.; Meijer, G.; Duncan, M.A. *Chem. Phys. Lett.* **2004**, *392*, 409.

(94) Jaeger, T.D.; van Heijnsbergen, D.; Klippenstein, S.J.; von Helden, G.; Meijer, G.; Duncan, M.A. *J. Am. Chem. Soc.* **2004**, *126*, 10981.

(95) Lemaire, J.; Boissel, P.; Heninger, M.; Mauclaire, G.; Bellec, G.; Mestdagh, H.; Simon, A.; Le Caer, S.; Ortega, J.M.; Glotin, F.; Maitre, P *Phys. Rev. Lett.* **2002**, *89*, 273002/1.

(96) Lemaire, J.; Boissel, P.; Heninger, M.; Mestdagh, H.; Mauclaire, G.; Le Caer, S.; Ortega, J.M.; Maitre, P. *Spectra Anal.* **2003**, *32*, 28.

(97) Le Caer, S.; Heninger, M.; Lemaire, J.; Boissel, P.; Maitre, P.; Mestdagh, H. *Chem. Phys. Lett.* **2004**, *385*, 273.

(98) Simon, A.; Jones, W.; Ortega, J.M.; Boissel, P.; Lemaire, J.; Maitre, P. *J. Am. Chem. Soc.* **2004**, *126*, 11666.

(99) Fielicke, A.; Meijer, G.; von Helden, G. *J. Am. Chem. Soc.* **2003**, *125*, 3659.

(100) Fielicke, A.; Meijer, G.; von Helden, G. *Eur. Phys. J. D.* **2003**, *24*, 69.

(101) Fielicke, A.; Meijer, G.; von Helden, G.; Simard, B.; Denommee, S.; Rayner, D. *J. Am. Chem. Soc.* **2003**, *125*, 11184.

(102) Fielicke, A.; Mitric, R.; Meijer, G.; Bonacic-Koutecky, V.; von Helden, G. *J. Am. Chem. Soc.* **2003**, *125*, 15716.

(103) Fielicke, A.; von Helden, G. ; Meijer, G. *J. Phys. Chem. B* **2004**, *108*, 14591.

(104) Fielicke, A.; Kirilyuk, A.; Ratsch, C.; Behler, J.; Scheffler, M.; von Helden, G. ; Meijer, G. *Phys. Rev. Lett.* **2004**, *93*, 023401/1.

(105) Oomens, J.; Moore, D.T.; von Helden, G. ; Meijer, G.; Dunbar, R.C. *J. Am. Chem. Soc.* **2004**, *126*, 724.

(106) Demtroder, W. *Laser Spectroscopy* Springer-Verlag: Berlin, 1996.

(107) Oepts, D.; van der Meer, A.F.G.; van Amersfoort, P.W. *Infrared. Phys. Technol.* **1995**, *36*, 297.

(108) FOM Plasma Physics Instiute homepage [http://www.rijnh.nl/n4/n3/f1234.htm]

(109) van Heijnsbergen, D.; von Helden, G.; Sartakov, B.; Meijer, G. *Chem. Phys. Lett.* **2000**, *321*, 508

(110) a)von Helden, G.; Holleman, I; Meijer, G.; Sartakov, B. *Opt. Express* **1999**, *4*, 46. b) von Helden, G.; Holleman, I.; Knippels, G.M.H.; van der Meer, A.F.G.; Meijer, G. *Phys. Rev. Lett.* **1997**, *79*, 5234.

(111) van Heijnsbergen, D.; von Helden, G.; Duncan, M.A.; van Roij, A.J.A.; Meijer, G. *Phys. Rev. Lett.* **1999**, *83*, 4983.

(112) van Heijnsbergen, D.; von Helden, G.; Meijer, G. *J. Phys. Chem. A* **2003**, *107*, 1671.

CHAPTER 3

PHOTODISSOCIATION OF TRANSITION METAL CATION COMPLEXES WITH BENZENE

Abstract

Transition metal cation-benzene complexes of the form $M^+(C_6H_6)_{1-7}$ (M=Ti, V, Ni) are produced in a laser vaporization pulsed nozzle cluster source. The clusters are mass-selected and photodissociated using the third harmonic of a Nd:YAG laser (355 nm). $Ti^+(C_6H_6)$ fragments via a ligand decomposition channel to produce $Ti^+C_4H_2$, $Ti^+C_2H_2$, and Ti^+. $V^+(C_6H_6)$ fragments by simple ligand elimination of neutral benzene to give V^+ as the primary fragment. $Ni^+(C_6H_6)$ fragments via both simple ligand elimination leaving Ni^+ and by a photoinduced charge transfer pathway to give benzene cation. Complexes with two benzene ligands fragment by the loss of a single neutral benzene to leave $M^+(C_6H_6)$ as the fragment. For clusters with more than two benzenes, all species fragment directly down to $M^+(C_6H_6)_2$ with a small amount of $M^+(C_6H_6)$ for M=Ti and Ni. This indicates that a stable core is established at $M^+(C_6H_6)_2$ and subsequent benzene ligands most likely do not attach as strongly as the first two. There is no evidence for threefold coordination in any of these complexes.

Introduction

Transition metal ion-molecule complexes that are produced, isolated, and studied in the gas phase provide models for metal-ligand interactions and insight into metal-ion solvation.[1-4] Metal ion-benzene complexes are of particular interest for their relevance to catalytic and biological processes.[5,6] Such π-aromatic bonded systems are prevalent throughout organometallic chemistry.[7,8] Metal-ion benzene complexes are also fascinating because they have the propensity to form sandwich structures.[7,8] These systems can be compared to similar complexes that are synthesized and isolated using conventional techniques.[7,8] Those complexes that can be produced using traditional condensed phase methods have been studied using infrared spectroscopy, and shifts in the ligand based vibrations give information on the metal-ligand interaction.[9-12] Until recently, such information has been limited for gas phase ion complexes. In the past, we have reported the application of infrared photodissociation spectroscopy for a variety of gas-phase transition metal-ion benzene complexes in the fingerprint region using a free electron laser.[13-15] Recently, IR photodissociation spectroscopy has been reported for $V^+(benzene)_x$ and $V^+(benzene)_xAr$ in the C-H stretch region using a tunable IR Optical Parametric Oscillator/Amplifier (OPO/OPA) laser system.[16] These IR studies have helped to elucidate structures for these complexes, however, the UV photochemistry of these systems has not been fully investigated. UV photodissociation of metal ion-benzene complexes has been implemented previously by this group, but has been limited for the most part to mono-benzene complexes.[17] This study focuses on the photodissociation of $M^+(C_6H_6)_{1-7}$ (M=Ti, V, Ni) using UV light (355 nm).

The field of sandwich complexes began with the discovery of ferrocene and the explanation of its bonding stability by metal-ligand charge transfer.[18] Shortly after, dibenzene chromium was synthesized and isolated. The relative stability of both complexes has been attributed to the familiar 18-electron rule.[9] Several neutral metal-benzene analogues have been isolated and studied via conventional techniques, as have several complexes that carry a net charge and are stabilized via counter ions.[7,8] Although qualitative trends of shifts in the ligand based modes were established, many uncertainties arose from solvent effects and the presence of counter ions. It is therefore advantageous to study metal-ion benzene complexes in the gas phase where such effects are absent.

Many metal ion-benzene complexes have been studied in the gas phase by mass spectrometry.[17,19-23] Bond energies have been determined for such systems using collision-induced dissociation (CID),[20] equilibrium mass spectrometry,[21] and UV-vis photodissociation.[18,19] Theory has investigated the structures and energetics of these systems.[2,3,24-30] Kaya and coworkers demonstrated that various metal-benzene complexes form multiple-decker sandwich structures of the form $M_x(benzene)_y$ at x:y values where $y = x + 1$.[22] This tendency was most pronounced for earlier transition metal complexes, such as those containing vanadium or titanium. Later transition metals clustered in a different manner, forming "rice-ball" structures of metal clusters surrounded by benzene ligands. The multiple-decker sandwich structures were confirmed by ion mobility measurements performed by Bowers and coworkers.[23] Photoelectron spectroscopy has been applied to metal-benzene anions.[22b,31] Recently, an IR absorption spectrum was obtained for $V^+(benzene)_2$ that was size-selected as a cation then deposited and subsequently neutralized in a rare gas matrix.[32] Lisy and coworkers have obtained gas phase IR photodissociation spectra for alkali cation-$(water)_x(benzene)_y$

complexes in the O-H stretch region.[33] We have reported the vibrational spectra for several metal-ion benzene complexes in the 600-1700 cm^{-1} region.[13-15] These studies demonstrated systematic shifts in the ring based vibrations of these complexes.[15] A comprehensive comparison to DFT calculations was also presented.[15] A recent communication showed that IR photodissociation spectroscopy could be applied to $V^+(benzene)_x$ and $V^+(benzene)_xAr$ complexes in the C-H stretch region.[16]

UV and visible photodissociation studies have been performed previously by our group for many metal cation-ligand systems including $M^+(benzene)_x$,[17] $M^+(C_{60})_x$,[34,35] $M^+(coronene)_x$.[35-37] and $M^+(cycloocatetraene)_x$.[38] Yeh and coworkers have employed photodissociation to study the binding in a variety of related systems including $M^+(C_5H_5N)$,[39] $M^+(furan)$,[40] and $M^+(benzene)$.[41] In many cases photodissociation occurs by simple ligand elimination in which an intact neutral ligand leaves the cluster and the metal cation or a smaller metal-ligand species is the charged fragment. In other cases ligand decomposition can occur, and the metal complex loses smaller stable neutral fragments. Yet another dissociation pathway is photoinduced charge transfer, as we have seen with several $M^+(benzene)_x$ systems.[17] Fragmentation of these complexes yields a charged organic and a neutral metal atom by either direct excitation into a charge transfer state at an energy above the dissociation limit or via an electronic curve crossing. For many metal ion-ligand systems, ligand elimination is expected based on the structural stability of the ligand studied. It is also interesting to see if a certain cluster size is observed as a common fragment from larger clusters. When this occurs, it is usually an indication that coordination around the metal ion is complete at this cluster size. In this way, the experiment helps to elucidate coordination numbers. The previous studies of $M^+(C_6H_6)$ performed by this group have focused on photoinduced charge transfer in complexes with only one benzene

ligand.[17] This study will expand this earlier work by studying complexes with multiple benzene ligands, and will focus on general fragmentation trends established at these larger cluster sizes.

Experimental Section

The experimental apparatus has been described previously.[42] Clusters are produced via laser vaporization (355 nm) in a pulsed nozzle cluster source and mass analyzed in a reflectron time-of-flight mass spectrometer. By using a "cutaway" type rod holder[17] a free expansion of excess benzene seeded in Ar produces clusters of the form $M^+(C_6H_6)_x$ efficiently. The molecular beam is skimmed from the source chamber into a differentially pumped mass spectrometer chamber. Cations are pulse accelerated into the first flight tube and mass selected by pulsed deflection plates located just prior to the reflection region. The ions of interest are then intersected by the third harmonic (355 nm) output of an Nd:YAG laser system. Excitation of these ions leads to subsequent fragmentation. Parent and fragment ions are mass analyzed in the second flight tube and detected using an electron multiplier tube and a digital oscilloscope (LeCroy 9310A). Data is transferred to a PC via an IEEE-488 interface.

Results and Discussion

The mass spectra of clusters obtained for C_6H_6 with titanium, vanadium, and nickel are shown in Figure 3.1. For all three metals shown, the mass spectra consist predominately of metal ion-benzene adducts of the form $M^+(C_6H_6)_x$. Because metal atom recombination is limited

Figure 3.1 Time-of-flight mass spectra for Ti, V, and Ni-$(C_6H_6)_x$ complexes formed in an Ar expansion.

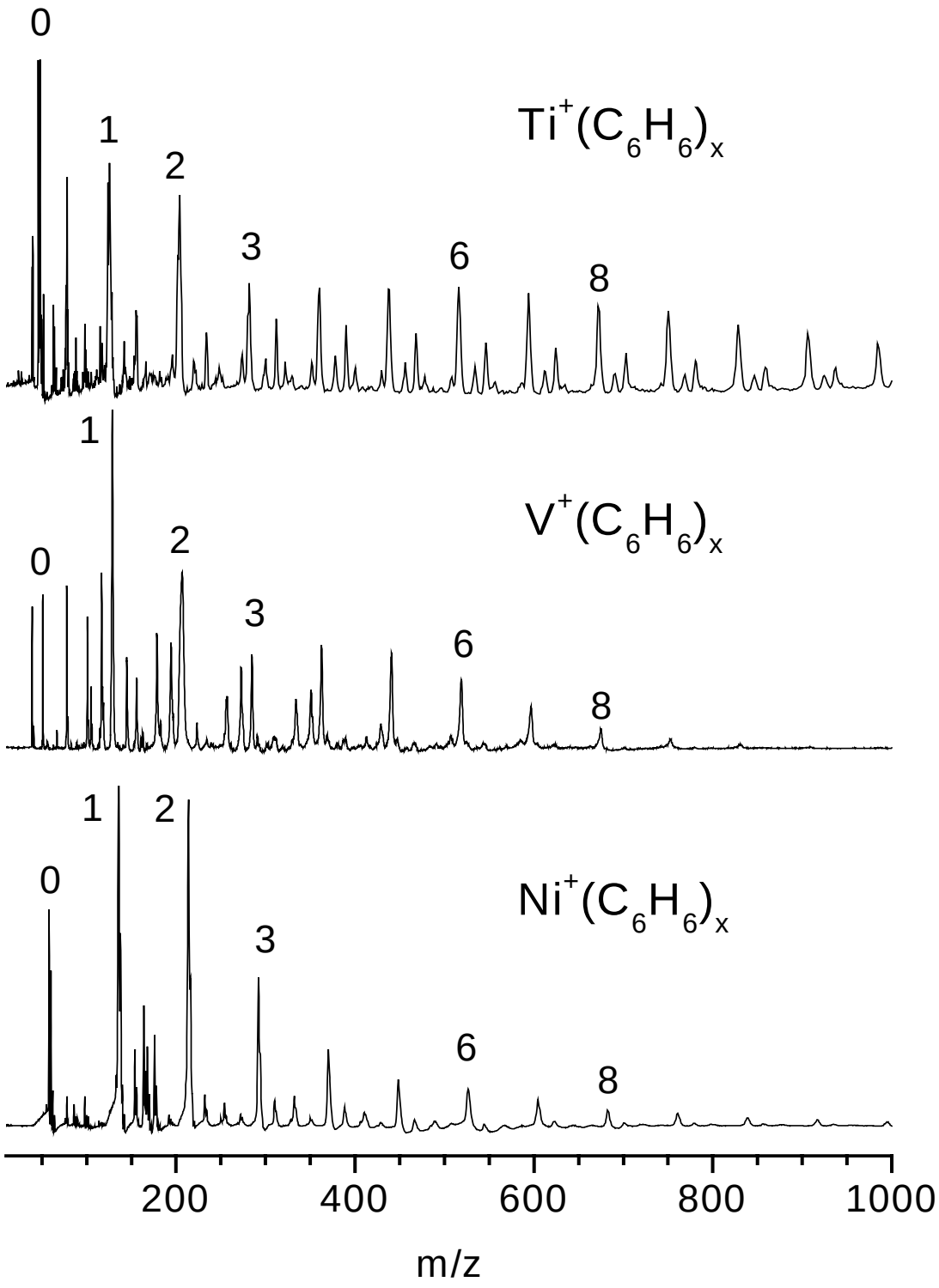
0
1
2
3
6
8
Ti+(C6H6)x
1
0
2
3
6
8
V+(C6H6)x
1
2
0
3
6
8
Ni+(C6H6)x
200
400
600
800
1000
m/z

in this particular cluster source configuration, multiple metal atom species, and in particular the possibility of multiple-decker sandwich or rice-ball clusters described by Kaya and coworkers,[22] are not produced efficiently. Clustering is efficient out to ten or more benzene ligands. After x=2, however, a sharp drop off in intensity occurs for all three metal ion-benzene species. This could indicate particular stability for complexes with one or two benzene ligands. Other masses not associated with metal ion-benzene adducts are also present in all three mass spectra. For Ti^+, these masses are assigned as $K^+(C_6H_6)$, $Ti^+(H_2O)(C_6H_6)_x$, $(C_6H_6)_x^+$, and $Ti^+(C_6H_6)_xAr$. In the mass spectrum of $V^+(C_6H_6)_x$, the other masses are metal ion-benzene adducts of sodium and potassium. For Ni^+, the other mass peaks are assigned as $Ni^+(H_2O)(C_6H_6)_x$, $Ni^+(C_6H_6)_xAr$, and $Ni_2^+(C_6H_6)_x$.

Each cluster size of interest is mass selected and photodissociated using the third harmonic (355 nm) of a Nd:YAG laser. This sequential process is shown for $Ti^+(C_6H_6)$ in Figure 3.2. The parent ion is first mass selected using pulsed deflection plates. This eliminates all clusters of higher and lower masses than the desired ion of study. The multiplet in this particular ion, $Ti^+(C_6H_6)$, is attributed to the naturally occurring isotopes of Ti (46,47, 48, 49, and 50). Because all higher masses have been deflected, any fragments observed can be attributed solely to the selected parent ion. Because all lower mass fragments have been eliminated, any photofragments created by photoexcitation can be detected on a zero background. Once the parent has been mass selected, the excitation laser can be aligned both spatially and temporally with the ion packet. Absorption and excitation occur, and fragmentation is subsequently seen. Parent and fragment ions are simultaneously mass analyzed in the second flight tube and a fragmentation mass spectrum, like that in Figure 3.2 is recorded. To highlight

Figure 3.2 A parent ion of interest is mass selected using pulsed deflection plates. This eliminates all clusters of higher and lower mass. The fragmentation laser is then aligned both spatially and temporally and fragmentation occurs. The mass spectrum with the laser off is subtracted from the mass spectrum with the laser on to give the difference mass spectrum.

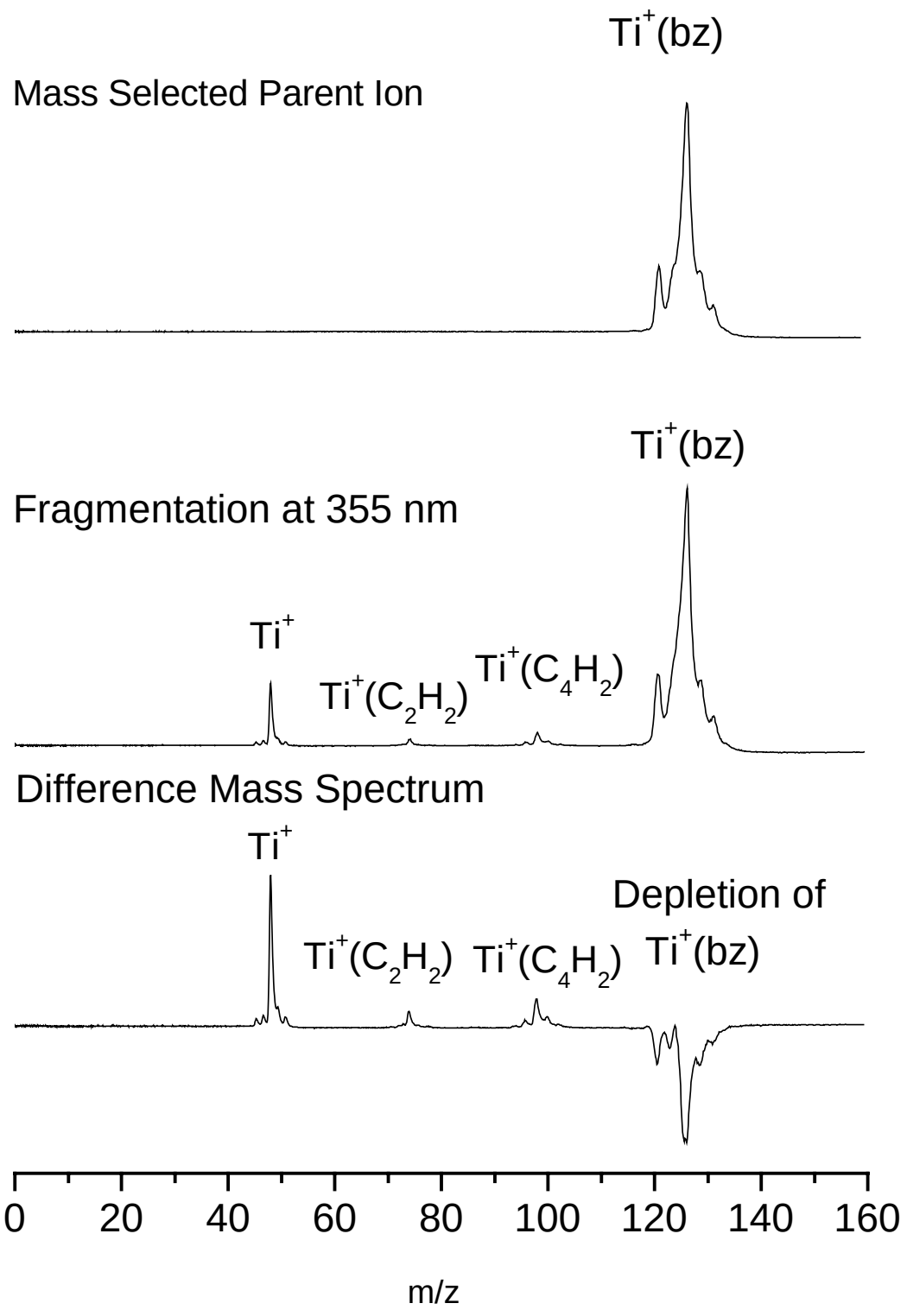
Ti+(bz)
Mass Selected Parent Ion
Ti+(bz)
Fragmentation at 355 nm
Ti+
Ti+(C2H2)
Ti+(C4H2)
Difference Mass Spectrum
Ti+
Depletion of
Ti+(C2H2)
Ti+(C4H2)
Ti+(bz)
0
20
40
60
80
100
120
140
160
m/z

the depletion of the parent ion and the appearance of fragment ions, a difference mass spectrum is obtained. This is accomplished by subtracting a mass spectrum taken with the laser off (top of Figure 3.2) from a mass spectrum taken with the fragmentation laser on (middle of Figure 3.2) to yield the difference mass spectrum (bottom of Figure 3.2).[17] This method gives a negative-going parent peak due to depletion and positive-going fragment peaks. All fragmentation mass spectra were obtained with this technique and are shown in this manner.

The fragmentation difference mass spectra taken at 355 nm of the $M^+(C_6H_6)$ parent ions for M=Ti, V, and Ni are shown in Figure 3.3. As mentioned earlier, three general types of photofragmentation can occur: ligand decomposition, ligand elimination, and photoinduced charge transfer. All three types of dissociation are observed in the fragmentation patterns of these selected transition metal cation-benzene complexes.

As shown in Figure 3.3, the photodissociation of $Ti^+(C_6H_6)$ appears to follow three possible fragmentation pathways:

1) $Ti^+(C_6H_6) \rightarrow Ti^+ + C_6H_6$

2) $Ti^+(C_6H_6) \rightarrow Ti^+C_2H_2 + C_4H_4$

3) $Ti^+(C_6H_6) \rightarrow Ti^+C_4H_2 + C_2H_2$

At firsts glance, it is not clear if the Ti^+ fragment occurs by ligand elimination from $Ti^+(C_6H_6)$ or by further fragmentation of $Ti^+(C_4H_2)$ or $Ti^+(C_2H_2)$. An examination of the thermodynamics of each pathway might help to understand which, if any, of these pathways is energetically favored and whether or not these processes are single or multiphoton.

For pathway number one, we can compare the bond energy of $Ti^+(C_6H_6)$ with the

Figure 3.3 Photofragmentation difference mass spectra of $M^+(C_6H_6)$ complexes at 355 nm where M=Ti, V, and Ni.

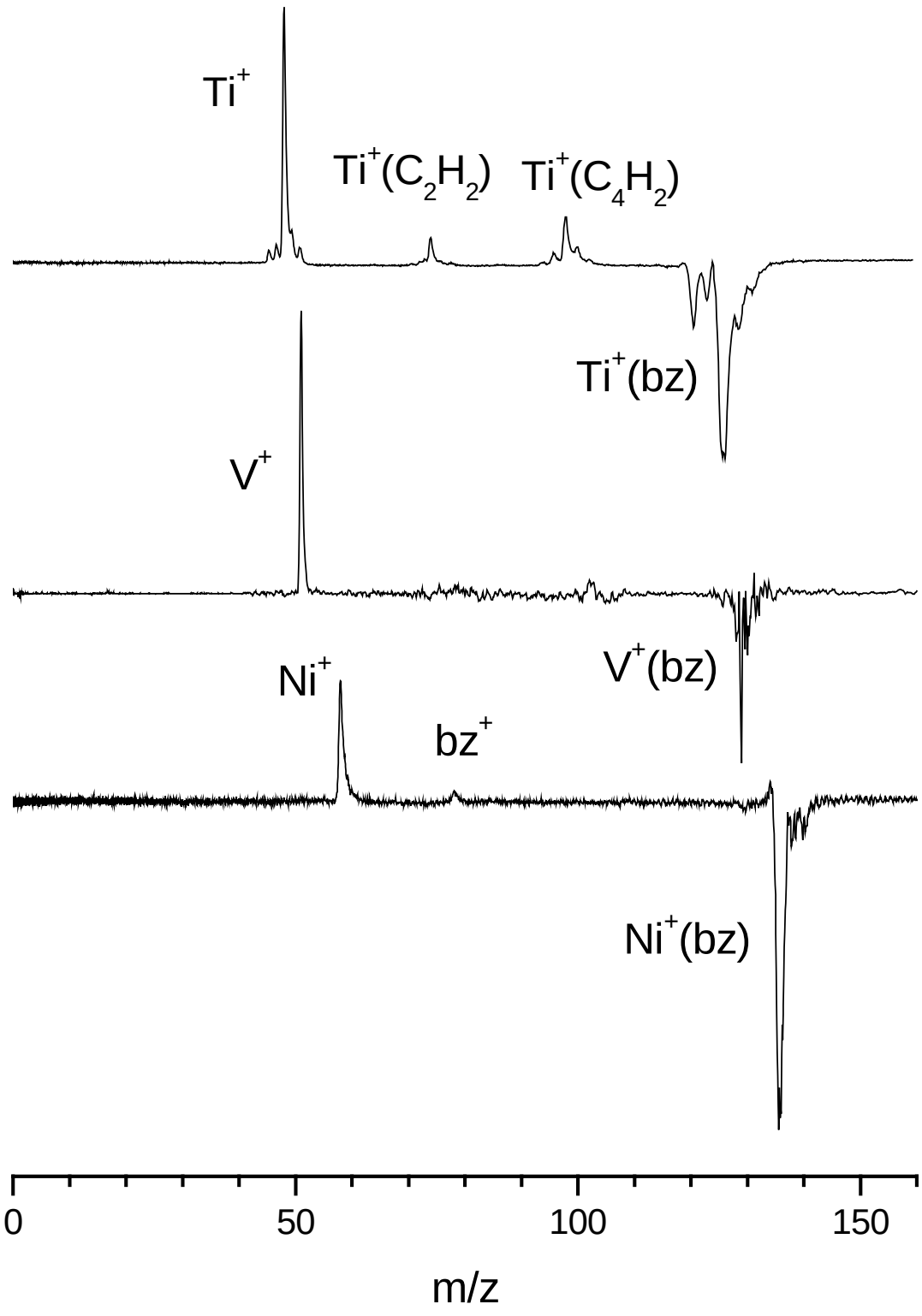
Ti+
Ti+(C2H2)
Ti+(C4H2)
Ti+(bz)
V+
V+(bz)
Ni+
bz+
Ni+(bz)
0
50
100
150
m/z

incident photon energy to see whether this process could be single or multiphoton. A table of metal ion-benzene bond energies derived from CID measurements is presented in Table 3.1. $Ti^+(C_6H_6)$ is bound by 61.9 kcal/mol (2.68 eV; ~22,000 cm^{-1}).[20] The incident photon energy at 355 nm is ~3.50 eV or ~28,000 cm^{-1}. This shows that the incident photon energy is enough to break this bond for simple ligand elimination. As laser fluence was systematically decreased, the intensity of all fragments decreased linearly, indicating that the process could be a single photon process. However, since higher order processes can sometimes appear linear, we cannot say for sure that this is a single photon process.

Besides ligand elimination, $Ti^+(C_6H_6)$ also undergoes ligand decomposition to give $Ti^+(C_4H_2)$ and $Ti^+(C_2H_2)$. This is somewhat surprising because benzene is generally considered to be a very stable ligand and is not expected to decompose readily. Titanium, though, is known to be extremely reactive towards hydrocarbons,[43-46] and this could account for the fragmentation patterns witnessed here. However, Schwarz and coworkers, using FT-ICR, found Ti^+ to be unreactive towards benzene.[43] Photoexcitation provides the activation energy necessary for a reaction to occur.

The appearance of $Ti^+(C_2H_2)$ is not too surprising. $C_2H_2^+$ is observed in large quantities in the EI mass spectrum of C_6H_6.[47] Acetylene is also rather strongly bound to Ti^+ with a D_0 of 60.4 kcal/mol (2.62 eV),[41] so it is makes sense that this appears as a fragment. The formation of $Ti^+(C_4H_2)$, however, is intriguing. This could occur because ethylene, C_2H_4, is a relatively good neutral leaving group, or because the $Ti^+(C_4H_2)$ fragment has particular stability. In fact, diacetylene, $C_4H_2^+$, is seen in large quantities in the electron-impact ionization (EI) mass spectrum of C_6H_6,[47] where high energy electron beams cause extensive fragmentation. It is possible that C_4H_2 takes the form of diacetylene when it complexes with Ti^+. Ti^+ must bind

Table 3.1 Table of Metal Ion-Benzene Bond Energies Determined by Collision-Induced Dissociation[a]

Complex	D_0 (loss of one C_6H_6; eV)	
	x=1	x=2
$Ti^+(C_6H_6)_x$	2.68	2.62
$V^+(C_6H_6)_x$	2.42	2.55
$Cr^+(C_6H_6)_x$	1.76	2.40
$Mn^+(C_6H_6)_x$	1.38	2.10
$Fe^+(C_6H_6)_x$	2.15	1.94
$Co^+(C_6H_6)_x$	2.65	1.73
$Ni^+(C_6H_6)_x$	2.52	1.52
$Cu^+(C_6H_6)_x$	2.26	1.61

[a] Reference 20b

rather strongly to diacetylene and is thus present in the photofragmentation spectrum. Unfortunately, to our knowledge, theoretical or experimental bond energies for this complex are not known. Because the thermodynamics of these complexes is not fully understood, it is not clear which fragmentation pathway observed is the lower energy pathway.

The photochemical nature of these reactions might be wavelength dependent. This is examined by changing the photodissociation wavelength to see if any alterations in the fragmentation patterns are observed. When 532 nm light is used for photodissociation, however, the same fragments in the same relative intensities are observed. This is somewhat surprising. As mentioned earlier, the metal-ligand bond energy of $Ti^+(C_6H_6)$ is 2.68 eV (~22,000 cm^{-1}). When the photodissociation wavelength is 355 nm (~28,000 cm^{-1}), the incident photon energy is greater than the bond energy and single photon excitation could lead to dissociation. This is not the case when the excitation wavelength is 532 nm (~19,000 cm^{-1}). Although multiphoton processes cannot be completely ruled out, the same fragmentation patterns are observed at low laser fluences, indicating that it is most likely single photon. This discrepancy can be accounted for if a fraction of the $Ti^+(C_6H_6)$ complexes present in the beam are in a metastable excited state. Previous DFT calculations[15] found $Ti^+(C_6H_6)$ to have a $^4A_1$ ground state with a $^2A_2$ some 0.42 eV (~3400 cm^{-1}) higher in energy. This then accounts for the ligand elimination pathway seen at 532 nm. The presence of a small fraction of an excited metastable state could also explain the ligand decomposition pathways seen here, as it is well known that the reactivities of metal ions are highly dependent on their electronic state.[48-51] In fact, for Ti^+ the first doublet excited state is known to be over 100 times more reactive towards certain hydrocarbons than its quartet ground state.[50]

Figure 3.3 also shows the photofragmentation of $V^+(C_6H_6)$ at 355 nm. This pattern is much simpler than that of $Ti^+(C_6H_6)$. As shown, $V^+(C_6H_6)$ fragments by simple ligand elimination of a whole neutral benzene ligand. These results are consistent with those previously presented by Yeh and coworkers for $V^+(C_6H_6)$ using both 532 nm and 355 nm light.[41] The binding energy of $V^+(C_6H_6)$ (55.9 kcal/mol; 2.42 eV)[20] is slightly less than that of $Ti^+(C_6H_6)$, and, as shown earlier, could conceivable occur via a single photon process.

Because no ligand decomposition is observed, it is tempting to say that V^+ is less reactive towards benzene than Ti^+. This trend has been observed for other various hydrocarbons in previous experiments investigating metal-carbide clusters.[45,46] In these experiments pure Ti and V targets were laser ablated in the presence of small hydrocarbons. Both metals dehydrogenate the hydrocarbons by insertion into the C-H bonds to form metal-carbide species, but the extent to which this occurred was far greater for Ti, indicating a higher reactivity for this metal. Similar results have been observed in reaction studies using several different hydrocarbons, all pointing to a greater reactivity of Ti^+ than V^+.[43,44]

The photofragmentation of $Ni^+(C_6H_6)$ at 355 nm is also shown in Figure 3.3. This complex fragments via two parallel pathways, simple ligand elimination of neutral benzene and a photoinduced charge transfer pathway. $Ni^+(C_6H_6)$ is bound by 58.1 kcal/mol (2.52 eV),[20] which is less than the incident photon energy (3.50 eV). The fact that a charge transfer is seen is somewhat intriguing. As reported earlier by this group,[17] an upper limit can be placed on the metal ion-ligand bond energy in systems that display photoinduced charge transfer according to the following equation:

$$D_0 \leq h\nu - \Delta IP$$

where $h\nu$ is the incident photon energy and ΔIP is equal to the difference in the ionization potentials between the metal and the ligand. In the case of $Ni^+(C_6H_6)$, an upper limit of $D_0 \sim$ 1.89 eV can be derived for excitation at 355 nm with ΔIP equal to 9.24–7.63 = 1.61 eV. Surprisingly, this does not agree with the experimentally obtained bond energy (2.52)[20] for this system. It is possible that this pathway is caused by a multiphoton process, but the fact that it is observed at low laser fluence suggests that this is not the case. Another possibility is that there could be a small fraction of $Ni^+(C_6H_6)$ in the molecular beam that is trapped in a metastable excited state. Ni^+ has a ^2D ground state with a spin-forbidden ^4F state ~1 eV higher in energy.[47] The difference between the CID bond energy and the upper limit on the dissociation energy found by photoinduced charge transfer is approximately equal to this value (0.92 eV) indicating that the charge transfer seen here is probably due to photoexcitation of a metastable excited state in the complex that correlates to this atomic state. If this is true, it would suggest an upper limit of 1.61 eV for the binding energy of the quartet $Ni^+(C_6H_6)$ complex.

It is interesting to see what happens to the fragmentation pattern of these complexes when more than one ligand is attached. The photofragmentation difference mass spectra at 355 nm for $M^+(C_6H_6)_2$ (M=Ti, V, Ni) are shown in Figure 3.4. As shown, all three complexes fragment primarily by the loss of a single neutral benzene ligand. Some further fragmentation is seen for $Ti^+(C_6H_6)_2$, but this is attributed to multiphoton processes. This pattern suggests that the interaction between the metal-ion and the second ligand is not as strong as the interaction with the first. If one examines the bond energies of the metal ion to the second benzene ligand, this is true for Ti and Ni (2.62 vs. 2.68 eV and 1.52 vs. 2.52 eV, respectively), but not for V (2.55 vs. 2.42).[20] In the case of all of these complexes, the incident photon energy (355 nm, 3.50 eV)

Figure 3.4 Photofragmentation difference mass spectra of $M^+(C_6H_6)_2$ complexes at 355 nm where M=Ti, V, and Ni.

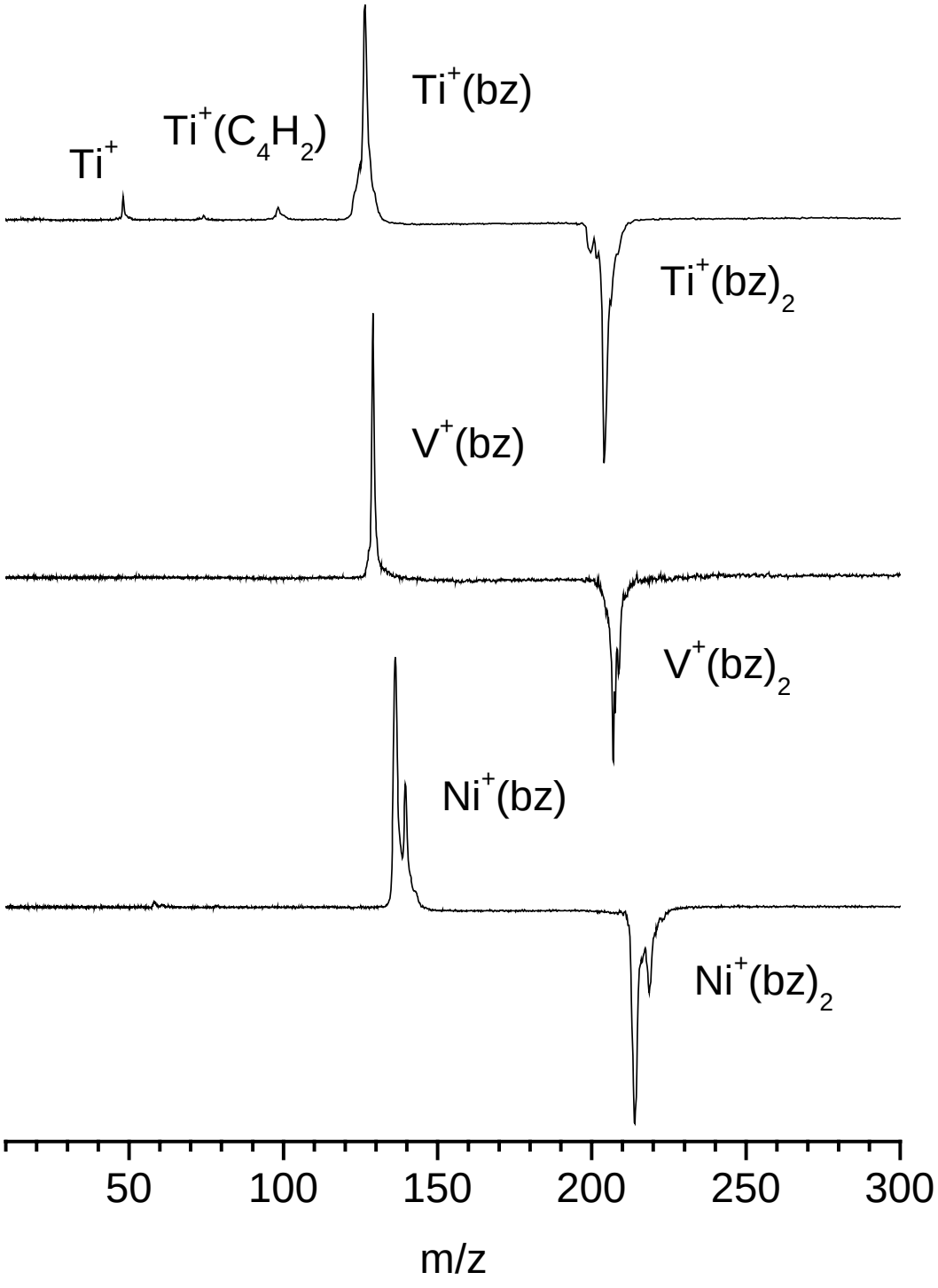
Ti+
Ti+(C4H2)
Ti+(bz)
Ti+(bz)2
V+(bz)
V+(bz)2
Ni+(bz)
Ni+(bz)2
50
100
150
200
250
300
m/z

exceeds the bond energy of the second ligand, and, therefore the loss of a whole benzene unit is not surprising. The same results were reported for $V^+(C_6H_6)_2$ by Yeh and coworkers.[41]

Transition metal ion-benzene complexes are usually expected to have a coordination number of two, as in the familiar sandwich structures. However, the rice-ball structures suggested by Kaya and coworkers[22] would imply that some metals have coordination numbers of three or more. Thus, it is interesting to study the photofragmentation of $M^+(C_6H_6)_x$ ($x \geq 2$) complexes to see if fragmentation patterns similar to those seen in the $M^+(C_6H_6)$ complexes arise. Interesting photochemistry occurs in complexes with more than two benzene ligands. As mentioned earlier, the coordination in these systems could be complete with two benzene ligands attached to the metal cation but the possibility of higher coordination numbers cannot be ruled out. These systems are expected to be strongly bound (~1.5 to 2.5 eV).[20] As more benzene ligands are attached to the cluster, at some point they will not be able to make direct contact with the metal cation because coordination is complete. The benzene ligands instead will attach to the "core" benzene ligands and essentially pile up on the outside of the cluster, solvating the stable core within. The binding of the external ligands would approximate that of a neutral benzene dimer (~1000 cm^{-1}).[52-54] The incident photon energy of 28,000 cm^{-1}, as used in this experiment, should be enough to evaporate all of these solvent ligands and leave only the stable core, whatever its coordination number might be. As shown in Figures 3.5, 3.6, and 3.7, this is exactly what is observed. In all three metal ion systems, all benzene molecules evaporate down to the $M^+(C_6H_6)_2$, as expected for bis-benzene sandwich complexes. For Ti and Ni, some $M^+(C_6H_6)$ is also produced at smaller cluster sizes. This is most likely due to multiphoton effects in which subsequent fragmentation of the sandwich core occurs, as these fragments are not observed at lower laser fluences. These results clearly demonstrate that coordination for these metal ion-

Figure 3.5 Photofragmentation difference mass spectra of $Ti^{+}(C_6H_6)_{3\text{-}7}$ complexes at 355 nm.

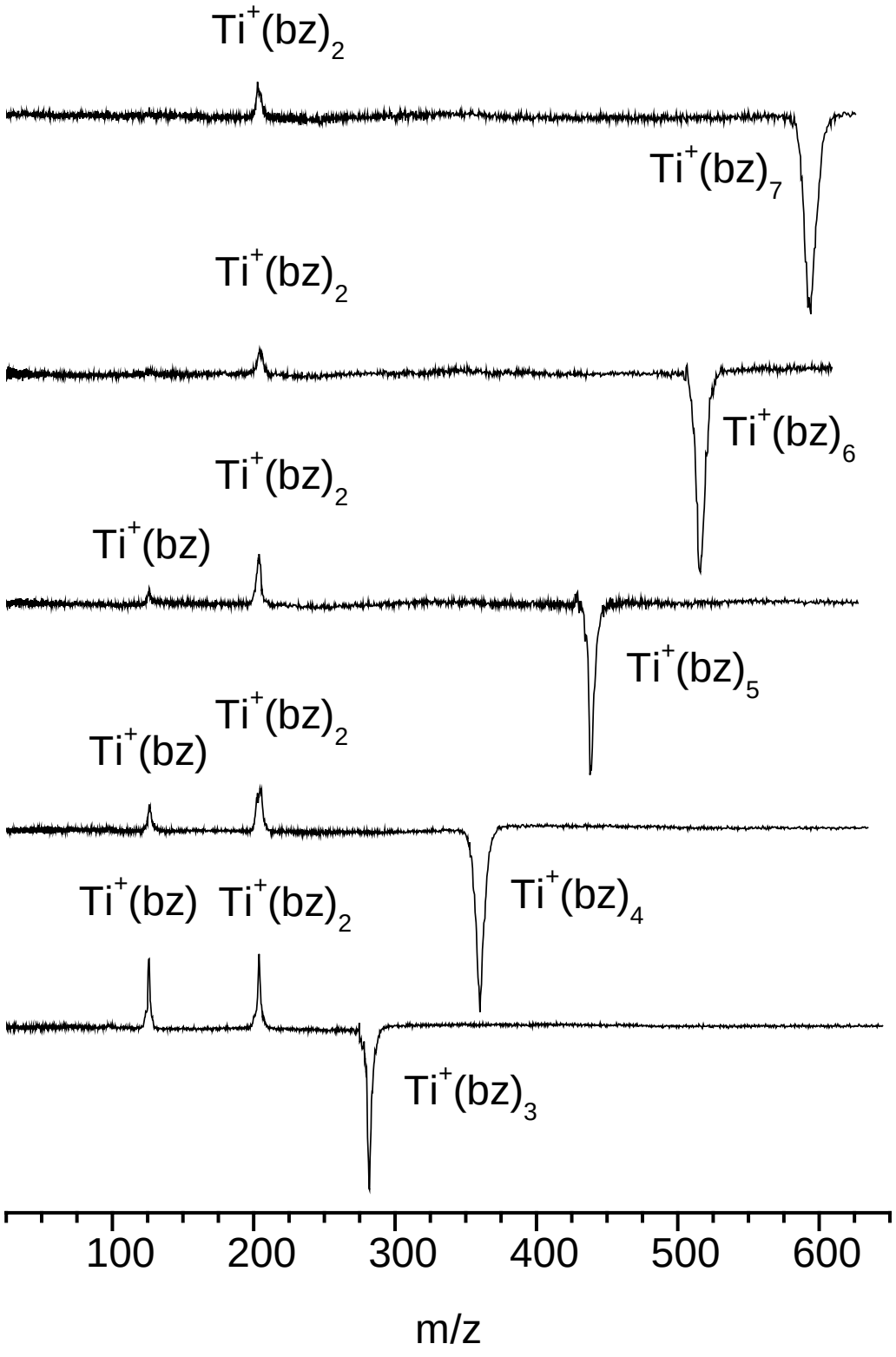
Ti+(bz)2
Ti+(bz)7
Ti+(bz)2
Ti+(bz)6
Ti+(bz)2
Ti+(bz)
Ti+(bz)5
Ti+(bz)2
Ti+(bz)
Ti+(bz)4
Ti+(bz)
Ti+(bz)2
Ti+(bz)3
100
200
300
400
500
600
m/z

Figure 3.6 Photofragmentation difference mass spectra of $V^+(C_6H_6)_{3\text{-}7}$ complexes at 355 nm.

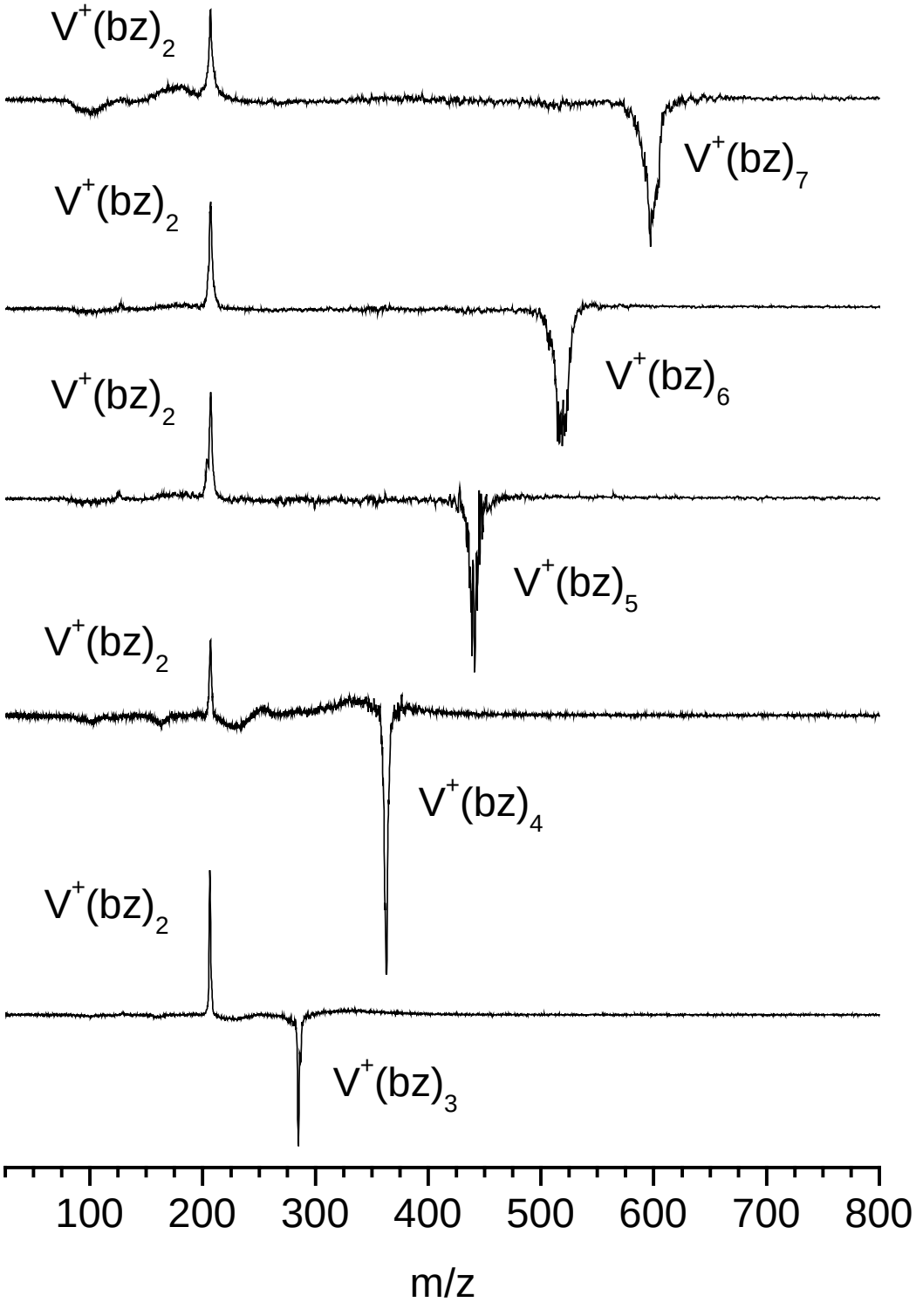
V+(bz)2
V+(bz)7
V+(bz)2
V+(bz)6
V+(bz)2
V+(bz)5
V+(bz)2
V+(bz)4
V+(bz)2
V+(bz)3
100
200
300
400
500
600
700
800
m/z

Figure 3.7 Photofragmentation difference mass spectra of $Ni^+(C_6H_6)_{3\text{-}6}$ complexes at 355 nm.

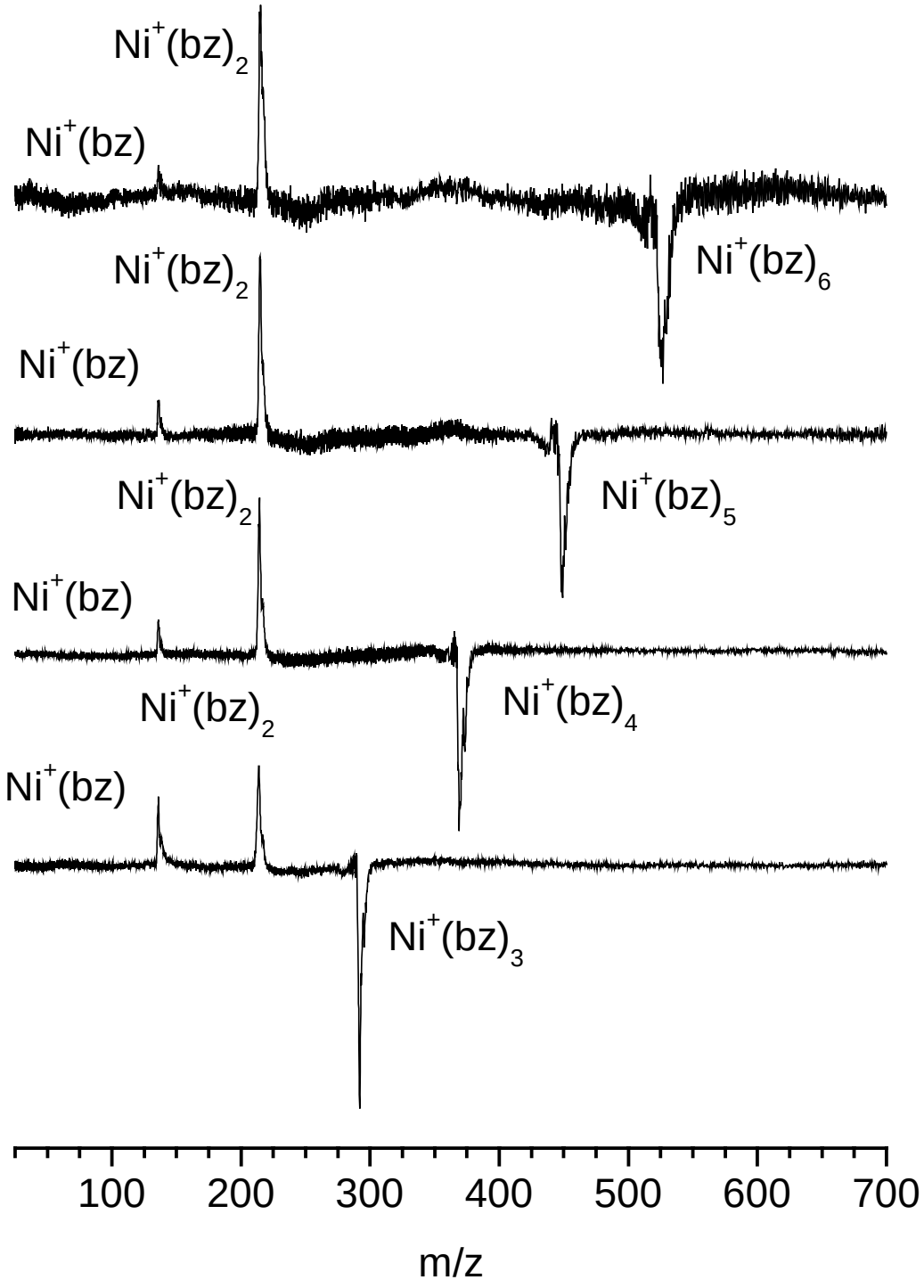
Ni+(bz)2
Ni+(bz)
Ni+(bz)6
Ni+(bz)2
Ni+(bz)
Ni+(bz)5
Ni+(bz)2
Ni+(bz)
Ni+(bz)4
Ni+(bz)2
Ni+(bz)
Ni+(bz)3
100
200
300
400
500
600
700
m/z

benzene complexes is complete at two. Additional ligands appear to solvate this stable sandwich core. It is interesting that none of the complexes show coordination numbers larger than two, especially since work performed by this group on $Ni^+(acetylene)_x$ complexes demonstrated the ability of Ni^+ to have a coordination number four.[55] Future studies should be performed using other metal ions to investigate if any metal ion-benzene systems can have a coordination number greater than two.

Conclusions

Titanium, vanadium, and nickel metal ion-benzene systems have been studied using fixed frequency photodissociation at 355 nm. $Ti^+(C_6H_6)$ fragments by ligand decomposition while $V^+(C_6H_6)$ and $Ni^+(C_6H_6)$ fragment by simple ligand elimination. There is evidence in dissociation mass spectra for $Ti^+(C_6H_6)$ and $Ni^+(C_6H_6)$ that metastable excited states are present in the molecular beam. For $Ni^+(C_6H_6)$ this results in a photoinduced charge transfer pathway. Complexes with two benzene ligands fragment via the loss of a whole benzene unit. Complexes with more than two benzene ligands fragment completely to the $M^+(C_6H_6)_2$ complex as a common fragment indicating coordination is complete with the addition of two benzene ligands and subsequent ligands act as solvent molecules. There is no evidence for complexes with a coordination number greater than two.

References

(1) Russell, D.H., ed., *Gas Phase Inorganic Chemistry*, Plenum, New York, 1989.

(2) Eller, K.; Schwarz, H. *Chem. Rev.* **1991**, *91*, 1121.

(3) Freiser, B.S., ed., *Organometallic Ion Chemistry*, Kluwer, Dordrecht, 1996.

(4) *Gas Phase Metal Ion Chemistry* (special issue), Leary, J.J.; Armentrout, P.B., eds., *Intl. J. Mass Spectrom.* **2001**, *204*, 1-294.

(5) a) Ma, J.C.; Dougherty, D.A. *Chem. Rev.* **1997**, *97*, 1303. b) Dougherty, D.A. *Science* **1996**, *271*, 163.

(6) Caldwell, J.W.; Kollman, P.A. *J. Am. Chem. Soc.* **1995**, *117*, 4177.

(7) Muetterties, E.L.; Bleeke, J.R.; Wucherer, E.J.; Albright, T.A. *Chem. Rev.* **1982**, *82*, 499.

(8) Long, N.J. *Metallocenes*, **1998**, Blackwell Sciences, Ltd., Oxford, UK.

(9) Fischer, E.O.; Hafner, W. *Z. fuer Naturforsch.* **1955**, *10B*, 665.

(10) Fritz, H.R. *Adv. Organometallic Chem.* **1964**, *1*, 239.

(11) Aleksanyan, V.T. *Vib. Spectra and Structure* **1982**, *11*, 107.

(12) K. Nakamoto, *Infrared and Raman Spectra of Inorganic and Organometallic Compounds,* 5th edition, Part B, Wiley Interscience, New York, 1997.

(13) van Heijnsbergen, D.; von Helden, G.; Meijer, G.; Maitre, P.; Duncan, M.A. *J. Am. Chem. Soc.* **2002**, *124*, 1562.

(14) van Heijnsbergen, D.; Jaeger, T.D.; von Helden, G.; Meijer, G.; Duncan, M.A. *Chem. Phys. Lett.* **2002**, *364*, 345.

(15) Jaeger, T.D.; van Heijnsbergen, D.; Klippenstein, S.J.; von Helden, G.; Meijer, G.; Duncan, M.A. *J. Am. Chem. Soc.*, **2004**, *126*, 10981.

(16) Jaeger, T.D.; Pillai, E.D.; Duncan, M.A. *J. Phys. Chem A* **2004**, *108*, 6605.

(17) a) Willey, K.F.; Cheng, P.Y.; Bishop, M.B.; Duncan, M.A. *J. Am. Chem. Soc.* **1991**, *113*, 4721. b) Willey, K.F.; Yeh, C.S.; Robbins, D.L.; Duncan, M.A. *J. Phys. Chem.* **1992**, *96*, 9106.

(18) Kealy, T.J.; Paulson, P.L. *Nature* **1951**, *168*, 1039.

(19) a) Jacobson, D.B.; Freiser, B.S. *J. Am. Chem. Soc.* **1984**, *106*, 3900. b) Jacobson, D.B.; Freiser, B.S. *J. Am. Chem. Soc.* **1984**, *106*, 4623. c) Rufus, D.; Ranatunga, A.; Freiser, B.S. *Chem. Phys. Lett.* **1995**, *233*, 319.

(20) a) Chen, Y.M.; Armentrout, P.B. *Chem. Phys. Lett.* **1993**, *210*, 123. b) Meyer, F.; Khan, F.A.; Armentrout, P.B. *J. Am. Chem. Soc.* **1995**, *117*, 9740. c) Armentrout, P.B.; Hales, D.A.; Lian, L. *Adv. Metal Semicon. Clusters* (M.A. Duncan, editor) **1994**, *2*, 1 (JAI Press, Greenwich, CT). d) Rogers, M.T., Armentrout, P.B. *Mass Spectrom. Rev.* **2000**, *19*, 215.

(21) a) Dunbar, R.C.; Klippenstein, S.J.; Hrusak, J.; Stöckigt, D.; Schwartz, H. *J. Am. Chem. Soc.* **1996**, *118*, 5277. b) Ho, Y.P.; Yang, Y.C.; Klippenstein, S.J.; Dunbar, R.C. *J. Phys. Chem. A* **1997**, *101*, 3338.

(22) a) Hoshino, K.; Kurikawa, T.; Takeda, H.; Nakajima, A.; Kaya, K. *J. Phys. Chem.* **1995**, *99*, 3053. b) Judai, K.; Hirano, M.; Kawamata, H.; Yabushita, S.; Nakajima, A.; Kaya, K. *Chem. Phys. Lett.* **1997**, *270*, 23. c) Yasuike, T.; Nakajima, A.; Yabushito, S.; Kaya, K. *J. Phys. Chem. A* **1997**, *101*, 5360. d) Kurikawa, T.; Takeda, H.; Hirano, M.; Judai, K.; Arita, T.; Nagoa, S.; Nakajima, A.; Kaya, K. *Organometallics* **1999**, *18*, 1430. e) Nakajima, A.; Kaya, K. *J. Phys. Chem. A*, **2000**, *104*, 176.

(23) Weis, P.; Kemper, P.R.; Bowers, M.T. *J. Phys. Chem. A* **1997**, *101*, 8207.

(24) a) Sodupe, M.; Bauschlicher, C.W. *J. Phys. Chem.* **1991**, *95*, 8640. b) Sodupe, M.; Bauschlicher, C.W.; Langhoff, S.R.; Partridge, H. *J. Phys. Chem.* **1992**, *96*, 2118. c) Bauschlicher, C.W.; Partridge, H.; Langhoff, S.R. *J. Phys. Chem.* **1992**, *96*, 3273. d) Sodupe, M.; Bauschlicher, C.W. *Chem. Phys.* **1994**, *185*, 163.

(25) Stöckigt, D. *J. Phys. Chem. A* **1997**, *101*, 3800.

(26) a) Yang, C.-N.; Klippenstein, S.J. *J. Phys. Chem.* **1999**, *103*, 1094. b) Klippenstein, S.J.; Yang, C.-N. *Intl. J. Mass Spectrom.* **2000**, *201*, 253.

(27) Chaquin, P.; Costa, D.; Lepetit, C.; Che, M. *J. Phys. Chem.* **2001**, *105*, 4541.

(28) Pandey, R.; Rao, B.K.; Jena, P.; Alvarez Blanco, M. *J. Am. Chem. Soc.* **2001**, *123*, 3799.

(29) Li, Y.; Baer, T. *J. Phys. Chem. A* **2002**, *106*, 9820.

(30) Kaczorwska, M.; Harvey, J.M. *Phys. Chem. Chem. Phys.* **2002**, *4*, 5227.

(31) Gerhards, M.; Thomas, O.C.; Nilles, J.M.; Zheng, W.-J.; Bowen, K.H., Jr. *J. Chem. Phys.* **2002**, *116*, 10247.

(32) Judai, K; Sera, K.; Amatsutsumi, S.; Yagi, K.; Yasuike, T.; Nakajima, A.; Kaya, K. *Chem. Phys. Lett.* **2001**, *334*, 277.

(33) a) Cabarcos; O.M.; Weinheimer, C.J.; Lisy, J.M. *J. Chem. Phys.* **1998**, *108*, 5151. b) Cabarcos; O.M.; Weinheimer, C.J.; Lisy, J.M. *J. Chem. Phys.* **1999**, *110*, 8429.

(34) a) Reddic, J.E.; Robinson, J.C.; Duncan, M.A. *Chem. Phys. Lett.* **1997**, *279*, 203. b) Grieves, G.A.; Buchanan, J.W.; Reddic, J.E.; Duncan, M.A. *Intl. J. Mass Spectrom.* **2001**, *204*, 223.

(35) Buchanan, J.W.; Grieves, G.A.; Reddic, J.E.; Duncan, M.A. *Intl. J. Mass Spectrom.* **1999**, *182/183*, 323.

(36) a) Buchanan, J.W.; Reddic, J.E.; Grieves, G.A.; Duncan, M.A. *J. Phys. Chem. A* **1998**, *102*, 6390. b) Buchanan, J.W.; Grieves, G.A.; Flynn, N.D.; Duncan, M.A. *Intl. J. Mass Spectrom.* **1999**, *185-187*, 617.

(37) Foster, N. R.; Grieves, G. A.; Buchanan, J. W.; Flynn, N. D.; Duncan, M. A. *J. Phys. Chem. A,* **2000**, *104*, 11055.

(38) Jaeger, T.D.; Duncan, M.A. *J. Phys. Chem. A*, in print.

(39) Hsu, H.C.; Lin, F.W.; Lai, C.C.; Su, P.H.; Yeh, C.S *New J. Chem.* **2002**, *26*,481.

(40) Su, P.H; Lin, F.W.; Yeh, C.S. *J. Phys. Chem. A* **2001**, *105*, 9643.

(41) Lee, H.F.; Lin, F.W.; Yeh, C.S. *J. Mass. Spec.* **2001**, *36*, 493.

(42) Duncan, M.A. *Intl. Rev. Phys. Chem.* **2003**, *22*, 407.

(43) Tunkyn, R.; Ronan, M.; Weisshaar, J.C. *J. Phys. Chem.* **1988**, *92*, 92.

(44) Eller, K.; Schwarz, H. *Chem. Rev.* **1991**, *91*, 1121.

(45) a) Guo, B.C.; Kerns, P.; Castleman, Jr., A.W. *Science* **1992**, *255*, 1411 b) Guo, B.C; Wei, S.; Purnell, J.; Buzza, S.; Castleman, Jr. A.W. *Science* **1992**, *256*, 515. c) Wei, S.; Guo, B.C.; Purnell, J.; Buzza, S.; Castleman, Jr. A.W. *Science* **1992**, *256*, 818. d) Guo, B.C; Wei, S.; Purnell, J.; Buzza, S.; Castleman, Jr. A.W. *J. Phys. Chem.* **1992**, *96*, 4166. e) Cartier, S.F.; Chen, Z.Y.; Walder, G.J.; Sleppy, C.R.; Castleman, Jr., A.W. *Science* **1993**, *260*, 195.

(46) a) Pilgrim, J.S.; Duncan, M.A. *J. Am. Chem. Soc.* **1993**, *115*, 6958. b) Pilgrim, J.S.; Duncan, M.A. *J. Am. Chem. Soc.* **1993**, *115*, 9724. c) Duncan, M.A. *J. Clust. Sci.* **1997**, *8*, 239.

(47) Stein, S.E., "Mass Spectrum" in NIST Chemistry WebBook, NIST Standard Reference Database Number 69, Eds. P.J. Linstrom and W.G. Mallard, March 2003, National

Institute of Standards and Technology, Gaithersburg MD, 20899 (http://webbook.nist.gov).

(48) a) Van Koppen, P.A.M.; Kemper, P.R.; Bowers, M.T. *J. Am Chem. Soc.* **1992**, *114*, 10941. b) Van Koppen, P.A.M.; Kemper, P.R.; Bowers, M.T. *J. Am. Chem. Soc.* **1992**, *114*, 1083.

(49) Weisshaar, J.C. *Acc. Chem. Res.* **1993**, *26*, 213.

(50) Armentrout, P.B. *Annu. Rev. Phys. Chem.* **1990**, *41*, 313.

(51) Fisher, E.R.; Elkind, J.L.; Clemmer, D.E.; Georgiadia, R.; Loh, S.K.; Aristov, N.; Sunderlin, L.S.; Armentrout, P.B. *J. Chem. Phys.* **1990**, *93*, 2676.

(52) Grover, J.R.; Walters, E.A.; Hui, E.T. *J. Phys. Chem.* **1987**, *91*, 3233.

(53) Krause, H.; Ernstberger, B.; Neusser, H.J. *Chem. Phys. Lett.* **1991**, *184*, 411.

(54) Sinnokrot, M.O.; Valeev, E.F.; Sherrill, C.D. *J. Am. Chem. Soc.* **2002**, *124*, 10887.

(55) Walters, R.S.; Jaeger, T.D.; Duncan, M.A. *J. Phys. Chem. A* **2002**, *106*, 10482.

CHAPTER 4

PHOTODISSOCIATION PROCESSES IN TRANSITION METAL CATION COMPLEXES WITH CYCLOOCTATETRAENE

Abstract

Transition metal cation complexes with 1,3,5,7-cyclooctatetraene of the form $M^+(C_8H_8)_{1,2}$ (M=V, Fe, Ni, and Ag) are produced by laser vaporization in a pulsed nozzle cluster source. The clusters are mass-selected and photodissociated using the second and third harmonics of an Nd:YAG laser (532 and 355 nm). The first row transition metal complexes undergo retro-cyclotrimerization to produce M^+(benzene). The photodissociation of $V^+(C_8H_8)$ also produces a significant amount of $V^+(C_5H_5)$. This is attributed to the ability of V^+ to donate electron density to stabilize a cyclopentadienyl anion. Dissociation of $Ag^+(C_8H_8)$ exhibits a photoinduced charge transfer pathway allowing an upper limit of 2.6 eV to be placed on the binding energy in this system. Complexes with two C_8H_8 molecules primarily dissociate by loss of intact C_8H_8 molecules with some fragmentation to $M^+(C_{10}H_{10})$ for M^+=V and Fe. Fragmentation of these $M^+(C_{10}H_{10})$ species indicates a structure that is not ferrocene-like in nature. Mixed sandwich complexes are produced with both COT and benzene as ligands, and these dissociate by eliminating benzene, indicating that COT is more strongly bound to these transition metal ions. The results of these experiments shed new insight on the bonding and photochemistry of these organometallic systems.

Introduction

A fascinating variety of unusual organometallic complexes have been produced by new molecular beam cluster studies, including many novel sandwich complexes.[1-18] The condensed phase synthesis of well-known complexes such as ferrocene[19] and dibenzene chromium[20] has over the years prompted extensive work to investigate sandwiches of various ligands in the gas phase. Theoretical and experimental work has investigated new sandwich complexes containing benzene,[1,13] fullerenes[5,6,13,] and polycyclic aromatic hydrocarbons (PAH's).[11-17] Multiple decker sandwiches have been described for transition metal-benzene complexes,[1,6e] metal-PAH complexes[12] and metal-fullerenes[6] as well as for lanthanide metal-cyclooctatetraene (COT)[6e,18] systems. Photodissociation has been employed to unravel the structures of some of these complexes.[4-5,12-15,21] In the present work, we use photodissociation measurements to investigate new complexes between transition metals and COT.

Sandwich complexes with COT have been produced previously in the condensed phase[22-25] and in the gas phase.[6e,18] Uranocene was discovered in 1968 by Streitwieser and Müller-Westerhoff[22] and is structurally analogous to ferrocene, but contains an actinide core of uranium sandwiched between two COT ligands. Also similar to ferrocene, the stability of the structure is attributed to charge transfer from the metal to the ligands.[23-25] COT itself is anti-aromatic with eight π electrons, lacking two electrons to satisfy the aromaticity requirement of 4n+2 as established by Huckel's rule. Uranium donates two electrons to each ligand creating aromatic COT di-anions, which stabilizes the complex.[23-25] Based on this same concept, Kaya and coworkers performed gas phase studies to investigate the possibility of an extended stacking motif of lanthanide metals with COT.[6e,18] The mass spectra observed in their experiments

showed a pattern of magic numbers corresponding to $M_n^+(COT)_{n+1}$ (M=Ce, Nd, Eu, Ho,Yb) species, which they assigned to multiple decker sandwiches. Photoelectron spectroscopy of these complexes gave further evidence for these structures.[18] Unfortunately, these studies were limited to the lanthanide metals mentioned above. Transition metal ion-COT complexes have not been investigated, and these species may be equally interesting. Photodissociation experiments allow the stability of such clusters to be tested.

UV and visible photodissociation studies have been performed previously by our group for many metal cation-ligand systems including $M^+(benzene)_n$,[21] $M^+(C_{60})_n$,[5,13] $M^+(coronene)_n$.[12-15] In many cases photodissociation occurs by simple ligand elimination in which an intact neutral ligand leaves the cluster and the metal cation or a smaller metal-ligand species is the charged fragment. In other cases ligand decomposition can occur, and the metal complex loses smaller stable neutral fragments. Yet another dissociation pathway is photoinduced charge-transfer, as we have seen with several $M^+(benzene)_n$ systems.[21] Fragmentation of these complexes yields a charged organic and a neutral metal atom by either direct excitation into a charge-transfer transfer state at an energy above the dissociation limit or via an electronic curve crossing. For many metal ion-ligand systems, ligand elimination is expected based on the structural stability of the ligand studied. However, because COT is less stable and can dissociate to form stable species such as benzene, ligand decomposition reactions may be expected in these systems, and this is in fact observed.

Experimental Section

The experimental apparatus has been described previously.[26] Clusters are produced via laser vaporization (355 nm) in a pulsed nozzle cluster source and mass analyzed in a reflectron time-of-flight mass spectrometer. By using a "cutaway" type rod holder a free expansion of excess cot seeded in Ar produces clusters of the form $M^+(C_8H_8)_n$ efficiently. The molecular beam is skimmed from the source chamber into a differentially pumped mass spectrometer chamber. Cations are pulse accelerated into the first flight tube and mass selected by pulsed deflection plates located just prior to the reflection region. The ions of interest are then intersected by the second or third harmonic output of an Nd:YAG laser system, at 532 and 355 nm respectively. Excitation of these ions leads to subsequent fragmentation. Parent and fragment ions are mass analyzed in the second flight tube and detected using an electron multiplier tube and a digital oscilloscope (LeCroy 9310A). Data is transferred to a PC via an IEEE-488 interface.

Results and Discussion

The mass spectra of clusters obtained for COT with vanadium, iron and nickel are shown in Figure 4.1. These have been cropped to show the ions of interest, with a solid line denoting where the intensities of the atomic ions are off scale. As shown, the higher mass region is dominated by clusters of the form $M^+(C_8H_8)_n$, which correspond to intact COT adducts with atomic metal cations. Because metal atom recombination is limited in this particular cluster source configuration, multiple metal atom species, and in particular the possible multiple-decker sandwich clusters, are not produced efficiently. Also present at lower mass are complexes

Figure 4.1 Time-of-flight mass spectra for V, Fe, and Ni-COT complexes formed in an Ar expansion. The solid line at the top of each mass spectra indicates that they have been cropped to highlight the complexes of interest. The * denotes complexes of the form $M^+(Ar)_n$.

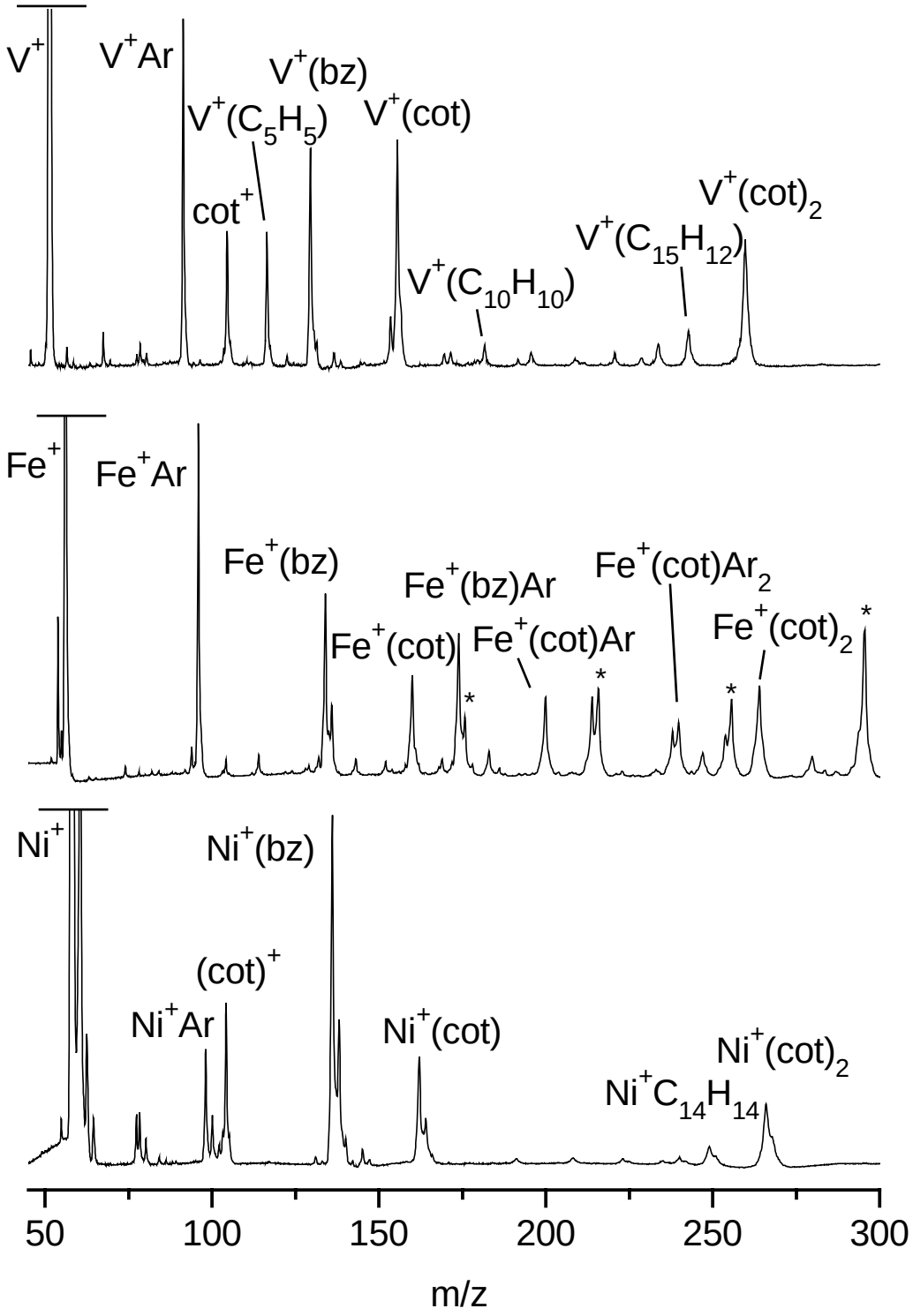
V+
V+Ar
V+(bz)
V+(C5H5)
V+(cot)
cot+
V+(cot)2
V+(C15H12)
V+(C10H10)
Fe+
Fe+Ar
Fe+(bz)
Fe+(bz)Ar
Fe+(cot)Ar2
Fe+(cot)
Fe+(cot)Ar
Fe+(cot)2
*
Ni+
Ni+(bz)
(cot)+
Ni+Ar
Ni+(cot)
Ni+(cot)2
Ni+C14H14
50
100
150
200
250
300
m/z

associated with COT dissociation products from the plasma chemistry, i.e. M^+(benzene), and the COT cation without any metal. The mass spectrum for vanadium also shows a significant amount of $V^+(C_5H_5)$. $Ag^+(COT)_n$ (not shown), on the other hand, forms only COT adducts with no ligand decomposition products. No clusters of pure metal, COT clusters, or multiple-decker sandwiches are observed in any of these systems. However, complexes of M^+Ar are observed for all species and M^+(ligand)Ar are formed extensively for M=Fe. Smaller peaks can be attributed to metal-water complexes or metal oxides from trace impurities either in the gas line or on the surface of the ablation target.

To begin the study of these metal-ligand complexes, it is first interesting to know how the ligand itself behaves. Neutral COT has been known to undergo a retro-cyclotrimerization reaction to form benzene and acetylene when exposed to light.[27] It is therefore interesting to see if similar behavior occurs for the COT cation. Figure 4.2 shows the photofragmentation mass spectrum of COT^+. For this study, the $C_8H_8^+$ cation was mass selected and excited at 532 nm. This data, as with all fragmentation spectra in this study, are generated with a previously described computer difference method.[26] A mass spectrum recorded with the laser off is subtracted from one with the laser on, producing a negative-going parent ion peak (i.e. depletion) and positive fragment peaks. Photodissociation spectra obtained previously for COT^+ demonstrate a large absorption cross section near 532 nm.[28] Thus, it is not surprising that COT^+ absorbs and fragments efficiently here. Fragmentation occurs by the loss of neutral H, leaving $C_8H_7^+$ and by the loss of neutral C_2H_2, leaving the benzene cation. A small amount of $C_7H_4^+$ is also observed from the loss of neutral CH_4. Fragmentation patterns with similar masses and intensities are observed in the electron impact and photoionization mass spectra of COT^+.[29-30] In these previous experiments, appearance energies were recorded for $C_8H_7^+$ (10.90 ± 0.10

Figure 4.2 Photofragmentation mass spectrum of cyclooctatetraene (COT) cation at 532 nm. The spectrum is generated by subtracting the mass spectrum with the laser off from the mass spectrum with the laser on leaving a negative-going peak for depleted complexes and positive peaks for fragments.

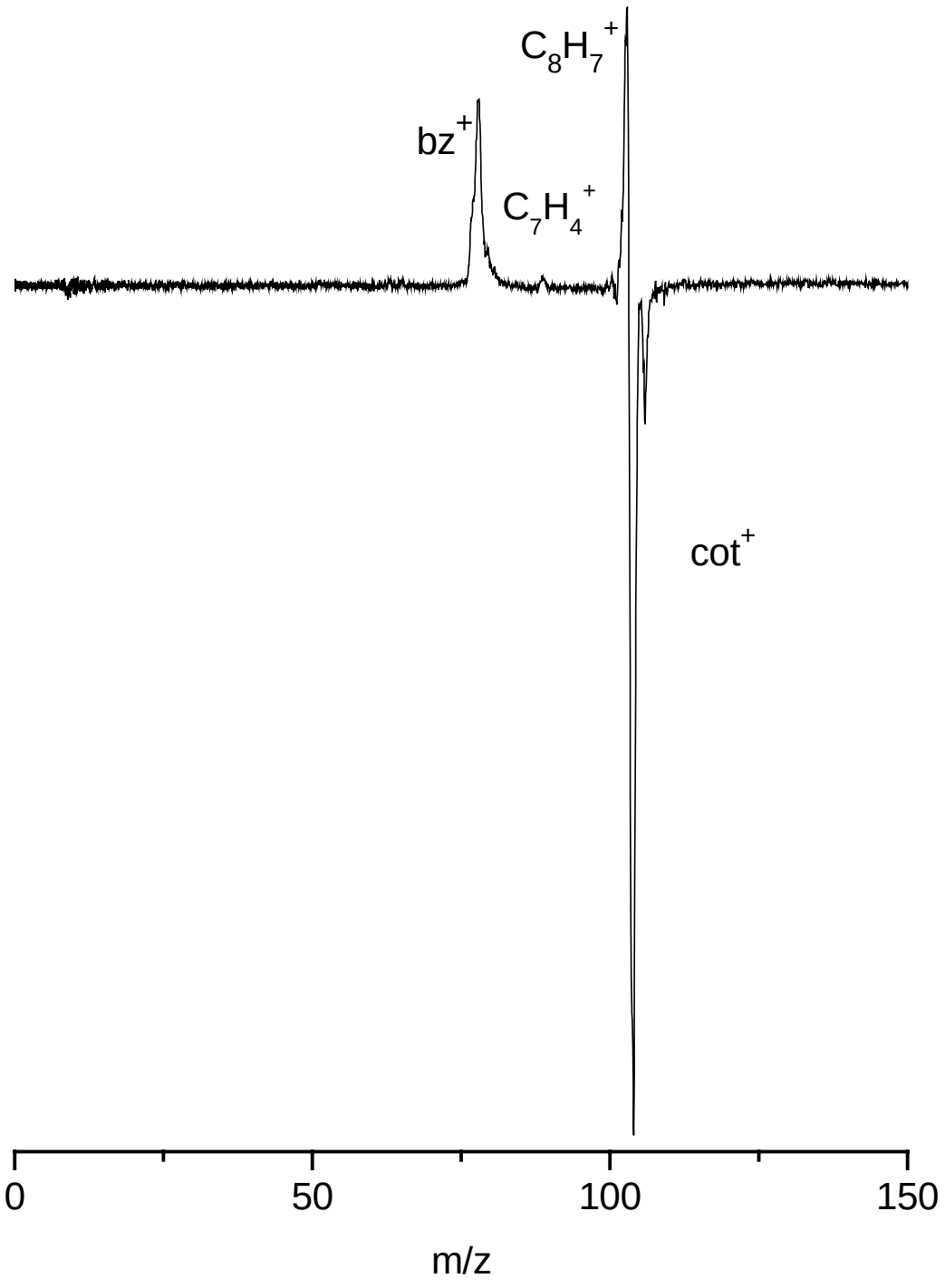
C8H7+
bz+
C7H4+
cot+
0
50
100
150
m/z

eV)[29]and for $C_6H_6^+$ (9.40 ± 0.05 eV).[30] When the IP of COT (8.2 ± 0.2 eV)[31] is subtracted from each of these measurements, the approximate energy for COT^+ dissociation into these channels can be calculated. This works out to 2.7 ± 0.2 eV for $C_8H_7^+$ and 1.2 ± 0.2 eV for $C_6H_6^+$. The incident photon energy in this experiment (532 nm=2.32 eV) is very close to these dissociation values. Hence, the photochemistry here could conceivably come from two different one-photon processes occurring in parallel, although we cannot rule out resonance-enhanced two photon processes.

As a first example of a metal-COT system, we examine $Ag^+(COT)$. Ag^+ has a d^{10} closed shell electronic configuration and the electronic structure of the complex should be relatively simple. The photofragmentation mass spectrum of $Ag^+(COT)$ at 355 nm is shown in Figure 4.3. The doublet in the negative going parent peak is attributed to the two naturally occurring isotopes (107,109) of Ag resolved in the $Ag^+(COT)$ parent. What appears to be a triplet is observed in the positive-going fragment portion of the spectrum. Actually, this triplet can be attributed to two distinct fragmentation channels: the Ag^+ fragment (mass 107 and 109) and the COT^+ fragment ion at mass 104. The former occurs from simple ligand elimination and the latter is a result of photoinduced charge-transfer dissociation. Just as there was no evidence of COT decomposition due to plasma chemistry in the mass spectrum of $Ag^+(COT)$, there also is no ligand decomposition upon photofragmentation. This experiment was performed with low laser fluence to ensure single photon processes. At higher photon energy subsequent fragmentation of COT^+ leads to the appearance of benzene$^+$. Previous work in this lab and others has demonstrated similar behavior from Ag^+(ligand) systems.[21,32] In this previous work it was shown that an upper limit could be placed on the metal ion-ligand bond energy according to the following equation:

Figure 4.3 Photofragmentation mass spectrum of $Ag^+(COT)$ at 355 nm. The complex fragments via two dissociation pathways: simple ligand elimination and photoinduced charge-transfer.

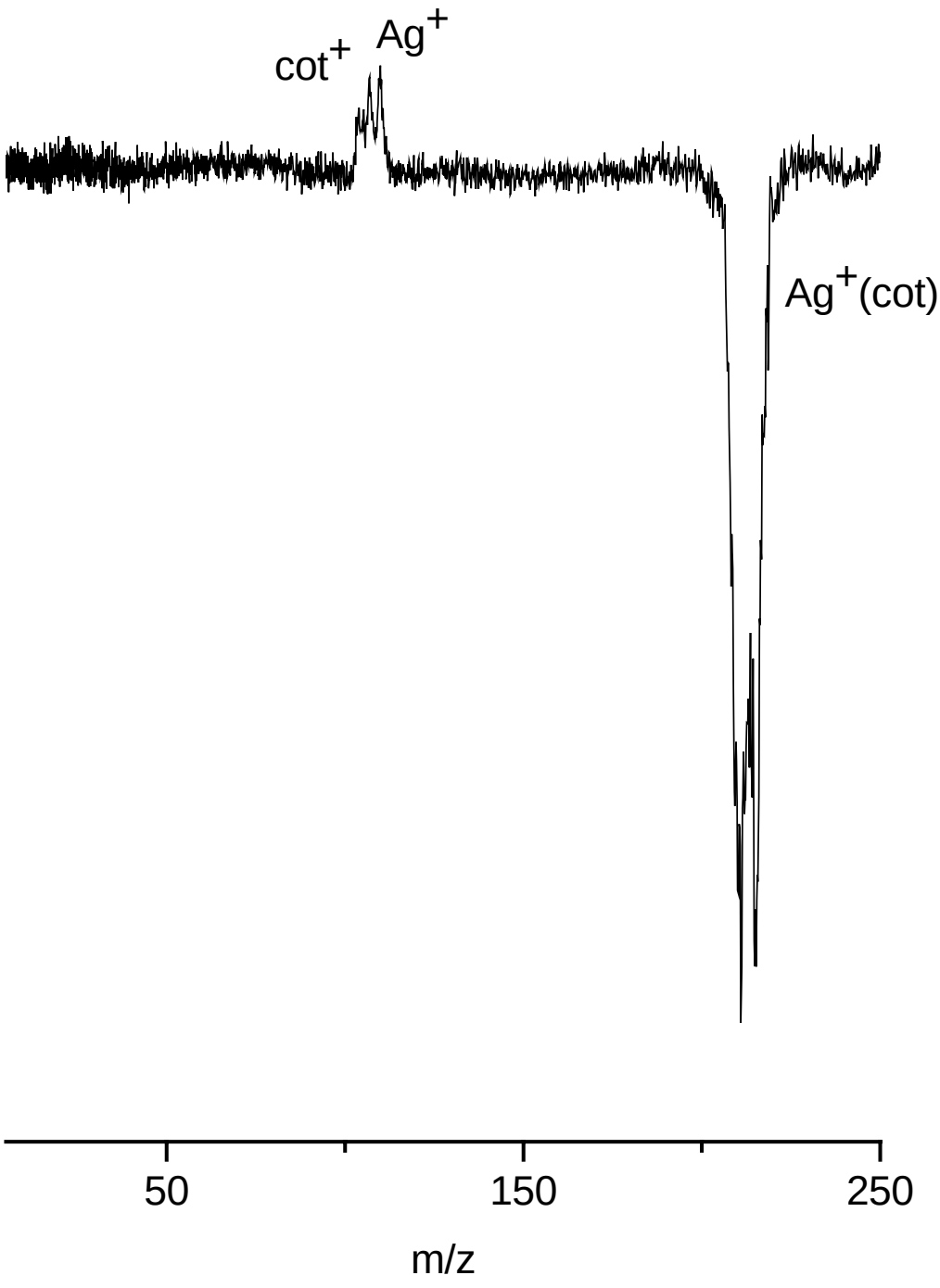
cot+
Ag+
Ag+(cot)
50
150
250
m/z

$$D_0 \leq h\nu - \Delta IP$$

where $h\nu$ is the incident photon energy and ΔIP is equal to the difference in the ionization potentials between the metal and the ligand. In the case of $Ag^+(COT)$, an upper limit of $D_0 \sim 2.8$ eV can be derived for excitation at 355 nm with ΔIP equal to 8.2–7.6 = 0.65 eV. However, this value is approximate because the ionization potential of COT has an uncertainty of ± 0.2 eV.

The photofragmentation mass spectra for the $M^+(COT)$ (M=V, Fe, Ni) systems with excitation at 355 nm are shown in Figure 4.4. Similar fragmentation patterns are seen with 532 nm, but with lower signal levels. The noise level is greater in the vanadium system, reflecting the lower photodissociation efficiency for this ion at this wavelength. All three systems are quite different from the $Ag^+(COT)$ system. There is no evidence for any charge transfer in these systems. Instead, the major fragmentation channel is the loss of C_2H_2 (i.e., acetylene) and the production of $M^+(C_6H_6)$, i.e., the metal-benzene complex. The different channels observed for these metals indicate perhaps a higher reactivity or a different bonding configuration for the transition metal species with partially filled d shells. The closed shell Ag^+ system would have more electrostatic bonding, while the open shelled species could have come covalent character in their binding. If the bonding is stronger in the V, Fe and Ni systems than it is in the Ag complex, the charge-transfer channel would lie at higher energy, perhaps explaining why it is not seen here. Although there is some evidence for elimination of intact COT in the nickel and iron complexes, it is not the main fragmentation pathway. It is also interesting that the channel corresponding to the loss of neutral H that was prevalent for the dissociation of COT^+ is absent from all metal ion-COT complexes. This probably indicates that the formation of a $M^+(C_8H_7)$

Figure 4.4 Photofragmentation mass spectra of V, Fe, and Ni cation mono-COT complexes at 355 nm.

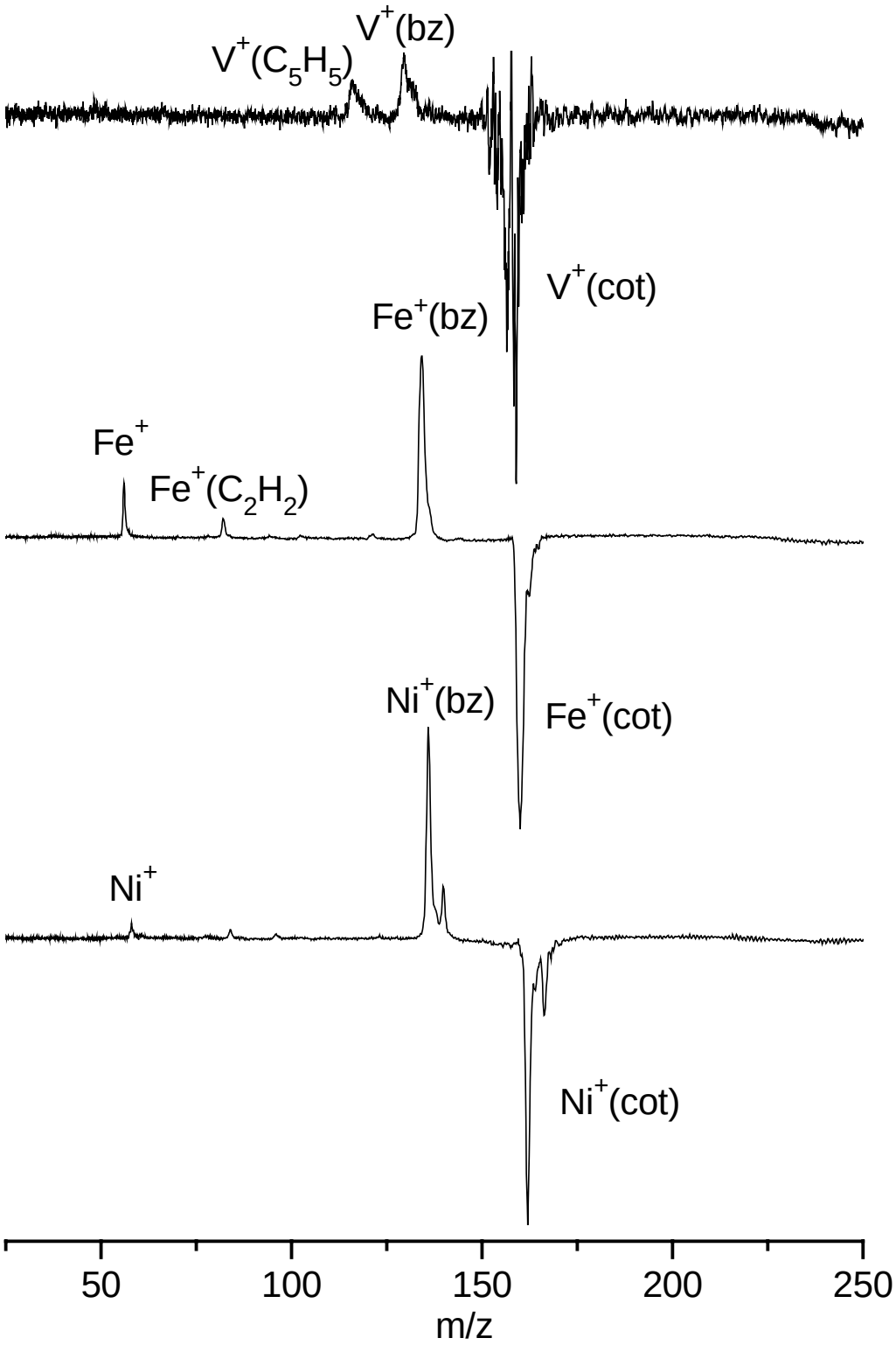
V+(bz)
V+(C5H5)
V+(cot)
Fe+(bz)
Fe+
Fe+(C2H2)
Ni+(bz)
Fe+(cot)
Ni+
Ni+(cot)
50
100
150
200
250
m/z

complex is energetically unfavorable compared to other possible channels. As noted earlier, the appearance energy of this channel in COT^+ is 1.5 eV higher in energy than the $C_6H_6^+$ channel. It is possible that the photon energy (355 nm = 3.49 eV) is not high enough in these metal-ligand systems to access this fragmentation pathway.

In many organometallic systems, stability is associated with 18 π electrons.[19,20,25] These mono-ligand systems are well shy of this number and so the relative stability of fragment ions must be examined in other contexts. The main fragmentation channel for V^+, Fe^+, and Ni^+ is the loss of neutral C_2H_2 to form M^+(benzene) complexes. This type of retro-cyclotrimerization of COT to benzene is seen in the photodissociation of COT^+ as well as in temperature-programmed desorption (TPD) experiments on Pt[33] and TiO_2[34] surfaces. It is known that first row transition metal cation-benzene complexes are relatively strongly bound. The dissociation energies of the relevant complexes are listed in Table 4.1.[35] High binding energies of the first row transition metals to benzene make the formation of such products quite favorable. The lower binding energy of Ag^+ to benzene might explain why metal-benzene formation is not seen upon photodissociation of its COT adduct. Another likely mechanism for the formation of these benzene complexes is excitation into metal cation-based excited states, which then lead to reaction with the COT ligand. The open-shelled transition metal cations all have low-lying excited states, and there will be molecular states of the complexes correlating to these that can be excited. Excited states of transition metal cations are often more reactive than ground states. Ag^+, however, has no low-lying atomic excited states, and therefore the only molecular state for the Ag^+(COT) complex is likely one correlating to the charge transfer asymptote. This could explain the lack of dissociative fragmentation in this system.

Table 4.1 Metal-ligand bond energies for various metal benzene complexes.

Species	D_0 (eV)[a]
$V^+(C_6H_6)$	2.42
$Fe^+(C_6H_6)$	2.15
$Ni^+(C_6H_6)$	2.42
$Ag^+(C_6H_6)$	1.62

[a]Ref. 35.

While the formation of M^+(benzene) fragments could be expected, it is surprising that we also detect an $M^+(C_5H_5)$ fragment in the case of the V^+ complex. $V^+(C_5H_5)$ appears here with an intensity almost equal to that of the V^+(benzene) fragment. The same kind of $M^+(C_5H_5)$ fragment is detected, but small, for Fe^+ and it is not detected for Ni^+. It is well known that C_5H_5 is not aromatic, but can become so as the cyclopentadienyl anion when it receives charge donation from metal in a complex.[19] The stability of ferrocene is known to occur by this mechanism, as two electrons from the metal core are donated to the two cyclopentadienyl ligands, thus stabilizing them and giving the overall complex 18 electrons.[19] It is likely that a similar charge transfer mechanism can occur to stabilize these mono-ligand complexes. Because the complexes studied here have a net charge, the metal could carry an effective oxidation state of +2 by donating one electron to stabilize C_5H_5, forming a complex of the nominal form $[M^{2+}(C_5H_5)^-]^+$. The tendency to do this should vary with the second ionization potential of the metal. The second IP of vanadium is in fact the lowest of the three metals studied here at 14.7 eV while those of Fe and Ni are 16.2 and 18.2 eV,[36] respectively. It is then reasonable that the vanadium cation is more likely to donate electron density to stabilize the C_5H_5 moiety. The higher second IP of Fe decreases the likelihood of this process, consistent with the low intensity of this photofragment, while the second IP of Ni is too high to allow the $Ni^+(C_5H_5)$ species to form. If this logic is correct, one might expect other metals with low second IP's, such as the lanthanides, to exhibit similar behavior. This has in fact been observed in our lab,[37] where M^+(COT) complexes of Sm^+, Dy^+, and Nd^+ (second IP's of 11.1, 11.7, and 10.8 eV, respectively) also photodissociate to produce the corresponding $M^+(C_5H_5)$ fragments.

Complexes with two COT ligands were also studied in order to investigate the stability of sandwich structures. The photofragmentation mass spectra for $V^+(COT)_2$, $Fe^+(COT)_2$, and

$Ni^+(COT)_2$ at 355 nm are shown in Figure 4.5. The fragmentation patterns at 532 nm are similar to these but with lower signal to noise. $Ag^+(COT)_2$ did not fragment at either wavelength and, therefore is not shown. All three di-COT complexes fragment primarily by the elimination of an intact COT unit. This is different from the mono-COT systems in which further ligand decomposition is seen as the primary dissociation pathway. This could indicate that the second COT ligand is less strongly bound than the first. This is not surprising if charge transfer from the metal is important in the bonding of these metal-COT complexes. COT requires two electrons to achieve aromatic character, and these metals just do not have enough electron-donating character to satisfy this need for two COT ligands. All three complexes show further fragmentation to M^+(bz) as is seen with the mono-COT complexes. It is not possible for our experiment to determine if this is a sequential process or a parallel fragmentation pathway. These same fragments are still seen at lower laser fluences, but power dependence studies cannot distinguish between a single photon process and a resonance enhanced two-photon process that has much higher cross section for one step.

$V^+(COT)_2$ has a minor fragmentation channel corresponding to the loss of C_2H_2 and both $V^+(COT)_2$ and $Fe^+(COT)_2$ have channels corresponding to the loss of C_6H_6, resulting in $M^+(C_{10}H_{10})$ fragment ions. This latter fragmentation is particularly interesting, because $M^+(C_{10}H_{10})$ could correspond either to a M^+(COT)(acetylene) complex or a $M^+(C_5H_5)_2$ complex analogous to ferrocene. Both Fe and V complexes with two cyclopentadienyl (Cp) ligands are well known in the condensed phase,[25] and the possibility of observing these complexes as dissociation products is intriguing. For either structure, the Fe and V complexes of $M^+(C_{10}H_{10})$ have a total of 17 and 16 electrons, respectively, and electron counts this close to 18 can result in relatively stable complexes. $Ni^+(C_{10}H_{10})$, on the other hand, would have 19 electrons, which

Figure 4.5 Photofragmentation mass spectra of V, Fe, and Ni cation di-COT complexes at 355 nm. These species fragment primarily by loss of intact COT molecules. Subsequent fragmentation follows the same patterns as observed for the mono-COT complexes.

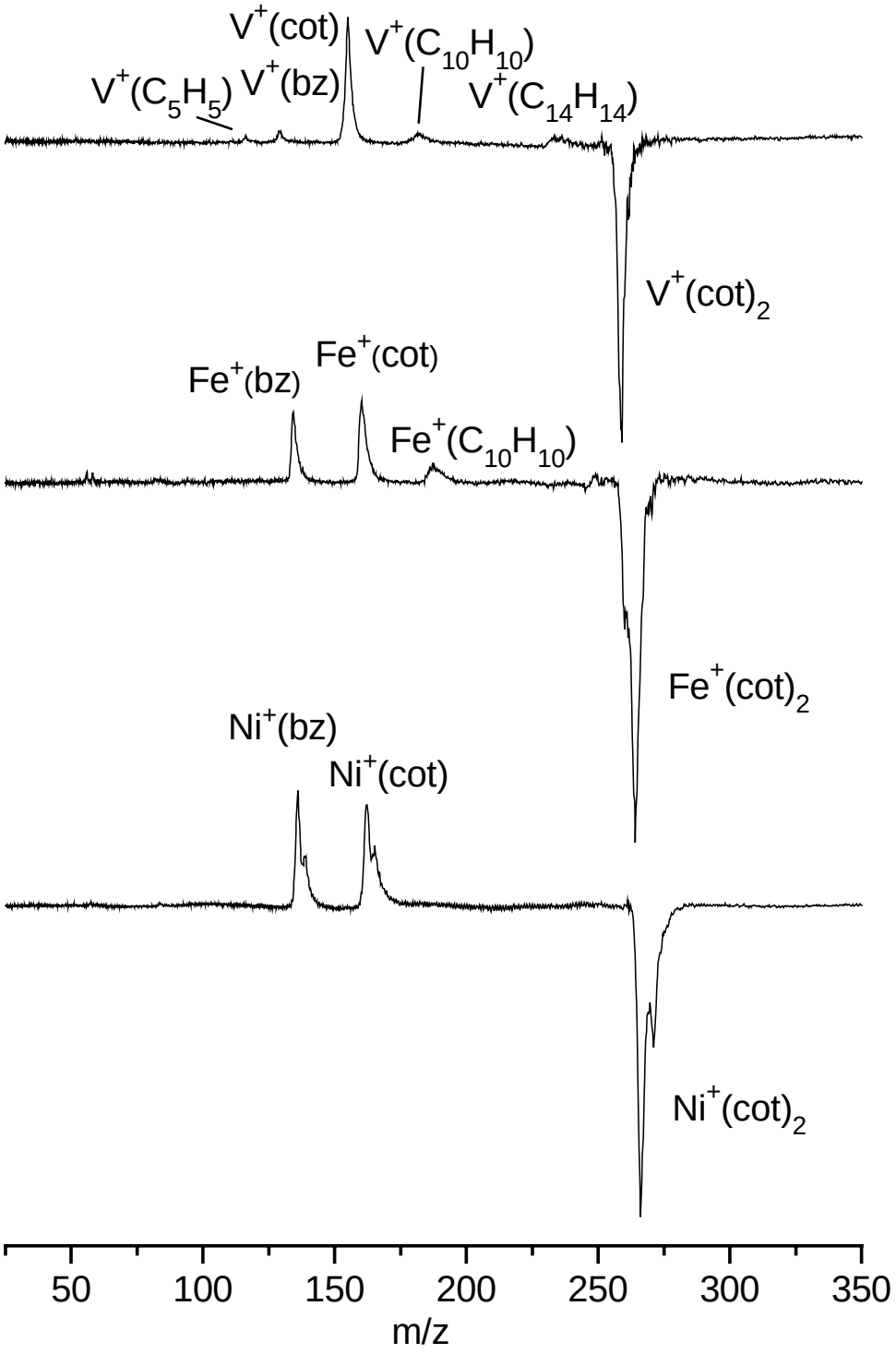
V+(cot)
V+(C10H10)
V+(C5H5)
V+(bz)
V+(C14H14)
V+(cot)2
Fe+(bz)
Fe+(cot)
Fe+(C10H10)
Fe+(cot)2
Ni+(bz)
Ni+(cot)
Ni+(cot)2
50
100
150
200
250
300
350
m/z

does not lead to stable complexes. Photodissociation measurements also make it possible to investigate the structures of these $M^+(C_{10}H_{10})$ ions. Because they are observed as plasma chemistry products in the mass spectra of V and Fe (see Figure 4.1), it is possible to mass select them and observe their fragmentation patterns. The photofragmentation mass spectra of $V^+(C_{10}H_{10})$ and $Fe^+(C_{10}H_{10})$ at 532 nm are shown in Figure 4.6. The primary fragment for both species is the loss of neutral C_2H_2 to form M^+(COT), with some formation of M^+(bz). This fragmentation pattern as well as the lack of any $M^+(C_5H_5)$ fragments indicates that these species are most likely the $M^+(COT)(C_2H_2)$ ions and not the ferrocene-like structures. This structure is apparently preferred because it leads to a species with nearly 18 electrons, with benzene as an excellent neutral leaving group, without the large-scale rearrangement necessary for the formation of ferrocene-like complexes.

Another interesting ion formed as a minor channel in the fragmentation of $Fe^+(C_{10}H_{10})$ is $Fe^+(C_9H_9)$. This ion is somewhat puzzling as CH is not generally considered to be a good neutral leaving group. It is possible that this complex could be Fe^+(cyclobutadiene)(Cp). Although cyclobutadiene does not exist on its own, it can be stabilized by a metal center, particularly in complexes with Fe, Co and Ni.[38,39] Unfortunately this species is not directly generated in the plasma and therefore could not be studied further.

As a final example of metal-COT complexes, we decided to make and study mixed species of the form M^+(COT)(benzene). If dissociation in these species proceeds by COT decomposition, it would be possible to produce $M^+(bz)_2$ or M^+(bz)(Cp) complexes as fragments. Figure 4.7 shows the fragmentation of V^+(COT)(bz) and Fe^+(COT)(bz) complexes. As indicated, the primary process in these systems is the loss of benzene to form the M^+(COT) fragment ion. At higher laser power, the smaller fragments that were formed by the

Figure 4.6 Photofragmentation mass spectra for $V^+(C_{10}H_{10})$ and $Fe^+(C_{10}H_{10})$ at 532 nm. Fragmentation patterns suggest that these complexes do not have ferrocene like structures.

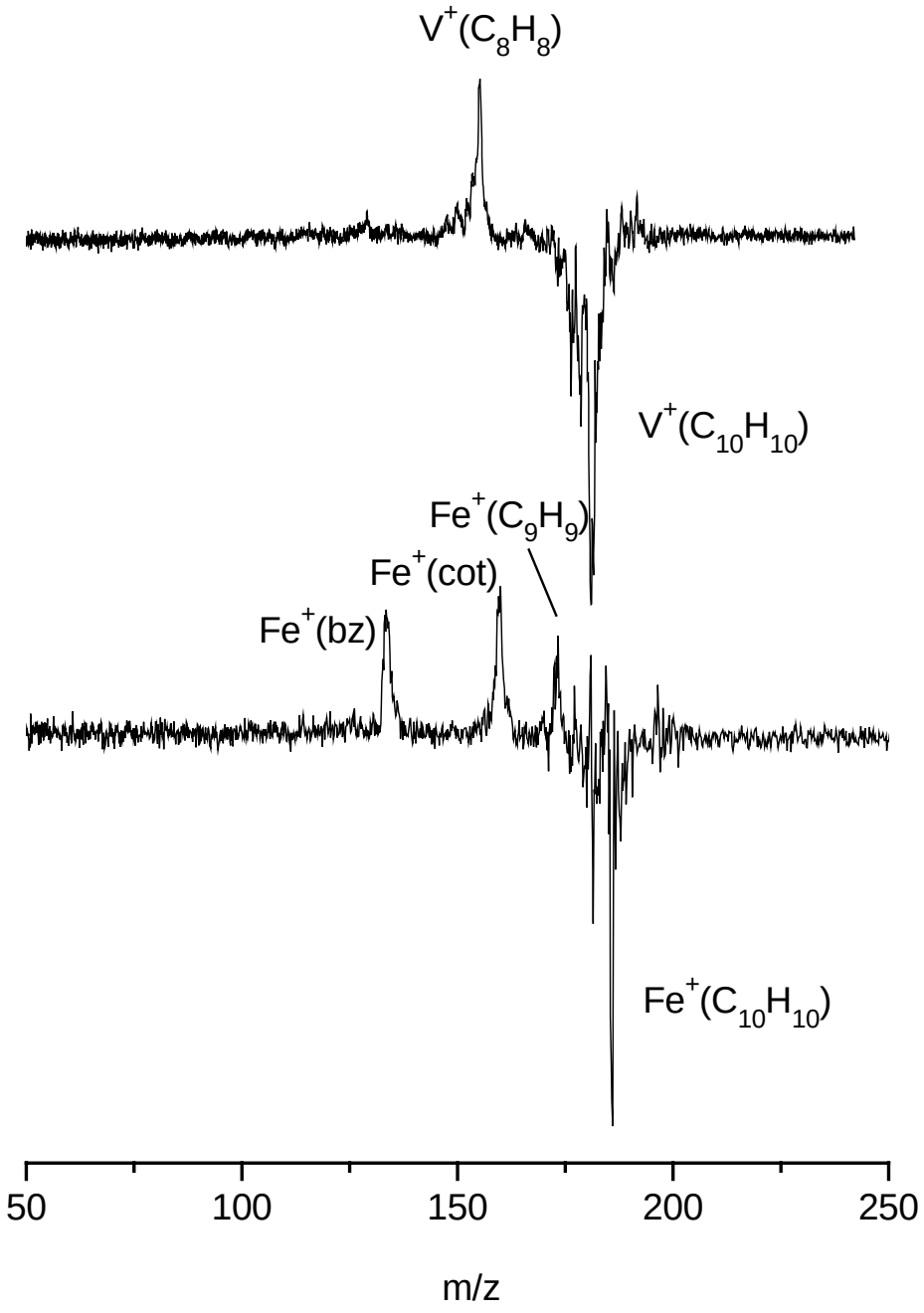
V+(C8H8)
V+(C10H10)
Fe+(C9H9)
Fe+(cot)
Fe+(bz)
Fe+(C10H10)
50
100
150
200
250
m/z

Figure 4.7 Photofragmentation mass spectrum for V^+(COT)(bz) and Fe^+(COT)(bz) at 532 nm.

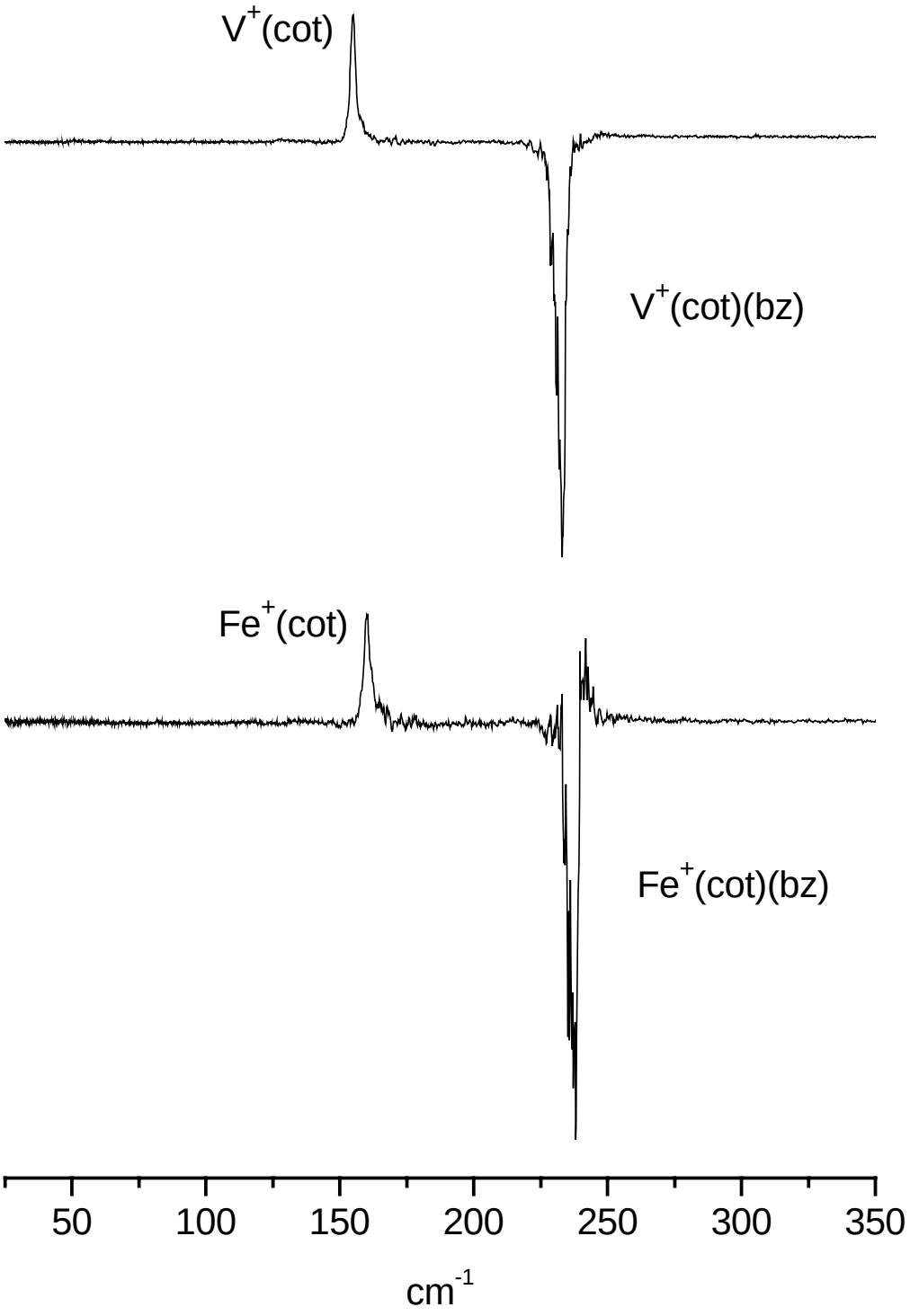
V+(cot)
V+(cot)(bz)
Fe+(cot)
Fe+(cot)(bz)
50
100
150
200
250
300
350
cm-1

fragmentation of these M^+(COT) ions are also seen. In data not shown, the corresponding Ag^+ and Ni^+ complexes were also studied and they produced these same M^+(COT) fragment ions. The data shown is for fragmentation at 532 nm, but all four metal complexes were also studied at 355 nm, with the same result. This fragmentation behavior is surprising, because it indicates that these metal ions bind more strongly to COT than they do to benzene. As we discussed in our earlier work on mixed complexes,[13] competitive elimination experiments can be used to determine relative ligand binding energies, as long as photo-excitation does not accidentally access some resonance leading to dissociation on an excited state potential. When excitation occurs by excited state absorption followed by internal conversion and dissociation in the ground state, the more weakly bound ligand will be preferentially eliminated first. Because all of these complexes exhibit the same behavior at both 532 and 355 nm, we can safely rule out excited state resonances, and thus conclude that these metal cations bind more strongly to COT than they do to benzene. The benzene binding energies listed in Table 4.1 are therefore lower limits for the corresponding M^+(COT) binding energies.

Stronger binding to COT than to benzene can be rationalized in at least two ways. Because COT is larger than benzene, its polarizability should be somewhat greater, thus enhancing the charge-induced dipole electrostatic component in bonding. However, the larger effect may be the greater amount of charge transfer in M^+(COT) binding. Because COT achieves greater stability by accepting charge from the metal ions and benzene is already aromatic without such charge donation, the charge transfer interaction should be greater in the COT complexes. This could explain the apparent stronger bonding in these complexes. To our knowledge, there are no previous studies of M^+(COT) dissociation energies, nor have these binding energies been calculated. These studies would be useful for future investigations.

Conclusions

Transition metal ion-cyclooctatetraene complexes of V, Fe, Ni, and Ag were produced by laser vaporization and studied by photodissociation at 355 and 532 nm. The mass spectra show simple adducts of $M^+(COT)_{1,2}$ as well as other smaller complexes formed via COT decomposition in the laser plasma. Mass selected photodissociation measurements on each complex showed various metal dependent fragmentation channels. $Ag^+(COT)$ was the only complex that demonstrated both simple ligand elimination and photoinduced charge-transfer. The mono-COT complexes of V, Fe, and Ni all show extensive ligand decomposition upon photofragmentation, yielding $M^+(C_6H_6)$ as the main fragment ion. Photofragmentation of both V and Fe mono-COT complexes also produced $M^+(C_5H_5)$ and this is attributed to their relatively low second IP's, which allow donation of electron density to the C_5H_5 ligand that stabilizes it. Fragmentation patterns for di-COT complexes of V, Fe, and Ni were also recorded. These systems exhibit primarily the elimination of intact COT ligands, indicating that the second ligand is more weakly interacting with the metal than the first. V and Fe di-COT complexes also fragment to form $M^+(C_{10}H_{10})$. Further investigation of these complexes indicates that they have an $M^+(COT)(C_2H_2)$ structure rather than a ferrocene-like structure. Dissociation of mixed complexes containing both COT and benzene takes place by the loss of benzene. This suggests that the binding energies of these transition metal cations with COT are greater than those with benzene.

References

(1) a) Hoshino, K.; Kurikawa, T.; Takeda, H.; Nakajima, A.; Kaya, K. *J. Phys. Chem.* **1995**, *99*, 3053. b) Judai, K.; Hirano, M.; Kawamata, H.; Yabushita, S.; Nakajima, A.; Kaya, K. *Chem. Phys. Lett.* **1997**, *270*, 23. c) Nagao, S. Negishi, Y.; Kato, A.; Nakamura, Y.; Nakajima, A.; Kaya, K. *J. Phys. Chem. A* **1999**, *103*, 8909.

(2) Basir, Y.; Anderson, S.L *Chem. Phys. Lett.* **1995**, *243*, 45.

(3) Welling, M.; Thompson, R.I.; Walther, H. *Chem. Phys. Lett.* **1996**, *253*, 37.

(4) a) Martin, T.P.; Malinowski, N.; Zimmermann, U.; Naher, U.; Schaber, H.J. *J. Chem. Phys.* **1993**, *99*, 4210. b) Zimmermann, U.; Malinowski, N.; Naher, U.; Frank, S.; Martin, T.P. *Phys. Rev. Lett.* **1994**, *72*, 3542. c) Tast, F.; Malinowski, N.; Frank, S.; Heinebrodt, M.; Billas, I.M.L.; Martin, T.P. *Phys. Rev. Lett.* 77 (1996) 3529. d) Tast, F.; Malinowski, N.; Billas, I.M.L.; Heinebrodt, M.; Martin, T.P. *Z. Phys. D: At., Mol. & Clusters* **1997**, *40*, 351. e) Branz, W.; Billas, I.M.L.; Malinowski, N.; Tast, F.; Heinebrodt, M.; Martin, T.P. *J. Chem. Phys.* **1998**, *109*, 3425.

(5) a) Reddic, J.E.; Robinson, J.C.; Duncan, M.A. *Chem. Phys. Lett*. **1997**, *279*, 203. b) Grieves, G.A.; Buchanan, J.W.; Reddic, J.E.; Duncan, M.A. *Intl. J. Mass Spectrom.* **2001**, *204*, 223.

(6) a) Nakajima, A.; Nagao, S.; Takeda, H.; Kurikawa, T.; Kaya, K. *J. Chem. Phys.* **1997**, *107*, 6491. b) Kurikawa, T.; Nagao, S.; Miyajima, K.; Nakajima, A.; Kaya, K. *J. Phys. Chem. A* **1998**, *102*, 1743. c) Nagao, S.; Kurikawa, T.; Miyajima, K.; Nakajima, A.; Kaya, K. *J. Phys. Chem. A* **1998**, *102*, 4495. d) Nagao, S.; Negishi, Y.; Kato, A.; Nakamura, A.; Nakajima, A.; Kaya, K. *J. Phys. Chem. A* **1999**, *103*, 8909. e) Nakajima,

A.; Kaya, K. *J. Phys. Chem. A* **2000**, *104*, 176. f) Suzumura, J.; Hosoya, S.; Nagao, S.; Mitsui, M.; Nakajima, A. *J. Chem. Phys.* **2004,** *121*, 2649.

(7) Nagao, S.; Kato, A.; Nakajima, A. *J. Am. Chem. Soc.* **2000**, *122*, 4221.

(8) Marty, P.; de Parseval, P.; Klotz, A.; Chaudret, B.; Serra, G.; Boissel, P. *Chem. Phys. Lett.* **1996**, *256*, 669.

(9) Marty, P.; de Parseval, P.; Klotz, A.; Serra, G.; Boissel, P. *Astron. Astrophys.* **1996**, *316*, 270.

(10) Klotz, A.; Marty, P.; Boissel, P.; de Caro, D.; Serra, G.; Mascetti, J.; de Parseval, P.; Deroualt, J.; Daudey, J.-P.; Chaudret, B. *Planet. Space Sci.* **1996**, *44*, 957.

(11) Pozniak, B.P.; Dunbar, R.C. *J. Am. Chem. Soc.* **1997**, *119*, 10439.

(12) Buchanan, J.W.; Reddic, J.E.; Grieves, G.A.; Duncan, M.A. *J. Phys. Chem. A* **1998**, *102*, 6390.

(13) Buchanan, J.W.; Grieves, G.A.; Reddic, J.E.; Duncan, M.A. *Intl. J. Mass Spectrom.* **1999**, *182/183*, 323.

(14) Buchanan, J.W.; Grieves, G.A.; Flynn, N.D.; Duncan, M.A. *Intl. J. Mass Spectrom.* **1999**, *185-187*, 617.

(15) Foster, N. R.; Grieves, G. A.; Buchanan, J. W.; Flynn, N. D.; Duncan, M. A. *J. Phys. Chem. A,* **2000**, *104*, 11055.

(16) Duncan, M.A.; Knight, A.M.; Negishi, Y.; Nagao, S.; Nakamura, Y.; Kato, A.; Nakajima, A.; Kaya, K. *Chem. Phys. Lett.* **1999**, *309*, 49.

(17) Duncan, M. A.; Knight, A. M.; Negishi, Y.; Nagao, S.; Judai, K.; Nakajima, A.; Kaya, K. *J. Phys. Chem. A* **2001**, *105,* 10093.

(18) a) Kurikawa, T.; Negishi, Y.; Hayakawa, F.; Nagao, S.; Miyajima, K.; Nakajima, A.; Kaya, K. *J. Am. Chem. Soc.* **1998**, *120*, 11766. b) Kurikawa, T.; Negishi, Y.; Hayakawa, F.; Nagao, S.; Miyajima, K.; Nakajima, A.; Kaya, K. *Eur. Phys. J. D* **1999**, *9*, 283. c) Miyajima, K.; Kurikawa, T.; Hashimoto, M.; Nakajima, A.; Kaya, K. *Chem. Phys. Lett.* **1999**, 306, 256.

(19) Kealy, T.J.; Paulson, P.L. *Nature* **1951**, *168*, 1039.

(20) Fischer, E.O.; Hafner, W. *Z. fuer Naturforsch.* **1955**, *10B*, 665.

(21) a) Willey, K.F.; Cheng, P.Y.; Bishop, M.B.; Duncan, M.A. *J. Am. Chem. Soc.* **1991**, *113*, 4721. b) Willey, K.F.; Yeh, C.S.; Robbins, D.L.; Duncan, M.A. *J. Phys. Chem.* **1992**, *96*, 9106.

(22) Streitwieser, A.; Müller-Westerhoff, U. *J. Am. Chem. Soc.*, **1968**, *90*, 7364.

(23) Streitwieser, A.; Müller-Westerhoff, U.; Sonnichsen, G.; Mares, F.; Morell, D.G.; Hodgson, K.O.; Harmon, C.A. *J. Am. Chem. Soc.*, **1973**, *95*, 8644.

(24) Hodgson, K.O.; Raymond, K.N. *Inorg. Chem.*, **1972**, *11*, 3030.

(25) Long, N.J. *Metallocenes*, **1998**, Blackwell Sciences, Ltd., Oxford, UK.

(26) a) Yeh, C.S.; Pilgrim, J.S.; Robbins, D.L.; Willey, K.F.; Duncan, M.A. *Intl. Rev. Phys. Chem.* **1994**, *13*, 231. b) Duncan, M.A. *Intl. Rev. Phys. Chem.* **2003**, *22*, 407.

(27) a) Tanaka, I.; Okuda, M. *J. Chem. Phys.* **1954**, *22*, 1780. b) Fonken, G.J.; *Chemistry & Industry* **1963**, *40*, 1625.

(28) Fu, E.W.; Dunbar, R.C *J. Am. Chem. Soc.* **1978**, *100*, 2283.

(29) Franklin, J.L.; Carroll, S.R. *J. Am. Chem. Soc.*, **1969**, *91*, 5940.

(30) Lifshitz, C.; Malinovich, Y. *Int. J. Mass Spectrom. Ion Processes*, **1984**, *60*, 99.

(31) Fu, E.W.; Dunbar, R.C. *J. Am. Chem. Soc.*, **1978**, *100*, 2283. Value is average of upper and lower energies presented in this reference.

(32) a) Yang, Y.S.; Hsu, W.Y.; Lee, H.F.; Huang, Y.C.; Yeh, C.S.; Hu, C.H. *J. Phys. Chem. A* **1999**, *103*, 11287. b) Su, P.H.; Lin, F.W.; Yeh, C.S. *J. Phys. Chem. A* **2001**, *105*, 9643.

(33) Hostetler, M.J.; Nuzzo, R.G.; Girolami, G.S.; Dubois, L.H. *J. Phys. Chem.* **1994**, *98*, 2952.

(34) a) Sherrill, A.B.; Lusvardi, V.S.; Barteau, M.A. *Langmuir* **1999**, *15*, 7615. b) Sherrill, A.B.; Medlin, J.W.; Chen, J.G.; Barteau, M.A. *Surf. Sci.* **2001**, *492*, 203.

(35) a) Chen, Y.M.; Armentrout, P.B. *Chem. Phys. Lett.* **1993**, *210*, 123. b) Meyer, F.; Khan, F.A.; Armentrout, P.B. *J. Am. Chem. Soc.* **1995**, *117*, 9740.

(36) WebElements [http://www.webelements.com/]

(37) Foster, N. R.; Grieves, G. A.; Flynn, N. D.; Duncan, M. A., unpublished results.

(38) Maitlis, P. M. *Advances in Organometallic Chemistry*; Stone, F. G. A., West, R., Eds.; Academic Press: New York, 1966; Vol. 4, p 95.

(39) Efraty, A. *Chem. Rev*. **1977**, *77*, 691.

CHAPTER 5

VIBRATIONAL SPECTROSCOPY AND DENSITY FUNCTIONAL THEORY OF TRANSITION METAL ION-BENZENE AND DI-BENZENE COMPLEXES IN THE GAS PHASE

Abstract

Metal-benzene complexes of the form $M(benzene)_n$ (M=Ti, V, Fe, Co, Ni) are produced in the gas phase using laser vaporization in a pulsed nozzle cluster source. These complexes are photoionized with an ArF excimer laser (193 nm; 6.42 eV), producing the corresponding $M^+(benzene)_n$ ions. The respective mono- and di-benzene complex ions are isolated in an ion-trap mass spectrometer and studied with infrared resonance enhanced multiple-photon dissociation (IR-REMPD) spectroscopy using the tunable Free Electron Laser for Infrared eXperiments (FELIX). Photodissociation of all complexes occurs by the elimination of intact neutral benzene molecules. This process is enhanced on resonances in the vibrational spectrum, making it possible to measure vibrational spectroscopy for size-selected complexes by monitoring fragment yield versus IR excitation wavelength. Vibrational bands in the 600-1700 cm^{-1} region are characteristic of the benzene molecular moiety with systematic shifts caused by the metal bonding. The spectra in this solvent-free environment exhibit periodic trends in band shifts and intensities relative to the free benzene molecule that vary with the metal. Density functional theory calculations are employed to investigate the structures, energetics and

vibrational frequencies of these complexes. The comparison between experiment and theory provides fascinating new insight into the bonding in these prototypical organometallic complexes.

Introduction

Transition metal ion complexes that can be produced, isolated, and examined in the gas phase provide simple models for metal-ligand interactions as well as metal ion-solvation.[1-4] Of these complexes, metal ion-benzene complexes hold special interest because of their relevance in catalysis and biological processes.[5,6] Such aromatic π-bonded systems are fundamental throughout organometallic chemistry.[7,8] These complexes are also known to form sandwich type structures and can be compared to similar complexes that have been synthesized and studied using conventional condensed-phase techniques.[7,8] Infrared spectroscopy has been useful for elucidating bonding characteristics based on observed shifts in the ligand based vibrational modes.[9,11] Such studies have been limited in the gas-phase due to low sample concentrations and the availability of high power, widely tunable IR light sources. Our group has reported previous success in studying $V^+(benzene)_n$ and $Al^+(benzene)$ complexes by utilizing Infrared Resonance Enhanced Multiple-photon Photodissociation (IR-REMPD) spectroscopy for obtaining vibrational spectra of complexes created in the gas-phase in low concentrations.[12,13] This work extends the previous experiments to several transition metal cation-benzene systems to investigate periodic trends in spectral shifts of the ligand-based modes and provide further understanding of their binding.

The study of sandwich complexes began with the synthesis of ferrocene and the understanding of it relative stability due to metal-ligand charge transfer.[14] Shortly after, dibenzene chromium was synthesized as the first metal-benzene analogue of these types of complexes. The stability of both complexes was attributed to the familiar 18-electron rule.[15] Since then, many neutral metal-benzene complexes have been synthesized using conventional condensed-phase techniques. These neutral complexes, as well as some with net charge stabilized by counter-ions, have been investigated for years in the condensed-phase.[7,8] These investigations have been complicated by the presence of solvent molecules. Gas phase studies using mass spectrometric techniques have been prevalent throughout the literature.[16-21] Collision-induced Dissociation (CID),[18] equilibrium mass spectrometry[19] and UV-visible photodissociation[16,17] experiments have been employed to determine the bond strengths for several of these complexes. Many theoretical investigations have ensued to calculate structures and investigate their energetics.[2,3,22-28] Kaya and coworkers demonstrated that various metal-benzene systems have the propensity to form multiple-decker sandwich structures.[20] Mass spectra of these systems showed prominent $M_m^+(benzene)_n$ stoichiometries where n = m+1. These tendencies were more pronounced for earlier transition metals, especially vanadium. The multiple-decker sandwich structure were confirmed by ion-mobility measurements performed by Bowers and coworkers[21] as well as by magnetic deflection experiments performed by Kaya and coworkers.[20f] The magnetic moments of $V_m^+(benzene)_n$ complexes were found to increase linearly with cluster size, giving further proof of the multiple-decker structure.[20f] Additionally, photoelectron spectroscopy has been applied to metal-benzene anions,[20b, 29] and a partial IR absorption spectra was obtained for $V^+(benzene)_2$ size-selected as a cation and deposited into a rare gas matrix.[30] Lisy and coworkers have applied IR photodissociation spectroscopy in the OH

stretch region of alkali cation $M^+(benzene)_m(H_2O)_n$ complexes.[31] Two earlier communications from this group reported the application of IR-REMPD to obtain vibrational spectra for vanadium and aluminum cation-benzene systems using a free electron laser.[12,13] Similar results have been reported by others on Cr^+(aniline) complexes.[32] The Free Electron Laser for Infrared eXperiments (FELIX) provides high-power, widely tunable light to make such experiments possible.

Although many transition metal-benzene complexes have been studied , several mysteries still remain concerning their structure and bonding. It is well known that metal-ligand bonding can contain both electrostatic and covalent components. Covalent interactions are extremely complex in transition metal ion systems due to the occurrence of low lying metal excited states that can mix or compete with the ground state for the most stable bonding configuration. Theoretical investigations have difficulty distinguishing between different electronic states and metal spin configurations to assign the proper ground states of such complexes. Also, some uncertainty remains in the geometric configurations of the metal ion-benzene systems. For instance, it is not always clear that η^6 π-bonding is preferred over η^2 or η^3 bonding sites. Benzene can also be distorted from its normal planar geometry by strong interactions with the metal cation. Other questions remain about the conformation of benzene ligands in sandwich structures. Both eclipsed (D_{6d}) and staggered (D_{6h}) isomers are possible and often lie close in energy to one another. The lack of detailed spectroscopy in a solvent free environment has prevented the possibility to probe these details in a systematic way. Since different electronic states and geometries should yield different vibrational spectra, IR-REMPD should be able to discern these differences and solve some the above mentioned problems.

Experimental Methods

Transition metal-benzene complexes of the form M-$(C_6H_6)_n$ (M= Ti, V, Fe, Co, and Ni) are produced by laser vaporization in a pulsed nozzle (Jordan) source using an argon expansion seeded with benzene vapor at ambient temperature. Neutral complexes in the molecular beam pass through the center of a quadrupole ion trap mass spectrometer (Jordan) and the corresponding cations are produced by photoionization with an ArF excimer laser (Neweks, PSX-100; 193 nm; 6.42 eV; 4 mJ/pulse). The ionization potentials of all of the neutral metal-benzene complexes studied here have been measured previously, and these are lower than the ArF photon energy, so that a one-photon process can cause efficient ionization.[20] The density of ions produced in this experiment is far too low for IR absorption spectroscopy, and therefore we use IR photodissociation to measure the vibrational spectroscopy. The experimental methodology for IR photodissociation has been described previously in the study of polycyclic aromatic hydrocarbon ions,[33] $Ti_8C_{12}^+$ clusters,[34] and both $V^+(C_6H_6)_{1,2}$ and $Al^+(C_6H_6)$ complexes.[12,13] The cation complexes produced by photoionization are trapped for several milliseconds and isolated by mass with the RF potentials of the ion trap (1 MHZ; up to ~1000 V p-p). In our implementation of the ion trap, it is not possible to stabilize the trajectories of the trapped ions by the use of a collisional gas. Unfortunately, this prohibits absolute mass selection of specific ions. However, ions below a selected mass threshold can be rejected from the trap by adjustment of the RF potential. In these experiments, all molecules below the mass of interest are eliminated allowing its fragments to be monitored on a zero background. For example, ions below $M^+(C_6H_6)_2$ are eliminated in order to monitor the appearance of the $M^+(C_6H_6)$ fragment.

Infrared excitation is accomplished with the tunable Free Electron Laser for Infrared eXperiments (FELIX),[35] which delivers intense 10-50 mJ pulses of infrared light throughout the spectral region of the main IR-active skeletal vibrations of benzene (600-1700 cm^{-1}).[36] After excitation with FELIX, the contents of the ion trap are extracted into a time-of-flight spectrometer (Jordan) for mass analysis. Infrared absorption leads to resonance enhanced multiple-photon dissociation (IR-REMPD). This is evident from the appearance of fragment ions following IR excitation. The infrared spectrum is obtained by monitoring the intensity of these fragment ions versus the frequency of the infrared laser.

Theoretical Methods

The molecular structures, harmonic vibrational frequencies, and infrared absorption intensities were calculated for a variety of transition metal benzene mono-benzene ("monomer") and di-benzene ("dimer") cation complexes using density functional theory (DFT). These calculations employ the Becke-3 Lee-Yang Parr (B3LYP) functional[37] and the 6-311++G(*d,p*) basis set.[38] The transition metal ions from Ti^+ to Cu^+ are investigated. In each complex, the metal cations were assumed to bind to the central region of the benzene aromatic rings for both the monomer and dimer calculations. The dimers were assumed to exist in a sandwich structure, with the metal ions separating the two benzene rings. The metal ions were allowed to deviate from the C_6 symmetry axis as necessary to obtain all real frequencies. Similarly, reduced symmetries were considered as appropriate for the benzene rings. In one or two instances, one imaginary frequency remained even in C_1 symmetry, which was likely an artifact of the numerical methods employed in the calculations. A variety of electronic states were considered

with the results presented expected to correlate with the ground electronic states. Spin restricted wavefunctions were employed for the singlet states, while unrestricted wavefunctions were employed for all other electronic states. The density functional calculations were performed on a Parallel Quantum Solutions[39] Linux cluster employing the Gaussian98 quantum chemistry software.[40]

Results and Discussion

Metal-benzene complexes with several transition metals are produced via the laser vaporization technique.[12,17] Neutral complexes photoionized using an ArF laser give a cluster distribution of $M^+(benzene)_n$ out to n=6-8. Excess benzene vapor in the cluster growth region produces primarily atomic metal cation with several benzene ligands attached. Due to these conditions, production of multiple-decker sandwich type complexes, similar to those seen by Kaya and coworkers,[20] is not efficient. Conditions are adjusted to maximize $M^+(benzene)$ and $M^+(benzene)_2$ signal intensities during infrared scans.

Figure 5.1 shows mass spectra of $V^+(benzene)_n$ complexes and how these ions fragment upon resonant vibrational excitation from the free electron laser. Because of the limitations of the ion trap, it is not possible to select only the $V^+(C_6H_6)$ ion for study, since the RF potentials only allow elimination of masses below a certain threshold. In the upper trace, both $V^+(C_6H_6)$ and $V^+(C_6H_6)_2$ are present, but no masses below $V^+(C_6H_6)$ are seen until resonant IR excitation occurs. After this, the V^+ ion appears as a fragment, however, it is not clear yet which parent ion produced this fragment. Clarification comes, however, by the data in the lower trace, where ions below $V^+(C_6H_6)_2$ are blocked before laser excitation. Only a small amount of $V^+(C_6H_6)$ appears

Figure 5.1 The mass spectra and fragment ions produced by IR-REMPD of trapped vanadium-benzene ions. In the upper trace, the RF potentials of the trap are adjusted so that all ions up to $V^+(bz)$ are ejected before IR excitation. The V^+ mass peak appears as a result of IR induced photodissociation. In the lower trace, all ions up to $V^+(bz)_2$ are blocked before the laser. The $V^+(bz)$ fragment appears following IR excitation. These measurements show that V^+ is the photofragment from $V^+(bz)$ and $V^+(bz)$ is the photofragment from $V^+(bz)_2$.

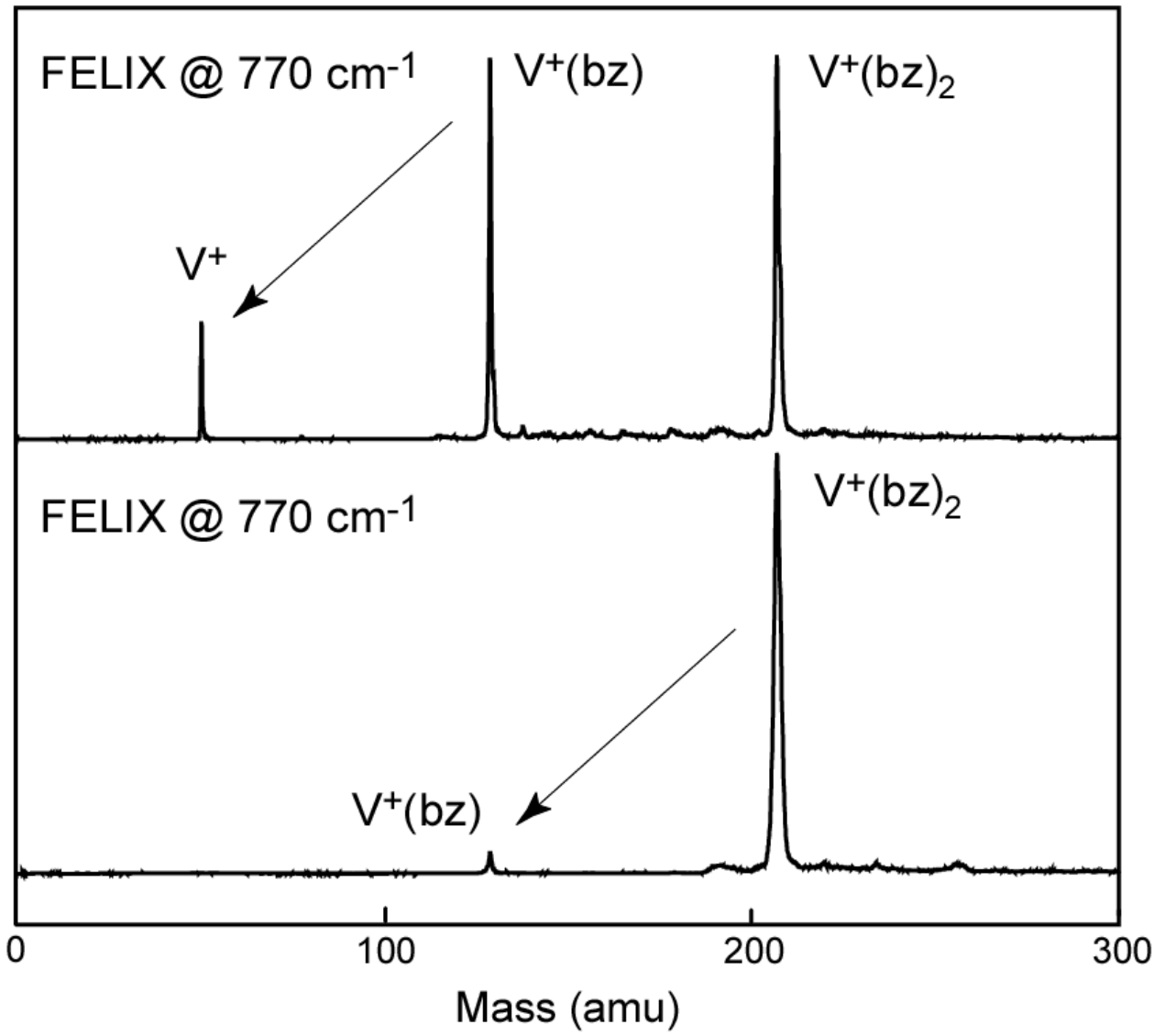
FELIX @ 770 cm-1
V+(bz)
V+(bz)2
V+
FELIX @ 770 cm-1
V+(bz)2
V+(bz)
0
100
200
300
Mass (amu)

here as a photofragment, and it is evident that no V^+ fragment is produced from the $V^+(C_6H_6)_2$ parent. V^+ and $V^+(C_6H_6)$ are therefore the fragments from $V^+(C_6H_6)$ and $V^+(C_6H_6)_2$, respectively, and these fragments can be used to measure uniquely the dissociation spectra of their parent ions, as shown previously.[12,13] This same methodology is employed for all of the $M^+(C_6H_6)_{1,2}$ complexes studied here.

All metal-ion benzene complexes studied here have relatively high dissociation energies ($D_0 \geq 12{,}000$ cm^{-1}) as measured by CID.[18] As mentioned earlier, the vibrational modes to be measured have IR excitation energies between 600-1700 cm^{-1}. It becomes clear that, in order for photodissociation to occur, many IR photons must be absorbed by these complexes. However, multiple-photon processes involving 100 or more photons have been observed using FELIX.[41-43] It is important to make a distinction between *multiphoton* processes, involving non-resonant absorption steps, and *multiple-photon* processes that involve resonant absorption, intramolecular vibrational relaxation (IVR) and continued resonant absorption within a single laser pulse. As discussed in previous papers,[41-43] the latter mechanism, which gives rise to efficient resonant enhancement on vibrational fundamentals, is believed to be observed in the present study. This process is facilitated by the temporal profile of the FELIX laser pulse. It consists of a 5-7 μsec macropulse which is made up of a train of picosecond micropulses separated in time by a nanosecond. Based on their metal-ligand bond energies,[18] all complexes in this study are expected to require multiple-photon dissociation.

Infrared multiple-photon photodissociation is enhanced when the laser is tuned to a vibrational resonance, as described previously.[12,13] Tuning the infrared light frequency while monitoring fragment yield gives the IR-REMPD spectrum with bands analogous to those that would be measured in a direct absorption experiment. These band might be shifted slightly to

the red of where they would be measured, if it were possible, in a typical direct absorption experiment due to the multiple-photon processes.[41,43] These multiple-photon processes also can cause broadening of spectral features.[41,43] The linewidths observed in these experiments (20-50 cm^{-1}) are substantially broader than the laser linewidth (5-7 cm^{-1}). It is also important to note that the observed band intensities are proportional to the dissociation yield and, hence, might not be directly related to the absorption intensities. Despite the aforementioned experimental limitations, vibrational spectra can be measured for several transition metal cation-benzene systems to investigate periodic trends in band positions and, to a limited degree, band intensities.

Figure 5.2 shows the IR-REMPD spectra of M^+(benzene) monomer systems where M = V, Co, and Ni. These complexes were the only mono-benzene complexes with enough signal intensity to be studied by this method. Vibrational resonances are observed in the 600-1700 cm^{-1} region. Dashed vertical lines in the figure are used to denote the IR active modes of free benzene in this region.[36] They occur at 673, 1038, and 1486 cm^{-1} for the ν_{11} out-of-plane C-H bend, ν_{18} in-plane C-H bend, and ν_{19} in-plane carbon ring distortion modes, respectively. Strong vibrational modes occur in all three M^+(benzene) complexes and are observed near the ν_{11} out-of-plane C-H bend and ν_{19} in-plane carbon ring distortion modes. A smaller intensity mode near the ν_{18} in-plane C-H bend of free benzene is also observed for the V^+(benzene) complex. All band positions are reported in Table 5.1.

Figures 5.3 and 5.4 show similar IR-REMPD vibrational spectra for several $M^+(benzene)_2$ complexes where M = Ti, V, Fe, Co, and Ni. Once again, the free benzene modes in this region are indicated by vertical dashed lines. Their assignments are the same as that of Figure 5.2. Just as observed for the monomer complexes, all dimer species studied exhibit strong vibrational bands near the ν_{11} and ν_{19} modes of free benzene. Ti and V complexes also have

Figure 5.2 The IR-REMPD vibrational spectra of V^+(bz), Co^+(bz) and Ni^+(bz) measured in the M^+ fragment ion channel. Experiments like those in Figure 5.1 were conducted to show that the M^+ fragment ion in each system comes from the corresponding M^+(bz) parent. The small peaks indicated with * in the Co^+(bz) spectrum are noise peaks that are not reproducible.

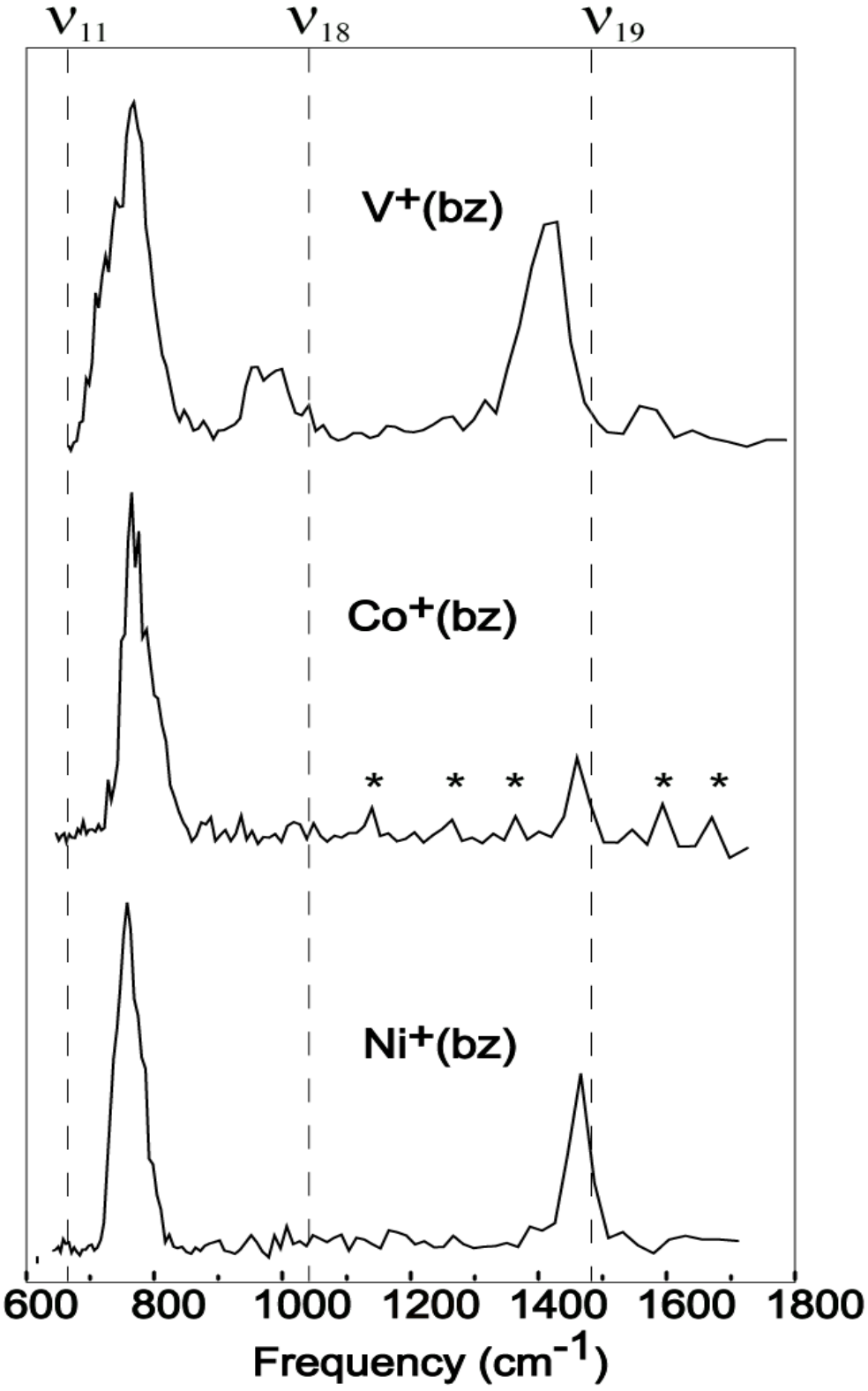
ν11
ν18
ν19
V+(bz)
Co+(bz)
Ni+(bz)
*
*
*
*
*
600
800
1000
1200
1400
1600
1800
Frequency (cm-1)

Table 5.1 The positions of the IR bands observed for transition metal ion-benzene complexes and their comparison to the spectra of neutral complexes and to the predictions of theory.

Complex	ν_{11} out-of-plane H bend		ν_1 C ring stretch (IR inactive in benzene)		ν_{18} in-plane C-H bend		ν_{19} in-plane C ring distortion	
	Exp.	Theory[a]	Exp.	Theory	Exp.	Theory[a]	Exp.	Theory[a]
C_6H_6	673	687(122)	992	979/981(0)	1038	1059/1059(6/6)	1486	1510/1510(7/7)
$Ti^+(bz)$		756(100)		899(4)		1003/1004(8/8)		1450/1450(11/11)
$Ti^+(bz)_2$	739	751(88)	946	922/974(10/19)	992	1011/1034(15/6)	1421	1466/1478/1530 (17/15/22)
$Ti(bz)_2$			946[b]		979[b]			
$V^+(bz)$	769	744[c]			980	1000/1016[c]	1425	1447/1458[c]
		791(103)		986/1001(5/11)		1005(2)		1423/1455/1528 (7/2/7)
$V^+(bz)_2$	769	724[c]	962		1005	1010/1023[c]	1449	1456/1465[c]
		761(75)		947/993(21/13)		998/1020(11/3)		1462/1535(16/58)
$V(bz)_2$	739[b]		959[b]		985[b]		1416[b]	
$Cr(bz)_2$	794[b]		971[b]		999[b]		1426[b]	
$Fe^+(bz)$		767(101)		926/931(2/2)		1004/1021(5/3)		1458/1465(16/20)
$Fe^+(bz)_2$	768	777(99)	996	955(7)		1005/1031(4/7)	1440	1453/1472(31/26)
$Co^+(bz)$	740	786(105)		929/931(1/1)		1012/1012(5/5)	1430	1456/1457(15/15)
$Co^+(bz)_2$	748	737(160)		927(2)		1023/1023(5/5)	1472	1469/1469(28/27)
$Ni^+(bz)$	744	764(105)				1005/1021(4/3)	1444	1454/1464(19/18)
$Ni^+(bz)_2$	732	733(205)		1006(1)		1021/1032(5/5)	1469	1469/1477(36/36)

[a]This work, except as noted. [b]Literature values from the condensed phase, references 9-11. [c]Reference 12.

Figure 5.3 The IR-REMPD vibrational spectra of $Ti^+(bz)_2$ and $V^+(bz)_2$ measured in the $M^+(bz)$ fragment ion channel. Experiments like those in Figure 1 were conducted to show that the $M^+(bz)$ fragment ion in each system comes from the corresponding $M^+(bz)_2$ parent.

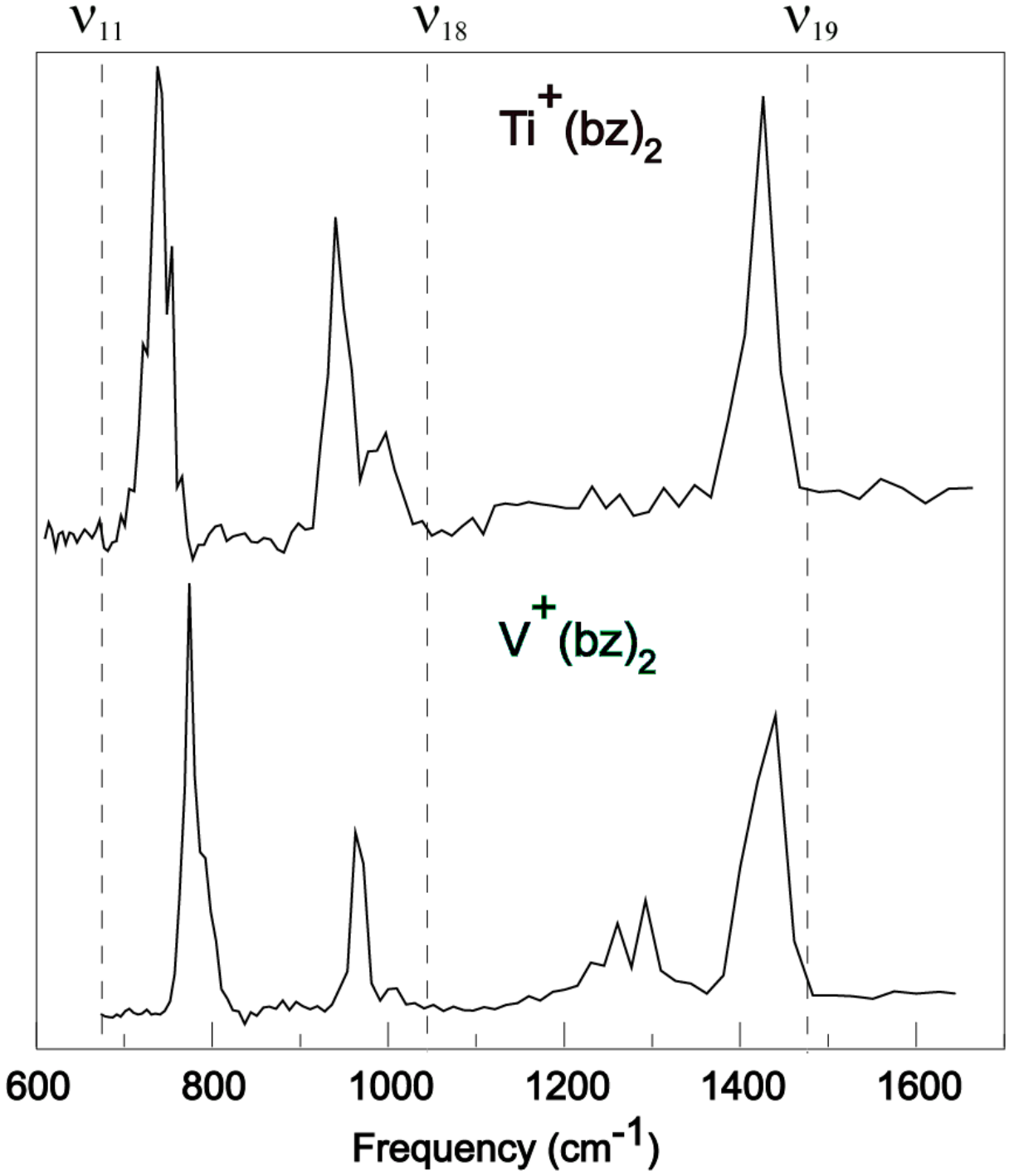
ν11
ν18
ν19
Ti+(bz)2
V+(bz)2
600
800
1000
1200
1400
1600
Frequency (cm-1)

Figure 5.4 The IR-REMPD vibrational spectra of $Fe^+(bz)_2$, $Co^+(bz)_2$ and $Ni^+(bz)_2$ measured in the $M^+(bz)$ fragment ion channel. Experiments like those in Figure 5.1 were conducted to show that the $M^+(bz)$ fragment ion in each system comes from the corresponding $M^+(bz)_2$ parent. The small peaks indicated with * in the $Ni^+(bz)$ spectrum are noise peaks that are not reproducible.

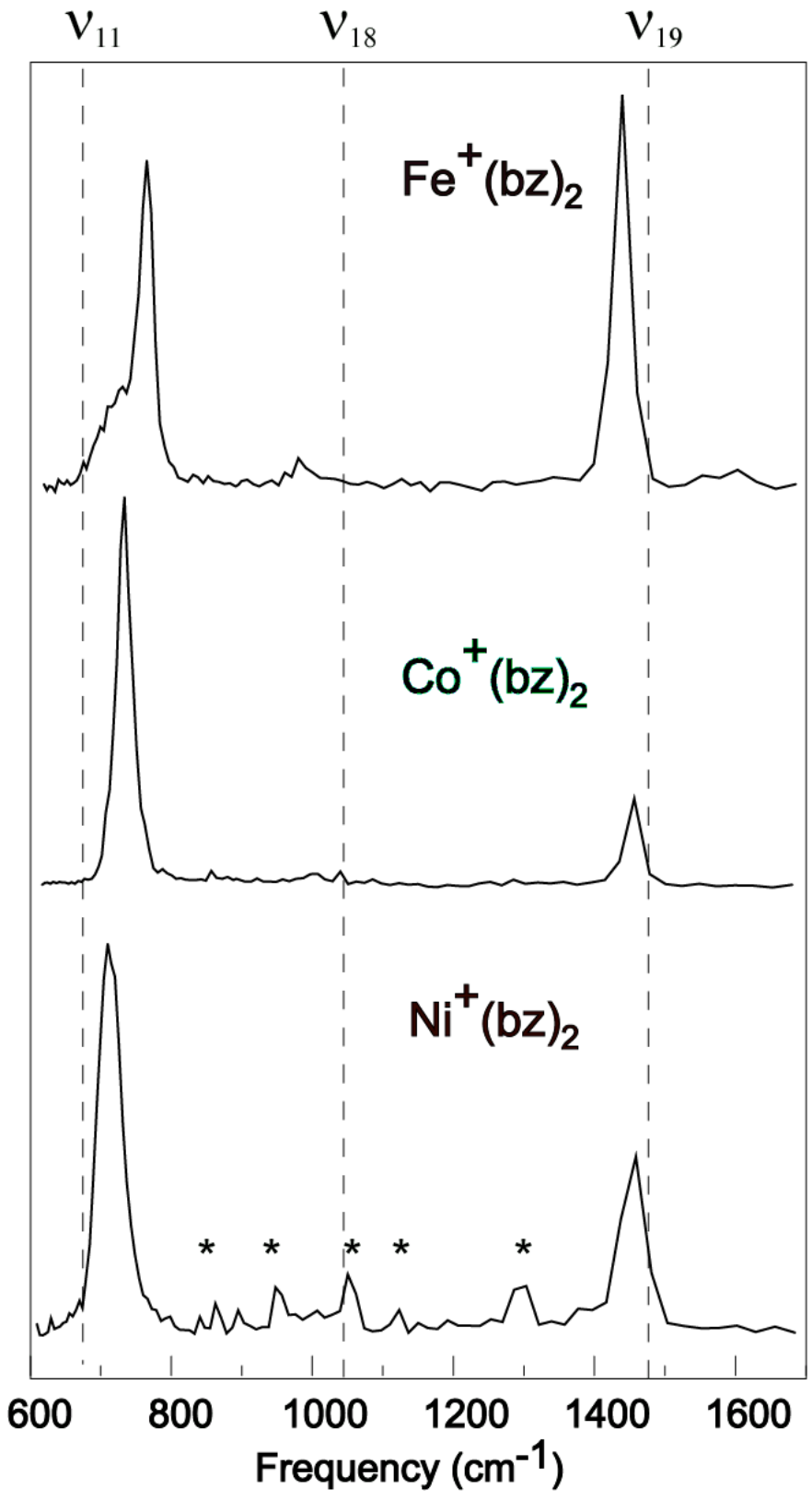
ν11
ν18
ν19
Fe+(bz)2
Co+(bz)2
Ni+(bz)2
*
*
*
*
*
600
800
1000
1200
1400
1600
Frequency (cm-1)

vibrational structure near that of the ν_{18} modes, but no intensity is observed in this region for Fe, Co, and Ni. All band positions are listed in Table 5.1.

Figures 5.2, 5.3 and 5.4 make it evident that all of these $M^+(benzene)_{1,2}$ complexes have vibrational modes near those of free benzene. It is interesting to further investigate the positions of these bands relative to those of free benzene. Bands which occur in the 730-770 cm^{-1} region all occur at higher frequency than the ν_{11} out-of-plane C-H bend of free benzene which lies at 673 cm^{-1}. Bands in the 900-1000 cm^{-1} region are not seen for all species, but, when observed, occur at lower frequency than that of the ν_{18} in-plane C-H bend of free benzene. This mode occurs at 1038 cm^{-1} in the unbound species. Vibrational bands in the 1420-1470 cm^{-1} region occur at lower frequencies than the ν_{19} in-plane carbon ring distortion mode of free benzene. Similar vibrational patterns have been observed and discussed for condensed-phase metal-benzene systems.[9-11] These complexes were studied in solution or in solid thin films, and, therefore, definitive vibrational band positions for isolated molecules are not generally known. These earlier studies still provide a convenient guide for this present work. Values for neutral $Ti(benzene)_2$ and $V(benzene)_2$, as well as those for $Cr(benzene)_2$, are provided for comparison in Table 5.1.[9-11]

The vibrational bands near the ν_{11} and ν_{19} modes are the most intense ones observed in condensed-phase studies. This is true for the gas-phase complexes studied here as well. The ν_{11} mode is generally observed to blue-shift while the ν_{18} and ν_{19} modes are usually red-shifted in the condensed-phase complexes. These trends have been discussed previously.[9,10] When a transition metal binds to a hydrocarbon such as benzene, there is σ-donation of electron density from the molecular π cloud to empty orbitals on the metal, and also π back-bonding from the populated metal orbitals into the antibonding molecular orbitals. These effects, analogous to

those seen for metal carbonyls and metal-olefin complexes, constitute the well-known Dewar-Chatt-Duncanson model of π-bonding.[44-46] The net result of these charge transfer processes is that the molecular bonding in the ligand is weakened, driving many of its vibrational frequencies to lower values. This explains the red shifts seen for the ν_{18} and ν_{19} vibrational bands. The exception to this trend occurs for the ν_{11} bands, in which a blue-shift is observed. While the red-shift of the ν_{18} and ν_{19} bands is a chemical bonding/charge transfer effect, the blue shift of the ν_{11} mode is due to a mechanical effect. The presence of the metal atom over the benzene ring provides an impediment to the out-of-plane hydrogen bend. The extra repulsion at the outer turning point of this vibration produces a steeper potential in this region, which drives the frequency higher. These trends have been observed previously in the condensed phase neutral di-benzene complexes that could be made and studied.[9-11] The same effect is seen here in cations of M^+(benzene) complexes, which could not be studied before as neutrals, and for $M^+(benzene)_2$ for a wider variety of transition metals.

Also observed in condensed phase IR studies is the activation of vibrational bands which would otherwise be IR-forbidden in free benzene. An example of this is the ν_1 symmetric C-H stretching mode which occurs at 992 cm^{-1}. Normally this mode is Raman active and, due to the mutual exclusion principle, is IR-forbidden for D_{6h} free benzene. In these metal-benzene complexes, this symmetry is broken and, in certain cases, the ν_1 mode becomes IR active.[9-11] Modes observed in 1000 cm^{-1} might be tentatively assigned to activation of this mode as well as IR activity in the ν_{18} mode.

Density functional theoretical (DFT) calculations have been performed by Klippenstein to help us better understand these experimental IR spectra and to investigate trends in the shifts of the ligand based vibrational modes. Previous theoretical studies have been performed by

several groups.[21-28] Bauschlicher and coworkers pioneered the field by performing modified coupled pair functional formalism (MCPF) calculations on several monomer species.[22] Klippenstein and Yang provided the first wide ranging density functional study of monomer binding.[24b] These B3LYP results agreed well with the MCPF results, validating the use of B3LYP here to investigate not only the monomer complexes but the dimers as well. Other studies on transition metal-acetylene and ethylene complexes further validate the use of DFT here.[24a] The dimer binding has been investigated by Rao and coworkers using the BPW91 density functional.[26] The present study utilizes B3LYP instead of BPW91. This provides a more detailed description of the electronic states involved, allows for symmetry breaking from D_{6h} to obtain true minima, and obtains vibrational frequencies for all states considered. This study is similar to an early study performed on monomer complexes by Klippenstein and Yang,[24b] but employs a larger basis set for better estimates of IR spectral properties for comparison with IR-REMPD results. More limited DFT studies have been performed by Bowers and coworkers,[21] Li and Baer,[27] and Kaczorowski and Harvey[28] on $V^+(benzene)_2$, $Cr^+(benzene)_2$, and $Fe^+(benzene)_2$, respectively.

The present B3LYP/6-311++G(*d,p*) calculations find stable minima for all the $M^+(benzene)$ and $M^+(benzene)_2$ complexes. The structures found and the low energy electronic states are indicated in Table 5.2. For the monomer complexes, the structures found are either the simple C_{6v}, or the C_{2v} in which the benzene ring has two carbon atoms distorted towards the metal. Ti^+, Cr^+, Mn^+ and Cu^+ complexes adopt the C_{6v} structure, while V^+, Mn^+, Fe^+, Co^+ and Ni^+ adopt the C_{2v}. Only Mn^+ exhibits both structures in different spin states. The dimer complexes may also have undistorted D_{6h} and D_{6d} structures, depending on whether the benzene rings are eclipsed or

Table 5.2 B3LYP/6-311++G(*d*,*p*) predicted metal ligand binding energies (kcal/mol) and bond lengths (Å) for cation metal benzene (bz) monomer and dimer complexes.

Species	State[a]	Sym.	D_0 (Theory)[b]	D_0 (Expt)	R_{MX1}[c]	R_{MX2}[d]	θ_{XMX}[e]
$Ti(bz)^+$	$^4A_1$ ($3de_2^2 3da_1$)	C_{6v}	54.5		1.886		
$Ti(bz)_2^+$	$^4A_1$ ($3de_2^2 3da_1$)	D_6	47.4		1.984		
$Ti(bz)_2^+$	^2A_g ($3de_2^3$)	D_{2h}	48.3	51.0-60.4[f]	1.938		
$Ti(bz)_2^+$	$^2B_{3g}$ ($3de_2^2 3da_1$)	D_{2h}	53.5		1.872		
$V(bz)^+$	$^5B_1$ ($3de_2^2 3da_1 3de_1$)	C_{2v}	47.5		1.959		
$V(bz)^+$	$^3A_2$ ($3de_2^3 3da_1$)	C_{2v}	48.4	49.6-58.8[f]	1.685		
$V(bz)_2^+$	^{5} ($3de_2^2 3da_1 3de_1$)	C_1	32.2		2.039	2.181	168.5
$V(bz)_2^+$	$^3B_{3g}$ ($3de_2^3 3da_1$)	D_{2h}	55.7		1.801		
$Cr(bz)^+$	$^6A_1$ ($3de_2^2 3da_1 3de_1^2$)	C_{6v}	36.4		2.114		
$Cr(bz)_2^+$	$^2A_{1g}$ ($3de_2^4 3da_1$)	D_{6h}	36.8	47.0-55.3[f] 57.9[g]	1.662		
$Mn(bz)^+$	$^7A_1$ ($3de_2^2 3da_1 3de_1^2 4s^1$)	C_{6v}	31.5		2.379		
$Mn(bz)^+$	$^5A_1$ ($3de_2^3 3da_1 3de_1^2$)	C_{2v}	27.8		1.816		
$Mn(bz)_2^+$	$^1A_1$ ($3de_2^4 3da_1^2$)	D_{6h}	29.9	40.6-48.4[f]	1.631		
$Fe(bz)^+$	$^6A_2$($3de_2^3 3da_1 3de_1^2 4s^1$)	C_{2v}	38.9		2.218		
$Fe(bz)^+$	$^4A_1$($3de_2^3 3da_1^2 3de_1^2$)	C_{2v}	49.0		1.810		
$Fe(bz)_2^+$	$^4A_{1g}$($3de_2^4 3da_1 3de_1^2$)	D_{6h}	32.5		1.865		
$Fe(bz)_2^+$	^4A($3de_2^3 3da_1^2 3de_1^2$)	C_2	36.2		2.040		
$Fe(bz)_2^+$	$^2B_{1g}$($3de_2^4 3da_1^2 3de_1$)	D_{2h}	40.6	37.8-44.7[f]	1.714		
$Co(bz)^+$	$^3A_2$($3de_2^4 3da_1^2 3de_1^2$)	C_{2v}	58.6		1.672		

$Co(bz)_2^+$	$^3A_1(3de_2^4 3da_1^2 3de_1^2)$	D_6	35.9	34.6-39.9[f]	1.857		
$Ni(bz)^+$	$^2B_2(3de_2^4 3da_1^2 3de_1^3)$	C_{2v}	57.4		1.738		
$Ni(bz)_2^+$	$^2(3de_2^4 3da_1^2 3de_1^3)$	C_1	33.7	30.7-35.1[f]	1.971		
$Cu(bz)^+$	$^2A_1(3de_2^4 3da_1^2 3de_1^4)$	C_{6v}	49.1		1.859		
$Cu(bz)_2^+$	$^2A_1(3de_2^4 3da_1^2 3de_1^4)$	C_1	35.2	32.1-37.1[f]	2.434	2.407	146.7

[a] The orbital prescription in parentheses corresponds to the occupation of the metal 3d and 4s orbitals using a notation corresponding to that of the metal orbitals in C_{6v} symmetry.
[b] B3LYP/6-311++G** predicted dissociation energy for the process $M^+(bz)_n \rightarrow M^+(bz)_{n-1}$ in kcal/mol including zero-point correction.
[c] Distance from metal cation to center of C6 ring. For asymmetric dimers this corresponds to the value for one of the rings.
[d] Distance from metal cation to center of second C6 ring for asymmetric dimers.
[e] Angle in degrees from the center of one C6 ring to the metal to the center of the other C6 ring. For the symmetric dimers this value is 180.
[f] Dissociation energy obtained from modeling of collision induced dissociation measurements of Ref. 18b. The first number corresponds to that obtained from a tight RRKM modeling while the second number corresponds to that obtained from a loose RRKM modeling.
[g] Dissociation energy obtained from modeling of photoelectron-photoion coincidence

experiments of Ref 27.

staggered with respect to each other. For most complexes, there is a negligible energy difference between the staggered and eclipsed forms. However, as in the monomers, many of the more strongly bound dimer complexes have structures in which the benzene rings are distorted. For example, a D_{2h} structure occurs for several complexes that has two carbons in each benzene ring displaced toward the metal, analogous to the monomer C_{2v} structure. A C_1 complex has the metal localized over an η^3 site on each benzene ring, with the benzene rings slipped parallel to each other. Selected structures for some of these monomer and dimer complexes are shown in Figure 5.5.

Calculated bond energies and metal-ligand bond lengths are reported in Table 5.2 and shown graphically in Figures 5.6 and 5.7, respectively. Experimental CID results for D_0 are also displayed in Table 5.2. These results are based on the coupling of purely theoretical estimates for the spin-conserving dissociation process with experimental values for the spin excitation process in the metal cation. The results for M^+(benzene) complexes are similar to those reported by Klippenstein and Yang,[24b] but with slightly decreased binding energies attributed to increased basis set size for C and H atoms. The decrease is fairly constant , ranging from 2.2-3.0 kcal/mol (2.5 kcal/mol on average). The present results also suggest that the $^3A_2$ state in the V^+(benzene) complex is slightly more strongly bound than either the $^5B_1$ or $^5B_2$ states, which is contrast to results originally reported by this group for this complex.[12]

$M^+(benzene)_2$ complexes are calculated to prefer lower spin states than those calculated for M^+(benzene) complexes. For example, Ti^+(benzene) is predicted to be a quartet while $Ti^+(benzene)_2$ is predicted to be a doublet. $V^+(benzene)_2$ is predicted to have a triplet state that is 23 kcal/mol lower in energy than that of the quintet species while V^+(benzene) has a triplet and

Figure 5.5 The schematic structures calculated for various metal di-benzene sandwich complexes. Hydrogens are removed and ring distortions are exaggerated in these structures compared to the actual predictions of theory.

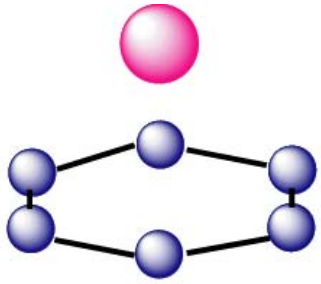

C_{6v}
(Ti,Cr,Mn,Cu)

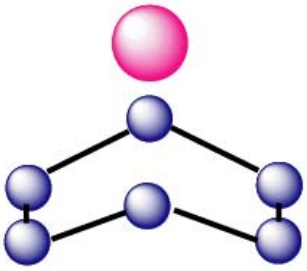

C_{2v}
(V,Fe,Co,Ni)

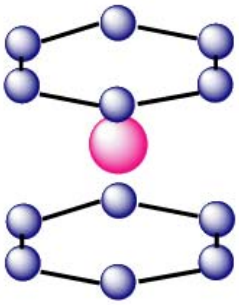

D_{6h} Eclipsed
(Cr,Mn,Co)

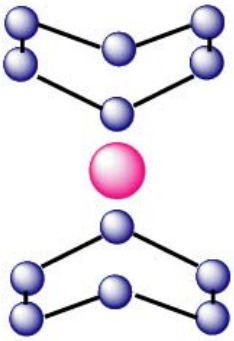

D_{2h} Eclipsed
(Ti,V,Fe)

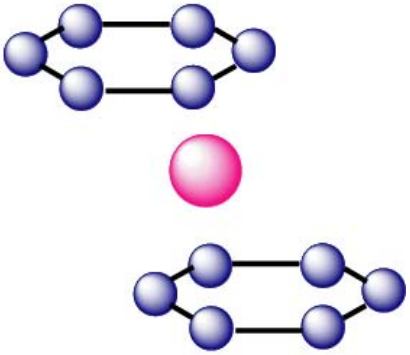

C_1 Slipped
(Ni,Cu)

Figure 5.6 Plot of the calculated dissociation energy, $M^+(bz)_n \rightarrow M^+(bz)_{n-1}$, versus number of valence electrons for the monomer and dimer metal benzene cations.

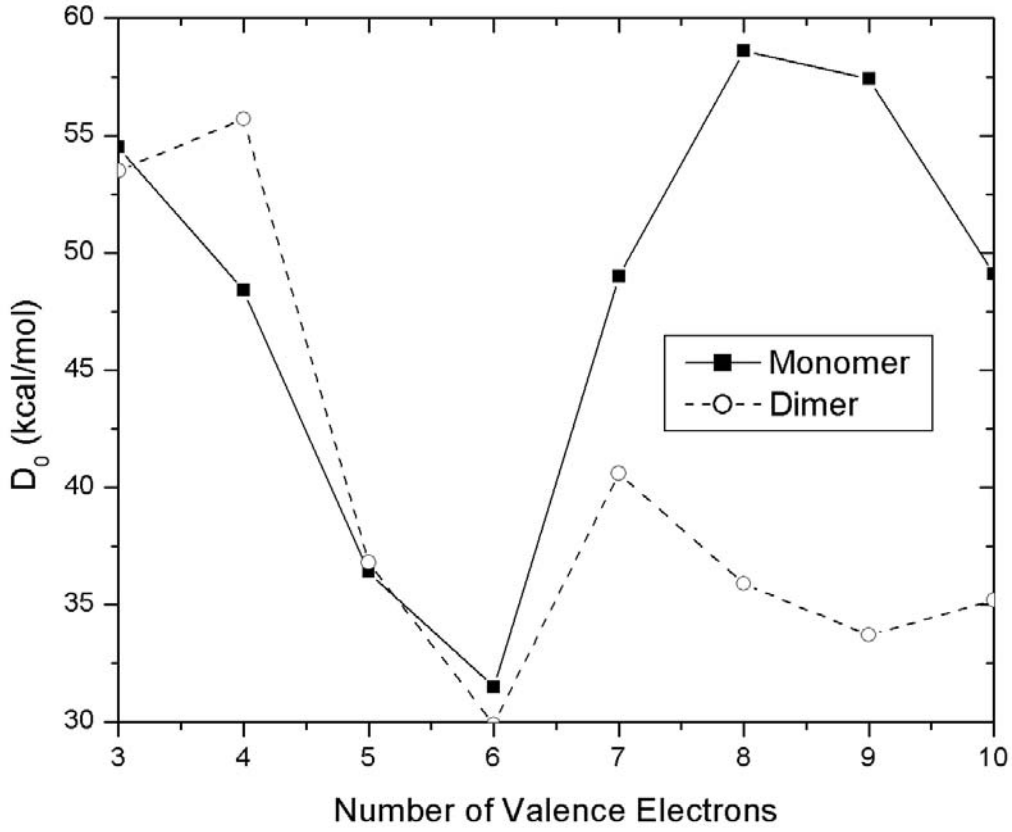
60
55
50
45
40
35
30
D_0 (kcal/mol)
3
4
5
6
7
8
9
10
Number of Valence Electrons
Monomer
Dimer

Figure 5.7 Plot of the calculated metal ligand bond length versus number of valence electrons for the monomer and dimer metal benzene cations.

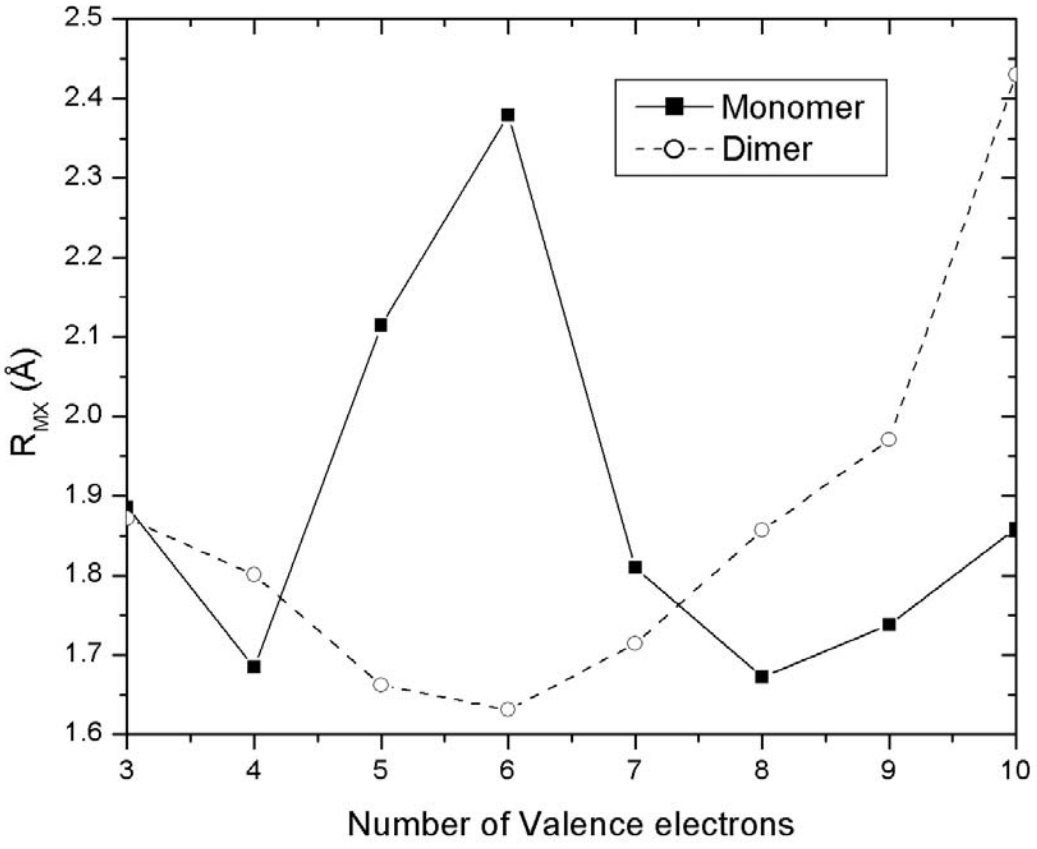
Monomer
Dimer
R_{MX} (Å)
Number of Valence electrons
2.5
2.4
2.3
2.2
2.1
2.0
1.9
1.8
1.7
1.6
3
4
5
6
7
8
9
10

quintet states within 1 kcal/mol of each other. $Cr^+(bz)_2$ is a doublet whereas $Cr^+(bz)$ is a sextet; $Mn^+(bz)_2$ is a singlet whereas $Mn^+(bz)$ is a septet; and $Fe^+(bz)_2$ is a doublet whereas $Fe^+(bz)$ is a quartet. The calculated spin states are a result of the balance between the promotion energy of pairing electrons in the metal and the increase in metal ion-ligand bond energy for paired spins.

The D_0 for the second benzene ligand in $Ti^+(benzene)_2$, $Cr^+(benzene)_2$, and $Mn^+(benzene)_2$ is approximately equal to the binding energy of the first benzene ligand. This demonstrates a near equivalence for the promotion energy and the increase in the metal ion-ligand bond energy. For both monomer and dimer V^+ complexes, a reduced spin is calculated even though V^+ on its own has a quintet configuration. The second benzene ligand is also predicted to have a stronger binding energy than the first. Later transition metal (Fe^+ through Cu^+) exhibit weaker bonding to the second ligand due to added repulsion from filling of the d electron cloud. The calculated dissociation energies of these complexes of later transition metals agree well with experimental CID results,[18] however, the calculated dissociation energies of Cr^+ and Mn^+ complexes are underestimated and those for Ti^+ and V^+ complexes are below the experimental lower limits. It should be noted, though, that the estimated kinetic shifts applied to the extraction of bond energies from CID experiments tend to be much greater for early transition metals. This makes it unclear as to whether the discrepancies between the calculated and theoretical values are from the theoretical method or experimental uncertainties.

The bond lengths calculated by the current theoretical method decrease with decreasing spin. A decrease in spin, however, competes with an increase in repulsion and, thus, competes with bond lengths when more than one ligand is involved. In complexes where a lower spin is calculated for the dimer than the monomer, monomer and dimer complexes have nearly equivalent bond lengths. When spin remains unchanged, the bond length increases from

monomer to dimer. For Cr^+ and Mn^+ the two dimer complexes have much smaller bond lengths due to the pairing of multiple sets of electrons. For Ni^+ and Cu^+ the nearly complete filling of the *d*-shell leads to increased repulsions and the dimer complexes have much greater bond lengths. In fact, for the Cu^+ case, the repulsions lead to a significant distortion away from the C_6 axis.

The present B3LYP/6-311++G(*d,p*) predictions for the vibrational properties of these complexes are reported in Table 5.1. For brevity, only those modes with significant infrared (IR) activity (i.e., predicted to have an intensity of greater than 1.0 km/mol) are provided. A complete listing of the vibrational and structural properties can be found in the Appendix. The entries in Table 5.1 have been scaled from those resulting directly from the DFT calculations. The unscaled values are listed in the Appendix. The scaling, which amounts to shifts of 10-20 cm^{-1}, is applied on a per-mode basis, using the difference between the calculated and experimental values for each vibration when free benzene is calculated at this same level of theory. These IR intensities and vibrational frequencies are used below as an aid in the interpretation of the IR spectra.

Theoretical calculations are helpful for confirming the vibrational mode assignments of the observed bands. The predicted IR spectra, in fact, confirm that the modes observed experimentally near the ν_{11} and ν_{19} modes of benzene are indeed the corresponding vibrations in the M^+(benzene) and M^+(benzene)$_2$ complexes. The qualitative shifts, a red-shift for ν_{19} and a blue-shift for ν_{11}, are also predicted, but their quantitative agreement is somewhat disappointing. For certain modes in certain species scaled predicted modes fall with 10-20 cm^{-1} of experimental observations, but others differed by 50-60 cm^{-1}. Although IR-REMPD is know to red-shift vibrational spectra, this shift is usually on the order of 10-20 cm^{-1}. Adjusting the predicted

values by this scaling factor would help agreement on some modes but would actually make some discrepancies much worse.

Theory could also possibly aid in the assignment of structure observed near 1000 cm^{-1}. Free benzene possesses one IR active mode (ν_{18}) and one IR-forbidden mode (ν_1) in this region. In the previous work in the condensed phase,[9-11] both of these modes have been assigned in the IR spectra of metal complexes. Doublet features in $Ti^+(benzene)_2$, $V^+(benzene)_2$, and $Fe^+(benzene)_2$ around 1000 cm^{-1} are assigned to IR activity in these two modes. Theory predicts that the lower frequency band should be the now IR-active ν_1 modes, similar to observations previously recorded for condensed-phase studies. This band is calculated to have similar intensity to that of the ν_{18} in plane C-H bend, which is IR-active in free benzene.

Theoretical predictions not only help in the assignment of vibrational bands, but they aid in the clarification of observed spectral shifts. Chaquin and coworkers have highlighted the magnitude of shift in the ν_{19} as a method of determining the degree of charge-transfer in metal benzene complexes.[25] Figure 5.8 shows graphically the shift in this mode versus metal for both experimental data and theoretical predictions. Substantial shifts in this mode are both measured and predicted, with greater shifts for early transition metals than the later ones. This trend seems at first to be related to the metal ion-ligand bond energy. For instance, Mn^+ and Cr^+ complexes are predicted to have low bond energies and small shifts. Unfortunately, we do not have experimental data for these species. The relation between large shifts and strong bond energies does not necessarily always hold true. This become apparent when one compares the shifts observed for monomer complexes to those seen for dimers. For metal ion-benzene complexes of V^+, Co^+, and Ni^+, the shift in ν_{19} is greater for the mono-benzene complexes than it is for the di-

Figure 5.8 The shift of the ν_{19} vibrational mode relative to the energy of the free benzene mode for the different mono- and di-benzene complexes studied here. The squares indicate the measured shift for di-benzene complexes, while the triangles represent those for mono-benzene complexes. The lines indicate the predictions of theory.

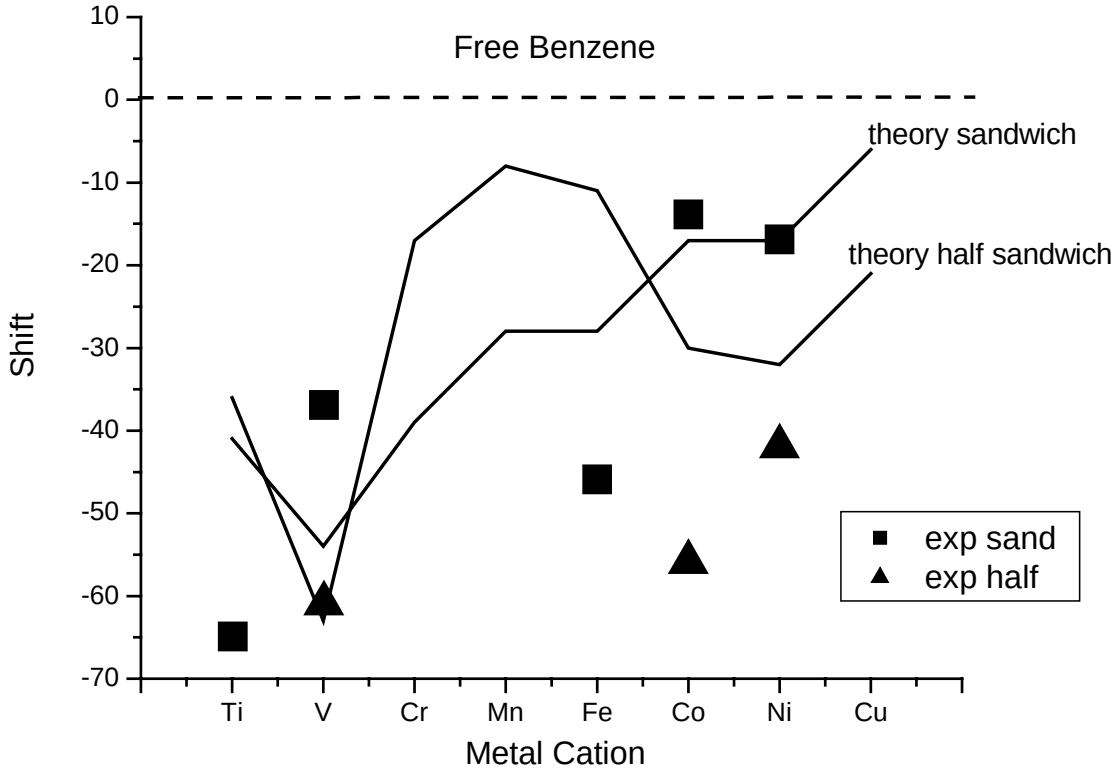
Free Benzene
theory sandwich
theory half sandwich
exp sand
exp half
Shift
Metal Cation
10
0
-10
-20
-30
-40
-50
-60
-70
Ti
V
Cr
Mn
Fe
Co
Ni
Cu

benzene complexes. For Co^+ and Ni^+, the monomer complexes are more strongly bound then the dimer complexes. This is consistent with our logic that stronger bounds induce greater shifts. However, in V^+ complexes the dimer is more strongly bound than the monomer, but its shift is less. These trends for all three metals are predicted correctly by DFT. This demonstrates that if ν_{19} is proportional to the degree of charge-transfer, then, charge-transfer is not directly related to bond strengths. The larger shifts in the ν_{19} mode for early transition metals make it apparent that charge-transfer is greater in these systems. Because these systems have fewer *d* electrons available for π-back bonding to the benzene ligand, it becomes apparent that σ-donation of charge towards the metal is the dominant bonding mechanism.

Although it is difficult to directly relate predicted IR absorption intensity to the intensity of peaks measured in IR-REMPD experiments, one trend in peak intensity becomes apparent in both theoretical predictions and experimental observations: the relative intensity of the ν_1 mode from metal to metal. Figure 5.9 compares the measured intensities of this band versus the DFT predicted IR absorption intensity. Because IR absorption intensities are not directly measured in these experiments, we have set the intensity of the band observed for $Ti^+(benzene)_2$ equal to its DFT predicted intensity. Data for all other complexes was normalized accordingly. This mode has much greater intensity for the early transition metals than the later ones. Although the data is incomplete for monomer complexes, ν_1 intensity is detected for V^+(benzene) but not for Co^+(benzene) and Ni^+(benzene). The appearance of this mode is apparently not related to a strong metal-ligand bond, as Co^+(benzene) and Ni^+(benzene) are more strongly bound than V^+(benzene) but show no activity in this vibration. Activity in this mode could, however, be an indication of large charge-transfer character as a large shift in ν_{19} correlates to large intensity in benzene ligands, i.e. C_{2v} monomers and D_{2h} dimers. This symmetry breaking distortion is what

Figure 5.9 The measured relative intensity of the ν_1 vibrational band (squares) compared to the predictions of theory (line) for the various di-benzene complexes.

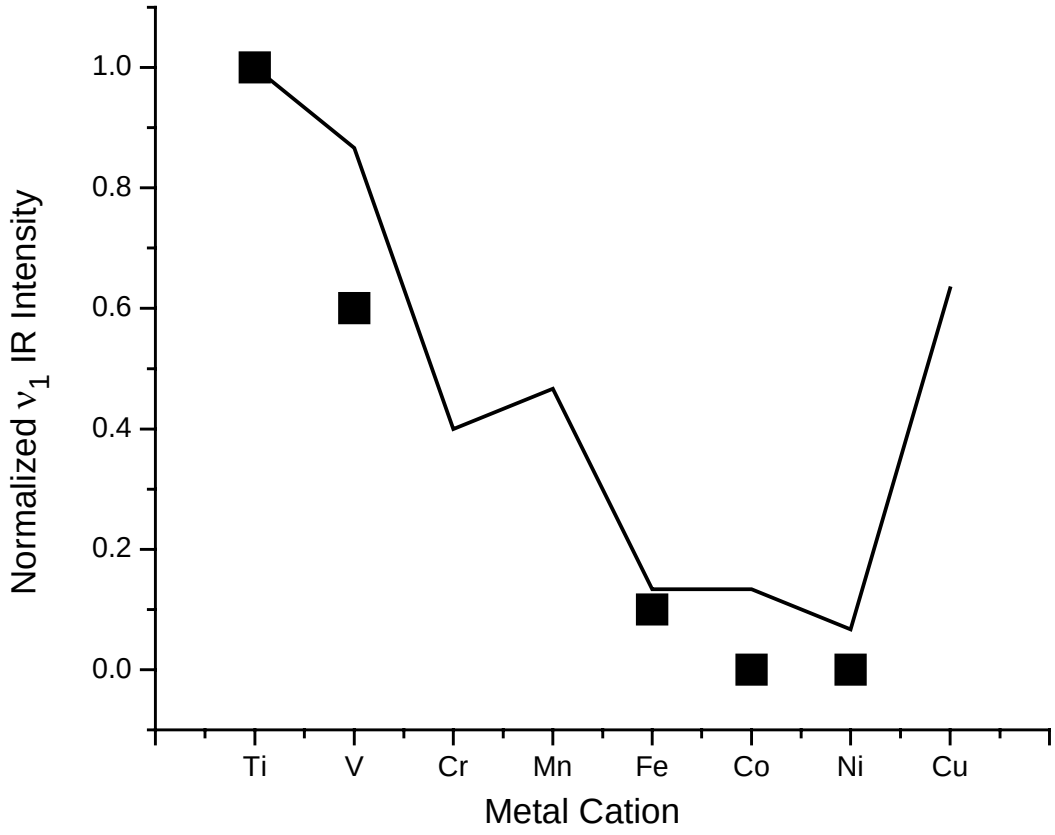
Normalized ν_1 IR Intensity
1.0
0.8
0.6
0.4
0.2
0.0
Ti
V
Cr
Mn
Fe
Co
Ni
Cu
Metal Cation

induces IR activity in this mode. The presence of the ν_1 mode, then, can be used as an indication of distorted benzene ligands.

As noted earlier, metal spin state is a big issue in the electronic structure of $M^+(benzene)_n$ complexes. It is therefore useful to compare experimental results with the predicted IR spectrum for different spin states of the same complex. $Ti^+(benzene)_2$ is used here as a convenient example. This complex is predicted to have a $^2B_{3g}$ ground state which lies ~6 kcal/mol lower in energy than a $^4A_1$ state. The predicted spectra for these complexes are compared to the IR-REMPD spectrum of $Ti^+(benzene)_2$ in Figure 5.10. The $^2B_{3g}$ spectrum is predicted to have several intense features with a few predicted around 1330 and 1510 cm^{-1}. These features are absent from the observed IR-REMPD spectrum. The predicted spectrum for the $^4A_1$ is simpler, however, and appears to match better with experimental measurements. The IR spectrum favors that of a quartet state even though a doublet is predicted to have stronger binding. Similar results were reported by this group for $V^+(benzene)_2$.[12] In this system a triplet state is predicted to be bound more strongly than the quintet state by some 23 kcal/mol. Experimental evidence, however, matched more closely to the quintet state. The simplest explanation for these discrepancies is that DFT does not handle the relative energetics of different spin states well. It tends to overestimate the bond energies for low spin states more than for higher ones, consistent with the results presented here. DFT is also known to have difficulty accurately calculating open-shelled systems.[47] It should be noted here that it is possible that the photoionization process could preferentially produce ions in metastable excited states that cannot relax before IR excitation. In the future it will be important to produce ions in other ways to investigate this effect.

Figure 5.10 A comparison of the vibrational spectrum measured for $Ti^+(benzene)_2$ with that calculated for the quartet versus doublet spin for the ground state.

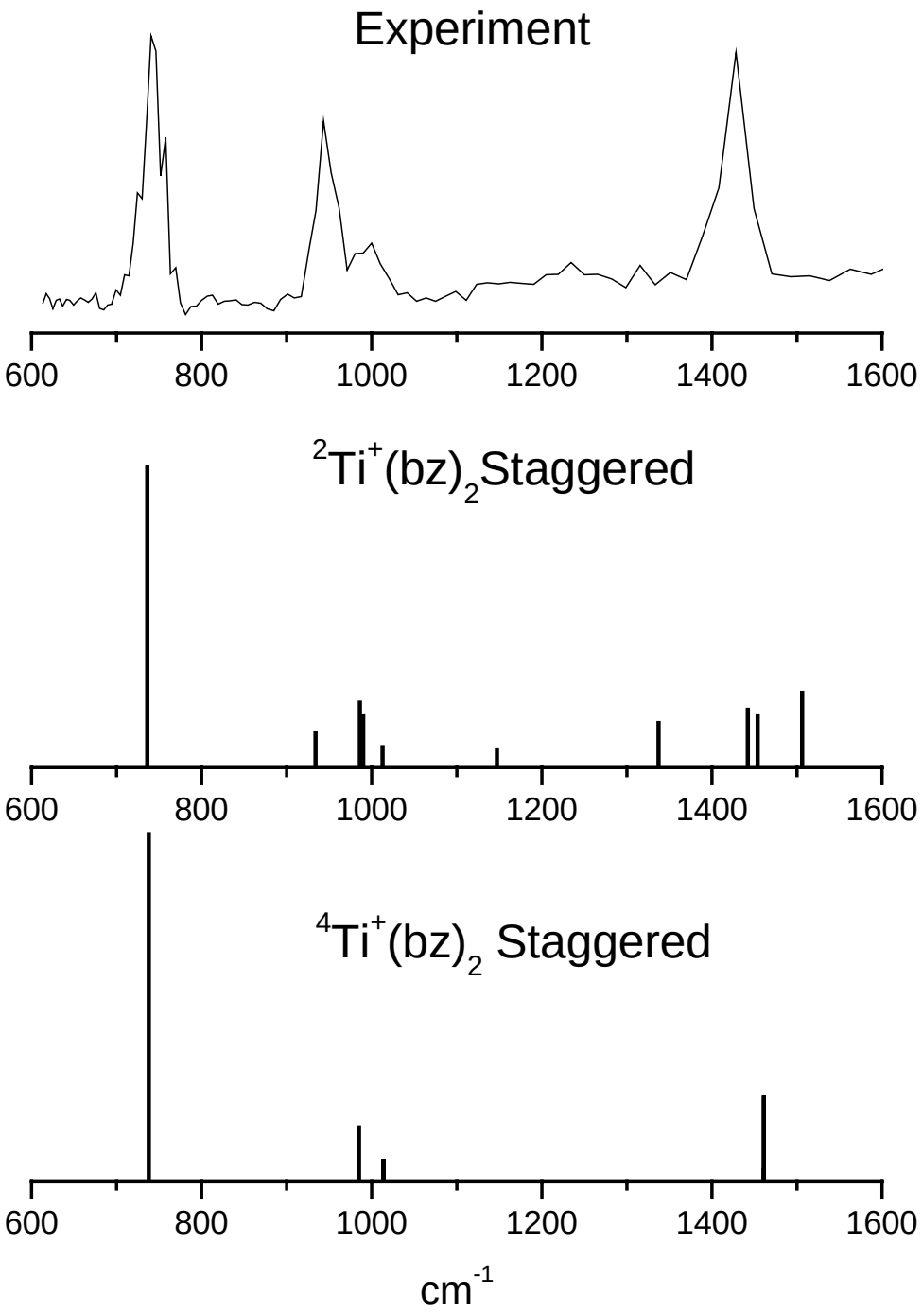
Experiment
600
800
1000
1200
1400
1600
$^{2}Ti^{+}(bz)_{2}$Staggered
600
800
1000
1200
1400
1600
$^{4}Ti^{+}(bz)_{2}$ Staggered
600
800
1000
1200
1400
1600
cm^{-1}

One other aspect of these experiments is the conformation of the benzene ligands in the dimer complexes. They have the possibility of either an eclipsed or staggered symmetry. This issue has been pervasive throughout the history of metal-benzene complexes.[8-11] It is interesting to see if comparing theory with experiment can yield insight into this issue. Figure 5.11 shows the comparison of the IR-REMPD spectrum of $Ti^+(benzene)_2$ with theoretically predicted spectra for both staggered and eclipsed conformations of the quartet state. The main difference in the two predicted spectra is the split in the ν_1 and ν_{18} modes. The staggered conformation is predicted to have a splitting of 42 cm^{-1} while the eclipsed conformation would have splitting of 20 cm^{-1}. The experimentally observed split is 46 cm^{-1}, which lies relatively close to that of the staggered conformation. It is tempting to assign the IR-REMPD spectra obtained to this complex. However, the IR-REMPD process is known to induce shifts of this magnitude, making a definitive assignment impossible. The predicted energies of the two conformers are close enough that it is possible that both are present in the molecular beam. The measured spectrum could, in fact, be a superposition of spectrum for both complexes. Because the temperature of the ions in the experiment is not known, it is also conceivable that they have enough internal energy to allow the benzene molecules to freely rotate about the C_6 axis.

Conclusion

A variety of transition metal mono- and di-benzene complexes have been studied for the first time with infrared photodissociation spectroscopy in the gas phase. Corresponding studies have investigated these complexes with density functional theory calculations, providing a systematic investigation of geometry, bond energies and electronic structure for the series of

Figure 5.11 A comparison of the vibrational spectrum measured for $Ti^+(benzene)_2$ with that predicted for the eclipsed versus staggered isomers for the quartet ground state.

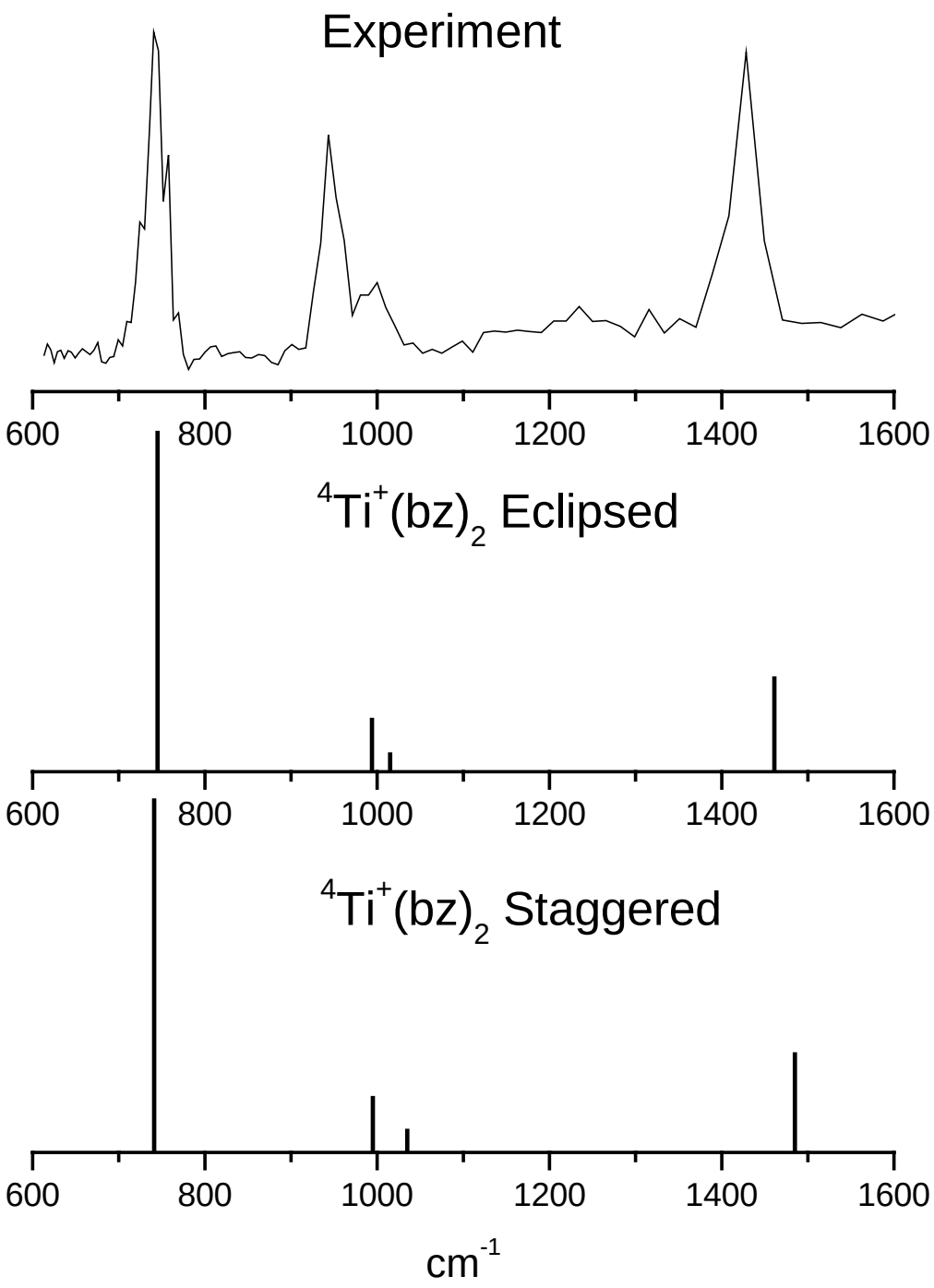
Experiment
600
800
1000
1200
1400
1600
$^4Ti^+(bz)_2$ Eclipsed
600
800
1000
1200
1400
1600
$^4Ti^+(bz)_2$ Staggered
600
800
1000
1200
1400
1600
cm^{-1}

first-row transition metals. Vibrational spectra exhibit sharp bands in the fingerprint region that can be compared to the spectra measured for condensed phase complexes produced by conventional synthesis. Through the interaction with theory, these vibrational bands can be assigned and related to corresponding vibrational motions in the free benzene molecule. In the region of this experiment (600-1700 cm^{-1}), vibrational bands are observed for the ν_{11}, ν_{18} and ν_{19} modes that are IR-active in benzene, as well as for the ν_1 mode that is IR-forbidden in benzene. The strong ν_{11} and ν_{19} bands are observed for essentially all complexes, while the ν_{18} and ν_1 bands are seen mostly for the earlier transition metals. In the same way seen previously for di-benzene sandwich complexes in the condensed phase, the systems studied here exhibit red shifts for the ν_{19} vibrational bands and blue shifts for the ν_{11} vibrational bands. The ν_{19} mode, that was predicted previously as an indicator for the degree of charge transfer in these complexes, exhibits a systematic trend with larger red shifts for the earlier transition metals. Likewise, we find a similar trend for the intensities of the ν_1 bands, which are also stronger for the earlier transition metals. Theory agrees with the qualitative trends revealed by these spectra, but the agreement on vibrational band positions is not highly quantitative.

The vibrational structure in these complexes was investigated together with theoretical predictions to determine if this would be a reliable indicator for different spin multiplicities and/or conformations (staggered versus eclipsed) in these complexes. Clear differences were found by theory for the vibrational structure in electronic states with different multiplicities. However, in selected systems where exact comparison was possible (di-benzene complexes of vanadium and titanium), the measured spectra do not agree with the patterns predicted for the lowest energy electronic states. It is conceivable that this discrepancy arises because the ions are produced in excited states, and so different ion formation methods need to be investigated to

clarify this. However, a more serious concern, which also warrants further investigation, is that DFT fails to identify the lowest energy electronic state in some of these open shell complexes. The vibrational spectra for different conformations were found to be so similar that we could not distinguish these with the present experimental resolution.

This data represents perhaps the most comprehensive study yet performed on the spectroscopy and ground state electronic structure of mono- and di-benzene transition metal ion complexes. It is clear from this study that IR spectroscopy has the potential to answer fundamental questions about the geometries and electronic structures of these complexes. Some striking patterns have been revealed here for the first time, involving the red shift of the ν_{19} bands and the intensities of the ν_1 bands. When these experiments can be extended to other regions of the IR spectrum (e.g., M-bz stretch; C-H stretch) and improved with regards to ion formation mechanism and spectroscopic resolution, further insights into the structure and bonding of these classic organometallic complexes can be anticipated.

Acknowledgements

We gratefully acknowledge support from the "Stichting voor Fundamenteel Onderzoek der materie" (FOM) and the "Nederlandse Organisatie voor Wetenschappelijk Onderzoek (NWO)". MAD acknowledges generous support for this work from the National Science Foundation (CHE-0244143). The theory work at Sandia is supported by the Division of Chemical Sciences, Geosciences, and Biosciences, the Office of Basic Energy Sciences of the U. S. Department of Energy. Sandia is a multi-program laboratory operated by Sandia Corporation, a Lockheed

Martin Company, for the United States Department of Energy's National Nuclear Security Administration under Contract No. DE-AC04-94-AL85000.

References

(1) Russell, D.H., ed., *Gas Phase Inorganic Chemistry*, Plenum, New York, 1989.

(2) Eller, K.; Schwarz, H. *Chem. Rev.* **1991**, *91*, 1121.

(3) Freiser, B.S., ed., *Organometallic Ion Chemistry*, Kluwer, Dordrecht, 1996.

(4) *Gas Phase Metal Ion Chemistry* (special issue), Leary, J.J.; Armentrout, P.B., eds., *Intl. J. Mass Spectrom.* **2001**, *204*, 1.

(5) a) Ma, J.C.; Dougherty, D.A., *Chem. Rev.* **1997**, *97*, 1303. b) Dougherty, D.A., *Science* **1996**, *271*, 163.

(6) Caldwell, J.W.; Kollman, P.A., *J. Am. Chem. Soc.* **1995**, *117*, 4177.

(7) Muetterties, E.L.; Bleeke, J.R.; Wucherer, E.J.; Albright, T.A., *Chem. Rev.* **1982**, *82*, 499.

(8) Long, N.J. *Metallocenes*, **1998**, Blackwell Sciences, Ltd., Oxford, UK.

(9) Fritz, H.R., *Adv. Organometallic Chem.* **1964**, *1*, 239.

(10) Aleksanyan, V.T., *Vib. Spectra and Structure* **1982**, *11*, 107.

(11) K. Nakamoto, *Infrared and Raman Spectra of Inorganic and Organometallic Compounds,* 5th edition, Part B, Wiley Interscience, New York, 1997.

(12) van Heijnsbergen, D.; von Helden, G.; Meijer, G.; Maitre, P.; Duncan, M.A. *J. Am. Chem. Soc.* **2002**, *124*, 1562.

(13) van Heijnsbergen, D.; Jaeger, T.D.; von Helden, G.; Meijer, G.; Duncan, M.A. *Chem. Phys. Lett.* **2002**, *364*, 345.

(14) Kealy, T.J.; Paulson, P.L., *Nature* **1951**, *168*, 1039.

(15) Fischer, E.O.; Hafner, W., *Z. fuer Naturforsch.* **1955**, *10B*, 665.

(16) a) Jacobson, D.B.; Freiser, B.S., *J. Am. Chem. Soc.* **1984**, *106*, 3900. b) Jacobson, D.B.; Freiser, B.S., *J. Am. Chem. Soc.* **1984**, *106*, 4623. c) Rufus, D.; Ranatunga, A.; Freiser, B.S., *Chem. Phys. Lett.* **1995**, *233*, 319.

(17) a) Willey, K.F.; Cheng, P.Y.; Bishop, M.B.; Duncan, M.A., *J. Am. Chem. Soc.* **1991**, *113*, 4721. b) Willey, K.F.; Yeh, C.S.; Robbins, D.L.; Duncan, M.A., *J. Phys. Chem.* **1992**, *96*, 9106.

(18) a) Chen, Y.M.; Armentrout, P.B., *Chem. Phys. Lett.* **1993**, *210*, 123. b) Meyer, F.; Khan, F.A.; Armentrout, P.B., *J. Am. Chem. Soc.* **1995**, *117*, 9740. c) Armentrout, P.B.; Hales, D.A.; Lian, L., *Adv. Metal Semicon. Clusters* (M.A. Duncan, editor) **1994**, *2*, 1(JAI Press, Greenwich, CT). d) Rogers, M.T., Armentrout, P.B., *Mass Spectrom. Rev.* **2000**, *19*, 215.

(19) a) Dunbar, R.C.; Klippenstein, S.J.; Hrusak, J.; Stöckigt, D.; Schwartz, H., *J. Am. Chem. Soc.* **1996**, *118*, 5277. b) Ho, Y.P.; Yang, Y.C.; Klippenstein, S.J.; Dunbar, R.C., *J. Phys. Chem. A* **1997**, *101*, 3338.

(20) a) Hoshino, K.; Kurikawa, T.; Takeda, H.; Nakajima, A.; Kaya, K., *J. Phys. Chem.* **1995**, *99*, 3053. b) Judai, K.; Hirano, M.; Kawamata, H.; Yabushita, S.; Nakajima, A.; Kaya, K., *Chem. Phys. Lett.* **1997**, *270*, 23. c) Yasuike, T.; Nakajima, A.; Yabushito, S.; Kaya, K., *J. Phys. Chem. A* **1997**, *101*, 5360. d) Kurikawa, T.; Takeda, H.; Hirano, M.; Judai, K.; Arita, T.; Nagoa, S.; Nakajima, A.; Kaya, K., *Organometallics* **1999**, *18*, 1430. e) Nakajima, A.; Kaya, K., *J. Phys. Chem. A*, **2000**, *104*, 176. f) Miyajima, K; Nakajima, A.; Yabushita, S; Knickelbein, M.B.; Kaya, K. *J. Am. Chem. Soc.* **2004**, *126*, 13202.

(21) Weis, P.; Kemper, P.R.; Bowers, M.T., *J. Phys. Chem. A* **1997**, *101*, 8207.

(22) a) Sodupe, M.; Bauschlicher, C.W., *J. Phys. Chem.* **1991**, *95*, 8640. b) Sodupe, M.; Bauschlicher, C.W.; Langhoff, S.R.; Partridge, H., *J. Phys. Chem.* **1992**, *96*, 2118. c)

Bauschlicher, C.W.; Partridge, H.; Langhoff, S.R., *J. Phys. Chem.* **1992**, *96*, 3273. d) Sodupe, M.; Bauschlicher, *Chem. Phys.* **1994**, *185*, 163.

(23) Stöckigt, D., *J. Phys. Chem. A* **1997**, *101*, 3800.

(24) a) Yang, C.-N.; Klippenstein, S.J., *J. Phys. Chem.* **1999**, *103*, 1094. b) Klippenstein, S.J.; Yang, C.-N., *Intl. J. Mass Spectrom.* **2000**, *201*, 253.

(25) Chaquin, P.; Costa, D.; Lepetit, C.; Che, M., *J. Phys. Chem.* **2001**, *105*, 4541.

(26) Pandey, R.; Rao, B.K.; Jena, P.; Alvarez Blanco, M., *J. Am. Chem. Soc.* **2001**, *123*, 3799.

(27) Li, Y.; Baer, T. *J. Phys. Chem. A* **2002**, *106*, 9820.

(28) Kaczorwska, M.; Harvey, J.M. *Phys. Chem. Chem. Phys.* **2002**, *4*, 5227.

(29) Gerhards, M.; Thomas, O.C.; Nilles, J.M.; Zheng, W.-J.; Bowen, K.H., Jr. *J. Chem. Phys.* **2002**, *116*, 10247.

(30) Judai, K; Sera, K.; Amatsutsumi, S.; Yagi, K.; Yasuike, T.; Nakajima, A.; Kaya, K., *Chem. Phys. Lett.* **2001**, *334*, 277.

(31) a) Cabarcos; O.M.; Weinheimer, C.J.; Lisy, J.M., *J. Chem. Phys.* **1998**, *108*, 5151. b) Cabarcos; O.M.; Weinheimer, C.J.; Lisy, J.M., *J. Chem. Phys.* **1999**, *110*, 8429.

(32) Oomens, J.; Moore, D.T.; von Helden, G.; Meijer, G.; Dunbar, R.C. *J. Am. Chem. Soc.* **2004**, *126*, 724.

(33) Oomens, J.; van Roij, A.J.A.; Meijer, G.; von Helden, G., *Astrophys. J.* **2000**, *542*, 404.

(34) van Heijnsbergen, D.; Duncan, M.A.; Meijer, G.; von Helden, G., *Chem. Phys. Lett.* **2001**, *349*, 220.

(35) Oepts, D.; van der Meer, A.F.G.; van Amersfoort, P.W., *Infrared Phys. Technol.* **1995**, *36*, 297.

(36) Shimanouchi, T., "Molecular Vibrational Frequencies" in NIST Chemistry WebBook, NIST Standard Reference Database Number 69, Eds. P.J. Linstrom and W.G. Mallard, July 2001, National Institute of Standards and Technology, Gaithersburg MD, 20899 (http://webbook.nist.gov).

(37) Becke, A. D. *J. Chem. Phys.*, **1993**, *98*, 5648.

(38) Hehre, W. J.; Radom, L.; Pople. J. A.; Schleyer, P. v. R. *Ab Initio Molecular Orbital Theory* (Wiley, New York, 1987).

(39) Parallel Quantum Solutions (PQS) QS16-2000R Parallel QuantumStation.

(40) Gaussian 98, Frisch, M. J.; Trucks, G. W.; Schlegel, H. B.; Scuseria, G. E.; Robb, M. A.; Cheeseman, J. R.; Zakrzewski, V. G.; Montgomery, J. A. Jr.; Stratmann, R. E.; Burant, J. C.; Dapprich, S.; Millam, J. M.; Daniels, A. D.; Kudin, K. N.; Strain, M. C.; Farkas, O.; Tomasi, J.; Barone, V.; Cossi, M.; Cammi, R.; Mennucci, B.; Pomelli, C.; Adamo, C.; Clifford, S.; Ochterski, J.; Petersson, G. A.; Ayala, P. Y.; Cui, Q.; Morokuma, K.; Malick, D. K.; Rabuck, A. D.; Raghavachari, K.; Foresman, J. B.; Cioslowski, J.; Ortiz, J. V.; Stefanov, B. B.; Liu, G.; Liashenko, A.; Piskorz, P.; Komaromi, I.; Gomperts, R.; Martin, R. L.; Fox, D. J.; Keith, T.; Al-Laham, M. A.; Peng, C. Y.; Nanayakkara, A.; Gonzalez, C.; Challacombe, M.; Gill, P. M. W.; Johnson, B.; Chen, W.; Wong, M. W.; Andres, J. L.; Gonzalez, C.; Head-Gordon, M.; Replogle, E. S.; Pople, J. A.; Gaussian, Inc., Pittsburgh PA, 1998.

(41) a) von Helden, G,; Holleman, I.; Meijer, G.; Sartakov, B., Optics Express **1999**, *4*, 46. b) von Helden, G.; Holleman, I.; Knippels, G.M.H.; van der Meer, A.F.G.; Meijer, G., *Phys. Rev. Lett.* **1997**, *79*, 5234.

(42) van Heijnsbergen, D.; von Helden, G.; Duncan, M.A.; van Roij, A.J.A.; Meijer, G., *Phys. Rev. Lett.* **1999**, *83*, 4983.

(43) van Heijnsbergen, D.; von Helden, G.; Meijer, G. *J. Phys. Chem. A* **2003**, *107*, 1671.

(44) Chatt, J.; Rowe, G. A.; Williams, A. A. *Proc. Chem. Soc.* **1957**, 208.

(45) Chatt, J.; Duncanson, L. A.; Guy, R. G. *J. Chem. Soc.* **1961**, 827.

(46) Chatt, J.; Duncanson, L. A.; Guy, R. G.; Thompson, D. T. *J. Chem. Soc.* **1963**, 5170.

(47) Cramer, C.J. *Essentials of Computational Chemistry*, John Wiley and Sons, West Sussex, UK, 2002.

CHAPTER 6

STRUCTURE, COORDINATION AND SOLVATION OF $V^+(BENZENE)_n$ COMPLEXES VIA GAS PHASE INFRARED SPECTROSCOPY

Abstract

$V^+(C_6H_6)_n$ (n=1-4) and $V^+(C_6H_6)_nAr$ (n=1,2) complexes are produced by laser vaporization in a pulsed nozzle cluster source. The clusters are mass-selected and studied by infrared laser photodissociation spectroscopy in the C-H stretch region of benzene. Photodissociation of $V^+(C_6H_6)_n$ complexes occurs by the elimination of intact neutral benzene molecules, while $V^+(C_6H_6)_nAr$ complexes lose Ar. The dissociation process is enhanced on vibrational resonances and the spectrum is obtained by monitoring fragment yield versus the infrared wavelength. Vibrational bands in the 2700-3300 cm^{-1} region are characteristic of the benzene molecular moiety with systematic shifts caused by the metal bonding. A dramatic change in the IR spectrum occurs at n=3, confirming that two ligands complete the coordination sphere and that additional benzenes act as solvent. The comparison between experiment and theory provides fascinating new insight into the bonding in these prototypical organometallic complexes.

Introduction

Transition metal ion-molecule complexes that are produced and studied in the gas phase are convenient examples of metal-ligand interactions and metal ion solvation.[1-4] Aromatic л-bonded complexes are relevant in many catalytic and biological processes.[5-8] These complexes are also interesting because they form sandwich structures.[7-8] Dibenzene chromium was among the first species to be synthesized using conventional techniques.[9] Gas-phase complexes can in principle be compared to those produced by conventional synthesis. Unfortunately, however, there are few spectroscopic studies that provide insight into the structures and bonding of these species. Conventional infrared (IR) spectroscopy has been applied to condensed-phase complexes,[10-12] but such measurements are difficult in the gas phase. However, gas phase measurements avoid complications from solvents or solid environments, and provide an ideal comparison to theory. We have recently measured IR spectroscopy for several metal ion-benzene complexes in the fingerprint region using a tunable free-electron laser.[13-15] In the present work, we extend these vibrational spectroscopy studies for the first time to the C-H stretch region. The vanadium-benzene system illustrates the effects of metal binding, sandwich formation and solvation on these vibrational modes.

Metal-benzene sandwiches, including bis-benzene vanadium, are familiar in the condensed phase and in gas-phase ion chemistry. In the latter area, collisional studies[16] and equilibrium mass spectrometry[17] have investigated bonding energetics, and theory has studied the details of electronic and geometric structure.[17-24] As shown by Kaya and coworkers, gas-phase $V_n(benzene)_m$ complexes form multiple-decker sandwiches.[25] Bowers and coworkers

probed these complexes with ion mobility measurements.[26] Kaya and coworkers reported a partial IR spectrum for the 1:2 complex that was size-selected as a cation, and then trapped in a rare gas matrix and neutralized.[27] However, there are few studies of gas phase spectroscopy for metal-benzene complexes. Electronic photodissociation spectroscopy has produced broad resonances associated with metal-ligand charge transfer,[28] and photoelectron spectroscopy of anions provides electron affinities.[25b,29] Lisy and coworkers have measured IR spectra of mixed-ligand alkali cation-$(water)_n(benzene)_m$ complexes in the O-H stretch region,[30] and we have recently reported the vibrational spectra of several transition metal-ion benzene complexes in the 600-1700 cm^{-1} region.[13-15] These latter studies included a detailed investigation of the spectrum of $V^+(C_6H_6)_{1,2}$ and theoretical calculations of the structures and vibrational frequencies of these complexes.[13,15] Unfortunately, these measurements were limited to the lower frequency region of the spectrum, and only complexes with one or two ligands could be studied. Further insight is expected here as these studies are extended into the C-H stretching region of the spectrum and to complexes with multiple benzene ligands.

Experimental Section

The experimental apparatus has been described previously.[31] Clusters are produced by laser vaporization at 355 nm in a pulsed nozzle cluster source and mass analyzed in a reflectron time-of-flight mass spectrometer. By using a "cutaway" type rod holder a free expansion with excess benzene produces clusters primarily of $V^+(C_6H_6)_n$ and $V^+(C_6H_6)_nAr$ (n=1,2,3,…). Metal atom recombination is not efficient in this source configuration and multiple-decker sandwich clusters are not produced efficiently. The molecular beam is skimmed from the source chamber

into a differentially pumped mass spectrometer chamber. Ions are pulse accelerated into the first flight tube, and mass selected by pulsed deflection plates located just before the reflection region. The selected ions are intersected by the infrared output of a Nd:YAG pumped optical parametric oscillator/amplifier (OPO/OPA) (LaserVision) in the turning region of the reflectron field. Photodissociation is enhanced on resonance with molecular vibrations of the ligand and infrared photodissociation spectra are obtained by monitoring the resulting fragment yield versus the laser wavelength. Parent and fragment ions are mass analyzed in the second flight tube and detected using an electron multiplier tube and a digital oscilloscope (LeCroy Waverunner LT-342). Data is transferred to a PC via an IEEE-488 interface.

Results and Discussion

IR excitation produces essentially no photodissociation signals for the $V^+(C_6H_6)_{1,2}$ complexes in the region of the IR-active C-H stretches of benzene near 3100 cm^{-1}.[32] The inefficiency of photodissociation for these complexes is consistent with their known binding energies (2.42 and 2.55 eV respectively),[16b] which are greater than the one-photon excitation energy here. To probe these complexes more effectively, we use the method of rare gas tagging with argon.[31,33-37] The binding energy of V^+-Ar is 0.38 eV (~3060 cm^{-1}),[38] and the binding energy of argon in these complexes should be less than this value. Therefore, single photon photodissociation should be possible by elimination of argon when excitation occurs near 3100 cm^{-1}. As shown in the past, tagging increases the photodissociation efficiency and argon is usually a minor perturbation on the spectrum of the complex. We find efficient photodissociation of $V^+(C_6H_6)Ar$ and $V^+(C_6H_6)_2Ar$, which occurs by the loss of argon.

Vibrational resonances occur for these species near 3100 cm^{-1}, as shown in Figure 6.1. Beginning at the n=3 complex and continuing for all larger complexes studied, the dissociation yield is substantial without argon tagging. The sudden increase in dissociation efficiency at n=3 and beyond is consistent with the presence of benzene molecules not attached to the metal ion. The binding energy of such external ligands should approximate that of the benzene dimer (about 800 cm^{-1}),[39] and so these external molecules can be eliminated via a one-photon process. Sharp vibrational spectra are measured for these complexes also in the 3100 cm^{-1} region. Spectra for the n=3-4 complexes are shown in Figures 6.1 and 6.2, and the line positions are given in Table 6.1.

The IR photodissociation spectrum of $V^+(C_6H_6)Ar$ monitored in the loss of Ar channel is shown in Figure 6.1. In the range from 2700-3300 cm^{-1} there is only one main peak. Based on the previous results of density functional theory,[13,15] this can be assigned to the ν_{12} C-H stretch of the benzene ligand in this complex, which is the only band expected to have strong IR intensity in this region. The peak occurs at 3088 cm^{-1} with a linewidth (FWHM) of ~12 cm^{-1}. A large peak with this same frequency and approximate linewidth is also recorded in the argon-loss channel for $V^+(C_6H_6)_2Ar$. For this complex a second smaller but reproducible peak is seen at 3108 cm^{-1}. For the $V^+(C_6H_6)_3$ complex, photodissociation occurs efficiently by the loss of benzene and no tagging experiments are required. The spectrum of this complex is dramatically different from those of the smaller complexes, containing a multiplet of at least four distinct features. In the center of this multiplet a band occurs at 3086 cm^{-1}, which is essentially the same position as the main band found for the $V^+(C_6H_6)Ar$ and $V^+(C_6H_6)_2Ar$ complexes. The multiplet and the band common to the n=1,2 complexes appear essentially unchanged in the spectra of the n=3,4 clusters.

Figure 6.1 Infrared photodissociation spectra for V^+(benzene)Ar, V^+(benzene)$_2$Ar and V^+(benzene)$_3$. The multiplet in the spectrum of V^+(benzene)$_3$ is assigned to the benzene Fermi triad.

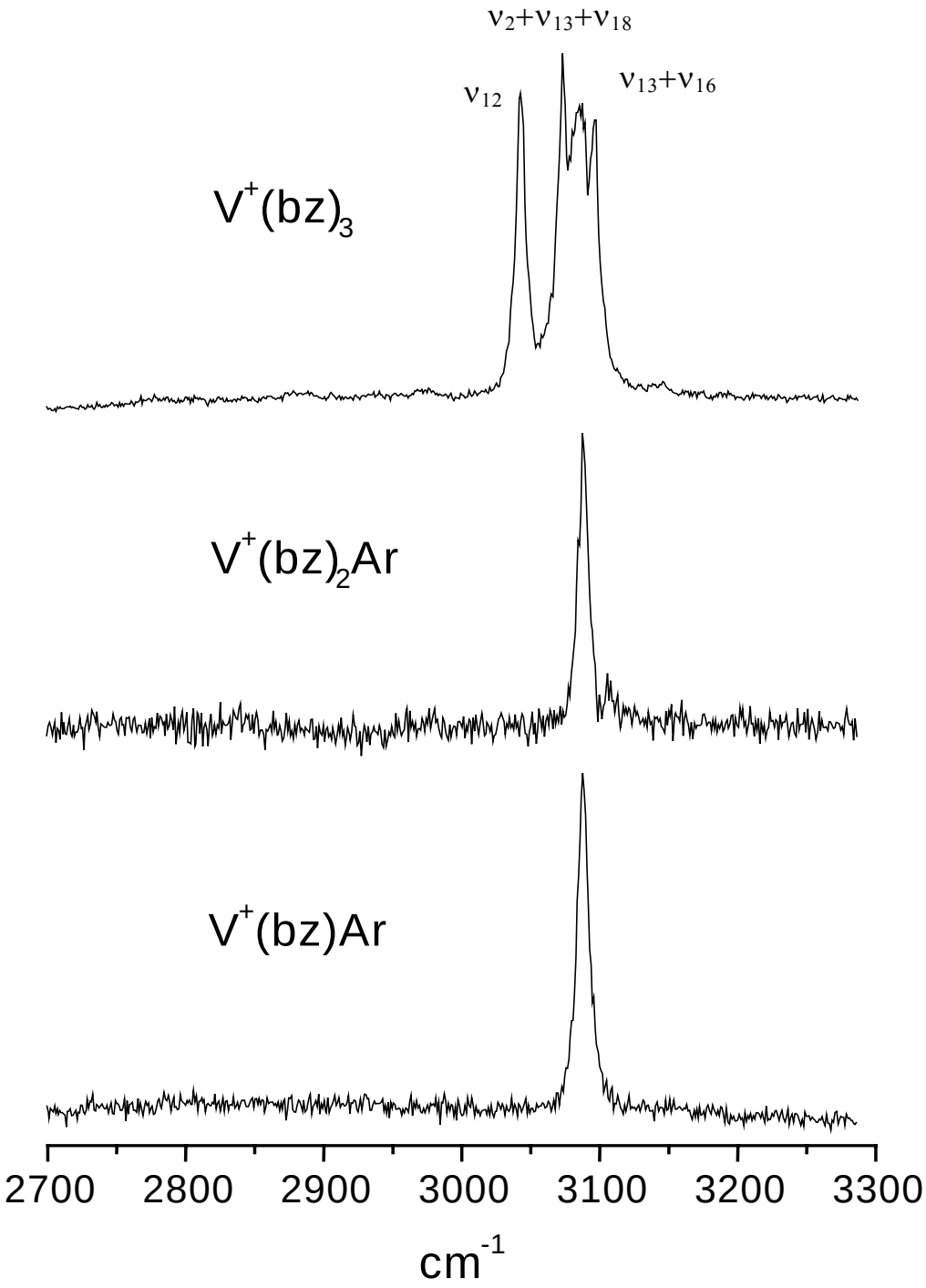
ν2+ν13+ν18
ν12
ν13+ν16
V+(bz)3
V+(bz)2Ar
V+(bz)Ar
2700
2800
2900
3000
3100
3200
3300
cm-1

Figure 6.2 Infrared photodissociation spectra for $V^+(benzene)_3$ and $V^+(benzene)_4$ measured in the C_6H_6 elimination channel. The infrared absorption spectrum of liquid benzene is shown for comparison.

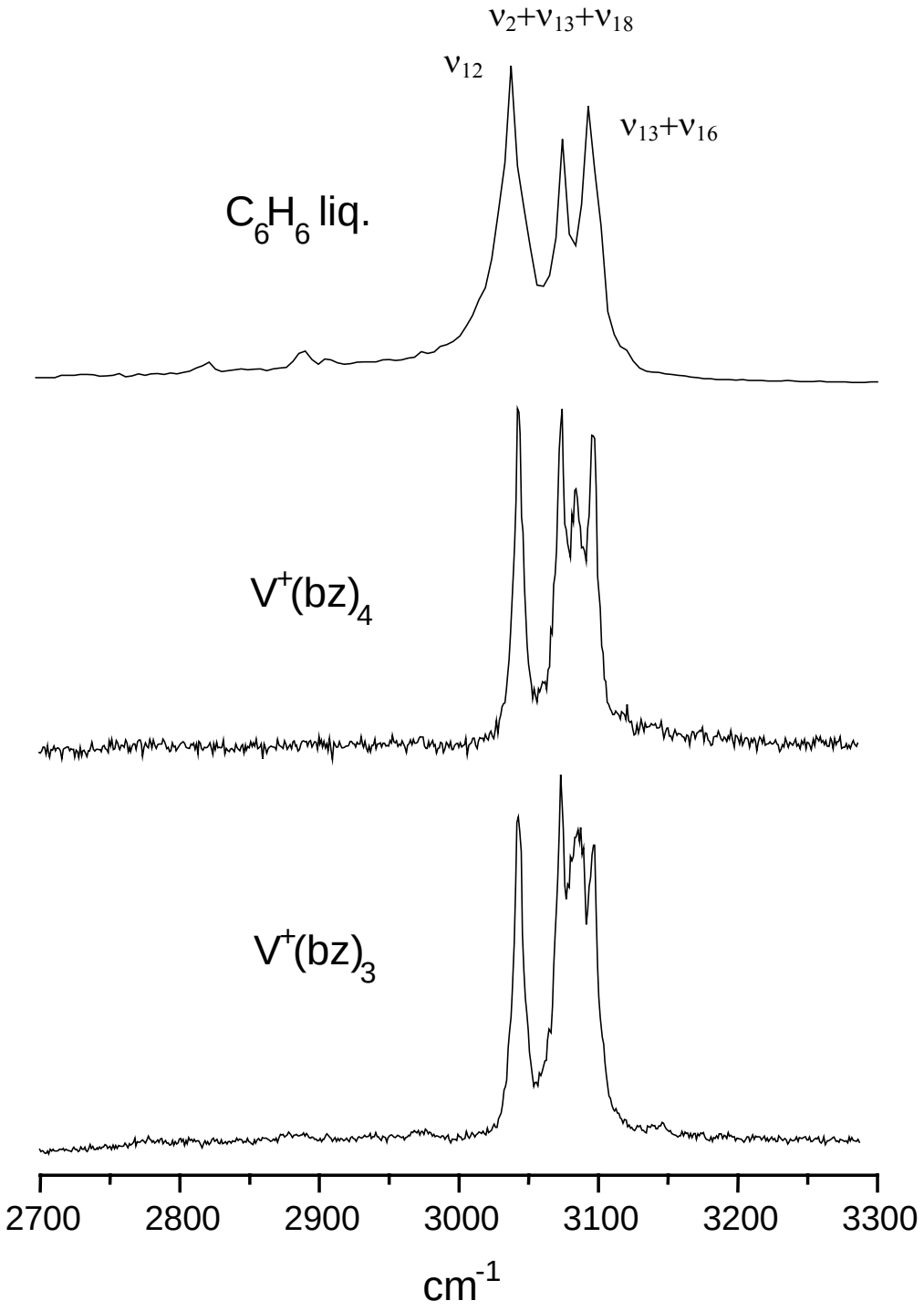
ν2+ν13+ν18
ν12
ν13+ν16
C6H6 liq.
V+(bz)4
V+(bz)3
2700
2800
2900
3000
3100
3200
3300
cm-1

Table 6.1 Experimental and theoretical line positions for various complexes.

Complex	Elect. State	Theoretical Line Position (cm^{-1})	Experimental Line Position (cm^{-1})
C_6H_6 (*l*)	$^1A_{1g}$	3063[a]	3037, 3074, 3093[b]
C_6H_6 (*g*)	$^1A_{1g}$	3063[a]	3048, 3079, 3101[c]
$V^+(C_6H_6)$	$^5B_1$ (C_{2v})	3082, 3087	3088
$V^+(C_6H_6)$	$^3A_2$ (C_{2v})	3066, 3079, 3090, 3093	3088
$V^+(C_6H_6)_2$	$^3B_{3g}$ (D_{2h})	3087, 3097, 3099	3088, 3108
$V^+(C_6H_6)_2$	$^5B_{2g}$ (D_{2h})	3087, 3091	3088, 3108
$V^+(C_6H_6)_3$			3043, 3073, 3086, 3096
$V^+(C_6H_6)_4$			3043, 3074, 3085, 3096

[a] Selected frequency value rating in the absence of Fermi triad (NIST).[32]

[b] Reference 32.

[c] Reference 40.

Figure 6.2 compares the spectra of $V^+(C_6H_6)_3$ and $V^+(C_6H_6)_4$ to the literature spectrum for liquid benzene. The liquid benzene spectrum has essentially the same appearance as the gas phase spectrum, containing three peaks at 3037, 3074 and 3093 cm^{-1}.[32] This multiplet arises from the well known Fermi triad of e_{1u} frequencies composed of the ν_{12} fundamental and the $\nu_2 + \nu_{13} + \nu_{18}$ and $\nu_{13} + \nu_{16}$ combination bands. These bands occur at 3048, 3079 and 3101 cm^{-1} in the gas phase.[40] It is apparent from the band positions and their intensities that the liquid benzene spectrum is essentially reproduced as the multiplet observed for the n=3 and 4 complexes. In addition to the features at 3086 (n=3) or 3085 (n=4) cm^{-1} corresponding to the 3088 cm^{-1} band in the smaller clusters, the multiplets have bands at 3043, 3073, and 3096 cm^{-1} (n=3) or 3043, 3074, 3096 cm^{-1} (n=4), all of which are all within 4-6 cm^{-1} of corresponding bands in the liquid spectrum. The simplest interpretation of these spectra, therefore, is that the n=1 and 2 complexes have benzene molecules attached directly to the metal cation, with concomitant shifts in their vibrational modes. These shifts, even though they may be small, are enough to remove the degeneracies that cause the Fermi triad, and this pattern simplifies to the single band from the ν_{12} fundamental expected here. At clusters beyond n=2, the ν_{12} fundamental band associated with the "core" complex persists, and the additional pattern associated with the triad re-appears. This indicates the presence of benzene molecules without any serious perturbation on their spectra, i.e., those not attached to the metal. The coordination to vanadium cation must therefore be two benzene molecules, exactly as expected for the sandwich complex, and the benzenes beyond these two act as solvating molecules in the cluster.

In the n=1,2 complexes, it is interesting to compare the vibrational mode observed to that of the free benzene molecule to investigate the effect of metal binding. Because of the Fermi resonance in isolated benzene, this comparison is not straightforward. However, the rated

frequency value for the ν_{12} mode in free benzene in the absence of the Fermi resonance is 3063 cm^{-1}.[32] This indicates that there is a 25 cm^{-1} shift to higher frequency for the ν_{12} mode in the $V^+(C_6H_6)_{1,2}$ complexes. While the presence of argon may introduce a small shift in vibrational bands, such a shift would usually go to the red.[31] Since the core band position for n=1,2 is essentially unchanged in the n=3,4 complexes which have no argon, it seems that argon plays a negligible role in this band position. However, the observation of a blue shift compared to the free molecule is somewhat surprising. In the classic Dewar-Chatt-Duncanson picture of π-bonding,[41-43] the metal-ligand interaction can be viewed from the standpoint of σ-donation of ligand bonding electron density into empty metal *d* orbitals and π back-bonding of *d* electron density into the π* antibonding orbitals. Both of these effects weaken the bonding on the benzene moiety and thus are expected to shift vibrational frequencies to *lower* values. In our recent studies of $M^+(C_6H_6)_n$ complexes, the ring distortion modes and in-plane C-H bends shifted to lower frequencies, consistent with this reasoning.[13,15] Likewise, in our previous work on metal cation-acetylene complexes of Ni^+ and Co^+, the symmetric and asymmetric C-H stretches were also red shifted.[44] However, the tendency is apparently reversed here for the C-H stretches in the vanadium-benzene complexes. However, such a blue shift has been seen previously for the C-H stretches of benzene by Dopfer and coworkers in their recent IR spectroscopy work on $C_6H_6^+$-L (L=Ar, N_2, CH_4) complexes.[45] IR photodissociation spectroscopy of such benzene *cation* complexes yielded ν_{12} resonances near 3095 cm^{-1}, some 30 cm^{-1} higher than the frequency of the neutral benzene species. This indicates that the C-H bonds become stiffer upon removal of an electron from the HOMO e_{1g} orbital of benzene. V^+ has a d^4 (^5D) configuration, with low *d* electron density compared to the later transition metals. This deficiency suggests that σ-donation will be more important than π back-bonding in its metal-benzene interaction,

resulting in greater charge transfer from the benzene toward the metal cation. In this sense, the benzene will become partially charged as in the cation, and a similar blue shift in the C-H stretches is reasonable.

In addition to the shifts induced by metal binding, the loss of the Fermi triad in the n=1 and 2 complexes is also an interesting feature of these spectra. If we derive a coupling strength for the ν_{12} mode with the $\nu_{13}+\nu_{16}$ combination mode based on the observed band splittings in the free benzene molecule,[46] and note that a Fermi resonance splitting would have to be greater than our linewidth of about 5 cm^{-1} to be detected, we can evaluate the likely proximity of these same vibrations in the metal-benzene complexes. From this analysis, we can conclude that the ν_{12} and $\nu_{13}+\nu_{16}$ combination modes, which are exactly degenerate in benzene, must be more than 18 cm^{-1} apart in the metal-benzene complex. According to the DFT results for the mono-benzene complex,[15] the $\nu_{13}+\nu_{16}$ combination occurs at 2966 cm^{-1} while the ν_{12} mode has a frequency in the 3080-3090 cm^{-1} region, depending on the spin state (see below). ν_{13} and ν_{16} are ring-distortion modes, and these shift substantially in the metal complexes because the metal binding distorts the benzene ring into a non-planar structure (see Figure 6.3), while the C-H stretching modes correlating to the ν_{12} in benzene shift to higher frequency, as noted above. It is therefore reasonable that these vibrations move away from each other in the metal complexes, resulting in the loss of the Fermi resonance.

Our previous work in the far IR on metal ion-benzene complexes featured extensive comparison with theoretical calculations.[13,15] The molecular structures, harmonic vibrational frequencies, and infrared absorption intensities were calculated for a variety of $M^+(benzene)_{1,2}$ complexes of the first-row transition metals via density functional theory (DFT) employing the

Figure 6.3 Calculated spectra for V^+(benzene) and V^+(benzene)$_2$ compared to the experimental spectra of V^+(benzene)Ar and V^+(benzene)$_2$Ar. Predicted intensities have been normalized for direct comparison. The molecular models have had their hydrogens removed and the distortion of the benzene ring has been exaggerated.

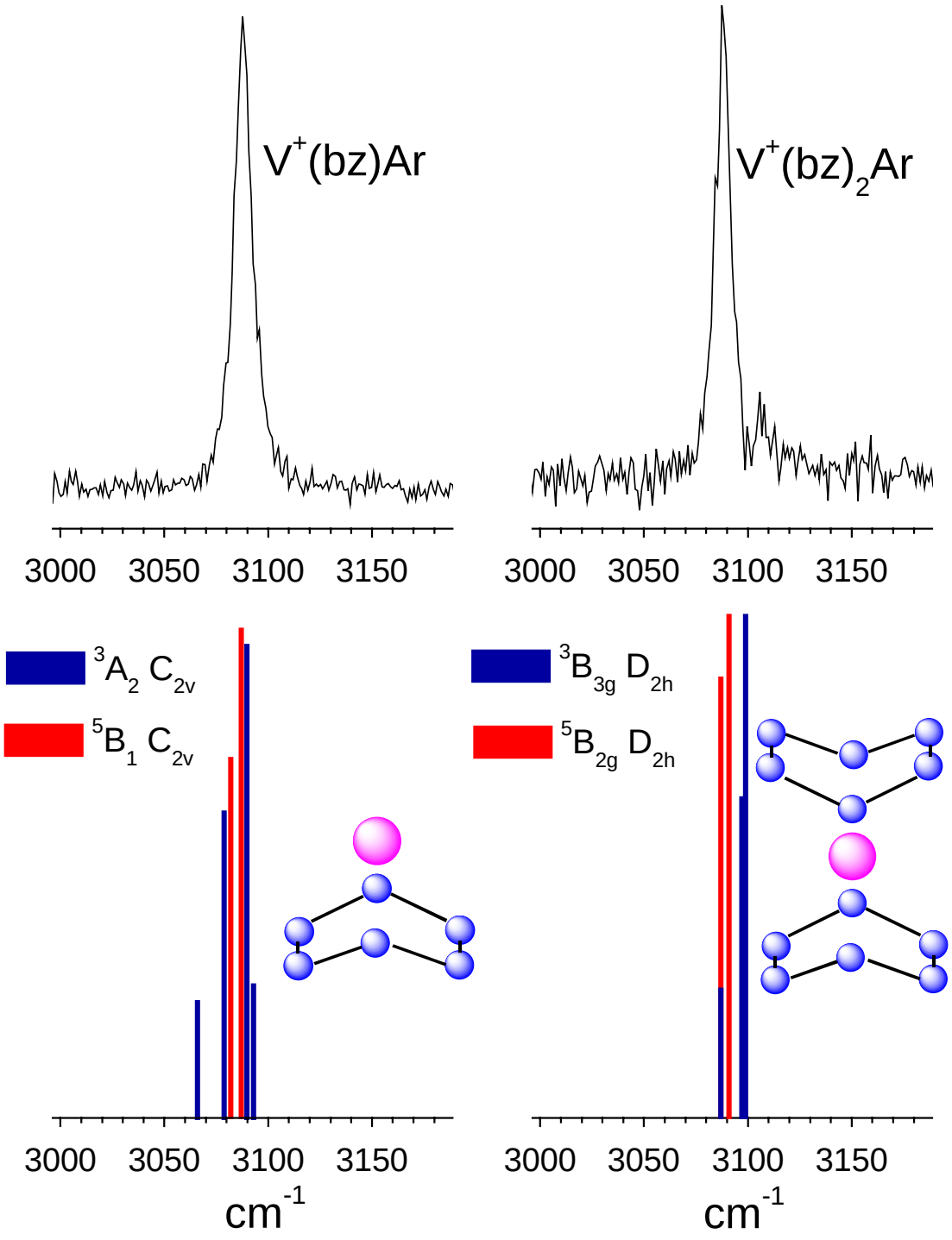
V+(bz)Ar
V+(bz)2Ar
3000
3050
3100
3150
3A2 C2v
5B1 C2v
3B3g D2h
5B2g D2h
cm-1

Becke-3 Lee-Yang-Parr (B3LYP) functional and the 6-311++G(*d*,*p*) basis set.[15] Although the trends in frequency shifts were predicted qualitatively, several discrepancies occurred between predicted IR spectra and those measured. Some issues could not be resolved due to experimental uncertainties. As the ions in that experiment were generated by photoionization (ArF, 193 nm) of neutral complexes, it was not clear that the spectra obtained were for complexes in their ground electronic state. The inherent linewidth of the free electron laser used in those multi-photon experiments, coupled with the possibility of thermally and/or electronically excited ions, led to spectral features with linewidths ranging from 20-50 cm^{-1}. These limitations caused ambiguities in the ground state symmetry and electronic structure assignment for these complexes. In the present experiments, ions are produced without photoionization and are cooled by supersonic expansion after their formation. The OPO laser linewidth is substantially narrower (0.3 cm^{-1}), resulting in sharper lines than we obtained previously. It is therefore interesting to compare these data on the C-H stretch vibrations to our previous theoretical predictions.

In the previous calculations,[13,15] the vanadium ion-benzene monomer complex was allowed to deviate from C_{6v} to C_{2v} symmetry by distortion of the benzene ring to obtain all real frequencies. The metal cation was assumed to bind to the central region of the benzene aromatic ring for both mono- and di-benzene complexes. Frequencies were scaled based on comparison of the calculated and experimental spectra of C_6H_6. The calculated spectra for $V^+(C_6H_6)$ and $V^+(C_6H_6)_2$ are compared to the experimental IR photodissociation spectra of $V^+(C_6H_6)Ar$ and $V^+(C_6H_6)_2Ar$ in Figure 6.3.

Two electronic configurations, each with C_{2v} symmetry because benzene is slightly distorted by the metal binding, were calculated as candidates for the ground state of $V^+(C_6H_6)$.[15]

The $^3A_2$ state (D_0 for loss of benzene=48.4 kcal/mol) was predicted to lie slightly lower in energy than the $^5B_1$ state (D_0=47.5 kcal/mol).[15] The binding of benzene is therefore predicted to change the spin configuration on V^+, which is a quintet in its isolated form. These two spin states have essentially the same geometric structure, but differences in the electronic structure lead to different vibrational band patterns for each. The predicted IR spectra for these two spin states are shown in Figure 6.3. The triplet is expected to have a quartet multiplet structure in the C-H stretching region, with outer peaks spaced by about 30 cm^{-1}. The quintet is predicted to have only two C-H stretching modes with similar band intensities more closely spaced at 3082 and 3087 cm^{-1}. In the experimental spectrum, only one peak is observed, with a linewidth of about 12 cm^{-1}, which is much broader than the laser linewidth. Even with this linewidth, we should have been able to see a widely spaced multiplet structure like that predicted for the triplet, but we do not. However, the two predicted peaks for the quintet species have such a small spacing (5 cm^{-1}) that these bands could easily be present but unresolved. Our spectrum therefore seems to be more consistent with the quintet electronic state, even though the triplet state is predicted to be more stable. This is not too surprising, because the energy difference predicted between the triplet and quintet species is quite small. Consistent with these observations, the vibrations in the lower frequency region observed for $V^+(C_6H_6)$ in our previous work also agreed with those predicted for the quintet ground state for this species.[13,15]

Although the measured spectra for $V^+(C_6H_6)Ar$ and $V^+(C_6H_6)_2Ar$ are quite similar, the theoretical predictions for $V^+(C_6H_6)$ and $V^+(C_6H_6)_2$ are quite different. A low-spin state like that predicted for the mono-benzene complex is also predicted as the second benzene ligand is attached to the vanadium ion, yielding a ($^3B_{3g}$) D_{2h} ground state. However, the energetic stabilization of this state is much more significant, and it is calculated to lie nearly 30 kcal/mol

lower in energy than the corresponding ($^5B_{2g}$) D_{2h} state.[13,15] However, this triplet species is predicted to have *three* IR-active bands in the C-H stretch region at 3087, 3097 and 3099 cm^{-1}.[15] While the latter two bands are too close to resolve with our linewidth, the 10 cm^{-1} splitting between the 3087 and 3097 cm^{-1} features is again great enough that we should be able to detect this splitting, but we do not. A small shift from the predicted band positions may occur in these complexes because of the presence of the argon tag. However, if there is any perturbation from argon it should be greater for the mono-benzene complex, where the binding can occur on the metal and is likely stronger. In the dibenzene complex, because the coordination is apparently filled, the argon must be bound externally to benzene through weaker van der Waals forces. Additionally, it is not clear that small shifts because of the argon would remove the multiplet predicted for the triplet state. We are therefore puzzled by the apparent poor agreement between the measured spectrum and the predicted one. A possible explanation is found in the prediction of theory for the quintet state of the sandwich complex. This species is predicted to have essentially the same vibrational spectrum as the corresponding quintet ground state for the mono-benzene complex, with two closely spaced modes (3087 and 3091 cm^{-1}) of similar intensity. Again, it is easily possible that such a doublet is present but not resolved within our linewidth. Indeed, the experiment finds spectra that are essentially identical for these two complexes. The occurrence of identical single-peak spectra can only be consistent with theory if both complexes are quintets. However, this can only be possible if density functional theory has grossly misjudged the relative energetics of the triplet and quintet spin states for the dibenzene complex.

Unfortunately, just such a problem with DFT is entirely possible, as this method is well known to be problematic for open-shell systems.[47] Indeed, we previously found the same kind of problem for $V^+(C_6H_6)_{1,2}$ complexes in the lower frequency region, where the measured spectrum

agreed with theory for the n=1 complex but did not for the dibenzene complex.[13,15] At the very least, these combined IR spectra from the fingerprint region and the C-H stretch region call into serious question the ability of DFT to handle the correct spin state for these complexes. To investigate this problem further, we performed a single point MP2 calculation (6-311++G** basis)[15] on the $V^+(C_6H_6)_2$ complex at the geometry determined by DFT. At this structure, MP2 also favors the triplet species by a large energy difference (27.9 kcal/mol). It is therefore not clear at this point why there is apparent disagreement between experiment and theory in these spectra. DFT either misses the spin state or does not accurately predict the vibrational patterns in these states. This is clearly an issue that needs to be investigated more thoroughly with a variety of theoretical methods.

The spectrum for $V^+(C_6H_6)_2Ar$ has an additional weak band occurring at 3108 cm^{-1}. There are a few possibilities for assignment of this lower intensity band. The $^3B_{3g}$ species is predicted to have modes with higher frequencies than those of the $^5B_{2g}$ species. This band could therefore result from an additional minor population of triplet species in the beam. Another possibility is a combination band on the benzene itself or for the benzene in combination with an argon stretch. Calculations on complexes like these that include the argon would be useful to assign this band and to provide further insight into the possibility of shifts it may introduce into these spectra.

Conclusion

We report here the first gas-phase infrared spectra for $V^+(C_6H_6)_{1,2}Ar$ and $V^+(C_6H_6)_{3,4}$ complexes, which are also apparently the first IR data for metal ion-benzene complexes in the C-

H stretching region. The smaller rare-gas tagged complexes yield simple spectra with one main band shifted to higher frequency than the C-H stretch of free benzene. Once the number of benzene ligands exceeds the coordination number of two a multiplet attributed to the Fermi triad of benzene is observed. This confirms that a stable core is established at n=2 and subsequent benzene molecules act as solvent for this core sandwich complex. The C-H stretching mode measured for $V^+(C_6H_6)Ar$ agrees with the pattern of IR-active bands predicted in this region for the mono-benzene complex in its $^5B_1$ state, which is predicted as one of the likely candidates for the ground state. However, the spectrum of the $V^+(C_6H_6)_2Ar$ complex exhibits systematic deviations from the spectrum predicted for the sandwich ion. Although the effects of argon cannot be completely excluded, it appears that the best assignment for the $V^+(C_6H_6)_2$ complex involves a quintet ground state rather than the triplet state predicted to be much more stable by DFT. This data is consistent with our previous IR measurements in the fingerprint region, which revealed the possible problems that DFT has in predicting the electronic spin state for these sandwich complexes.

Density functional theory is being applied widely to organometallic complexes, and further work is needed to explore the potential problems found here. These new IR measurements can be extended to other metal cation-benzene complexes. Systematic studies are underway to investigate trends in the vibrational shifts for different transition metal-benzene complexes and the details of the theory-experimental comparison for these systems.

References

(1) Russell, D.H., ed., *Gas Phase Inorganic Chemistry*, Plenum, New York, 1989.

(2) Eller, K.; Schwarz, H. *Chem. Rev.* **1991**, *91*, 1121.

(3) Freiser, B.S., ed., *Organometallic Ion Chemistry*, Kluwer, Dordrecht, 1996.

(4) *Gas Phase Metal Ion Chemistry* (special issue), Leary, J.J.; Armentrout, P.B., eds., *Intl. J. Mass Spectrom.* **2001**, *204*, 1-294.

(5) a) Ma, J.C.; Dougherty, D.A. *Chem. Rev.* **1997**, *97*, 1303. b) Dougherty, D.A. *Science* **1996**, *271*, 163.

(6) Caldwell, J.W.; Kollman, P.A. *J. Am. Chem. Soc.* **1995**, *117*, 4177.

(7) Muetterties, E.L.; Bleeke, J.R.; Wucherer, E.J.; Albright, T.A. *Chem. Rev.* **1982**, *82*, 499.

(8) Long, N.J. *Metallocenes*, **1998**, Blackwell Sciences, Ltd., Oxford, UK.

(9) Fischer, E.O.; Hafner, W. *Z. fuer Naturforsch.* **1955**, *10B*, 665.

(10) Fritz, H.R. *Adv. Organometallic Chem.* **1964**, *1*, 239.

(11) Aleksanyan, V.T. *Vib. Spectra and Structure* **1982**, *11*, 107.

(12) K. Nakamoto, *Infrared and Raman Spectra of Inorganic and Organometallic Compounds,* 5th edition, Part B, Wiley Interscience, New York, 1997.

(13) van Heijnsbergen, D.; von Helden, G.; Meijer, G.; Maitre, P.; Duncan, M.A. *J. Am. Chem. Soc.* **2002**, *124*, 1562.

(14) van Heijnsbergen, D.; Jaeger, T.D.; von Helden, G.; Meijer, G.; Duncan, M.A. *Chem. Phys. Lett.* **2002**, *364*, 345.

(15) Jaeger, T.D.; van Heijnsbergen, D.; Klippenstein, S.J.; von Helden, G.; Meijer, G.; Duncan, M.A. *J. Am. Chem. Soc.*, in press.

(16) a) Chen, Y.M.; Armentrout, P.B. *Chem. Phys. Lett.* **1993**, *210*, 123. b) Meyer, F.; Khan, F.A.; Armentrout, P.B. *J. Am. Chem. Soc.* **1995**, *117*, 9740. c) Armentrout, P.B.; Hales, D.A.; Lian, L. *Adv. Metal Semicon. Clusters* (M.A. Duncan, editor) **1994**, *2*, 1 (JAI Press, Greenwich, CT). d) Rogers, M.T., Armentrout, P.B. *Mass Spectrom. Rev.* **2000**, *19*, 215.

(17) a) Dunbar, R.C.; Klippenstein, S.J.; Hrusak, J.; Stöckigt, D.; Schwartz, H. *J. Am. Chem. Soc.* **1996**, *118*, 5277. b) Ho, Y.P.; Yang, Y.C.; Klippenstein, S.J.; Dunbar, R.C. *J. Phys. Chem. A* **1997**, *101*, 3338.

(18) a) Sodupe, M.; Bauschlicher, C.W. *J. Phys. Chem.* **1991**, *95*, 8640. b) Sodupe, M.; Bauschlicher, C.W.; Langhoff, S.R.; Partridge, H. *J. Phys. Chem.* **1992**, *96*, 2118. c) Bauschlicher, C.W.; Partridge, H.; Langhoff, S.R. *J. Phys. Chem.* **1992**, *96*, 3273. d) Sodupe, M.; Bauschlicher, C.W. *Chem. Phys.* **1994**, *185*, 163.

(19) Stöckigt, D. *J. Phys. Chem. A* **1997**, *101*, 3800.

(20) a) Yang, C.-N.; Klippenstein, S.J. *J. Phys. Chem.* **1999**, *103*, 1094. b) Klippenstein, S.J.; Yang, C.-N. *Intl. J. Mass Spectrom.* **2000**, *201*, 253.

(21) Chaquin, P.; Costa, D.; Lepetit, C.; Che, M. *J. Phys. Chem.* **2001**, *105*, 4541.

(22) Pandey, R.; Rao, B.K.; Jena, P.; Alvarez Blanco, M. *J. Am. Chem. Soc.* **2001**, *123*, 3799.

(23) Li, Y.; Baer, T. *J. Phys. Chem. A* **2002**, *106*, 9820.

(24) Kaczorwska, M.; Harvey, J.M. *Phys. Chem. Chem. Phys.* **2002**, *4*, 5227.

(25) a) Hoshino, K.; Kurikawa, T.; Takeda, H.; Nakajima, A.; Kaya, K. *J. Phys. Chem.* **1995**, *99*, 3053. b) Judai, K.; Hirano, M.; Kawamata, H.; Yabushita, S.; Nakajima, A.; Kaya, K. *Chem. Phys. Lett.* **1997**, *270*, 23. c) Yasuike, T.; Nakajima, A.; Yabushito, S.; Kaya, K. *J. Phys. Chem. A* **1997**, *101*, 5360. d) Kurikawa, T.; Takeda, H.; Hirano, M.; Judai,

K.; Arita, T.; Nagoa, S.; Nakajima, A.; Kaya, K. *Organometallics* **1999**, *18*, 1430. e) Nakajima, A.; Kaya, K. *J. Phys. Chem. A*, **2000**, *104*, 176.

(26) Weis, P.; Kemper, P.R.; Bowers, M.T. *J. Phys. Chem. A* **1997**, *101*, 8207.

(27) Judai, K; Sera, K.; Amatsutsumi, S.; Yagi, K.; Yasuike, T.; Nakajima, A.; Kaya, K. *Chem. Phys. Lett.* **2001**, *334*, 277.

(28) a) Willey, K.F.; Cheng, P.Y.; Bishop, M.B.; Duncan, M.A. *J. Am. Chem. Soc.* **1991**, *113*, 4721. b) Willey, K.F.; Yeh, C.S.; Robbins, D.L.; Duncan, M.A. *J. Phys. Chem.* **1992**, *96*, 9106.

(29) Gerhards, M.; Thomas, O.C.; Nilles, J.M.; Zheng, W.-J.; Bowen, K.H., Jr. *J. Chem. Phys.* **2002**, *116*, 10247.

(30) a) Cabarcos; O.M.; Weinheimer, C.J.; Lisy, J.M. *J. Chem. Phys.* **1998**, *108*, 5151. b) Cabarcos; O.M.; Weinheimer, C.J.; Lisy, J.M. *J. Chem. Phys.* **1999**, *110*, 8429.

(31) Duncan, M.A. *Intl. Rev. Phys. Chem.* **2003**, *22*, 407.

(32) Shimanouchi, T., "Molecular Vibrational Frequencies" in NIST Chemistry WebBook, NIST Standard Reference Database Number 69, Eds. P.J. Linstrom and W.G. Mallard, July 2001, National Institute of Standards and Technology, Gaithersburg MD, 20899 (http://webbook.nist.gov).

(33) a) Okumura, M.; Yeh, L.I.; Lee, Y.T. *J. Chem. Phys.* **1985**, *83*, 3705. b) Okumura, M.; Yeh, L.I.; Lee, Y.T. *J. Chem. Phys.* **1988**, *88*, 79.

(34) a) Meuwly, M.; Nizkorodov, S.A.; Maier, J.P.; Bieske, E.J. *J. Chem. Phys.* **1996**, *104*, 3876. b) Dopfer, O.; Roth, D.; Maier, J.P. *J. Phys. Chem. A* **2000**, *104*, 11702. c) Bieske, E.J.; Dopfer, O. *Chem. Rev.* **2000**, *100*, 3963.

(35) Ayotte, P.; Weddle, G.H.; Kim, J.; Johnson, M.A. *J. Am. Chem. Soc.* **1998**, *120*, 1236.

(36) Pino, T.; Boudin, N.; Brechignac, P. *J. Chem. Phys.* **1999**, *111*, 7337.

(37) Satink, R.G.; Piest, H.; von Helden, G.; Meijer, G. *J. Chem. Phys.* **1999**, *111*, 10750.

(38) Lessen, D.L.; Brucat, P.J. *J. Chem. Phys.* **1989**, *91*, 4522.

(39) Grover, J.R.; Walters, E.A.; Hui, E.T. *J. Phys. Chem.* **1987**, *91*, 3233.

(40) Snavely, D.L.; Walters, V.A.; Colson, S.D.; Wiberg, K.B. *Chem. Phys. Lett.* **1984**, *103*, 423.

(41) Chatt, J.; Rowe, G. A.; Williams, A. A. *Proc. Chem. Soc.* **1957**, 208.

(42) Chatt, J.; Duncanson, L. A.; Guy, R. G. *J. Chem. Soc.* **1961**, 827.

(43) Chatt, J.; Duncanson, L. A.; Guy, R. G.; Thompson, D. T. *J. Chem. Soc.* **1963**, 5170.

(44) Walters, R.S.; Jaeger, T.D.; Duncan, M.A. *J. Phys. Chem. A* **2002**, *106*, 10482.

(45) Dopfer, O.; Olkhov, R.V.; Maier, J.P. *J. Chem. Phys.* **1999**, *111*, 10754.

(46) Herzberg, G., *Molecular Spectra and Molecular Structure II. Infrared and Raman Spectra*, Van Nostrand Reinhold, New York (1945), p. 216.

(47) Cramer, C.J. *Essentials of Computational Chemistry*, John Wiley and Sons, West Sussex, UK, 2002.

CHAPTER 7

VIBRATIONAL SPECTROSCOPY OF $NI^+(BENZENE)_n$ COMPLEXES IN THE GAS PHASE

Abstract

$Ni^+(benzene)_n$ (n=1,2,3,...) and $Ni^+(benzene)_nAr_{1,2}$ (n=1,2) are produced by laser vaporization in a pulsed nozzle cluster source. The clusters are mass-selected and studied by laser photodissociation spectroscopy in a reflectron time-of-flight mass spectrometer. The excitation laser is an OPO/OPA system that produces tunable infrared light near the C-H stretch region of benzene. Photodissociation of $Ni^+(benzene)_n$ complexes occurs by the elimination of intact neutral benzene molecules while $Ni^+(benzene)_nAr_{1,2}$ complexes lose Ar. This process is enhanced on resonances and the vibrational spectrum is obtained by monitoring fragment yield versus infrared wavelength. Vibrational bands in the 2700-3300 cm^{-1} region are characteristic of the benzene molecular moiety with systematic shifts caused by the metal bonding. A dramatic change in the IR spectrum is seen at n=3, and is attributed to the superposition of spectra for two and three coordinate isomers in the molecular beam. Density functional theory calculations are employed to investigate the structures, energetics and vibrational frequencies of these complexes. The comparison between experiment and theory provides intriguing new insight into the bonding in these prototypical π-bonded organometallic complexes.

Introduction

Transition metal ion-molecule complexes that are produced, isolated, and studied in the gas phase provide models for metal-ligand interactions and metal-ion solvation.[1-4] Metal ion-benzene complexes are of particular interest for their relevance to catalytic and biological processes.[5,6] Such π-aromatic bonded systems are prevalent throughout organometallic chemistry.[7,8] Metal-ion benzene complexes are also fascinating because they form sandwich structures.[7,8] These systems can be compared to similar complexes that are synthesized and isolated using conventional techniques.[7,8] Those complexes that can be produced using traditional condensed phase methods have been studied using infrared spectroscopy, and shifts in the ligand based vibrations give information on the metal-ligand interaction.[9-12] Until recently, such information has been limited for gas phase ion complexes. In the past, we have reported the application of Infrared Resonance Enhanced Multiple-photon Photodissociation (IR-REMPD) for a variety of gas-phase transition metal-ion benzene complexes in the fingerprint region using a free electron laser (FEL).[13-15] Recently, IR photodissociation spectroscopy has been reported for $V^+(benzene)_n$ and $V^+(benzene)_nAr$ in the C-H stretch region using a tunable IR Optical Parametric Oscillator/Amplifier (OPO/OPA) laser system.[16] In the present work, we apply this technique to $Ni^+(benzene)_n$ and $Ni^+(benzene)_nAr_{1,2}$ complexes to investigate the bonding of a late transition metal-ion benzene complex.

Interest in sandwich structure complexes started with the discovery of ferrocene and the explanation of its bonding stability due to metal-ligand charge-transfer.[17] Shortly after, dibenzene chromium was synthesized and isolated.[9] The stability of both complexes was attributed to the familiar 18-electron rule.[9] Several neutral metal-benzene analogues have been

isolated and studied via conventional techniques, as have several complexes that carry a net charge and are stabilized via counter ions.[7,8] Although qualitative trends of shifts in the ligand based modes were established, many uncertainties arose from solvent effects and the presence of counter ions. It is therefore advantageous to study metal-ion benzene complexes in the gas phase where such effects are absent.

Many metal ion-benzene complexes have been studied in the gas phase by mass spectrometry.[18-23] Bond energies have been determined for such systems using collision-induced dissociation (CID),[20] equilibrium mass spectrometry,[21] and UV-vis photodissociation.[18,19] Theory has investigated the structures and energetics of these systems.[2,3,24-30] Kaya and coworkers demonstrated that various metal-benzene complexes form multiple-decker sandwich structures with alternating layers of ligands and metal ions, while other metal-benzene systems seemed to form "rice-ball" structures with metal cluster cores surrounded by ligands.[22] The tendency to form multiple-decker sandwiches is most pronounced for earlier transition metal complexes, such as those containing vanadium or titanium, while later transition metals were more likely to form rice-ball geometries. The multiple-decker sandwich structures were confirmed by ion mobility measurements performed by Bowers and coworkers,[23] as well as by magnetic deflection experiments by Kaya and coworkers.[22f] Photoelectron spectroscopy has been applied to metal-benzene anions.[22b,31] Recently, an IR absorption spectrum was obtained for $V^+(benzene)_2$ that was size-selected as a cation then deposited and subsequently neutralized in a rare gas matrix.[32] Lisy and coworkers have obtained gas phase IR photodissociation spectra for alkali cation-$(water)_x(benzene)_y$ complexes in the O-H stretch region.[33]

We have reported the vibrational spectra for several metal-ion benzene complexes in the 600-1700 cm^{-1} region.[13-15] These studies demonstrated systematic shifts in the ring based

vibrations of these complexes.[15] A comprehensive comparison to DFT calculations was also presented.[15] Unfortunately these studies were limited to complexes with only one or two benzene molecules. A recent communication showed that IR-REPD could be applied to $V^+(benzene)_n$ and $V^+(benzene)_nAr$ complexes in the C-H stretch region.[16] This study not only demonstrated that coordination is complete at two benzene molecules, but the onset of solvation is clearly marked by the appearance of the Fermi triad associated with free benzene upon the addition of a third benzene ligand.[16] Comparison with theory highlighted its difficulty to accurately describe the ground electronic state for such species.[16] This study focuses on $Ni^+(benzene)_n$ and $Ni^+(benzene)_nAr_{1,2}$ complexes to investigate spectral shifts and coordination numbers for late transition metal ion-benzene systems. Comparison with theoretical calculations are also discussed.

Experimental Section

The experimental apparatus has been described previously.[34] Briefly, clusters are produced by laser vaporization in a pulsed nozzle cluster source and mass analyzed in reflectron time-of-flight (R-TOF) mass spectrometer. The molecular beam is skimmed from the source chamber into a differentially pumped mass spectrometer chamber. Cations that form directly in the source are pulse accelerated into the first flight tube where they are mass selected by pulsed deflection plates prior to the reflectron region. The selected ions are intersected by the infrared output of a Nd:YAG pumped optical parametric oscillator/amplifier (OPO/OPA, LaserVision) in the turning region of the reflectron field. Photodissociation is enhanced on resonance with molecular vibrations of the ligand and infrared photodissociation spectra are obtained by

monitoring the resulting fragmentation yield versus the laser wavelength. Parent and fragment ions are mass analyzed in the second flight tube and detected using an electron multiplier tube and a digital oscilloscope (LeCroy Waverunner LT-342). Data is transferred to a PC via an IEEE-488 interface.

Results and Discussion

The mass spectrum of nascent cluster ions is shown in Figure 7.1. A "cutaway" type rod holder[19] is used to limit metal atom recombination. In this way, the distribution is dominated by $Ni^+(C_6H_6)_n$ (n=1,2,3,…) adducts. Clusters with multiple metal atoms, associated with multiple-decker sandwich or rice-ball type structures as seen by Kaya and coworkers,[22] are absent from this distribution. Although clustering is efficient out to n =12, a significant drop in signal intensity is seen after n=2, indicating that n=1,2 might possess greater structural stability than larger cluster sizes. Smaller intensity mass peaks in between $Ni^+(C_6H_6)_n$ peaks are attributed to $Ni^+(H_2O)(C_6H_6)_n$, $Ni^+(C_6H_6)_nAr$, and $Ni_2^+(C_6H_6)_n$ clusters.

IR excitation produces virtually no photodissociation signals for $Ni^+(C_6H_6)_{1,2}$ complexes in the region of the IR-active C-H stretches of benzene near 3100 cm^{-1}.[35] The inefficient photofragmentation for these complexes is not surprising considering their known binding energies (2.52 and 1.52 eV, respectively),[20b] which are greater than the incident photon excitation energy. To obtain photodissociation spectra of these complexes "rare gas tagging" is utilized. As shown in the past, tagging with Ar increases the photodissociation yield and is usually only a small perturbation to the system.[34,36-40] The binding energy of Ni^+-Ar is 0.55 eV (~4436 cm^{-1}),[3] and should be less in these complexes. For $Ni^+(C_6H_6)Ar$, essentially no

Figure 7.1 Mass spectrum of $Ni^+(C_6H_6)_n$ nascent ion cluster distribution. The mass spectrum is dominated by metal ion-benzene adducts. Lower intensity peaks between these adducts are attributed to $Ni^+(H_2O)(C_6H_6)_n$, $Ni^+(C_6H_6)_nAr$, and $Ni_2^+(C_6H_6)_n$ complexes.

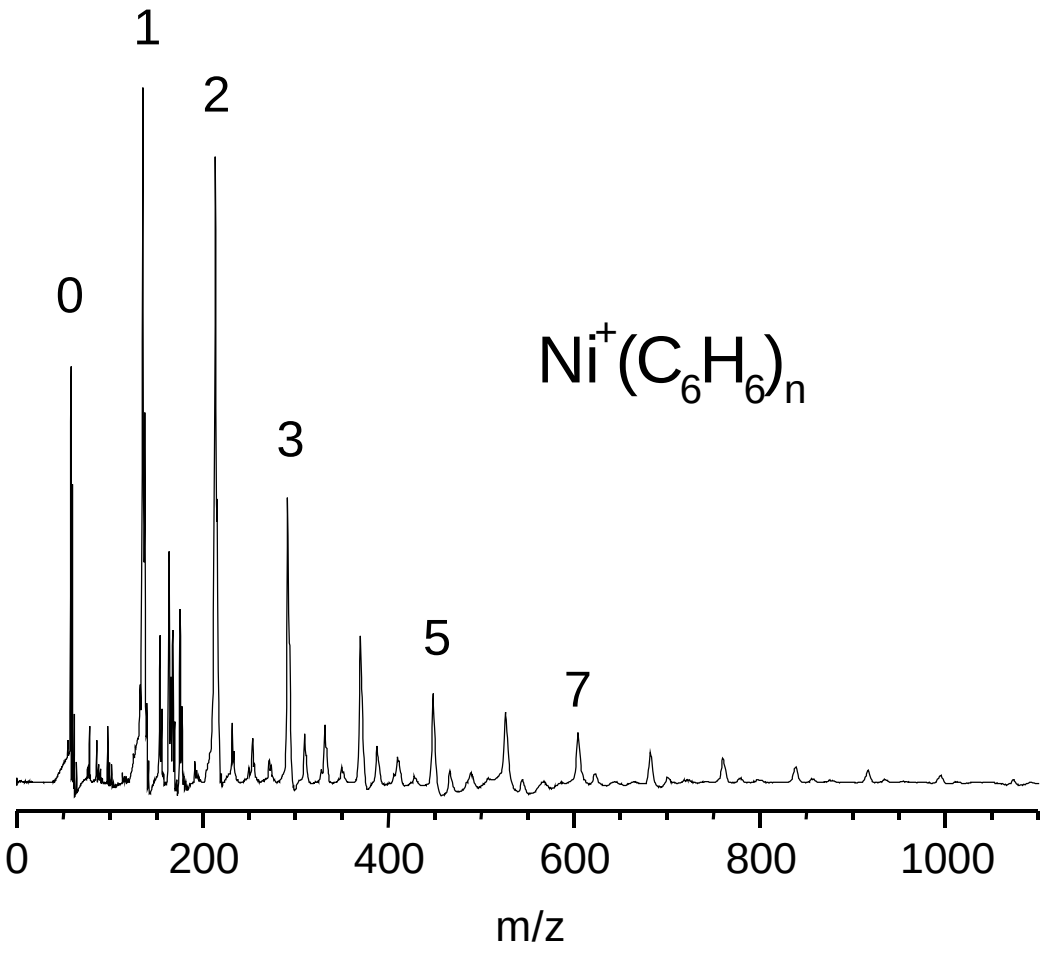
1
2
0
3
5
7
$Ni^+(C_6H_6)_n$
0
200
400
600
800
1000
m/z

photodissociation is observed, indicating that the Ar is still bound more strongly than the incident excitation energy. With the addition of a second Ar, however, efficient photofragmentation is observed near 3100 cm^{-1} by the loss of a single Ar. For $Ni^+(C_6H_6)_2Ar$, however, efficient photofragmentation is observed by the loss of Ar. Vibrational resonances occur for these two species around 3100 cm^{-1}, as shown in Figure 7.2. Beginning at the n=3 complex and continuing for all larger cluster sizes studied, the dissociation yield is substantial without argon tagging. The sudden increase in dissociation yield at n=3 and beyond is consistent with the presence of benzene molecules not attached directly to the metal ion. The binding energy of such external ligands should be similar to that of benzene dimer (~800-1000 cm^{-1}).[41-43] These external ligands can be eliminated via a one-photon process. Sharp vibrational spectra are measured for these species in the region around 3100 cm^{-1}. Spectra for n=3-6 are shown in Figure 7.3, and the line positions for all species measured are given in Table 7.1.

The IR photodissociation spectrum of $Ni^+(C_6H_6)Ar_2$ monitored in the loss of Ar channel is shown in Figure 7.2. In the range from 2700-3300 cm^{-1} a doublet is present at 3093 and 3099 cm^{-1}. Each peak has a line width (FWHM) of ~6 cm^{-1}. From the previous results of density functional theory,[15] these peaks can be attributed to the ν_{12} C-H stretch of the benzene ligand in this complex, which is the only band expected to have significant IR intensity in this region. DFT also predicts that two bands are observed because the benzene molecular moiety has been distorted from its normal planar geometry.[15] Two carbons on opposite sides of the benzene ring are drawn upwards towards the metal ion. The hydrogens on these atoms are also shifted out of the plane. The benzene ligand now has two types of non-equivalent hydrogens, and, therefore, two non-degenerate C-H stretches with frequencies close to 3100 cm^{-1}. The loss of Ar channel for $Ni^+(C_6H_6)_2Ar$, shown in Figure 7.2, shows one main feature centered at about the same

Figure 7.2 Infrared photodissociation spectra for $Ni^+(C_6H_6)Ar_2$, $Ni^+(C_6H_6)_2Ar$ and $Ni^+(C_6H_6)_3Ar$. The loss of Ar channel was monitored for these complexes. The multiplet in the spectra of $Ni^+(benzene)_3Ar$ is assigned to the benzene Fermi triad.

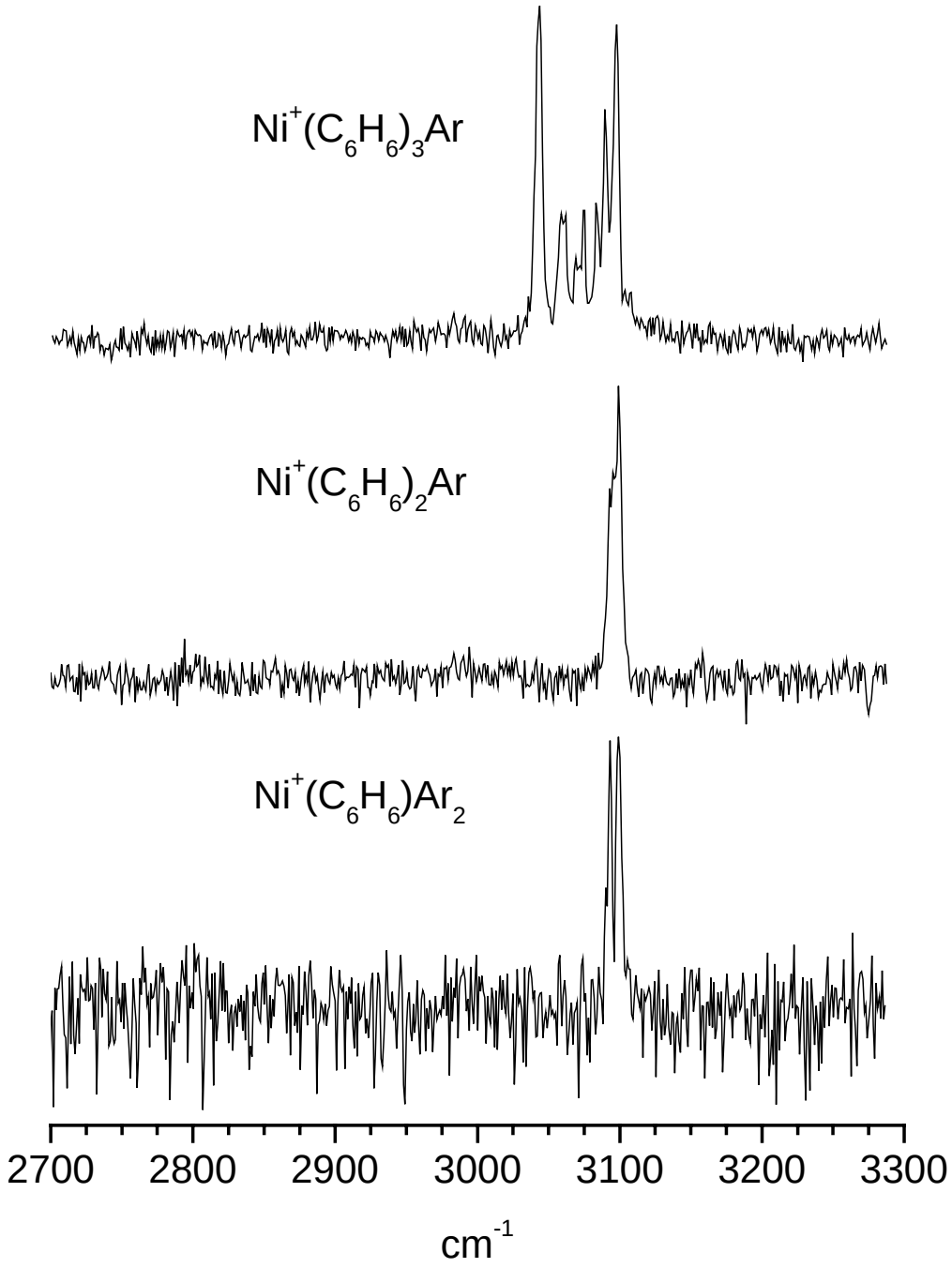
Ni+(C6H6)3Ar
Ni+(C6H6)2Ar
Ni+(C6H6)Ar2
2700
2800
2900
3000
3100
3200
3300
cm-1

Figure 7.3 Infrared photodissociation spectra for $Ni^+(C_6H_6)_3$ through $Ni^+(C_6H_6)_6$ measured in the C_6H_6 elimination channel. The infrared absorption spectra of benzene in the condensed phase is shown for comparison. The Fermi triad in liquid benzene has been labeled accordingly.

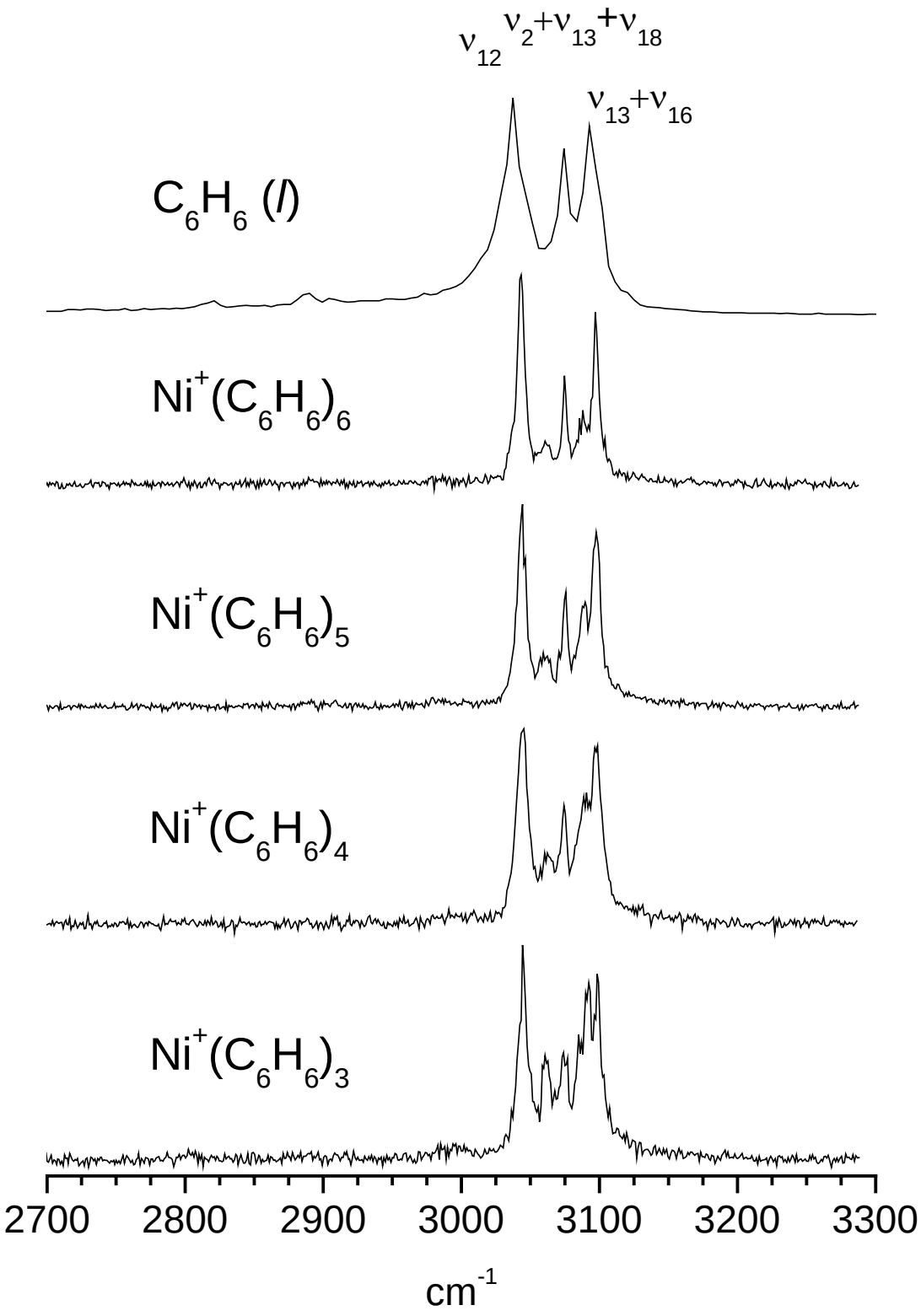
ν12
ν2+ν13+ν18
ν13+ν16
C6H6 (l)
Ni+(C6H6)6
Ni+(C6H6)5
Ni+(C6H6)4
Ni+(C6H6)3
2700
2800
2900
3000
3100
3200
3300
cm-1

Table 7.1 Experimental and Theoretical Line Positions for Various Complexes.

Complex	Elect. State	Theoretical Line Position (cm^{-1})	Experimental Line Position (cm^{-1})
C_6H_6 (*l*)	$^1A_{1g}$ (D_{6h})	3063[a]	3037, 3074, 3093[b]
C_6H_6 (*g*)	$^1A_{1g}$ (D_{6h})	3063[a]	3048, 3079, 3101[c]
$Ni^+(C_6H_6)$	$^2B_2$ (C_{2v})	3073, 3089, 3093	3093, 3099
$Ni^+(C_6H_6)_2$	^2A (C_1)	3062, 3069, 3071, 3081, 3082	3096
$Ni^+(C_6H_6)_2$	$^2B_{2g}$ (D_{2h})	3067, 3084, 3087 3092	3096
$Ni^+(C_6H_6)_3$			3044, 3060, 3074, 3084, 3090, 3098
$Ni^+(C_6H_6)_4$			3044, 3062, 3074, 3089, 3098
$Ni^+(C_6H_6)_5$			3044, 3060, 3076, 3089, 3098
$Ni^+(C_6H_6)_6$			3044, 3061, 3075, 3088, 3097

[a] Selected frequency value rating in the absence of Fermi triad (NIST)[35]

[b] Reference 35

[c] Reference 44

frequency as the doublet observed for $Ni^+(C_6H_6)Ar_2$. The peak appears to be somewhat asymmetrical, with a slight shoulder to the red. This peak occurs at 3096 cm^{-1} and has a line width (FWHM) of ~10 cm^{-1}. Due to its position and overall shape, it is reasonable that this band could contain features similar to those described for $Ni^+(C_6H_6)Ar_2$ that are unresolved. As mentioned earlier, complexes with n=3 and greater fragment efficiently without argon tagging. However, $Ni^+(C_6H_6)_3Ar$ has a similar but much sharper spectrum than $Ni^+(C_6H_6)_3$, and has therefore been shown for comparison in Figure 7.2. As can be seen, the IR photodissociation spectrum of $Ni^+(C_6H_6)_3Ar$ looks drastically different from the spectra of $Ni^+(C_6H_6)Ar_2$ and $Ni^+(C_6H_6)_2Ar$, containing a multiplet of at least six features. As shown in Figure 7.3, this multiplet appears virtually unchanged as cluster size increases. The assignment of these multiplet features requires the insight gained by previous experiments on an analogous complex.

In a recent related study, we measured IR photodissociation spectra of $V^+(C_6H_6)_n$ in the same C-H stretch region.[16] In this work, single bands were observed for n=1 and 2 and then a multiplet of four distinct features was observed for $V^+(C_6H_6)_3$. When compared with the condensed phase IR spectrum of liquid benzene, the multiplet of peaks observed for $V^+(C_6H_6)_3$ were attributed to the well known Fermi triad of e_{1u} frequencies. This triad consists of the ν_{12} fundamental and the $\nu_2 + \nu_{13} + \nu_{18}$ and $\nu_{13} + \nu_{16}$ combination bands and occur at 3037, 3074, and 3093 cm^{-1} for liquid benzene[35] and 3048, 3079, and 3101 cm^{-1} for benzene in the gas phase.[44] The remaining peak at 3086 cm^{-1} occurs slightly red-shifted from the mode observed for $V^+(C_6H_6)Ar$ and $V^+(C_6H_6)_2Ar$. The interpretation for this previous work was that $V^+(C_6H_6)Ar$ and $V^+(C_6H_6)_2Ar$ complexes have benzene molecules directly attached to the metal cation, with one vibrational band associated with the ν_{12} fundamental. In complexes with more than two benzene ligands, this "core" mode persists, slightly red-shifted, and the Fermi triad reappears,

indicating the presence of benzene molecules with little perturbation on their spectra. Based on these observations, a coordination number of two was assigned to the vanadium cation-benzene system, as expected for a sandwich complex, and further benzene molecules were concluded to act as a solvent around this stable core.

For the $Ni^+(C_6H_6)_x$ complexes, similar reasoning can be applied. The doublet observed for the n=1 occurs at 3093 and 3099 cm^{-1} and an asymmetric peak at 3096 cm^{-1} occurred for n=2. In the n=3 complex this same doublet reappears at 3084 and 3090 cm^{-1}, slightly red-shifted but with the same 6 cm^{-1} split as that observed for the n=1 complex. Likewise, as shown in Figure 7.3, a comparison of the larger cluster sizes with the condensed phase IR spectrum of liquid benzene allows for the assignment of the modes observed at 3044, 3074, and 3098 cm^{-1} to the Fermi triad of benzene. In this way, coordination is complete at n=2 and further benzene molecules merely solvate this stable core. This logic, however, does not account for the mode observed in the n=3 and larger complexes occurring at 3060 cm^{-1}. These will be discussed in detail later.

For the n=1,2 complexes, it is interesting to compare the vibrational modes observed to those of the free benzene molecule to investigate the effect of metal binding in this organometallic system. Because of the presence of a Fermi triad in free benzene, this comparison is not straightforward. However, the rated frequency value of the ν_{12} mode in free benzene in the absence of the Fermi triad (3063 cm^{-1})[35] can be used to investigate the subsequent shift caused by binding to the metal cation. This number gives shifts of 30/36 and 33 cm^{-1} to higher frequency for the n=1 and n=2 complexes, respectively. Previous work on $V^+(C_6H_6)_{1,2}$ demonstrated shifts of 25 cm^{-1} to higher frequency. Although the Ni^+ and V^+ systems were both measured using Ar tagging, a shift due to the Ar atom would be small (~2-3cm^{-1}) and generally

would go towards lower frequency.[34] Also, since the core position remains essentially unchanged in complexes with more than two benzenes, which were measured without Ar, it seems that Ar has a negligible effect on vibrational frequencies.

It is somewhat unexpected that these systems exhibit a blue shift in frequency when compared to the free molecule. In the classic Dewar-Chatt-Duncanson model of π-bonding,[45-47] the metal-ligand interaction is composed of σ-donation of ligand bonding electron density into the empty metal d orbitals and π back-bonding of d electron density into the π* antibonding orbitals of the ligand. Both of these effects weaken the bonding on the benzene molecule and are expected to shift vibrational frequencies to *lower* values. In our recent studies of $M^+(C_6H_6)_n$ complexes in the far-IR, the ring distortion modes as well as the in-plane C-H bends shifted to lower frequencies, consistent with this reasoning.[13,15] Likewise, in our previous work on metal cation-acetylene complexes of Co^+ and Ni^+, the asymmetric and symmetric C-H stretches were observed to red-shift.[48] This tendency appears to be reversed for V^+ and $Ni^+(C_6H_6)_n$ complexes. For investigation of C-H stretching frequencies it seems that the Dewar-Chatt-Duncanson model falls somewhat short in describing what occurs in these metal ion-benzene systems.

Interestingly, a blue-shift has been observed for the C-H stretches of benzene cation by Dopfer and coworkers in their IR photodissociation studies of $C_6H_6^+$-L (L=Ar, N_2, CH_4) complexes.[49] IR photodissociation of these benzene cation complexes yielded a ν_{12} fundamental of 3095 cm^{-1}, approximately 30 cm^{-1} higher in frequency than that of neutral benzene. Apparently, the C-H bonds actually become stiffer upon removal of an electron from the HOMO e_{1g} orbital of benzene. The blue shift observed in $Ni^+(C_6H_6)_n$ complexes is likely due, therefore, to charge-transfer from the benzene ligand to the metal ion, leaving benzene with a partial

positive charge. This suggest that the σ-donation does appear to be more important than π back-bonding in these metal ion-benzene complexes.

The magnitude of the blue shift observed for $Ni^+(C_6H_6)_n$ is larger than that observed for $V^+(C_6H_6)$. This is an interesting trend in the data which warrants further investigation. For $V^+(C_6H_6)$, we stated that the low *d* electron density of an early transition metal causes the σ-donation to become more important than the π back-bonding in the metal-ligand binding interaction, resulting in greater charge-transfer from the benzene to the metal cation and partial positive charge on the benzene.[16] Nickel, however, is a later transition metal with higher *d* electron density, and should, therefore, have more π back-bonding character based on this same logic. In practice, though, the $Ni^+(C_6H_6)_n$ complexes exhibit a *larger* blue shift than the $V^+(C_6H_6)_n$ complexes. This suggest that although the σ-donation does appear to be more important than π back-bonding in these metal ion-benzene complexes, it is not entirely due to the total *d* electron density.

Perhaps the magnitude of the blue shift is related to the bond strength in each of these clusters. $Ni^+(C_6H_6)$ (D_0=2.52 eV) is more strongly bound than $V^+(C_6H_6)$ (D_0=2.42 eV), however, $Ni^+(C_6H_6)_2$ (D_0=1.52) is not as strongly bound as $V^+(C_6H_6)_2$ (D_0=2.55).[20b] If the degree of shift were related to bond energy, than we would expect the monomer Ni^+ complex to have a greater blue-shift than V^+ complex, as observed experimentally. This trend, however, would switch for the dimer complexes. This is not observed experimentally, and suggests that bond energy is neither directly related to the observed spectral shift nor to the degree of charge-transfer.

The effective blue shift seems somewhat more related to the partial charges of the components of the complex. If we examine the difference in ionization potential (ΔIP) between

metal atom and benzene ligand we can get some estimate as to where the charge will reside in these complexes. The IP of benzene is 9.24 eV[50] and V and Ni have IP's of 6.75 and 7.64 eV, respectively.[51] The ΔIP of V and Ni in $M^+(C_6H_6)_n$ complexes is, therefore, 2.49 and 1.60 eV, respectively. Because Ni has an IP closer to that of C_6H_6, It is more likely that benzene could carry a partial charge in a $Ni(C_6H_6)$ cation complex than in a $V(C_6H_6)$ cation complex. A comparison of ΔIP's only gives us an estimate of this charge-transfer interaction. In order to fully understand these systems, theoretical calculations must be compared to experimental data.

Our previous work in the far-IR on metal-ion benzene complexes highlighted extensive comparison with density functional theoretical calculations.[13,15] Although the trends in frequency shifts were predicted qualitatively, several discrepancies occurred between predicted IR spectra and those obtained experimentally. Because the ions were obtained via photoionization (ArF, 193 nm) of neutral complexes, it was unclear if the spectra obtained were for their ground electronic state. Also, the inherent line width of the free electron laser and line-broadening due to multiphoton events, coupled with the possibility of thermally and/or electronically excited ions, led to spectral features with line widths ranging from 20 to 50 cm^{-1}. These limitations caused ambiguities in the analysis of these spectra. In the present experiment, nascent ions directly from the cluster source, cooled via supersonic expansion, are probed with an OPO with a laser line width of ~0.3 cm^{-1}. This results in much sharper lines than previously measured. The data in the C-H stretch region can now be compared more directly to the predictions of theory, with fewer experimental uncertainties.

The molecular structures, harmonic vibrational frequencies, and infrared absorption intensities were calculated for a variety of $M^+(C_6H_6)_{1,2}$ complexes of the first-row transition metals via DFT employing the Becke-3 Lee-Yang-Parr (B3LYP) functional and the 6-

311++G(d,p) basis set.[15] Frequencies were scaled mode by mode on the basis of comparison of the calculated and experimental spectra of C_6H_6. In the previous calculations,[15] the nickel ion-benzene monomer complex was allowed to deviate from C_{6v} to C_{2v} symmetry by distortion of the benzene ring to obtain all real frequencies. The metal cation remains in the η^6 position, centered in the middle of the benzene ring. The calculated ground state for the $Ni^+(C_6H_6)$ complex is a $^2B_2$ bound by 57.4 kcal/mol. This is the same multiplicity as the Ni^+, which has a $3d^9$ valence configuration.

The comparison of the predicted vibrational frequencies to those observed experimentally is shown in Figure 7.4. The dashed line indicates the position of the ν_{12} C-H stretch fundamental of C_6H_6 in the absence of the Fermi triad. Theory predicts two modes of large intensity at 3089 and 3093 cm^{-1}, with a smaller intensity mode at 3073 cm^{-1}. Although the experiment was conducted on species with an Ar tag, agreement is rather good. The two high frequency modes agree well with experiment both in their predicted frequencies and relative intensity to each other. Although the lower intensity mode is not observed, it is possible that the experiment is simply not sensitive enough to detect it. It is feasible to say that the spectra obtained experimentally matches the theoretically predicted ground electronic state of $^2B_2$ with C_{2v} geometry, and that the Ar tag does not perturb the system greatly.

For $Ni^+(C_6H_6)_2$, two geometries are predicted, both with doublet spin states. The lower energy state is a ^2A of C_1 symmetry in which the Ni ion resides over the η^3 position of both benzene rings, but the rings are slipped parallel to each other. This state is predicted to be bound by 33.7 kcal/mol. The second geometry is a $^2B_{2g}$ electronic state with D_{2h} symmetry in which the Ni ion resides in the η^6 position of both rings. The benzenes are distorted with two carbon atoms opposite of each other on each ring pulled toward the ion. The rings reside in an eclipsed

Figure 7.4 Calculated spectrum for $Ni^+(C_6H_6)$ is compared with the experimental spectrum of $Ni^+(C_6H_6)Ar_2$. The dashed line indicates the rated frequency value of the ν_{12} C-H stretch fundamental of benzene in the absence of the Fermi triad.

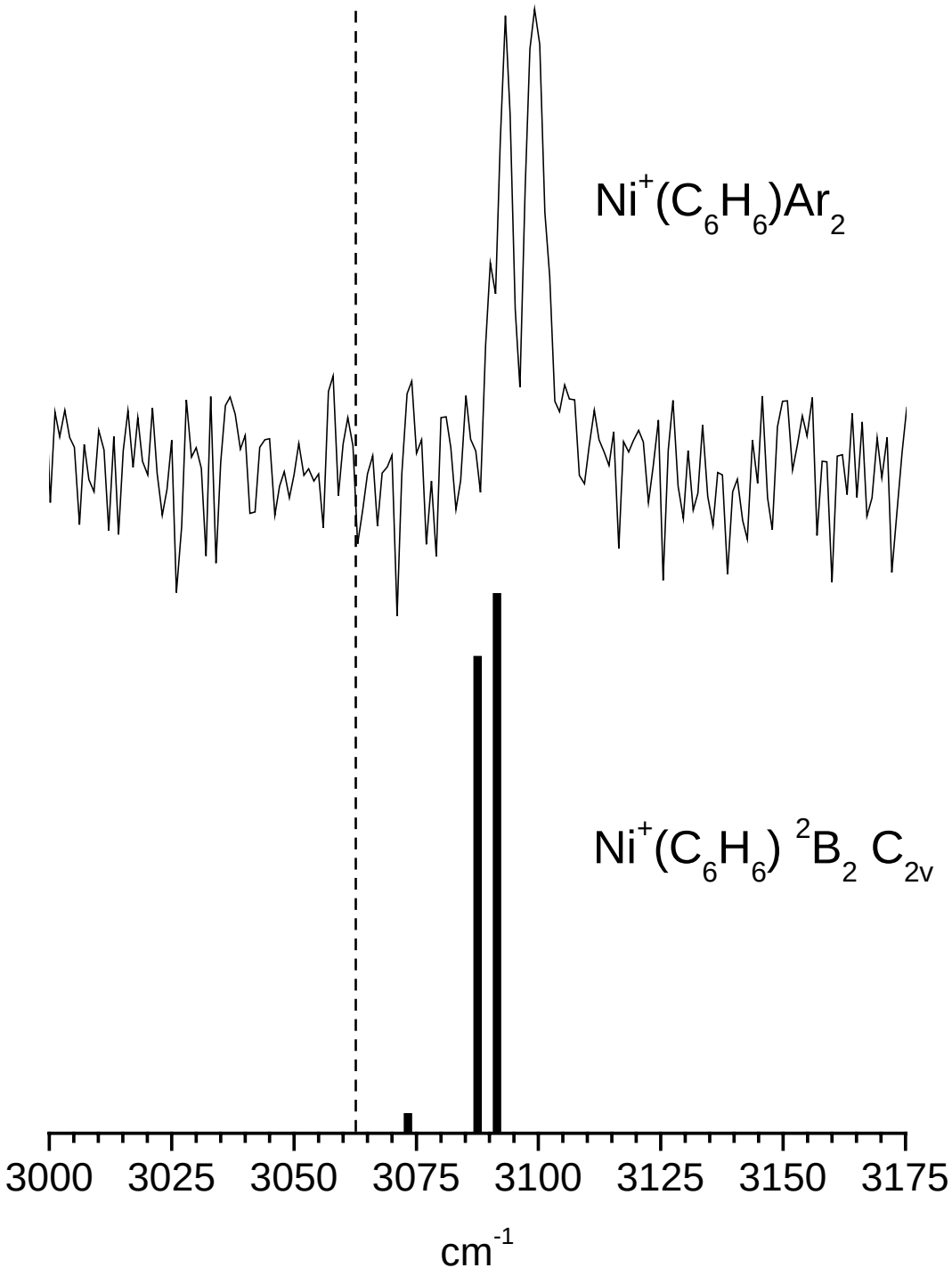
Ni+(C6H6)Ar2
Ni+(C6H6) 2B2 C2v
3000
3025
3050
3075
3100
3125
3150
3175
cm-1

configuration with each carbon on one ring aligned with a carbon on the opposite ring. The structure lies 5.4 kcal higher in energy with D_0=28.3 kcal/mol. The predicted infrared spectra are compared to experimental observations in Figure 7.5. Once again, a dashed line is used to indicate the position of the ν_{12} C-H stretch fundamental of C_6H_6 in the absence of the Fermi triad. As shown, the predicted ground state geometry, ^{2}A C_1, does not match well with experimental observations. Not only are the frequencies predicted too far to the red, the multiplet of peaks predicted is clearly not observed experimentally. The $^2B_{2g}$ D_{2h}, however, has a predicted spectrum that does appear to agree with experiment. The predicted line positions seem to agree well except for that of the lower frequency mode predicted at 3067 cm^{-1}. The intensity of this peak is predicted to be small, and it is likely that the experiment is not sensitive enough to detect this mode.

It is interesting that the lowest predicted energy state is not observed experimentally. Similar results were seen in the work with $V^+(C_6H_6)_n$ complexes.[16] In these systems the predicted ground state for both the n=1 and n=2 species is a triplet. However, experimental results matched the predicted spectra for species with a quintet spin state. Unfortunately, it is well known that DFT has a problem with misjudging the relative energetics in these systems.[52] It is clear from this comparison that the spectrum obtained experimentally is that of $^2B_{2g}$ D_{2h} species.

Although the shifts induced by metal binding are interesting to examine, the disappearance of the Fermi triad in the n=1 and 2 complexes is a fascinating feature worth further investigation. As outlined in our previous work with $V^+(C_6H_6)_n$ complexes, if we derive a coupling strength for the ν_{12} mode with the ν_{13} + ν_{16} combination mode on the basis of the splittings in the free benzene molecule[53] and note that a Fermi resonance splitting would have to

Figure 7.5 Calculated spectra for $Ni^+(C_6H_6)_2$ is compared with the experimental spectrum of $Ni^+(C_6H_6)_2Ar$. The predicted modes are shown with their relative intensities. The dashed line indicates the rated frequency value of the ν_{12} C-H stretch fundamental of benzene in the absence of the Fermi triad.

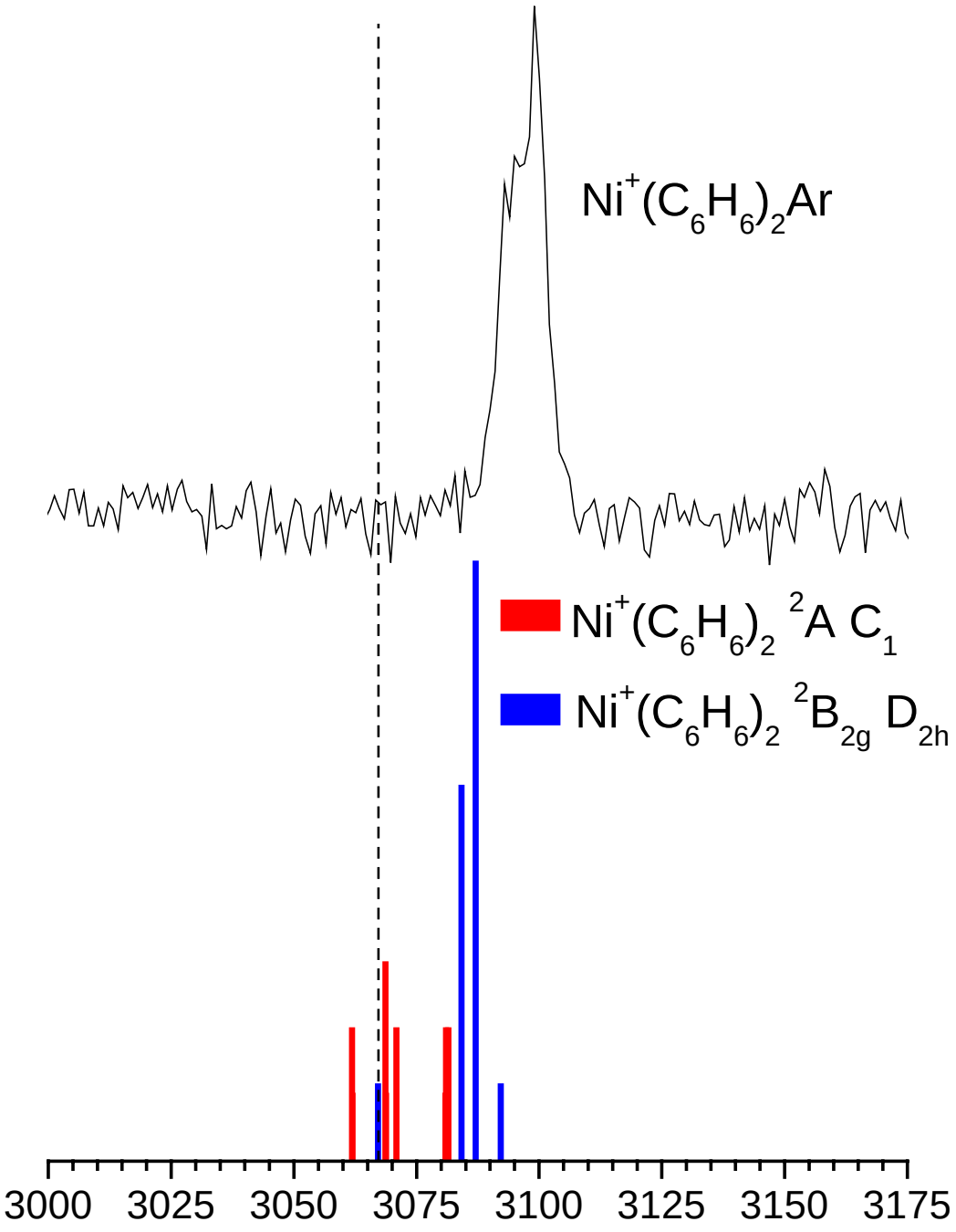
Ni+(C6H6)2Ar
Ni+(C6H6)2 2A C1
Ni+(C6H6)2 2B2g D2h
3000
3025
3050
3075
3100
3125
3150
3175

be greater than our linewidth of about 3-5 cm^{-1} to be detected, we can evaluate the likely proximity of these same vibrations in the metal ion-benzene complexes.[16] From this analysis, we can conclude that the ν_{12} and $\nu_{13} + \nu_{16}$ combination modes, which are exactly degenerate in benzene, must be more than 18 cm^{-1} apart in the metal-benzene complex. According to the DFT calculations for the nickel cation-monobenzene complex,[15] the $\nu_{13} + \nu_{16}$ combination should occur at 2989 cm^{-1} whereas the ν_{12} mode has frequencies in the 3085-3095 cm^{-1} region. ν_{13} and ν_{16} are ring-distortion modes, which shift substantially in the metal complexes due to the distortion of the benzene ring into a non-planar, C_{2v} structure, whereas the C-H stretching modes correlating to the ν_{12} mode of benzene shift to higher frequency, as previously noted. It is hence reasonable that these vibrations move away from each other in the metal complexes, resulting in the loss of the Fermi resonance.

Earlier in this paper, the spectrum of $Ni^+(C_6H_6)_3Ar$ was presented. A magnification of this spectrum is shown in Figure 7.6. The peaks associated with the Fermi triad have been labeled and the predicted IR spectra for the two geometries of $Ni^+(C_6H_6)_2$ are shown. The modes at 3084 and 3090 cm^{-1} were tentatively assigned to the $Ni^+(C_6H_6)_2$ core modes red-shifted slightly by solvation. These modes match well with those predicted by theory for the $^2B_{2g}$ D_{2h} geometry. Unfortunately, the remaining mode at 3060 cm^{-1} has not yet been assigned. There are a few possibilities for their assignment. The first possibility is that the third benzene molecule could shift the energetics of the system such that an isomer with a C_1 type $Ni^+(C_6H_6)_2$ core is established. If this occurred the Fermi triad would still be present as the third benzene molecule would be acting as a solvent. The C_1 core modes would occur slightly red shifted from their free value. The C_1 modes, shown in Figure 7.6, do not appear to match well with the observed

Figure 7.6 Calculated spectra for $Ni^+(C_6H_6)_2$ is compared with the experimental spectra of $Ni^+(C_6H_6)_3Ar$. The peaks associated with the Fermi triad have been labeled accordingly. The mode at 3060 cm^{-1} attributed to a portion of the $Ni^+(C_6H_6)_2$ core trapped in a metastable excited state is indicated by an arrow.

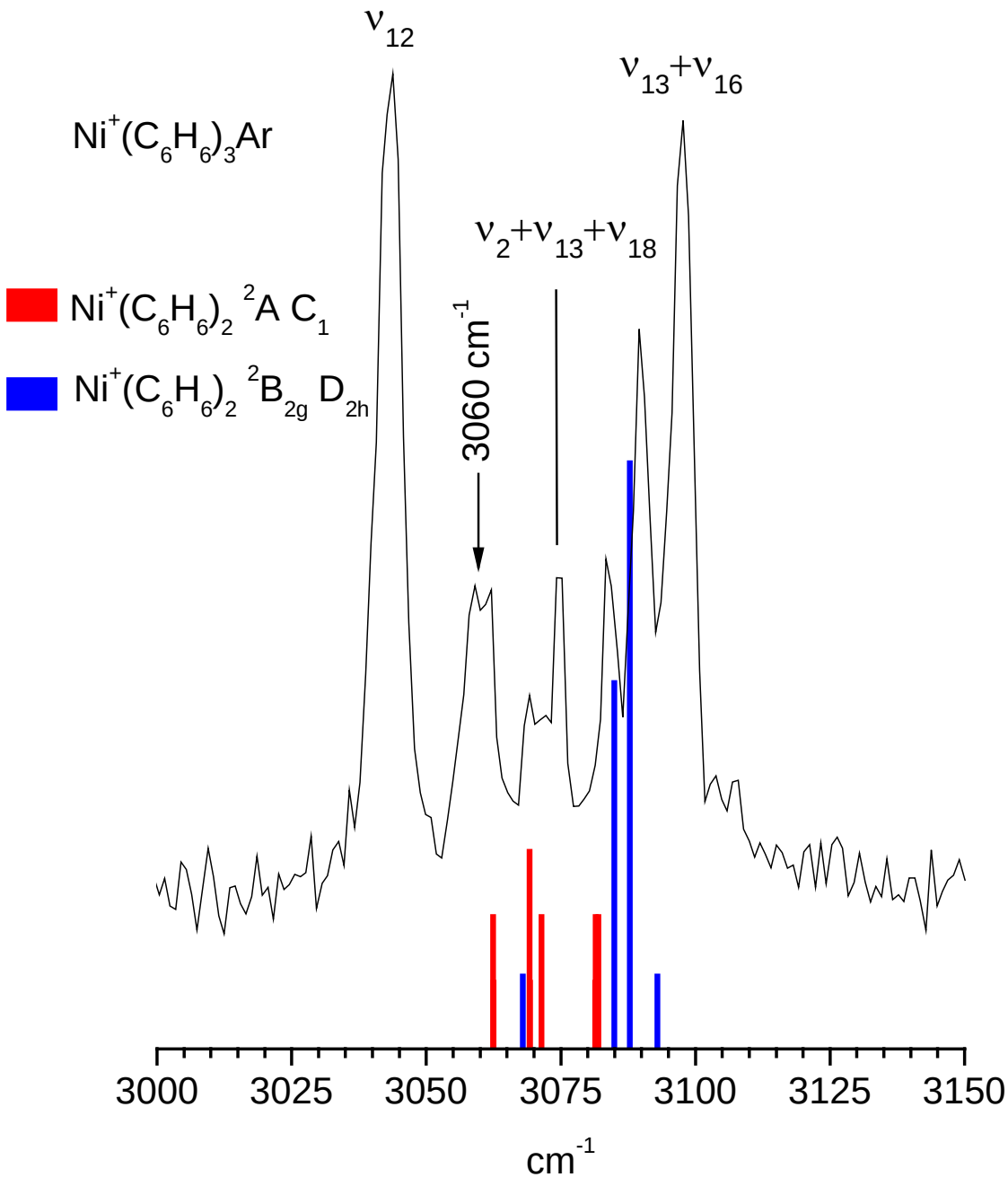
ν12
ν13+ν16
Ni+(C6H6)3Ar
ν2+ν13+ν18
Ni+(C6H6)2 2A C1
3060 cm-1
Ni+(C6H6)2 2B2g D2h
3000
3025
3050
3075
3100
3125
3150
cm-1

peak at 3060 cm^{-1} both in their predicted frequencies and relative intensities and, therefore, is most likely not a good assignment for this mode. Another possibility is that an isomer exists in the molecular beam with a coordination number of three. Studies performed by this group on $Ni^+(C_2H_2)_n$ complexes demonstrated that coordination for such complexes is complete at four.[48] Thus, it is possible that more than two benzene ligands could fit around a single nickel cation. Unfortunately, we do not have theory for the IR-active frequencies of such a complex. The mode observed here at 3060 cm^{-1} occurs closer to the rated frequency value of the ν_{12} fundamental of free benzene (3063 cm^{-1}) than those modes assigned to the $Ni^+(C_6H_6)_2$ core. This is consistent with previous IR photodissociation spectroscopy which shows that the magnitudes of shifts in ligand-based vibrations due to interaction with the metal cation decrease as more ligands are attached. However, UV photodissociation experiments performed by this group have clearly shown a coordination number of two for $Ni^+(benzene)_n$ complexes,[54] and, this too, is no the proper assignment of this mode. The third, and most likely, interpretation is that we have a metastable complex in the beam. Ni^+ has a quartet excited state roughly 1 eV higher in energy than its doublet ground state.[55] It is highly possible that $Ni^+(benzene)_n$ complexes trapped in a similar metastable excited state are created in the laser vaporization process and can not relax to the ground state before they are probed with the IR laser. UV photodissociation studies performed by this group also pointed to the existence of such a state.[54] What is observed experimentally, then, is the superposition of IR photodissociation spectra for ground state doublet and metastable quartet $Ni^+(benzene)_n$ complexes.

Conclusion

We report here the first gas phase infrared spectra for $Ni^+(C_6H_6)Ar_2$, $Ni^+(C_6H_6)_{2,3}Ar$, and $Ni^+(C_6H_6)_{3\text{-}6}$ complexes in the C-H stretch region. The $Ni^+(C_6H_6)Ar_2$ complex yields a simple spectrum with a doublet shifted to higher frequency that that of neutral benzene. The $Ni^+(C_6H_6)_2Ar$ complex has a spectrum with one main mode shifted to higher frequency than neutral benzene. Once the number of benzene ligands exceeds the coordination number of two a multiplet attributed to the Fermi triad of benzene is observed. This confirms that a stable core is established at x=2 and subsequent molecules act as a solvent for the stable sandwich core. The C-H stretching mode measured for $Ni^+(C_6H_6)Ar_2$ matches the predicted IR-active bands of the $^2B_2$ C_{2v} structure of $Ni^+(C_6H_6)$, which is the predicted ground state of this complex. The $Ni^+(C_6H_6)_2Ar$ spectrum matches that of the predicted IR-active bands of the $^2B_{2g}$ D_{2h} structure of $Ni^+(C_6H_6)_2$, which is not the predicted ground state structure of $Ni^+(C_6H_6)_2$. The IR spectra of $Ni^+(C_6H_6)_3Ar$ and $Ni^+(C_6H_6)_{3\text{-}6}$ also have a mode at 3060 cm^{-1} which becomes active in addition to the Fermi triad and $^2B_{2g}$ D_{2h} $Ni^+(C_6H_6)_2$ core modes. This mode is assigned to an isomer in the beam which is trapped in a quartet metastable electronic state. Further investigations using theoretical calculations need to be employed.

Acknowledgement

We acknowledge generous support from the National Science Foundation (CHE-0244143).

References

(1) Russell, D.H., ed., *Gas Phase Inorganic Chemistry*, Plenum, New York, 1989.

(2) Eller, K.; Schwarz, H. *Chem. Rev.* **1991**, *91*, 1121.

(3) Freiser, B.S., ed., *Organometallic Ion Chemistry*, Kluwer, Dordrecht, 1996.

(4) *Gas Phase Metal Ion Chemistry* (special issue), Leary, J.J.; Armentrout, P.B., eds., *Intl. J. Mass Spectrom.* **2001**, *204*, 1-294.

(5) a) Ma, J.C.; Dougherty, D.A. *Chem. Rev.* **1997**, *97*, 1303. b) Dougherty, D.A. *Science* **1996**, *271*, 163.

(6) Caldwell, J.W.; Kollman, P.A. *J. Am. Chem. Soc.* **1995**, *117*, 4177.

(7) Muetterties, E.L.; Bleeke, J.R.; Wucherer, E.J.; Albright, T.A. *Chem. Rev.* **1982**, *82*, 499.

(8) Long, N.J. *Metallocenes*, **1998**, Blackwell Sciences, Ltd., Oxford, UK.

(9) Fischer, E.O.; Hafner, W. *Z. fuer Naturforsch.* **1955**, *10B*, 665.

(10) Fritz, H.R. *Adv. Organometallic Chem.* **1964**, *1*, 239.

(11) Aleksanyan, V.T. *Vib. Spectra and Structure* **1982**, *11*, 107.

(12) K. Nakamoto, *Infrared and Raman Spectra of Inorganic and Organometallic Compounds,* 5th edition, Part B, Wiley Interscience, New York, 1997.

(13) van Heijnsbergen, D.; von Helden, G.; Meijer, G.; Maitre, P.; Duncan, M.A. *J. Am. Chem. Soc.* **2002**, *124*, 1562.

(14) van Heijnsbergen, D.; Jaeger, T.D.; von Helden, G.; Meijer, G.; Duncan, M.A. *Chem. Phys. Lett.* **2002**, *364*, 345.

(15) Jaeger, T.D.; van Heijnsbergen, D.; Klippenstein, S.J.; von Helden, G.; Meijer, G.; Duncan, M.A. *J. Am. Chem. Soc.*, **2004**, *126*, 10981.

(16) Jaeger, T.D.; Pillai, E.D.; Duncan, M.A. *J. Phys. Chem A* **2004**, *108*, 6605.

(17) Kealy, T.J.; Paulson, P.L. *Nature* **1951**, *168*, 1039.

(18) a) Jacobson, D.B.; Freiser, B.S. *J. Am. Chem. Soc.* **1984**, *106*, 3900. b) Jacobson, D.B.; Freiser, B.S. *J. Am. Chem. Soc.* **1984**, *106*, 4623. c) Rufus, D.; Ranatunga, A.; Freiser, B.S. *Chem. Phys. Lett.* **1995**, *233*, 319.

(19) a) Willey, K.F.; Cheng, P.Y.; Pearce, K.D.; Duncan, M.A. *J. Phys. Chem.* **1990**, *94*, 4769. b) Willey, K.F.; Cheng, P.Y.; Bishop, M.B.; Duncan, M.A. *J. Am. Chem. Soc.* **1991**, *113*, 4721. c) Willey, K.F.; Yeh, C.S.; Robbins, D.L.; Duncan, M.A. *J. Phys. Chem.* **1992**, *96*, 9106.

(20) a) Chen, Y.M.; Armentrout, P.B. *Chem. Phys. Lett.* **1993**, *210*, 123. b) Meyer, F.; Khan, F.A.; Armentrout, P.B. *J. Am. Chem. Soc.* **1995**, *117*, 9740. c) Armentrout, P.B.; Hales, D.A.; Lian, L. *Adv. Metal Semicon. Clusters* (M.A. Duncan, editor) **1994**, *2*, 1 (JAI Press, Greenwich, CT). d) Rogers, M.T., Armentrout, P.B. *Mass Spectrom. Rev.* **2000**, *19*, 215.

(21) a) Dunbar, R.C.; Klippenstein, S.J.; Hrusak, J.; Stöckigt, D.; Schwartz, H. *J. Am. Chem. Soc.* **1996**, *118*, 5277. b) Ho, Y.P.; Yang, Y.C.; Klippenstein, S.J.; Dunbar, R.C. *J. Phys. Chem. A* **1997**, *101*, 3338.

(22) a) Hoshino, K.; Kurikawa, T.; Takeda, H.; Nakajima, A.; Kaya, K. *J. Phys. Chem.* **1995**, *99*, 3053. b) Judai, K.; Hirano, M.; Kawamata, H.; Yabushita, S.; Nakajima, A.; Kaya, K. *Chem. Phys. Lett.* **1997**, *270*, 23. c) Yasuike, T.; Nakajima, A.; Yabushito, S.; Kaya, K. *J. Phys. Chem. A* **1997**, *101*, 5360. d) Kurikawa, T.; Takeda, H.; Hirano, M.; Judai, K.; Arita, T.; Nagoa, S.; Nakajima, A.; Kaya, K. *Organometallics* **1999**, *18*, 1430. e) Nakajima, A.; Kaya, K. *J. Phys. Chem. A*, **2000**, *104*, 176. f) Miyajima, K; Nakajima, A; Yabushita, S; Knickelbein, M.B.; Kaya, K. *J. Am Chem. Soc.* **2004**, *126*, 13202.

(23) Weis, P.; Kemper, P.R.; Bowers, M.T. *J. Phys. Chem. A* **1997**, *101*, 8207.

(24) a) Sodupe, M.; Bauschlicher, C.W. *J. Phys. Chem.* **1991**, *95*, 8640. b) Sodupe, M.; Bauschlicher, C.W.; Langhoff, S.R.; Partridge, H. *J. Phys. Chem.* **1992**, *96*, 2118. c) Bauschlicher, C.W.; Partridge, H.; Langhoff, S.R. *J. Phys. Chem.* **1992**, *96*, 3273. d) Sodupe, M.; Bauschlicher, C.W. *Chem. Phys.* **1994**, *185*, 163.

(25) Stöckigt, D. *J. Phys. Chem. A* **1997**, *101*, 3800.

(26) a) Yang, C.-N.; Klippenstein, S.J. *J. Phys. Chem.* **1999**, *103*, 1094. b) Klippenstein, S.J.; Yang, C.-N. *Intl. J. Mass Spectrom.* **2000**, *201*, 253.

(27) Chaquin, P.; Costa, D.; Lepetit, C.; Che, M. *J. Phys. Chem.* **2001**, *105*, 4541.

(28) Pandey, R.; Rao, B.K.; Jena, P.; Alvarez Blanco, M. *J. Am. Chem. Soc.* **2001**, *123*, 3799.

(29) Li, Y.; Baer, T. *J. Phys. Chem. A* **2002**, *106*, 9820.

(30) Kaczorwska, M.; Harvey, J.M. *Phys. Chem. Chem. Phys.* **2002**, *4*, 5227.

(31) Gerhards, M.; Thomas, O.C.; Nilles, J.M.; Zheng, W.-J.; Bowen, K.H., Jr. *J. Chem. Phys.* **2002**, *116*, 10247.

(32) Judai, K; Sera, K.; Amatsutsumi, S.; Yagi, K.; Yasuike, T.; Nakajima, A.; Kaya, K. *Chem. Phys. Lett.* **2001**, *334*, 277.

(33) a) Cabarcos; O.M.; Weinheimer, C.J.; Lisy, J.M. *J. Chem. Phys.* **1998**, *108*, 5151. b) Cabarcos; O.M.; Weinheimer, C.J.; Lisy, J.M. *J. Chem. Phys.* **1999**, *110*, 8429.

(34) Duncan, M.A. *Intl. Rev. Phys. Chem.* **2003**, *22*, 407.

(35) Shimanouchi, T., "Molecular Vibrational Frequencies" in NIST Chemistry WebBook, NIST Standard Reference Database Number 69, Eds. P.J. Linstrom and W.G. Mallard, July 2001, National Institute of Standards and Technology, Gaithersburg MD, 20899 (http://webbook.nist.gov).

(36) a) Okumura, M.; Yeh, L.I.; Lee, Y.T. *J. Chem. Phys.* **1985**, *83*, 3705. b) Okumura, M.; Yeh, L.I.; Lee, Y.T. *J. Chem. Phys.* **1988**, *88*, 79.

(37) a) Meuwly, M.; Nizkorodov, S.A.; Maier, J.P.; Bieske, E.J. *J. Chem. Phys.* **1996**, *104*, 3876. b) Dopfer, O.; Roth, D.; Maier, J.P. *J. Phys. Chem. A* **2000**, *104*, 11702. c) Bieske, E.J.; Dopfer, O. *Chem. Rev.* **2000**, *100*, 3963.

(38) a) Headrick, J.M.; Bopp, J.C.; Johnson, M.A. *J. Chem. Phys.* Submitted. b) Ayotte, P.; Weddle, G.H.; Kim, J.; Johnson, M.A. *J. Am. Chem. Soc.* **1998**, *120*, 1236. c) Bailey, C.G.; Kim, J.; Dessent, C.E.H.; Johnson, M.A. *Chem. Phys. Lett.* **1997**, *269*, 122. d) Bailey, C.G.; Kim, J.; Johnson, M.A. *J. Phys. Chem.* **1996**, *100*, 16782.

(39) Pino, T.; Boudin, N.; Brechignac, P. *J. Chem. Phys.* **1999**, *111*, 7337.

(40) Satink, R.G.; Piest, H.; von Helden, G.; Meijer, G. *J. Chem. Phys.* **1999**, *111*, 10750.

(41) Grover, J.R.; Walters, E.A.; Hui, E.T. *J. Phys. Chem.* **1987**, *91*, 3233.

(42) Krause, H.; Ernstberger, B.; Neusser, H.J. *Chem. Phys. Lett.* **1991**, *184*, 411.

(43) Sinnokrot, M.O.; Valeev, E.F.; Sherrill, C.D. *J. Am. Chem. Soc.* **2002**, *124*, 10887.

(44) Snavely, D.L.; Walters, V.A.; Colson, S.D.; Wiberg, K.B. *Chem. Phys. Lett.* **1984**, *103*, 423.

(45) Chatt, J.; Rowe, G. A.; Williams, A. A. *Proc. Chem. Soc.* **1957**, 208.

(46) Chatt, J.; Duncanson, L. A.; Guy, R. G. *J. Chem. Soc.* **1961**, 827.

(47) Chatt, J.; Duncanson, L. A.; Guy, R. G.; Thompson, D. T. *J. Chem. Soc.* **1963**, 5170.

(48) Walters, R.S.; Jaeger, T.D.; Duncan, M.A. *J. Phys. Chem. A* **2002**, *106*, 10482.

(49) Dopfer, O.; Olkhov, R.V.; Maier, J.P. *J. Chem. Phys.* **1999**, *111*, 10754.

(50) Duncan, M.A.; Dietz, T.G.; Smalley, R.E. *J. Chem. Phys.* **1981**, *75*, 2118

(51) Lias, S.G., "Gas Phase Ion Energetics" in NIST Chemistry WebBook, NIST Standard Reference Database Number 69, Eds. P.J. Linstrom and W.G. Mallard, March 2003, National Institute of Standards and Technology, Gaithersburg MD, 20899 (http://webbook.nist.gov).

(52) Cramer, C.J. *Essentials of Computational Chemistry*, John Wiley and Sons, West Sussex, UK, 2002.

(53) Herzberg, G. *Molecular Spectra and Molecular Structure II. Infrared and Raman Spectra*; Van Nostrand Reinhold: New York, 1945; p. 216.

(54) Jaeger, T.D.; Duncan, M.A. *Intl. J. Mass Spectrom.*, submitted.

(55) "Atomic Spectra Database Leves for Ni II" in NIST Atomic Spectra Database, NIST Standard Reference Database Number 78, Eds. W. C. Martin, J. Sugar, and A. Musgrove, March 1999, National Institute of Standards and Technology, Gaithersburg MD, 20899 (http://webbook.nist.gov).

CHAPTER 8

CONCLUSIONS

Metal ion-benzene systems have been investigated using UV/visible photodissociation and IR photodissociation spectroscopy. These techniques have elucidated fragmentation patterns, coordination numbers, and characterized the structure and binding in these novel organometallic systems. A thorough comparison with theoretical calculations has also been presented. IR-active vibrations in the fingerprint region, especially the ν_{19} modes, have red shifts of ~60 cm^{-1} while those in the C-H stretch region only shift by ~25 cm^{-1}. Because the shifts are larger and vary with metal, the modes in the fingerprint region are more descriptive of the bonding interaction between the metal ion and the benzene ligand than those in the C-H stretch region. Due to experimental limitations, however, spectra in the fingerprint region were only obtained for mono- and di-benzene systems. Therefore, information on solvation was only obtained in the C-H stretch region. Future work with other metal ion-aromatic systems should focus on obtaining spectra in the fingerprint region.

Because IR transitions are generally weaker than electronic transitions and because IR photon energy is sufficiently lower than metal ion-benzene dissociation energies, it was not at first clear that these experiments would work. However, it is obvious from the results presented here that infrared photodissociation spectroscopy does, in fact, work for metal ion-benzene systems. The spectra obtained by monitoring fragment yield versus IR wavelength are analogous to the vibrational spectra that would be obtained from direct absorption experiments, if these

could in fact be measured. The clearest example of this is the comparison of the spectra obtained for condensed phase metal-benzene systems[1,2] to those presented here for the gas phase species.[3-7] As explained earlier,[3-5] the same ligand based vibrational modes are observed in the fingerprint region for both condensed and gas phase species. As in condensed phase measurements,[1,2] an analysis of the shifts in these vibrations from those of the free benzene molecule yield insight into the bonding in these complexes.[3-5]

In many ways, spectra obtained using IR photodissociation are superior to those obtained for condensed phase species. First, vibrational spectra can be obtained for complexes with too low of a sample density for traditional absorption spectroscopy. Second, studying species in the gas phase eliminates perturbations induced by solvent effects or by counter ions present in condensed phase studies. Third, measurements can be made on species that could not be isolated in the gas phase, i.e. metal ion-benzene half sandwich complexes. Finally, the sensitivity of the techniques allows for study of the C-H stretches of these complexes. This is not possible in condensed phase studies because the oscillator strengths for these vibrations are too low to be detected above the solvent background.

The IR photodissociation experiments have the advantage of measuring vibrational spectra in both the fingerprint and C-H stretch regions for these molecules. As described earlier, shifts in the ligand based vibrations were observed in both regions.[3-7] The shifts recorded in the fingerprint region, however, were of a larger magnitude than those seen in the C-H stretch region. The shifts in the modes in the fingerprint region are also more dependent on the electronic state of the complex than those in the C-H stretch region. These modes, therefore, are more descriptive of which state is present in the experiment. Their potential to elucidate the

bonding properties of these complexes is better than that for modes in the C-H stretch region, and future experiments should concentrate on the fingerprint region.

The linewidth of the free electron laser, multiple-photon effects, and ion production (photoionization with ArF) problems gave broad spectral features. The low resolution spectra obtained made quantitative comparison with theoretical predictions difficult.[3-5] The use of an OPO system with improved resolution to probe supersonically cooled ions gave sharper spectra in the C-H stretch region.[6,7] Since the modes in the fingerprint region are more descriptive of the bonding in these systems it will be important to investigate metal ion-benzene systems and similar complexes using higher resolution lasers in the future. Because the fingerprint region lies below 2000 cm^{-1}, these experiments have not been possible with our OPO (scanning range of the LaserVision OPO ~2000-4500 cm^{-1}). Our lab has recently acquired a $AgGaSe_2$ crystal that expands our scanning range to 700-1900 cm^{-1}. This will allow us to obtain spectra of supersonically cooled ions in the fingerprint region for a variety of organometallic complexes.

The incident photon energy for these experiments is lower than that in the experiments performed in the C-H stretch region. In fact, the excitation energy in the fingerprint region is lower than the bond strength of many metal ion-argon complexes (see Table 1.1). This will make obtaining the spectra of many complexes difficult. Other rare gas atoms with weaker binding interactions (i.e Ne, He, etc.) will most likely need to be used. The results of this future work will, hopefully, allow for a more complete understanding of metal-ligand bonding interactions and provide for direct comparison to theoretical calculations.

Although the fingerprint region is better for describing the bonding in small metal-benzene complexes, experimental constraints prevented a thorough investigation of larger systems. Our work has shown that the C-H stretch region is good for investigating the solvation

process in larger metal-benzene systems. As mentioned earlier,[6,7] once the number of benzene ligands exceeded two, the Fermi triad of benzene is observed in the C-H stretch region. This is clear-cut evidence of unperturbed benzene molecules attached to metal ion-benzene complex core. This is interpreted as confirmation of the predicted coordination number of two for these complexes. Preliminary experiments performed in the fingerprint region also show bands present near the frequencies of free benzene when the number of ligands exceeds two. Further work should be performed in the fingerprint region using better mass selection and a high-resolution OPO to confirm that solvation begins with the addition of the third benzene ligand.

It would be interesting to find a metal-ion benzene system in which the coordination number is greater than two. Possible candidates could be those systems which Kaya and coworkers[8] found to have rice-ball structures (i.e. Fe, Co, and Ni). We have investigated Ni-benzene complexes and find no evidence for a coordination number greater than two. This does not, however, eliminate the possibility that Fe and Co could have a coordination number greater than two. Studies should also investigate larger metal ions such as gold or platinum to see if a coordination number other than two is possible.

The previous chapters provided a thorough comparison of our experimental results with DFT calculations.[5] It was found that the predicted ground electronic state for many of these metal ion-benzene complexes did not match the IR photodissociation spectra obtained. This is attributed to the difficulty DFT has in dealing with open-shelled systems and in dealing with the relative energetics of different spin states.[9] DFT has a tendency to erroneously predict higher bond energies for low spin states than for high spin states. Because these faults have been found and highlighted by this work, it has become apparent that improvements must be made in the theoretical techniques. Either changes must be made to the framework of DFT, or more

powerful processors must be developed so higher order calculations (MP2, CCSD, etc.) can be implemented.

Although the work presented here has concentrated on metal ion-benzene complexes, there are many other systems worth investigating. As described previously, much insight into the charge transfer character in metal ion-benzene systems is gained by examining the amount of shift in the υ_{19} in plane carbon ring distortion mode.[5,10] This mode is not present solely in these systems. Any complex with an aromatic ring or phenyl group will have a ring distortion vibration analogous to the υ_{19} mode. IR photodissociation spectra of metal ion complexes with naphthalene, C_{60}, coronene, or other polyaromatic hydrocarbons (PAH's) would most likely contain a ring distortion mode shifted from that of the free molecule. Several studies using a variety of metals and ligands would help to elucidate trends in shifts of this mode. From these, the charge transfer interactions could be better understood.

Ligands with multiple aromatic rings have more than one possible binding site for the metal ion.[11-13] Along with description of the charge transfer character, the shifts in the modes in the fingerprint region would also help to determine where the metal ion binds. Larger ligands could also bind to multiple metal atoms. IR photodissociation spectra would show whether multiple metal atoms bind as a cluster or in individual sites on the ligand. Additionally, complexes of multiple metal atoms and multiple ligands could be studied. For example, IR photodissociation spectroscopy of $M_x(benzene)_y$ complexes could confirm or refute the multiple-decker sandwich and rice-ball structures proposed by Kaya and coworkers.[13] This work could be expanded to similar systems involving multiple metal atoms bound to cyclooctatetraene, coronene, C_{60}, etc. because all of these complexes should possess IR-active ring distortion modes in the fingerprint region.

The work presented here demonstrates that IR photodissociation spectroscopy is a versatile technique. It will no doubt be used in the future for a wide variety of organometallic systems. The diversity of systems which can be studied increases as IR light sources improve. These will no doubt help to further the overall understanding of bonding in many novel organometallic systems. The applications, at this point, seems to be limited only by the imagination.

References

(1) Fritz, H.R., *Adv. Organometallic Chem.* **1964**, *1*, 239.

(2) K. Nakamoto, *Infrared and Raman Spectra of Inorganic and Organometallic Compounds,* 5th edition, Part B, Wiley Interscience, New York, 1997.

(3) van Heijnsbergen, D.; von Helden, G.; Meijer, G.; Maitre, P.; Duncan, M.A. *J. Am. Chem. Soc.* **2002**, *124*, 1562.

(4) van Heijnsbergen, D.; Jaeger, T.D.; von Helden, G.; Meijer, G.; Duncan, M.A. *Chem. Phys. Lett.* **2002**, *364*, 345.

(5) Jaeger, T.D.; van Heijnsbergen, D.; Klippenstein, S.J.; von Helden, G.; Meijer, G.; Duncan, M.A. *J. Am. Chem. Soc.*, **2004**, *126*, 10981.

(6) Jaeger, T.D.; Pillai, E.D.; Duncan, M.A. *J. Phys. Chem A* **2004**, *108*, 6605.

(7) Jaeger, T.D.; Duncan, M.A. *J. Phys. Chem A.*, submitted.

(8) a) Hoshino, K.; Kurikawa, T.; Takeda, H.; Nakajima, A.; Kaya, K. *J. Phys. Chem.* **1995**, *99*, 3053. b) Judai, K.; Hirano, M.; Kawamata, H.; Yabushita, S.; Nakajima, A.; Kaya, K. *Chem. Phys. Lett.* **1997**, *270*, 23. c) Yasuike, T.; Nakajima, A.; Yabushito, S.; Kaya, K. *J. Phys. Chem. A* **1997**, *101*, 5360. d) Kurikawa, T.; Takeda, H.; Hirano, M.; Judai, K.; Arita, T.; Nagoa, S.; Nakajima, A.; Kaya, K. *Organometallics* **1999**, *18*, 1430. e) Nakajima, A.; Kaya, K. *J. Phys. Chem. A*, **2000**, *104*, 176. f) Miyajima, K; Nakajima, A; Yabushita, S; Knickelbein, M.B.; Kaya, K. *J. Am Chem. Soc.* **2004**, *126*, 13202.

(9) Cramer, C.J. *Essentials of Computational Chemistry*, John Wiley and Sons, West Sussex, UK, 2002.

(10) Chaquin, P.; Costa, D.; Lepetit, C.; Che, M., *J. Phys. Chem.* **2001**, *105*, 4541.

(11) Mulliken, R.S; Person, W.B *Molecular Complexes*, Wiley Interscience: New York, 1969.

(12) a) Ma, J.C.; Dougherty, D.A. *Chem. Rev.* **1997**, *97*, 1303. b) Dougherty, D.A. *Science* **1996**, *271*, 163.

(13) Caldwell, J.W.; Kollman, P.A. *J. Am. Chem. Soc.* **1995**, *117*, 4177.

APPENDIX

CALCULATED VIBRATIONAL FREQUENCIES FOR TRANSITION METAL ION-BENZENE COMPLEXES

Complex	**Grnd. State**	**Symmetry**	**D_0 (kcal/mol)**	**IR Freq. (cm^{-1})**	**Intensity (km/mol)**
C_6H_6	---	D_{6h}		409.3	0.0
				410.1	0.0
				622.2	0.0
				622.2	0.0
				686.5	122.2
				719.3	0.0
				861.1	0.0
				863.7	0.0
				979.0	0.0
				980.5	0.0
				1010.5	0.0
				1011.1	0.0
				1022.4	0.0
				1058.6	6.4
				1058.9	6.4
				1174.6	0.0
				1197.1	0.0
				1197.2	0.0
				1335.4	0.0
				1380.8	0.0
				1509.9	7.1
				1510.2	7.1
				1633.0	0.0
				1633.0	0.0
				3155.5	0.0
				3165.7	0.0
				3181.4	37.3
				3181.5	37.3
				3191.6	0.0
$Ti^+(C_6H_6)$	$^4B_2$	C_{2v}	54.5	291	0.0

				292	0.0
				310	0.0
				414	0.0
				415	0.0
				615	0.0
				616	0.0
				639	0.0
				770.7	100.0
				885.9	4.2
				887	4.2
				965	0.0
				965	0.0
				975	1
				983	0.0
				1024.1	7.9
				1024.7	7.9
				1028	0.0
				1170	0.0
				1170	0.0
				1177	0.0
				1332	0.0
				1336	0.0
				1474.1	10.9
				1474.4	10.9
				1530	0.0
				1530	0.0
				3186	0.0
				3192	0.0
				3201.9	5.0
				3202.0	5.0
				3208	1.0
$Ti^{+}(C_6H_6)_2$	$^4A_{1g}$	D_6	47.4	14	0.0
				80	0.0
				83	0.0
				184	0.0
				229	0.0
				305.2	55.0
				329.2	9.5
				329.5	9.4
				402	0.0
				405	0.0
				426	0.0
				428	0.0
				611	0.0
				612	0.0

616	0.0
617	0.0
667	0.0
671	0.0
751.6	97.4
763	0.0
885	0.0
888	0.0
895	0.0
900	0.0
966	0.0
970	0.0
978	0.0
982	0.0
983.4	15.1
983	0.0
999	0.0
999	0.0
1030	0.0
1033	0.0
1033	0.0
1034	0.0
1035.4	5.4
1035.8	5.2
1175	0.0
1175	0.0
1181	0.0
1183	0.0
1184	0.0
1340	0.0
1345	0.0
1371	0.0
1371	0.0
1484.6	9.5
1484.7	13.2
1485.1	12.9
1485.2	17
1544	0.0
1545	0.0
1563	0.0
1564	0.0
3188	0.0
3189	0.0
3193	0.0
3194	0.0
3194	0.0

				3194	0.0
				3204	0.0
				3205.0	1.1
				3205.0	1.1
				3210.7	4.4
				3211	0.0
$Ti^{+}(C_6H_6)_2$	$^4A_{1g}$	D_{6d}	47.5	-34.7	0.0
				65.4	0.0
				65.4	0.0
				180.8	0.0
				226.7	0.0
				226.7	0.0
				303.9	55.1
				328.4	9.3
				328.4	9.3
				398.3	0.0
				399.0	0.0
				426.6	0.0
				427.0	0.0
				610.8	0.0
				611.2	0.0
				615.2	0.0
				615.6	0.0
				668.1	0.0
				668.2	0.0
				752.1	0.0
				752.6	97.0
				886.4	0.0
				886.4	0.0
				890.7	0.1
				890.7	0.1
				969.2	0.0
				970.6	0.0
				971.6	0.0
				973.9	0.0
				983.2	15.0
				983.4	0.0
				996.2	0.0
				996.2	0.0
				1030.8	0.0
				1031.1	0.0
				1032.7	0.0
				1032.7	0.0
				1035.3	5.5
				1035.3	5.5

				1176.0	0.0
				1176.1	0.0
				1181.7	0.0
				1181.7	0.0
				1182.0	0.0
				1182.1	0.0
				1342.3	0.0
				1342.3	0.0
				1371.5	0.0
				1371.8	0.0
				1484.6	3.1
				1484.7	2.8
				1485.0	23.5
				1485.0	23.1
				1543.8	0.0
				1544.3	0.0
				1562.5	0.0
				1563.0	0.0
				3188.0	0.0
				3188.0	0.0
				3193.2	0.0
				3193.4	0.0
				3193.6	0.0
				3203.9	0.2
				3203.9	0.2
				3204.5	1.1
				3210.3	4.5
				3210.6	0.0
$Ti^{+}(C_6H_6)_2$	$^4A_{1g}$	D_{6h}	47.5	-19.6	0.0
				77.2	0.0
				78.4	0.0
				184.4	0.0
				231.0	0.0
				231.9	0.0
				309.7	55.1
				330.3	9.6
				331.1	9.5
				400.9	0.0
				402.5	0.0
				425.5	0.0
				427.1	0.0
				610.7	0.0
				611.0	0.0
				616.2	0.0
				616.5	0.0

662.6	0.0
663.8	0.0
757.1	98.2
766.8	0.0
888.8	0.0
890.7	0.0
898.7	0.1
901.7	0.0
962.6	0.0
965.3	0.0
980.9	0.0
982.1	14.7
982.1	0.0
986.8	0.0
998.3	0.0
998.4	0.0
1028.3	0.0
1032.7	0.0
1032.8	0.0
1033.1	0.1
1034.5	5.7
1034.6	5.8
1174.5	0.0
1174.5	0.0
1181.2	0.0
1184.4	0.0
1184.6	0.0
1184.7	0.0
1336.4	0.0
1344.1	0.0
1371.3	0.0
1371.7	0.0
1484.5	0.0
1484.6	0.0
1484.7	26.6
1484.8	26.6
1541.7	0.0
1542.3	0.0
1561.7	0.0
1562.2	0.0
3182.6	0.0
3183.1	0.0
3187.7	0.0
3188.1	0.0
3188.6	0.0
3188.8	0.0

				3198.6	0.0
				3199.0	0.0
				3199.1	1.4
				3205.1	4.4
				3205.4	0.0
$Ti^{+}(C_6H_6)_2$	^2A_g	D_{2h}	48.3	21.5	0.0
				80.7	0.0
				165.7	0.0
				198.6	0.0
				226.8	0.0
				252.5	101.6
				262.0	0.0
				335.1	16.1
				382.0	3.7
				410.2	0.0
				426.0	0.0
				436.5	0.0
				600.4	0.0
				606.3	0.3
				618.4	0.0
				629.8	0.0
				661.0	0.0
				663.0	1.6
				760.2	43.2
				780.2	0.0
				856.6	0.0
				875.1	0.4
				898.2	0.0
				908.8	0.7
				928.5	74.2
				937.7	0.0
				972.9	26.8
				974.8	0.0
				998.5	0.0
				1001.7	12.3
				1004.2	0.0
				1006.0	0.0
				1011.8	0.0
				1015.2	1.9
				1029.5	0.0
				1034.7	0.1
				1042.5	0.0
				1042.9	0.0
				1045.2	0.0
				1157.2	0.0

				1179.5	0.0
				1182.2	1.9
				1188.7	33.1
				1195.0	0.0
				1335.8	0.0
				1341.4	53.6
				1366.0	0.0
				1366.1	0.0
				1449.3	0.0
				1468.6	0.0
				1468.7	22.7
				1496.2	13.4
				1497.0	0.0
				1507.9	0.0
				1584.6	188.9
				1594.1	0.0
				3185.6	0.0
				3186.0	0.6
				3187.6	0.0
				3191.4	0.0
				3196.4	2.1
				3199.4	0.0
				3199.8	0.5
				3212.7	0.0
				3212.9	2.3
				3214.8	8.3
				3214.9	0.0
$Ti^{+}(C_6H_6)_2$	^2A_g	D_{2d}	47.9	21.5	0.0
				80.0	0.0
				80.7	0.0
				165.7	0.0
				198.6	0.0
				226.8	0.0
				252.5	101.6
				262.0	0.0
				335.1	16.1
				382.0	3.7
				410.2	0.0
				426.0	0.0
				436.5	0.0
				600.4	0.0
				606.3	0.3
				618.4	0.0
				629.8	0.0
				661.0	0.0

663.0	1.6
760.3	43.2
780.2	0.0
856.6	0.0
875.1	0.4
898.2	0.0
908.8	0.7
928.6	74.2
937.7	0.0
972.10	26.8
974.8	0.0
998.5	0.0
1001.8	12.3
1004.2	0.0
1006.0	0.0
1011.8	0.0
1015.3	1.9
1029.5	0.0
1034.7	0.1
1042.5	0.0
1042.9	0.0
1045.2	0.0
1157.2	0.0
1179.5	0.0
1182.2	1.9
1188.8	33.1
1195.0	0.0
1335.8	0.0
1341.4	53.6
1366.0	0.0
1366.1	0.0
1449.3	0.0
1468.6	0.0
1468.8	22.7
1496.3	13.4
1497.0	0.0
1507.9	0.0
1584.7	188.9
1594.1	0.0
3185.6	0.0
3186.0	0.0
3187.6	0.0
3191.4	0.0
3196.4	0.0
3196.5	2.1
3199.4	0.0

				3199.8	0.5
				3212.7	0.0
				3112.9	2.3
				3214.8	8.3
				3214.9	0.0
$Ti^{+}(C_6H_6)_2$	$^2B_{3g}$	D_{2h}	53.5	-16.5	0.0
				45.0	0.1
				65.0	0.0
				16.3.8	0.0
				227.4	0.0
				249.5	0.0
				266.3	0.0
				324.6	76.4
				358.7	12.2
				385.0	7.9
				390.1	6.1
				405.1	0.0
				406.0	0.0
				598.5	0.0
				602.8	0.0
				611.0	0.0
				615.7	0.0
				640.9	0.0
				646.2	0.6
				751.1	88.3
				766.1	0.0
				852.3	0.0
				860.9	0.0
				869.4	0.0
				875.1	0.3
				915.8	0.0
				919.6	0.0
				922.3	9.8
				958.0	0.0
				973.5	0.0
				974.3	19.4
				980.0	0.0
				983.1	0.1
				1009.2	0.0
				1010.7	15.3
				1028.4	0.0
				1033.6	0.0
				1034.5	6.2
				1040.3	0.0
				1132.4	0.0

				1156.6	0.0
				1168.4	4.9
				1173.1	0.0
				1175.6	0.0
				1177.6	0.3
				1341.8	0.0
				1360.2	0.0
				1360.6	0.0
				1360.9	13.3
				1463.4	0.0
				1466.2	0.0
				1466.4	17.0
				1478.1	0.0
				1478.3	15.5
				1501.2	0.0
				1530.2	22.1
				1539.6	0.0
				3193.7	0.0
				3195.1	0.4
				3195.9	0.0
				3197.0	0.0
				3201.6	0.0
				3201.9	0.1
				3208.0	0.0
				3208.7	4.1
				3213.3	0.0
				3213.8	6.8
				3217.4	9.6
				3217.5	0.0
$V^+(C_6H_6)$	$^5B_1$	C_{2v}	47.5	160.3	6.3
				220.6	0.0
				235.7	0.0
				243.5	0.7
				410.5	0.1
				547.0	0.0
				613.2	0.2
				661.5	0.0
				761.3	89.6
				892.1	1.4
				910.9	1.4
				980.5	0.6
				983.0	0.0
				996.2	0.0
				1006.7	0.0
				1026.6	5.3

				1029.9	0.0
				1042.4	3.7
				1182.0	0.0
				1182.1	0.1
				1182.9	0.0
				1325.8	0.1
				1373.1	0.0
				1480.2	16.5
				1489.6	12.2
				1554.7	0.0
				1568.0	0.7
				3186.4	0.2
				3189.9	0.1
				3192.8	0.0
				3201.3	5
				3206.0	6.8
				3210.1	0.2
$V^+(C_6H_6)$	$^3A_2$	C_{2v}	48.4	249.2	0.0
				322.1	0.2
				347.9	0.5
				366.0	0.6
				398.3	0.8
				597.1	0.0
				607.8	0.0
				625.2	5.6
				805.9	103.3
				837.0	10.6
				882.0	1.0
				890.4	4.9
				965.8	0.5
				967.7	0.0
				974.1	5.0
				989.3	11.2
				1026.4	1.5
				1029.2	0.6
				1106.9	0.0
				1164.2	0.5
				1177.7	0.2
				1328.3	27.4
				1350.1	0.0
				1425.0	0.0
				1446.5	6.7
				1478.9	2.1
				1551.6	7.4
				3184.9	0.5

				3186.9	0.0
				3195.1	0.0
				3198.4	6.2
				3209.3	11.2
				3212.4	1.0
$V^+(C_6H_6)_2$	$^5B_{2g}$	D_{2h}	32.0	-159.1	0.0
				-106.4	0.0
				-81.0	0.0
				-17.6	0.0
				69.7	0.0
				87.0	0.0
				88.1	0.1
				100.0	0.0
				141.4	0.0
				196.2	5.0
				390.2	0.1
				400.6	0.0
				406.4	0.0
				571.7	0.0
				611.0	0.1
				611.7	0.0
				612.7	0.0
				652.2	3.3
				655.9	0.0
				737.9	147.8
				746.4	0.0
				874.3	0.0
				881.6	0.2
				901.7	0.0
				909.2	0.4
				973.0	2.0
				977.6	0.0
				990.6	1.5
				990.9	0.0
				991.1	0.0
				992.1	0.0
				1008.6	0.0
				1009.4	0.0
				1023.4	3.0
				1023.8	0.0
				1034.7	0.0
				1036.0	6.0
				1047.7	0.2
				1048.2	5.8
				1176.8	0.0

				1180.6	0.0
				1180.8	1.1
				1184.9	0.0
				1189.5	0.1
				1192.4	0.0
				1315.7	7.0
				1325.1	0.0
				1375.5	0.0
				1375.8	0.0
				1487.3	1.3
				1487.7	31.5
				1496.4	0.1
				1497.3	30.2
				1568.4	0.0
				1570.7	0.9
				1574.2	0.0
				1582.9	0.0
				3184.8	0.0
				3184.9	0.3
				3189.1	0.0
				3189.7	0.0
				3193.2	0.0
				3193.4	0.0
				3200.4	0.0
				3200.6	0.8
				3205.5	1.4
				3205.6	0.5
				3210.3	1.6
				3210.3	0.2
$V^+(C_6H_6)_2$	Quintet	C_1	32.2	20.8	0.0
				58.9	0.0
				71.5	0.0
				107.7	0.2
				129.0	0.2
				142.2	4.9
				163.7	1.3
				184.7	1.3
				256.9	19.2
				388.0	0.2
				405.3	1.3
				411.8	1.5
				419.2	0.3
				596.1	0.1
				606.0	2.5
				612.3	0.1

613.6	0.1
656.3	0.2
662.7	0.4
735.1	98.4
750.0	27.5
872.5	0.8
886.5	0.0
887.6	0.6
905.5	0.4
969.6	1.7
978.1	0.6
981.8	0.2
986.9	14.1
987.3	0.4
993.3	0.1
1002.5	0.7
1009.1	0.0
1019.4	2.2
1022.1	2.1
1026.9	0.7
1034.8	3.1
1046.0	2.4
1050.9	3.3
1177.3	1.1
1181.4	0.3
1183.4	3.4
1184.0	0.9
1185.8	3.0
1188.1	0.0
1329.2	4.4
1337.6	4.6
1372.4	0.0
1374.1	0.0
1478.4	12.5
1486.8	16.6
1494.3	9.3
1495.1	18.6
1552.2	0.1
1567.7	0.2
1577.2	2.5
1589.7	35.7
3180.0	0.2
3186.0	1.3
3186.8	0.0
3187.7	0.0
3191.5	0.0

				3194.4	0.0
				3197.4	0.1
				3199.6	0.6
				3202.3	1.1
				3205.7	1.4
				3207.3	0.9
				3210.9	1.2
$V^+(C_6H_6)_2$	$^3B_{3g}$	D_{2h}	61.7	13.6	0.0
				101.0	0.0
				107.1	0.1
				191.6	0.0
				217.7	0.0
				262.1	0.0
				280.1	0.0
				331.4	78.9
				384.9	22.4
				405.4	7.0
				406.0	12.4
				417.1	0.0
				424.5	0.0
				609.5	0.0
				615.3	0.0
				617.5	0.0
				654.3	0.0
				656.5	0.7
				776.3	75.2
				786.2	0.0
				867.6	0.0
				882.4	0.6
				891.5	0.0
				900.0	1.6
				935.3	20.6
				937.6	0.0
				954.2	0.0
				980.5	12.5
				981.2	0.0
				984.7	0.0
				996.5	0.0
				1000.3	0.0
				1010.7	0.0
				1012.9	11.3
				1029.7	0.0
				1039.2	0.0
				1039.4	0.0
				1041.4	2.5

				1133.1	0.0
				1160.4	0.0
				1177.0	0.0
				1179.2	10.8
				1181.5	0.5
				1186.2	0.0
				1349.7	0.0
				1363.7	0.0
				1364.0	0.0
				1365.9	21.4
				1460.7	0.0
				1470.2	20.3
				1470.3	0.0
				1486.0	16.3
				1486.3	0.0
				1514.8	0.0
				1556.0	58.1
				1568.9	0.0
				3191.1	0.0
				3192.3	0.5
				3193.4	0.0
				3193.9	0.0
				3201.0	0.3
				3201.2	0.0
				3204.9	0.0
				3205.7	1.4
				3215.1	0.0
				3215.9	3.2
				3217.9	5.5
				3218.4	0.0
$V^+(C_6H_6)_2$	$^3B_1$	D_{2d}	61.6	-31.2	0.0
				106.2	0.0
				114.1	0.0
				114.1	0.0
				220.9	0.0
				265.9	0.6
				265.9	0.6
				328.2	81.0
				396.9	16.4
				396.9	16.4
				403.2	6.3
				422.5	0.0
				427.8	0.0
				607.8	0.1
				611.0	0.0

618.1	0.0
622.1	0.0
659.2	0.6
659.2	0.6
778.5	73.3
793.1	0.0
877.2	0.0
877.2	0.0
903.9	1.3
903.9	1.3
933.9	20.3
946.2	0.0
951.5	0.0
980.8	12.7
981.9	0.0
995.9	0.0
1002.2	0.2
1002.2	0.2
1013.1	5.1
1013.1	5.1
1036.6	0.0
1036.6	0.0
1040.7	1.2
1040.7	1.2
1128.7	0.0
1162.9	0.0
1178.9	0.3
1178.9	0.3
1179.2	11.9
1184.7	0.0
1358.8	10.3
1364.7	0.0
1365.0	0.0
1454.4	0.0
1470.7	10.2
1470.7	10.2
1485.8	8.2
1485.8	8.2
1515.6	0.0
1552.3	61.7
1573.5	0.0
3192.7	0.2
3193.9	0.0
3195.4	0.0
3201.1	0.8
3201.5	0.0

				3206.2	0.7
				3206.2	0.7
				3214.2	1.5
				3214.2	1.5
				3217.3	5.6
				3217.6	0.0
$Cr^+(C_6H_6)$	$^6A_1$	C_{6v}	36.4	85.8	1.4
				88.0	1.4
				184.2	6.7
				407.8	0.0
				409.0	0.0
				614.1	0.0
				614.6	0.0
				679.0	0.0
				768.4	107.4
				905.9	0.8
				906.4	0.7
				988.3	0.6
				1004.6	0.0
				1005.2	0.0
				1017.3	0.0
				1029.7	0.0
				1043.0	3.9
				1043.3	3.9
				1181.1	0.0
				1194.9	0.0
				1195.2	0.0
				1312.5	0.0
				1378.7	0.0
				1493.1	16.2
				1493.5	16.3
				1590.5	0.0
				1590.6	0.0
				3186.1	0.0
				3192.6	0.0
				3192.7	0.0
				3202.8	4.1
				3202.8	4.1
				3209.1	0.0
$Cr^+(C_6H_6)_2$	$^2A_{1g}$	D_{6h}	36.8	31.0	0.0
				146.1	0.2
				147.4	0.2
				257.7	0.0
				304.8	0.0

306.8	0.0
393.4	0.0
393.7	6.4
401.9	100.8
443.6	29.6
443.8	29.8
445.4	0.0
447.4	0.0
616.1	0.0
616.2	0.0
617.1	0.0
617.4	0.0
636.7	0.0
642.5	0.0
808.6	78.7
816.7	0.0
882.7	0.0
884.1	0.0
897.0	4.6
899.1	4.5
939.9	0.0
942.7	0.0
956.2	0.0
958.2	0.0
980.9	0.0
987.5	0.0
988.2	5.6
989.7	0.0
1026.4	0.0
1026.7	0.0
1028.0	8.7
1028.2	8.6
1032.9	0.0
1044.5	0.0
1163.4	0.0
1165.1	0.0
1171.7	0.0
1173.7	0.0
1174.7	0.0
1178.9	0.0
1357.9	0.0
1358.8	0.0
1372.8	0.0
1405.1	0.0
1470.5	16.8
1471.4	16.8

				1471.5	0.0
				1472.2	0.0
				1521.5	0.0
				1522.6	0.0
				1540.1	0.0
				1541.0	0.0
				3198.5	0.0
				3200.6	0.0
				3203.9	0.0
				3203.9	0.0
				3204.2	0.0
				3204.4	0.0
				3214.1	0.0
				3214.3	0.0
				3215.0	3.7
				3215.4	3.7
				3220.6	3.3
				3221.3	0.0
$Mn^{+}(C_6H_6)$	$^7A_1$	C_{6v}	31.5	97.6	0.3
				97.6	0.3
				160.0	37.1
				374.6	0.0
				376.5	0.0
				612.8	0.0
				612.9	0.0
				674.8	0.0
				755.8	134.4
				915.6	1.0
				916.9	1.1
				995.3	5.0
				1015.0	0.0
				1015.5	0.0
				1023.0	0.0
				1031.3	0.0
				1050.5	0.7
				1050.5	0.7
				1188.4	0.0
				1202.2	0.0
				1202.4	0.0
				1330.1	0.0
				1384.3	0.0
				1501.4	31.6
				1501.5	31.6
				1604.2	0.0
				1604.8	0.0

				3179.4	0.0
				3186.2	0.0
				3186.3	0.0
				3196.3	5.8
				3196.4	5.8
				3202.6	0.0
$Mn^+(C_6H_6)$	$^5A_1$	C_{2v}	27.8	166.0	0.8
				166.8	0.0
				240.4	0.1
				260.3	1.6
				398.0	0.0
				604.8	0.0
				610.6	0.0
				659.8	3.3
				770.5	101.7
				875.9	4.1
				897.8	0.8
				944.4	2.1
				967.1	0.0
				968.4	0.6
				1002.6	6.0
				1010.1	4.9
				1029.7	0.4
				1037.3	2.5
				1133.3	0.0
				1176.5	0.5
				1185.6	1.8
				1312.7	9.4
				1365.0	0.0
				1464.3	0.0
				1465.4	10.1
				1482.0	11.4
				1567.3	14.4
				3191.4	0.2
				3193.7	0.0
				3200.1	0.1
				3204.6	7.2
				3211.8	10.7
				3215.2	0.6
$Mn^+(C_6H_6)_2$	$^1A_1$	D_{6h}	29.9	30.2	0.0
				169.8	0.2
				171.4	0.2
				257.2	0.0
				308.1	0.0

310.4	0.0
399.1	0.0
399.7	2.9
412.7	105.8
439.3	0.0
442.4	0.0
444.3	39.2
444.7	39.3
618.7	0.0
618.7	0.0
631.3	0.0
631.4	0.0
631.8	0.0
650.3	0.0
835.8	60.7
839.5	0.0
913.7	0.0
916.0	0.0
934.2	6.3
938.9	6.3
980.0	0.0
983.0	0.0
990.5	0.0
994.7	0.0
995.9	0.0
999.3	0.0
999.4	1.8
1002.4	0.0
1032.3	0.0
1035.4	0.0
1035.5	0.0
1038.0	3.9
1038.3	3.9
1042.6	0.2
1172.7	0.0
1174.7	0.0
1178.0	0.0
1180.0	0.0
1181.0	0.0
1185.9	0.0
1364.9	0.0
1365.9	0.0
1387.8	0.0
1413.5	0.0
1481.3	21.5
1482.2	21.5

				1482.4	0.0
				1483.1	0.0
				1548.4	0.0
				1549.5	0.0
				1558.5	0.0
				1559.4	0.0
				3192.4	0.0
				3194.1	0.0
				3197.8	0.0
				3198.1	0.0
				3198.7	0.0
				3199.2	0.0
				3208.4	0.0
				3208.7	0.0
				3209.2	0.1
				3209.6	0.1
				3214.8	0.3
				3215.5	0.0
$Mn^{+}(C_6H_6)_2$	$^1A_1$	D_{6d}	29.5	-41.2	0.0
				173.0	0.3
				173.0	0.3
				260.4	0.0
				300.9	0.0
				404.8	107.3
				407.0	1.6
				407.1	0.0
				431.5	0.0
				431.6	0.0
				445.9	38.0
				445.9	38.0
				622.9	0.0
				623.2	0.0
				626.8	0.0
				627.1	0.0
				658.8	0.0
				661.5	0.0
				830.8	59.8
				840.2	0.0
				912.4	0.0
				912.4	0.0
				940.4	7.0
				940.5	7.0
				985.2	0.0
				986.9	0.0
				993.9	0.0

				994.5	0.0
				999.5	1.9
				999.8	0.0
				1006.1	0.0
				1006.6	0.0
				1035.4	0.0
				1035.4	0.0
				1039.6	2.4
				1039.6	3.2
				1039.7	0.7
				1040.0	0.0
				1177.2	0.0
				1177.3	0.0
				1178.9	0.0
				1178.9	0.0
				1183.6	0.0
				1183.7	0.0
				1367.4	0.0
				1368.5	0.0
				1402.2	0.0
				1402.2	0.0
				1482.4	21.1
				1482.4	21.2
				1484.0	0.1
				1484.0	0.1
				1548.7	0.0
				1549.5	0.0
				1560.5	0.0
				1561.2	0.0
				3192.1	0.0
				3192.1	0.0
				3196.7	0.0
				3196.8	0.0
				3197.5	0.0
				3197.7	0.0
				3207.1	0.0
				3207.2	0.0
				3208.1	0.1
				3208.1	0.1
				3213.4	0.3
				3214.1	0.0
$Fe^{+}(C_6H_6)$	$^6A_2$	C_{2v}	38.9	108.5	0.1
				126.4	0.1
				166.7	27.1
				321.0	0.0

				361.5	0.1
				607.5	0.0
				609.8	0.0
				668.2	0.0
				761.5	125.1
				917.8	1.2
				919.6	1.3
				995.0	3.4
				1008.2	0.0
				1015.7	0.0
				1025.0	0.0
				1032.6	0.0
				1047.7	0.6
				1050.7	0.6
				1190.1	0.0
				1197.3	0.0
				1201.3	0.0
				1333.1	0.0
				1383.0	0.0
				1498.9	33.4
				1500.5	34.0
				1593.4	0.0
				1597.5	0.1
				3188.2	0.0
				3194.5	0.0
				3194.6	0.0
				3204.2	10.7
				3204.2	10.7
				3210.2	0.1
$Fe^{+}(C_6H_6)$	$^6A_1$	C_{2v}	38.8	106.7	0.1
				128.4	0.1
				165.9	27.1
				358.9	0.1
				367.2	0.0
				607.6	0.0
				610.4	0.0
				668.1	0.0
				764.6	125.1
				920.2	1.2
				921.7	1.4
				994.8	3.4
				1016.4	0.0
				1017.9	0.0
				1025.1	0.0
				1034.3	0.0

				1048.6	0.6
				1050.5	0.6
				1191.0	0.0
				1201.2	0.0
				1202.1	0.0
				1333.2	0.0
				1383.9	0.0
				1499.7	33.5
				1500.7	34.0
				1598.7	0.1
				1598.7	0.0
				3183.5	0.0
				3189.7	0.0
				3190.1	0.0
				3199.2	10.6
				3199.7	10.7
				3205.5	0.1
$Fe^{+}(C_6H_6)$	$^4A_1$	C_{2v}	49.0	-228.1	0.0
				166.6	1.3
				234.1	0.2
				240.6	0.7
				413.7	0.0
				604.7	0.0
				616.0	0.0
				675.3	1.4
				779.4	100.9
				911.5	2.4
				917.8	1.5
				967.3	0.0
				982.8	0.4
				992.4	0.3
				1013.5	0.0
				1025.1	5.6
				1035.8	0.0
				1043.0	2.6
				1156.3	0.0
				1181.6	0.2
				1190.7	0.5
				1318.3	2.6
				1373.8	0.0
				1480.4	16.8
				1489.3	18.3
				1504.6	0.0
				1581.8	3.9
				3189.9	0.0

				3193.2	0.0
				3197.3	0.1
				3204.0	6.2
				3206.8	6.9
				3211.6	0.0
$Fe^{+}(C_6H_6)$	$^4A_2$	C_{2v}	49.0	-49.5	0.0
				162.8	1.4
				236.4	0.2
				238.9	0.7
				419.8	0.0
				607.6	0.0
				613.9	0.0
				647.9	1.4
				781.5	100.9
				914.2	1.9
				919.0	1.6
				962.8	0.0
				982.4	0.4
				1008.0	0.3
				1014.1	0.1
				1024.5	4.9
				1036.3	0.1
				1044.7	2.8
				1171.1	0.0
				1182.6	0.3
				1185.0	0.5
				1317.9	2.9
				1375.0	0.0
				1482.4	15.7
				1488.8	19.6
				1534.8	0.0
				1559.9	3.8
				3183.4	0.0
				3187.4	0.1
				3190.3	0.0
				3198.0	6.1
				3199.8	6.8
				3205.0	0.0
$Fe^{+}(C_6H_6)_2$	$^4A_{1g}$	D_{6h}	32.5	-22.6	0.0
				79.3	0.0
				80.0	0.0
				112.7	0.0
				113.1	0.0
				176.3	0.00

200.9	17.9
218.0	1.9
218.5	1.9
396.5	0.0
396.9	0.0
408.1	0.0
409.4	0.0
472.3	0.0
474.2	0.0
615.5	0.0
615.8	0.0
652.6	0.0
664.4	0.0
750.0	152.9
762.6	0.0
883.1	0.0
883.3	0.0
890.0	1.5
891.8	1.6
899.1	0.0
902.1	0.0
978.0	0.0
979.5	0.0
986.5	1.6
987.8	0.0
1001.9	0.0
1007.6	0.0
1021.8	0.0
1031.5	0.0
1035.2	0.0
1036.1	0.0
1036.8	7.7
1037.8	7.8
1171.0	0.0
1175.4	0.0
1176.2	0.0
1180.2	0.0
1181.0	0.0
1181.2	0.0
1292.9	0.0
1329.6	0.0
1368.9	0.0
1369.5	0.0
1483.7	0.0
1484.5	0.0
1485.1	26.9

				1485.7	26.8
				1557.8	0.0
				1558.7	0.0
				1562.7	0.0
				1563.6	0.0
				3191.6	0.0
				3191.6	0.0
				3191.7	0.0
				3193.1	0.0
				3198.4	0.0
				3198.6	0.0
				3208.9	0.0
				3209.1	0.0
				3209.7	2.8
				3209.8	2.8
				3215.7	2.5
				3216.3	0.0
$Fe^{+}(C_6H_6)_2$	$^4B_{3g}$	$D2_h$	36.5	-60.2	0.0
				-27.7	0.0
				79.7	0.0
				80.8	0.1
				86.4	0.0
				97.6	0.0
				119.3	2.1
				144.1	0.0
				179.1	0.1
				182.7	0.8
				402.4	0.0
				405.5	0.7
				411.8	0.0
				603.9	0.0
				611.0	0.0
				611.1	0.0
				612.5	0.0
				670.4	0.0
				674.2	0.5
				749.7	172.4
				758.5	0.0
				897.5	0.0
				901.5	0.0
				908.6	0.7
				910.4	1.0
				956.5	0.0
				990.7	0.0
				993.3	0.0

				993.5	0.1
				999.2	0.0
				1003.7	2.8
				1015.1	0.0
				1016.1	0.0
				1024.8	0.0
				1028.6	0.0
				1037.6	0.0
				1039.6	5.1
				1049.9	0.0
				1051.7	3.2
				1172.3	0.0
				1180.2	0.0
				1182.1	0.5
				1190.2	4.0
				1192.0	0.0
				1193.5	0.0
				1320.1	0.0
				1322.0	3.4
				1377.3	0.0
				1377.5	0.0
				1492.5	0.0
				1493.8	32.5
				1497.4	0.0
				1498.8	37.3
				1541.4	0.0
				1584.8	18.3
				1586.9	0.0
				1598.1	0.0
				3185.1	0.0
				3185.6	0.0
				3190.2	0.0
				3190.9	0.5
				3192.7	0.0
				3193.2	0.0
				3202.4	0.0
				3202.8	0.3
				3204.0	0.0
				3204.5	0.6
				3210.0	0.1
				3210.3	0.0
$Fe^{+}(C_6H_6)_2$	Quartet	C_2	36.2	17.7	0.1
				44.1	0.0
				62.5	0.0
				64.6	2.1

81.1	0.0
92.4	1.2
169.6	0.0
182.9	0.7
244.1	4.5
361.2	0.0
406.3	1.8
413.9	0.4
414.0	0.0
609.0	0.0
610.2	0.0
612.0	0.0
613.2	0.0
680.6	0.0
684.6	0.2
748.9	172.2
755.6	0.0
896.9	0.0
899.9	0.0
906.4	1.6
910.1	0.6
981.4	0.0
988.9	0.5
990.1	0.0
990.7	0.3
1007.1	1.1
1007.1	2.6
1016.0	0.0
1018.0	0.1
1029.2	0.0
1031.7	0.0
1039.0	0.0
1040.6	4.6
1045.4	0.0
1049.0	3.3
1179.2	0.0
1180.1	0.5
1189.3	0.0
1190.5	3.5
1192.2	0.0
1194.6	0.0
1322.5	3.7
1323.0	0.0
1377.9	0.0
1378.0	0.0
1493.0	0.0

				1493.3	0.0
				1493.8	35.3
				1496.2	35.2
				1582.1	0.0
				1584.2	14.3
				1586.6	0.0
				1598.5	1.3
				3184.3	0.0
				3184.5	0.0
				3189.7	0.0
				3190.0	0.4
				3192.1	0.0
				3192.1	0.1
				3201.5	0.0
				3202.0	0.3
				3202.8	0.0
				3203.1	0.5
				3209.3	0.2
				3209.3	0.0
$Fe^{+}(C_6H_6)_2$	$^2B_{1g}$	D_{2h}	40.6	-17.3	0.0
				135.3	0.2
				146.0	0.1
				149.8	0.0
				180.4	0.0
				217.2	0.0
				244.9	0.0
				278.2	9.5
				309.2	48.8
				356.5	14.5
				395.6	0.2
				396.0	0.0
				422.9	0.0
				569.2	0.0
				611.7	1.1
				616.1	0.0
				620.6	0.0
				653.5	0.0
				658.9	1.1
				792.0	98.8
				803.7	0.0
				886.5	0.0
				899.5	1.6
				922.6	0.0
				942.5	7.1
				982.9	0.0

				990.2	0.3
				990.3	0.0
				993.4	0.0
				999.5	0.4
				1006.0	0.0
				1007.1	0.0
				1013.6	0.1
				1022.3	0.0
				1025.7	3.7
				1031.1	0.0
				1038.5	0.4
				1050.6	0.0
				1052.4	6.8
				1177.9	0.2
				1178.7	0.0
				1179.6	0.0
				1181.1	0.0
				1181.6	0.0
				1184.9	0.5
				1356.1	0.0
				1371.0	0.0
				1371.1	0.0
				1371.4	7.0
				1477.1	30.6
				1478.0	0.0
				1495.4	0.0
				1496.2	25.7
				1545.3	0.0
				1550.8	0.0
				3195.3	0.0
				3197.7	0.0
				3198.1	0.0
				3205.4	0.0
				3206.2	0.4
				3209.2	0.0
				3210.1	0.8
				3214.3	0.3
				3214.8	0.0
$Co^{+}(C_6H_6)$	$^3A_2$	C_{2v}	58.6	245.4	0.9
				245.5	0.9
				279.3	0.0
				412.2	0.0
				413.1	0.0
				622.7	0.0
				623.0	0.0

				667.3	0.0
				799.7	105.3
				917.0	1.4
				918.8	1.3
				983.1	0.0
				985.7	0.5
				999.8	0.0
				1000.7	0.0
				1033.2	5.1
				1033.3	5.1
				1037.8	0.0
				1156.6	0.0
				1182.6	0.0
				1182.8	0.0
				1278.4	0.0
				1371.0	0.0
				1480.4	15.1
				1480.6	15.1
				1558.9	0.0
				1559.4	0.0
				3185.3	0.0
				3192.8	0.0
				3193.0	0.0
				3201.9	9.6
				3202.1	9.6
				3208.2	0.0
$Co^{+}(C_6H_6)_2$	$^3A_1$	D_6	35.9	23.0	0.0
				100.0	0.0
				102.6	0.0
				103.5	0.1
				104.6	0.1
				167.3	0.0
				196.6	5.6
				208.4	3.2
				208.4	3.2
				401.5	0.0
				402.6	0.0
				410.4	0.0
				410.4	0.0
				616.4	0.0
				616.4	0.0
				618.9	0.0
				619.0	0.0
				674.8	0.0
				680.4	0.0

759.6	161.0
768.9	0.0
899.4	0.0
900.3	0.0
909.7	2.1
910.3	2.2
994.6	0.0
995.2	0.0
995.7	0.0
997.4	0.0
1000.0	0.0
1000.5	0.0
1015.5	0.0
1020.2	0.0
1027.9	0.0
1031.6	0.0
1043.3	0.1
1043.3	0.0
1045.1	4.9
1045.1	4.9
1177.7	0.0
1182.7	0.0
1188.7	0.0
1188.9	0.0
1190.5	0.0
1190.6	0.0
1315.4	0.0
1333.3	0.0
1375.0	0.0
1375.2	0.0
1492.5	1.7
1492.8	5.4
1493.8	26.1
1494.0	29.8
1585.0	0.0
1585.1	0.0
1585.5	0.0
1585.6	0.0
3188.7	0.0
3189.5	0.0
3195.1	0.0
3195.5	0.0
3196.0	0.0
3196.3	0.0
3206.0	0.1
3206.2	0.1

				3207.0	0.6
				3207.1	0.7
				3213.0	0.4
				3213.5	0.0
$Co^{+}(C_6H_6)_2$	$^3A_{1g}$	D_{6d}	35.8	-19.7	0.0
				101.6	0.0
				101.6	0.0
				110.1	0.1
				110.2	0.1
				170.4	0.0
				197.3	5.9
				211.3	3.1
				211.3	3.1
				403.6	0.0
				406.5	0.0
				408.0	0.0
				411.4	0.0
				616.4	0.0
				616.9	0.0
				618.3	0.0
				618.9	0.0
				678.7	0.0
				681.3	0.0
				761.5	160.0
				775.8	0.0
				901.2	0.0
				901.2	0.0
				915.1	2.2
				915.1	2.2
				994.4	0.0
				995.3	0.0
				997.1	0.0
				998.0	0.0
				1002.8	0.0
				1004.1	0.0
				1018.6	0.0
				1018.9	0.0
				1032.1	0.0
				1032.8	0.0
				1042.4	0.1
				1042.4	0.1
				1044.5	4.6
				1044.5	4.6
				1180.3	0.0
				1180.4	0.0

				1188.6	0.0
				1188.8	0.0
				1190.0	0.0
				1190.4	0.0
				1322.7	0.0
				1322.7	0.0
				1375.6	0.0
				1375.9	0.0
				1492.2	2.8
				1492.2	2.7
				1493.3	28.7
				1493.3	28.8
				1583.6	0.0
				1583.7	0.0
				1584.4	0.0
				1584.6	0.0
				3190.0	0.0
				3190.1	0.0
				3196.6	0.0
				3196.4	0.0
				3196.7	0.0
				3196.9	0.0
				3207.1	0.0
				3207.1	0.0
				3207.7	0.8
				3207.7	0.8
				3213.9	0.4
				3214.2	0.0
$Co^{+}(C_6H_6)_2$	$^3A_{1g}$	D_{6h}	35.9	-22.6	0.0
				103.1	0.1
				103.5	0.1
				106.6	0.0
				107.0	0.0
				169.9	0.0
				203.5	6.1
				211.1	3.2
				211.4	3.3
				401.3	0.0
				401.8	0.0
				409.9	0.0
				411.4	0.0
				615.6	0.0
				616.0	0.0
				618.8	0.0
				619.2	0.0

669.7	0.0
673.4	0.0
759.6	161.1
769.5	0.0
899.0	0.0
899.2	0.0
909.1	2.2
910.7	2.3
993.6	0.0
994.5	0.0
995.1	0.0
995.5	0.0
998.8	0.0
994.4	0.0
1013.2	0.0
1018.2	0.0
1024.3	0.0
1030.1	0.0
1041.6	0.0
1042.5	0.0
1043.8	4.9
1044.7	5.0
1177.2	0.0
1183.2	0.0
118.8.1	0.0
1190.4	0.0
1190.7	0.0
1313.4	0.0
1332.4	0.0
1374.0	0.0
1374.6	0.0
1491.4	0.0
1492.2	0.0
1492.8	31.8
1493.5	31.7
1583.0	0.0
1583.6	0.0
1583.9	0.0
1584.5	0.0
3188.9	0.0
3190.0	0.0
3195.7	0.0
3195.8	0.0
3196.4	0.0
3196.5	0.0
3206.5	0.0

				3206.6	0.0
				3207.3	0.8
				3207.3	0.8
				3213.3	0.4
				3213.9	0.0
$Ni^{+}(C_6H_6)$	$^2B_2$	C_{2v}	57.4	146.9	0.9
				192.8	0.5
				205.8	0.0
				240.4	0.6
				412.8	0.0
				547.0	0.0
				618.4	0.0
				679.3	0.1
				779.0	105.3
				906.0	1.2
				924.3	0.4
				984.9	0.9
				997.7	0.0
				1011.8	0.3
				1016.7	0.0
				1026.6	3.6
				1037.4	0.2
				1043.0	3.5
				1180.7	0.0
				1184.9	0.0
				1185.8	0.0
				1313.5	0.1
				1373.7	0.0
				1478.9	19.5
				1488.9	18.4
				1561.1	0.0
				1576.3	0.0
				3192.3	0.3
				3196.3	0.0
				3198.9	0.0
				3206.5	9.0
				3210.5	10.2
				3214.9	0.0
$Ni^{+}(C_6H_6)_2$	$^2B_{2g}$	D_{2h}	28.3	-135.2	0.0
				-85.8	0.1
				-72.4	0.0
				-25.9	0.0
				79.9	0.1
				84.8	0.0

90.2	0.4
138.3	0.0
146.5	3.0
177.1	0.0
395.7	0.0
403.3	0.1
410.3	0.0
577.3	0.0
614.1	0.0
614.5	0.0
616.4	0.0
684.4	0.0
685.4	0.2
746.5	205.4
755.9	0.0
890.1	0.0
899.1	0.7
905.7	0.0
915.9	1.9
994.1	1.3
995.3	0.0
1000.7	0.0
1004.5	0.0
1007.4	0.8
1011.2	0.0
1019.5	0.0
1021.2	0.0
1030.6	0.0
1033.5	0.4
1039.8	0.0
1042.0	4.6
1051.6	0.0
1053.2	5.1
1179.2	0.0
1181.2	0.4
1191.9	0.0
1192.0	0.1
1194.2	0.0
1195.3	0.0
1315.8	0.0
1317.1	2.4
1378.8	0.0
1378.9	0.0
1492.0	0.0
1493.5	35.5
1499.3	0.0

				1501.6	35.8
				1585.6	0.0
				1592.5	0.0
				1601.6	0.2
				1602.7	0.0
				3185.8	0.0
				3186.2	0.1
				3191.4	0.0
				3191.9	0.0
				3193.7	0.0
				3194.3	0.0
				3202.6	0.0
				3203.2	0.5
				3205.6	0.0
				3206.1	0.8
				3211.2	0.1
				3211.6	0.0
$Ni^{+}(C_6H_6)_2$	Doublet	C_1	33.7	11.2	0.0
				58.0	1.6
				61.2	0.0
				71.0	0.0
				72.1	0.0
				76.1	1.6
				129.5	0.5
				225.3	0.0
				281.4	0.5
				371.8	0.0
				399.4	1.6
				438.1	0.0
				438.7	1.0
				605.2	0.0
				612.6	0.1
				613.6	0.4
				614.8	0.0
				692.8	5.9
				693.5	1.1
				741.1	191.5
				745.6	0.0
				897.9	0.0
				901.4	0.0
				901.7	0.2
				904.6	0.3
				985.4	0.0
				985.6	3.0
				1000.8	3.1

				1001.4	0.0
				1006.6	0.0
				1007.3	1.7
				1021.4	0.2
				1021.8	0.0
				1031.7	0.1
				1031.9	0.7
				1040.5	0.0
				1041.5	3.7
				1049.5	0.0
				1049.9	4.5
				1177.8	0.0
				1178.4	0.0
				1189.5	0.0
				1192.8	0.2
				1197.6	1.0
				1198.1	0.0
				1316.2	0.0
				1329.8	0.7
				1378.5	0.0
				1378.6	0.0
				1491.9	0.0
				1492.5	34.0
				1497.8	33.8
				1498.4	0.0
				1591.5	0.0
				1595.0	7.1
				1598.5	0.0
				1598.9	2.5
				3180.9	0.2
				3181.0	0.1
				3187.7	0.3
				3187.8	0.1
				3189.0	0.2
				3189.7	0.0
				3199.9	0.1
				3200.0	0.2
				3200.2	0.1
				3200.5	0.2
				3207.7	0.0
				3207.8	0.0
$Cu^{+}(C_6H_6)$	$^{1}A_1$	C_{6v}	49.1	79.8	0.5
				82.5	0.5
				197.8	3.5
				408.5	0.0

				410.0	0.0
				617.2	0.0
				617.6	0.0
				690.0	0.0
				767.4	115.4
				916.4	0.6
				917.6	0.5
				986.1	2.8
				1012.4	0.0
				1012.8	0.0
				1021.2	0.0
				1038.0	0.1
				1039.1	3.1
				1039.7	3.2
				1180.2	0.0
				1194.6	0.0
				1194.7	0.0
				1301.8	0.0
				1379.0	0.0
				1489.1	20.5
				1489.1	20.5
				1584.3	0.0
				1584.8	0.0
				3185.3	0.0
				3191.4	0.0
				3191.5	0.0
				3200.8	7.6
				3200.9	7.6
				3207.0	0.1
$Cu^{+}(C_6H_6)_2$	$^1A_{1g}$	D_{6h}	10.9	-135.3	0.0
				-135.3	0.0
				-122.2	0.0
				-122.2	0.0
				-16.5	0.0
				72.3	0.0
				72.3	0.0
				123.0	0.0
				136.9	20.3
				403.4	0.0
				403.4	0.0
				408.9	0.0
				408.9	0.0
				614.6	0.0
				614.6	0.0
				615.6	0.0

615.6	0.0
695.4	0.0
695.8	0.0
740.1	243.7
746.7	0.0
896.7	0.0
896.7	0.0
903.4	0.2
903.4	0.2
999.9	0.0
999.9	0.0
1001.8	9.5
1002.9	0.0
1002.9	0.0
1003.7	0.0
1018.8	0.0
1019.1	0.0
1028.5	0.0
1029.3	0.0
1054.9	0.0
1054.9	0.0
1056.3	3.2
1056.3	3.2
1186.7	0.0
1187.9	0.0
1204.5	0.0
1204.5	0.0
1206.3	0.0
1206.3	0.0
1326.9	0.0
1327.5	0.0
1387.6	0.0
1387.9	0.0
1512.2	0.0
1512.2	0.0
1514.3	34.6
1514.3	34.6
1621.3	0.0
1621.3	0.0
1622.7	0.0
1622.7	0.0
3213.9	0.0
3214.1	0.0
3221.0	0.0
3221.0	0.0
3221.3	0.0

				3221.3	0.0
				3232.2	0.0
				3232.2	0.0
				3232.5	0.0
				3232.5	0.0
				3239.0	0.0
				3239.3	0.0
$Cu^{+}(C_6H_6)_2$	^1A	C_1	35.2	-14.1	0.0
				27.9	0.0
				38.7	0.0
				59.3	0.1
				74.2	0.0
				78.1	0.0
				90.9	0.8
				224.0	0.2
				283.0	1.6
				413.7	0.2
				416.9	0.1
				424.9	0.1
				426.4	0.1
				613.3	0.1
				613.7	0.2
				614.1	0.2
				614.8	0.0
				698.2	0.2
				699.1	0.3
				733.1	224.8
				736.5	1.0
				886.6	0.0
				889.5	0.0
				908.2	3.4
				910.4	0.4
				986.7	10.9
				988.4	0.8
				992.0	1.5
				993.9	2.7
				1008.3	0.1
				1008.7	0.6
				1023.6	0.3
				1024.1	0.7
				1032.6	0.2
				1033.3	0.1
				1044.7	3.4
				1045.1	2.7
				1050.4	1.2

1050.9	2.1
1176.8	0.1
1198.0	0.1
1198.2	0.2
1199.4	0.0
1199.7	0.1
1335.0	1.3
1337.2	8.2
1379.6	0.1
1379.8	0.1
1496.8	12.8
1496.9	16.1
1497.4	10.7
1497.9	21.8
1599.9	1.0
1600.6	2.3
1612.7	2.3
1613.4	2.8
3166.2	0.3
3166.9	0.3
3177.3	0.6
3178.3	0.7
3184.6	0.2
3184.9	0.2
3192.7	0.0
3192.8	0.0
3199.2	0.0
3199.6	0.0
3205.5	0.1
3205.6	0